frontiers

RESEARCH TOPICS

STRUCTURAL BIOLOGY FOR VIRUS RESEARCH

Hosted by
Akio Adachi, Yasuyuki Miyazaki, Masako Nomaguchi and Mikako Fujita

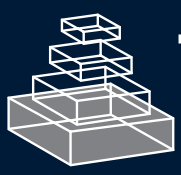

frontiers in MICROBIOLOGY

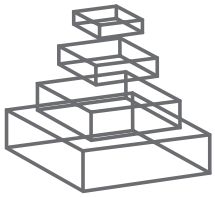

frontiers

Cover image provided by Ibbl sarl, Lausanne CH

ISSN 1664-8714
ISBN 978-2-88919-024-9
DOI 10.3389/978-2-88919-024-9

ABOUT FRONTIERS

Frontiers is more than just an open-access publisher of scholarly articles: it is a pioneering approach to the world of academia, radically improving the way scholarly research is managed. The grand vision of Frontiers is a world where all people have an equal opportunity to seek, share and generate knowledge. Frontiers provides immediate and permanent online open access to all its publications, but this alone is not enough to realize our grand goals.

FRONTIERS JOURNAL SERIES

The Frontiers Journal Series is a multi-tier and interdisciplinary set of open-access, online journals, promising a paradigm shift from the current review, selection and dissemination processes in academic publishing.
All Frontiers journals are driven by researchers for researchers; therefore, they constitute a service to the scholarly community. At the same time, the Frontiers Journal Series operates on a revolutionary invention, the tiered publishing system, initially addressing specific communities of scholars, and gradually climbing up to broader public understanding, thus serving the interests of the lay society, too.

DEDICATION TO QUALITY

Each Frontiers article is a landmark of the highest quality, thanks to genuinely collaborative interactions between authors and review editors, who include some of the world's best academicians. Research must be certified by peers before entering a stream of knowledge that may eventually reach the public - and shape society; therefore, Frontiers only applies the most rigorous and unbiased reviews.
Frontiers revolutionizes research publishing by freely delivering the most outstanding research, evaluated with no bias from both the academic and social point of view.
By applying the most advanced information technologies, Frontiers is catapulting scholarly publishing into a new generation.

WHAT ARE FRONTIERS RESEARCH TOPICS?

Frontiers Research Topics are very popular trademarks of the Frontiers Journals Series: they are collections of at least ten articles, all centered on a particular subject. With their unique mix of varied contributions from Original Research to Review Articles, Frontiers Research Topics unify the most influential researchers, the latest key findings and historical advances in a hot research area!
Find out more on how to host your own Frontiers Research Topic or contribute to one as an author by contacting the Frontiers Editorial Office: researchtopics@frontiersin.org

STRUCTURAL BIOLOGY FOR VIRUS RESEARCH

Hosted By
Akio Adachi, The University of Tokushima Graduate School, Japan
Yasuyuki Miyazaki, The University of Tokushima Graduate School, Japan
Masako Nomaguchi, The University of Tokushima Graduate School, Japan
Mikako Fujita, Kumamoto University, Japan

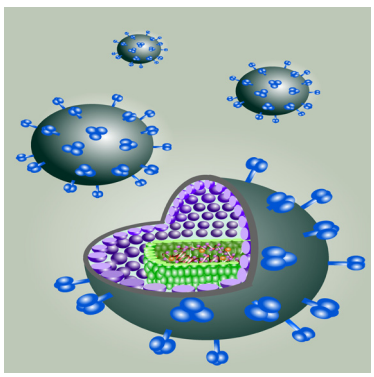

Viruses are absolutely and strictly dependent on target host cells for their replication. However, they have their own unique strategies at each replication step from the entry into cells, transcription, translation, assembly of viral genome/proteins, and up to the release of progeny virions from cells. We virologists have to understand these complex biological interactions between viruses and host cells. Importantly, extensive studies based on bio-structural technology have revealed in succession the detailed and bottom line mechanisms of viral replication processes otherwise impossible. We now know the highly dynamic nature of viral genome/proteins, and are impressed by their ingeniously organized functionality in hostile host environments. For characterization of viruses as a unique genetic entity and pathogenic agent, it has been critical to investigate thoroughly the individual viral components and host factors involved in the virus replication cycle. Because many viral and cellular factors essential for viral replication and pathogenicity have been newly discovered through the efforts of virologists, the necessity of contribution to the progress of virology by the structural biology is now greatly increasing. To fully understand precise mechanisms underlying the functional interaction of viral and host molecules, needless to say, it is crucially required to have their structural information. We need to know molecular details of the nucleic acids, proteins, and interacting molecules. The information indispensable for understanding certain biological phenomena may only be provided by high-resolution three-dimensional structures. Of note, a number of anti-viral drugs have been generated based on the structural information. The interacting interfaces between virus and host components, which are important for viral replication, can be potent targets for anti-viral drugs. Their structural characterization would lead to designing rigid anti-viral drugs and/or vaccines.

In this Research Topic, we wish to summarize and review what the structural biology has accomplished so far to resolve the important virological issues. We also wish to describe the perspective of the structural biology for the future virology. Finally, the presentation of ongoing original works is greatly encouraged.

Table of Contents

frontiers in
MICROBIOLOGY

EDITORIAL
published: 13 March 2012
doi: 10.3389/fmicb.2012.00091

Structural biology for virus research

Yasuyuki Miyazaki[1], Mikako Fujita[2], Masako Nomaguchi[1] and Akio Adachi[1]*

[1] *Department of Microbiology, Institute of Health Biosciences, The University of Tokushima Graduate School, Tokushima, Japan*
[2] *School of Pharmacy, Research Institute for Drug Discovery, Kumamoto University, Kumamoto, Japan*
**Correspondence: adachi@basic.med.tokushima-u.ac.jp*

Viruses are strictly dependent on target host cells for their amplification. However, each virus has a unique strategy at each replication step, beginning with entry into the cell, followed by transcription, translation, assembly of viral genome/proteins, and finishing with the cellular release of progeny virions. Extensive studies utilizing bio-structural technology have revealed detailed, bottom line mechanisms of viral replication processes that we virologists need to understand these complex interactions between viruses and host cells. We now know that viral genome/proteins are highly dynamic in nature, and are impressed by their ingeniously organized functionality in hostile host environments.

To characterize viruses as unique genetic entities and pathogenic agents, individual viral components and host factors involved in the virus replication cycle must be thoroughly investigated. Many viral and cellular factors essential for viral replication and pathogenicity have been recently revealed through the efforts of gifted and diligent virologists, and understanding the functional interactions of these viral and host molecules will require an increased use of structural biology and the generation of high-resolution three-dimensional structures. Of note, a number of anti-viral drugs have been generated based on such structural information, and structural characterization of interacting interfaces between virus and host components should reveal potent targets for the design of future specific anti-viral drugs and/or vaccines.

In this Research Topic, a number of structural and molecular biological studies on various viruses by influential researchers have been published as either original research articles, reviews, mini-reviews, or commentary articles. The viruses covered are measles virus (MV), influenza virus, hepatitis C virus (HCV), hantavirus, murine leukemia virus (MuLV), and human/simian immunodeficiency viruses (HIV/SIVs). General remarks applicable to a wide range of viruses are also included. Consequently, papers comprising this Research Topic on diverse aspects of viral replication will be relevant to many different viruses. Hashiguchi et al. (2011) review the molecular basis for the interaction of MV hemagglutinin and cellular receptors. Inoue et al. (2011) present a study on the translation of MV nucleocapsid mRNA. Noda (2012) describes a model of native influenza virion morphology. Molecular mechanisms underlying the genesis of infectious HCV have been summarized by Suzuki (2012). Estrada et al. (2011) report the structural analysis of viral membrane glycoprotein Gn from pathogenic and non-pathogenic hantaviruses. Many articles focusing on retroviruses are also presented. Ghanam et al. (2012) review the structural and functional role of the HIV-1 matrix protein for virus assembly. Masuda (2011) focuses on the non-enzymatic functions of HIV-1 integrase and discusses future targeted drug development. Sakuragi (2011) has clarified the morphogenesis of infectious HIV-1 virions and discussed the importance of such research for anti-viral therapy. Comprehensive, informative reviews on cellular anti-viral factors, i.e., APOBEC3 family (against HIV-1) and BST-2/tetherin (against HIV-2, SIV, Ebola virus, and Kaposi's sarcoma-associated herpesvirus), are provided by Kitamura et al. (2011) and Arias et al. (2011) respectively. Seki and Matano (2012) describe viral structure/function (HIV/SIV) and host cytotoxic T lymphocyte responses, while Miyazaki et al. (2011) focus on the structural dynamics of retroviral genome packaging (MuLV, HIV-1, and HIV-2). In a review article, Binning et al. (2012) discuss the potential roles of aptamers in structural virology and in clinical virology, with a commentary by Miyazaki and Fujita (2012). Finally, another commentary on the article dealing with the human/virus protein interaction network is offered by Adachi et al. (2011).

We are proud to present "Structural biology for virus research" as one of the Research Topic in Frontiers in Virology. We believe that all readers should taste the essence and possibility of structural virology in a broad sense. We are optimistic that this Research Topic will provide or re-generate/re-organize strategic insights into the important issues of today's virology.

REFERENCES

Adachi, S., Adachi, A., and Nomaguchi, M. (2011). Commentary on a new era of investigating 3D structure-based human-virus protein network dynamics. *Front. Microbiol.* 2:186. doi: 10.3389/fmicb.2011.00186

Arias, J. F., Iwabu, Y., and Tokunaga, K. (2011). Structural basis for antiviral activity of BST-2/tetherin and its viral antagonism. *Front. Microbiol.* 2:250. doi: 10.3389/fmicb.2011.00250

Binning, J. M., Leung, D. W., and Amarasinghe, G. K. (2012). Aptamers in virology: recent advances and challenges. *Front. Microbiol.* 3:29. doi: 10.3389/fmicb.2012.00029

Estrada, D. F., Conner, M., Jeor, S. C., and De Guzman, R. N. (2011). The structure of the hantavirus zinc finger domain is conserved and represents the only natively folded region of the Gn cytoplasmic tail. *Front. Microbiol.* 2:251. doi: 10.3389/fmicb.2011.00251

Ghanam, R. H., Samal, A. B., Fernandez, T. F., and Saad, J. S. (2012). Role of the HIV-1 matrix protein in Gag intracellular trafficking and targeting to the plasma membrane for virus assembly. *Front. Microbiol.* 3:55. doi: 10.3389/fmicb.2012.00055

Hashiguchi, T., Maenaka, K., and Yanagi, Y. (2011). Measles virus hemagglutinin: structural insights into cell entry and measles vaccine. *Front. Microbiol.* 2:247. doi: 10.3389/fmicb.2011.00247

Inoue, Y., Sato, H., Fujita, K., Tsukiyama-Kohara, K., Yoneda, M., and Kai, C. (2011). Selective translation of the measles virus nucleocapsid mRNA by La protein. *Front. Microbiol.* 2:173. doi: 10.3389/fmicb.2011.00173

Kitamura, S., Ode, H., and Iwatani, Y. (2011). Structural features of antiviral APOBEC3 proteins are linked to their functional activities. *Front. Microbiol.* 2:258. doi: 10.3389/fmicb.2011.00258

Masuda, T. (2011). Non-enzymatic functions of retroviral integrase: the next target for novel anti-HIV drug development. *Front. Microbiol.* 2:210. doi: 10.3389/fmicb.2011.00210

Miyazaki, Y., and Fujita, M. (2012). Commentary on aptamers for virus

research. *Front. Microbiol.* 3:52. doi: 10.3389/fmicb.2012.00052
Miyazaki, Y., Miyake, A., Nomaguchi, M., and Adachi, A. (2011). Structural dynamics of retroviral genome and the packaging. *Front. Microbiol.* 2:264. doi: 10.3389/fmicb.2011.00264
Noda, T. (2012). Native morphology of influenza virions. *Front. Microbiol.* 2:269. doi: 10.3389/fmicb.2011.00269
Sakuragi, J. (2011). Morphogenesis of the infectious HIV-1 virion. *Front. Microbiol.* 2:267. doi: 10.3389/fmicb.2011.00267
Seki, S., and Matano, T. (2012). CTL escape and viral fitness in HIV/SIV infection. *Front. Microbiol.* 2:247. doi: 10.3389/fmicb.2011.00247
Suzuki, T. (2012). Morphogenesis of infectious hepatitis C virus particles. *Front. Microbiol.* 3:38. doi: 10.3389/fmicb.2012.00038

Received: 12 February 2012; accepted: 23 February 2012; published online: 13 March 2012.
Citation: Miyazaki Y, Fujita M, Nomaguchi M and Adachi A (2012) Structural biology for virus research. Front. Microbio. ***3****:91. doi: 10.3389/fmicb.2012.00091*
This article was submitted to Frontiers in Virology, a specialty of Frontiers in Microbiology.

frontiers in
MICROBIOLOGY

REVIEW ARTICLE
published: 16 December 2011
doi: 10.3389/fmicb.2011.00247

Measles virus hemagglutinin: structural insights into cell entry and measles vaccine

Takao Hashiguchi [1,2] ****, Katsumi Maenaka*** [3,4] ***and Yusuke Yanagi*** [1]

[1] *Department of Virology, Faculty of Medicine, Kyushu University, Fukuoka, Japan*
[2] *Department of Immunology and Microbial Science, The Scripps Research Institute, La Jolla, CA, USA*
[3] *Laboratory of Biomolecular Science, Hokkaido University, Sapporo, Japan*
[4] *Core Research for Evolutional Science and Technology, Japan Science and Technology Agency, Saitama, Japan*

Edited by:
Akio Adachi, The University of Tokushima, Japan

Reviewed by:
Kaoru Takeuchi, University of Tsukuba, Japan
Hak Hotta, Kobe University, Japan

****Correspondence:***
Takao Hashiguchi, Department of Virology, Kyushu University, Fukuoka 812-8582, Japan; Department of Immunology, The Scripps Research Institute, 10550 North Torrey Pines Road, La Jolla, CA 92037, USA.
e-mail: takaoh@scripps.edu

Measles is one of the most contagious viral diseases, and remains a major cause of childhood morbidity and mortality worldwide. The measles virus (MV), a member of the family *Paramyxoviridae*, enters cells through a cellular receptor, the signaling lymphocyte activation molecule (SLAM), CD46 or nectin-4. Entry is mediated by two MV envelope glycoproteins, the hemagglutinin (H) and the fusion (F) protein. The H protein mediates receptor attachment, while the F protein causes membrane fusion. The interaction between the H and F proteins is essential to initiate the cell entry process. Recently determined crystal structures of the MV-H protein unbound and bound to SLAM or CD46 have provided insights into paramyxovirus entry and the effectiveness of measles vaccine.

Keywords: measles virus, hemagglutinin, structure, fusion, entry, measles vaccine, glycoprotein, receptor

INTRODUCTION

Measles virus (MV), the agent that causes measles, is an enveloped, non-segmented, negative-strand RNA virus, a member of the genus *Morbillivirus*, the family *Paramyxoviridae* (Griffin, 2007). Paramyxoviruses also include, among others, mumps virus, Newcastle disease virus (NDV), human parainfluenza viruses (hPIV), and emerging Hendra virus (HeV) and Nipah virus (NiV), members of the genus *Henipavirus* (Lamb and Parks, 2007). MV enters cells through membrane fusion in a pH-independent manner, like other paramyxoviruses. MV possesses two glycoproteins on its envelope, an attachment protein hemagglutinin (H) (MV-H) and a fusion (F) protein (MV-F) (Griffin, 2007). MV-H and MV-F form hetero-oligomer, which is required to induce membrane fusion. Upon receptor binding, MV-H is thought to undergo a conformational change, which in turn would trigger a structural rearrangement of MV-F from the metastable pre-fusion form to the intermediate and post-fusion forms (Plemper et al., 2011). This conformational change of MV-F would drive the fusion between the viral envelope and the host cell membrane. Currently, the detailed structural organization of MV-H and MV-F remains elusive.

The paramyxovirus attachment proteins are classified into three groups based on their functions, the hemagglutinin–neuraminidase (HN) protein, the H protein, and the G protein. Although these attachment proteins may have a common assembly process, their interaction with the F protein may be viral species-dependent, and different paramyxoviruses may use different strategies for fusion activation (Lamb and Parks, 2007; Iorio and Mahon, 2008; Connolly et al., 2009; Smith et al., 2009; Plemper et al., 2011). Among paramyxoviruses, only those belonging to the genera *Morbillivirus* and *Henipavirus* recognize protein receptors expressed on the target cell surface. This is in marked contrast to most other members of the family *Paramyxoviridae*, which contain the neuraminidase domain in their HN proteins and recognize sialic acid-containing receptors.

Three protein molecules have been identified as MV receptors, the signaling lymphocyte activation molecule (SLAM), CD46, and nectin-4. On the other hand, NiV and HeV utilize as receptors ephrin (Eph) B2 and EphB3, which belong to the highly conserved Eph family of tyrosine kinase receptors (Bonaparte et al., 2005; Negrete et al., 2005, 2006). Although both MV and henipaviruses recognize protein receptors, there is a large structural difference between MV-H and henipavirus G proteins (Bowden et al., 2010). The G proteins exhibit a structural-fold property closer to that of HN proteins. This suggests that MV-H and henipavirus G proteins have independently evolved the ability to recognize protein receptors.

One clinical isolate obtained from a child in 1954 known as the Edmonston strain gave rise to the majority of current MV vaccine strains (Katz, 2009). After 50 years, its progeny (Edmonston lineage) are still effective as live attenuated vaccines. It is estimated that more than 4.5 million measles deaths have been prevented annually through implementation of the vaccination strategies developed by WHO and UNISEF (Bellini and Rota, 2011).

Here, we review recent advances in our understanding of MV entry, based on crystal structures of MV-H–receptor complexes as well as functional studies. We compare the attachment protein-receptor complex of MV with those of other paramyxoviruses, and provide a general principle of paramyxovirus entry. We also discuss why MV has only one major serotype and why our current

MV vaccine prepared more than five decades ago from a single strain is still effective.

MV RECEPTORS

CD46

Currently, three receptors are identified, which facilitate MV entry. CD46 (also called membrane cofactor protein) is the first MV receptor discovered by two groups independently in 1993 (Dorig et al., 1993; Naniche et al., 1993). CD46 is a type I membrane protein that belongs to the regulators of complement activation (RCA) family. CD46 comprises an N-terminal signal sequence, four short consensus repeats (SCR1–SCR4), a transmembrane region, and a C-terminal cytoplasmic tail. Each SCR module contains ∼60 amino acids that fold into a compact β-barrel structure (Persson et al., 2010). N-terminal domains SCR1 and SCR2 participate in the interaction with MV-H (Santiago et al., 2010).

CD46 is expressed on all nucleated human cells, and acts as a cofactor in the proteolytic inactivation of C3b and C4b by factor I. Monkey, but not human, erythrocytes express CD46, allowing hemagglutination by MV (Cole et al., 1985; Kemper and Atkinson, 2009). Interestingly, only vaccine and laboratory-adapted strains of MV can utilize CD46 as a receptor, while clinically isolated MV strains employ different receptors for entry.

SIGNALING LYMPHOCYTE ACTIVATION MOLECULE

Measles viruses were found to be efficiently isolated from clinical specimens by using the marmoset B cell line B95a or other human B cell lines (Kobune et al., 1990; Schneider-Schaulies et al., 1995). Further, MVs obtained using these cell lines were unable to downregulate CD46 or induce cell-to-cell fusion in CD46-positive cell lines (Lecouturier et al., 1996; Bartz et al., 1998; Tanaka et al., 1998). These observations suggested the presence of MV receptor(s) other than CD46. In 2000, SLAM (also known as CD150) was identified as a principal cellular receptor for all MV strains (Tatsuo et al., 2000).

Signaling lymphocyte activation molecule, a member of the immunoglobulin (Ig) superfamily, is a type I membrane protein that possesses an N-terminal signal sequence, two Ig-like domains (V-set and C2-set), a transmembrane region, and a cytoplasmic tail (Cocks et al., 1995). Each Ig-like domain has ∼110 amino acid residues. Only the membrane-distal V-set domain is necessary and sufficient for MV-H binding. The V domain is comprised of the BED and AGFCC′C″ β-sheet, which utilize a Cys32–Cys132 disulfide bond to stabilize the A–G interstrand interaction (Hashiguchi et al., 2011).

In humans, SLAM is expressed on thymocytes, activated lymphocyte, mature dendritic cells, macrophages, and platelets. However, it is absent from monocytes, natural killer cells, and granulocytes (Schwartzberg et al., 2009). The distribution of SLAM nicely explains the tropism and immunosuppressive nature of MV (Yanagi et al., 2009).

NECTIN-4

Although epithelial cells do not express SLAM, MV antigens, and syncytia have been observed in the epithelia of various organs from measles patients and experimentally infected monkeys. It was found that a human lung adenocarcinoma cell line NCI-H358 supports SLAM- and CD46-independent MV infection (Takeda et al., 2007). Furthermore, several polarized epithelial cell lines have been reported to be susceptible to MV (Takeda et al., 2007; Leonard et al., 2008; Tahara et al., 2008). Together, these data hinted at the presence of a third MV receptor.

Recent studies have identified nectin-4 as an epithelial cell receptor (Muhlebach et al., 2011; Noyce et al., 2011). Human nectin-4 is expressed mainly in placenta cells, and to a lesser degree in trachea cells (Reymond et al., 2001). Nectin-4 is a member of the poliovirus receptor-like proteins (PVRLs), which are adhesion receptors of the Ig superfamily. Similar to SLAM, this type I membrane protein contains an N-terminal signal sequence, three Ig-like domains (V-set and two C2-set), a transmembrane region, and a cytoplasmic tail. Each Ig-like domain is predicted to be ∼105 amino acid residues. Both wild type and the Edmonston lineage MV strains can use nectin-4 as a receptor.

MV-H PROTEIN

The MV-H is a type II membrane glycoprotein comprised of an N-terminal cytoplasmic tail, a transmembrane region, a stalk, and a C-terminal receptor-binding head domain. The head domain of MV-H exhibits a six-bladed β-propeller fold, a feature conserved among all head domains of paramyxovirus attachment proteins thus far crystallized (Colf et al., 2007; Hashiguchi et al., 2007). Without a neuraminidase domain, MV-H targets protein receptors, SLAM, CD46, and nectin-4. The difference in receptor preference between H and HN proteins reflects the difference in their head domain structures (see below).

Crystal structure of the MV-H head domain reveals a top pocket reminiscent of the sialic acid binding cavity found in both HN proteins and the neuraminidase (NA) of influenza virus (Flu). However, the pocket in MV-H is enlarged and lacks several key residues that contribute to sialic acid binding. In addition, the N-linked sugar at position 215 of MV-H (located at the rim of the pocket) renders the top pocket inaccessible to sialic acid, antibodies or other molecules. The MV-H head domain exhibits a cubic shape, and forms a homodimer (Hashiguchi et al., 2007). Two neighboring N-linked sugars at position 200 (one each from both monomers), located at the homodimer interface, likely block access to the region, which in HN of NDV, has been proposed to contain a second sialic acid binding site. Similarly, HNs of hPIV3 and PIV5 do not contain a second sialic acid binding site due to N-linked sugar at Asn523 and Asn497, respectively.

INTERACTION BETWEEN MV-H AND RECEPTORS

Mutagenesis studies have suggested that receptor-binding sites on MV-H are located on the side of the β-propeller, which was subsequently confirmed by the crystal structures of MV-H complexed with SCR1 and SCR2 of CD46 or with the V domain of SLAM (**Figure 1A**; Santiago et al., 2010; Hashiguchi et al., 2011). By contrast, attachment proteins of NDV, hPIV3, and PIV5, NA of Flu and G proteins of NiV and HeV utilize the top pocket of the β-propeller structure for binding to their corresponding receptors or ligand (**Figure 1B**; Burmeister et al., 1992; Crennell et al., 2000; Lawrence et al., 2004; Yuan et al., 2005; Bowden et al., 2008; Xu et al., 2008).

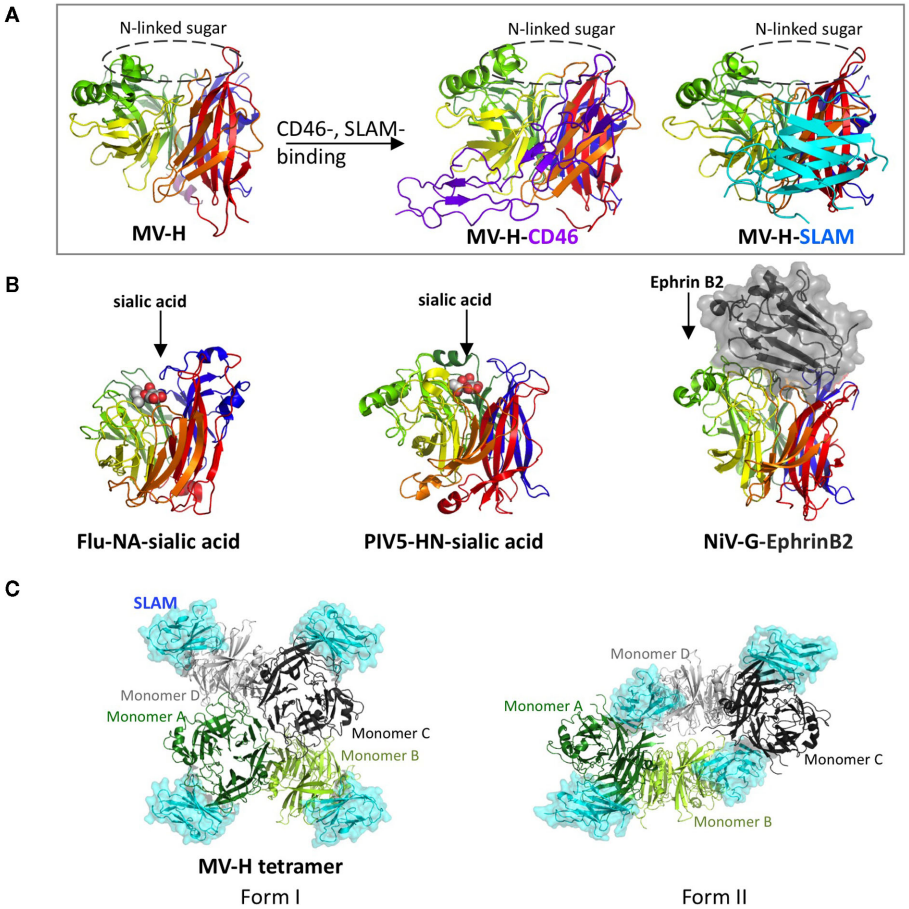

FIGURE 1 | Structures of viral glycoproteins exhibiting the β-propeller fold unbound or bound to their receptors or ligand. (A) Side view of the MV-H monomer (rainbow colors) unbound (left) or bound to CD46 (middle) or SLAM (right). CD46 (purple) and SLAM (cyan) are indicated in a ribbon diagram. The top pocket of the MV-H monomer is masked by N-linked sugar. **(B)** Side views of Flu-NA bound to sialic acid (left), PIV5-HN bound to sialic acid (middle), and NiV-G bound to ephrin B2 (right). Sialic acid (white and red) is indicated as sphere models, whereas ephrin B2 (black) is shown in surface presentation. **(C)** Top views of two forms of MV-H tetramer with each monomer bound to SLAM (cyan). MV-H monomers A (green) and B (light green) form one dimer, whereas monomers C (black) and D (gray) form another.

Crystal structure of MV-H bound to CD46 reveals that β-sheet 4 (β4) and β5 of the β-propeller structure interact with SCR1 and SCR2 of CD46 (**Figure 1A**; Santiago et al., 2010). Key residues Tyr481 and Gly546 on MV-H make hydrogen bonds with the main chain oxygen group of Cys65 and the main chain amino group of Glu63 on CD46, respectively. Furthermore, a serine-to-glycine mutation at position 546 on MV-H (found in some CD46-using MV strains) likely increases flexibility of the β5s3–β5s4 region, which is favorable for CD46 binding. Pro38 and Pro39 on CD46 are sandwiched between β4 residues Leu464 and Leu500 and β5 residues Tyr541 and Tyr543 on MV-H, while Tyr67 on CD46 makes a hydrophobic interaction with Val451 on MV-H. The interaction between MV-H and CD46 is relatively week (K_d, 2.2 μM; Hashiguchi et al., 2007).

Crystal structure of MV-H in complex with SLAM shows that β4–6 and loop regions on the lateral surface of the MV-H β-propeller structure interact with GFCC′C″ region of the SLAM-V domain (**Figure 1A**; Hashiguchi et al., 2011). This interaction is also confirmed by functional assays, surface plasmon resonance and infectious assay *in vitro*. Salt bridges formed by residues Asp530 and Arg533 on MV-H and Glu123 on SLAM play a key role in stabilizing the MV-H–SLAM complex. An intermolecular β-sheet, comprised of residues Pro191-Arg195 (β6) of MV-H and residues Ser127-Phe131 (G sheet) of SLAM-V, further stabilizes the MV-H–SLAM complex. Mouse SLAM does not contain the MV-H-interacting key residues, including His61 and Arg130, and therefore does not act as a MV receptor (Ono et al., 2001). Although SLAM interacts with another SLAM through its V domain, the affinity of SLAM–SLAM interaction (K_d of ∼200 μM) is over 400-fold lower than that of the MV-H–SLAM interaction (K_d of 0.29 ∼ 0.43 μM; Hashiguchi et al., 2007). Therefore, upon MV infection, SLAM preferentially interacts with MV-H rather than adjacent SLAM.

Mutagenesis studies have mapped nectin-4 binding sites in a region partly shared by SLAM-binding sites (Leonard et al., 2008; Tahara et al., 2008). Amino acids in this region are highly conserved

among morbilliviruses, whereas CD46 binding sites are not. Thus, it is likely that many morbilliviruses utilize this region of the H protein to infect immune and epithelial cells.

Like other paramyxovirus attachment proteins, MV-H forms a homodimer (or tetramer, see below). Interestingly, two monomers forming the MV-H dimer are highly tilted from each other, in contrast to other paramyxovirus attachment proteins (Hashiguchi et al., 2007). As a result, the receptor-binding sites on MV-H (located at the side of the β-propeller) are oriented upward in such a way that they are readily accessible to cellular receptors. This structural property and the inaccessibility of the top pocket due to N-linked sugar at position 215 account for the difference in receptor-binding sites between MV-H and other paramyxovirus attachment proteins.

MV-H TETRAMER AND MEMBRANE FUSION TRIGGERING

The mechanism by which receptor-binding leads to F protein-mediated membrane fusion is not well understood. However, crystal structures of MV-H–CD46 and MV-H–SLAM have also provided clues for this intriguing process (Santiago et al., 2010; Hashiguchi et al., 2011). No large structural change is observed in the MV-H monomer between receptor-free and receptor-bound forms. Furthermore, the relative orientation of two monomers in the MV-H dimer also remains essentially identical before and after receptor binding (r.m.s. deviation of 1.95 Å for 751 Ca atoms in MV-H–SLAM; r.m.s. deviation of 1.33 Å for 791 Ca atoms in MV-H–CD46).

Interestingly, crystal structures of the MV-H–SLAM complex reveal two different tetrameric configurations (dimer of dimers), form I and form II (**Figure 1C**; Hashiguchi et al., 2011). The tetrameric formation of MV-H is also detected by native PAGE and immunoblotting when the full-length MV-H is transiently expressed in cells. Recently reported crystal structures of NDV and PIV5 also reveal a four-helix bundle stalk (Bose et al., 2011; Yuan et al., 2011). MV-H monomers A and B form one dimer, while monomers C and D form another, and SLAM is bound to each MV-H monomer. Form I exhibits a conformation similar to previously reported head domains of NDV-HN, hPIV3-HN, PIV5-HN, and Flu-NA, although the relative position of monomers in the dimer units varies depending on the viral protein. In form II, a shift in the dimer of dimers occurs, enabling SLAM to bridge two neighboring monomers. Monomers A and C form the dimer–dimer interface in form I (contact area of 1.312 Å), whereas monomers B and D mainly form the dimer–dimer interface in form II (contact area of 2.099 Å). Based on these structural features, we propose the following fusion triggering mechanism. Upon the virus–cell interaction, the MV-H–SLAM complex in form I is formed. This structure renders the orientation of SLAM parallel rather than perpendicular in relation to the host membrane, and substantially reduces the distance between viral envelope and host membrane. This may prepare the environment suitable for subsequent conformational changes of MV-H and MV-F. The ensuing conformational shift of MV-H from form I to form II reorganizes the stalk region, allowing MV-F to refold and interact with the target cell membrane (Hashiguchi et al., 2011).

In a recent study, disulfide bonds were introduced at the protein interface to covalently anchor the two head domains in the MV-H dimer, leading to the block of its fusion-support activity (Navaratnarajah et al., 2011). The authors proposed that the two head domains in an MV-H dimer twist relative to each other upon receptor binding, which triggers membrane fusion. However, twisting of the head domains is not consistent with crystal structures of MV-H bound and unbound to receptors (Hashiguchi et al., 2007, 2011; Santiago et al., 2010). These introduced disulfide bonds might somehow prevent the proper formation of MV-H tetramer or its conformational shift upon receptor binding (Saphire and Oldstone, 2011). The similar experiment with the NDV-HN protein did not affect its fusion-support activity (Mahon et al., 2008).

Two models have been proposed for fusion triggering in paramyxoviruses. In one model, the attachment protein undergoes a conformational change upon receptor binding. This conformational change directly affects the F protein, causing its refolding which in turn drives membrane fusion. This model is consistent with the data for viruses using sialic acid as a receptor. In cells infected with hPIV3 and PIV5, the HN protein is associated with the F protein on the cell surface, but not in the endoplasmic reticulum (ER) (Paterson et al., 1997). Furthermore, the increased strength of the HN-F interaction enhances fusion activity. These results suggest that upon receptor binding, HN actively acts on the F protein and facilitates its refolding (Connolly et al., 2009). In the second model, the attachment protein serves as a clamp that stabilizes the F protein in its pre-fusion state. Receptor binding of the attachment protein releases the F protein from the clamp to facilitate its spontaneous conformational change. MV entry is consistent with this model. MV-H is already associated with MV-F within the ER (Plemper et al., 2001), and the conformational shift of the tetramer is likely to facilitate the release of MV-F from the heteromeric H–F oligomers. This release model is also supported by the data that a weaker interaction between MV-H and MV-F results in increased fusogenicity (Plemper et al., 2002; Corey and Iorio, 2009). A similar release model has also been proposed for NiV and HeV (Aguilar et al., 2006, 2007; Bishop et al., 2007). Thus, different paramyxoviruses may use different mechanisms of fusion triggering, although the overall cell entry mechanism may be similar among them.

STRUCTURAL INSIGHT INTO MV SEROTYPE AND VACCINE

Crystal structure of MV-H sheds light on why measles vaccine has been successful for a long time (Hashiguchi et al., 2007, 2011; Ruigrok and Gerlier, 2007). The structure suggests that N-linked sugars (at positions 168, 187, 200, and 215) on MV-H cover a considerable portion of its surface, only exposing a small area for receptor and antibody bindings (**Figures 2A,B**). Indeed, crystal structures of MV-H–SLAM and MV-H–CD46 complexes indicate that both receptors target this exposed area. Mutagenesis studies have also revealed that nectin-4 binds to this region as well. Furthermore, a majority of MV-H monoclonal antibodies are mapped onto this exposed receptor-binding area, indicating that this area acts as the epitope "hot spot." This overlap of binding sites for receptors and neutralizing antibodies explains why measles vaccine, derived from a single strain, remains effective against all 23 distinct MV genotypes. A functional importance (receptor binding) likely exerts a restrain that renders this region highly unfavorable to mutation. As a result, MV still occurs in

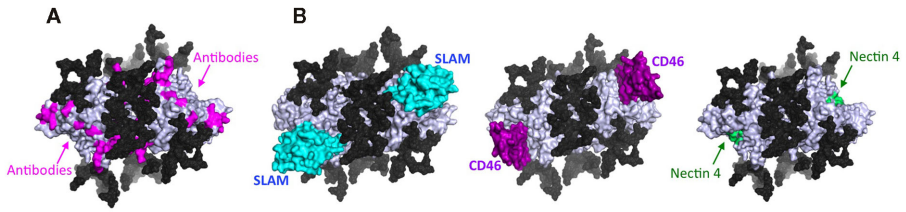

FIGURE 2 | Structural basis of the effectiveness of measles vaccine. **(A)** Epitopes of anti-MV-H monoclonal antibodies (red) on the MV-H homodimer (blue white) with potential N-linked sugars (mesh, black) as viewed downwards from the top. **(B)** Receptor-binding sites on MV-H. Left, crystal structure of MV-H–SLAM (SLAM shown in cyan). Middle, crystal structure of MV-H–CD46 (CD46 in purple). Right, putative nectin-4 binding sites (green), based on site-directed mutagenesis of MV-H.

only a single serotype (Hashiguchi et al., 2011). Interestingly, this receptor-binding area is highly conserved not only among MV strains but also among morbilliviruses, suggesting that this region could serve as a template for a universal vaccine targeting all morbilliviruses (Hashiguchi et al., 2007). The human immunodeficiency virus glycoprotein lacks the similarly conserved region to be targeted by antibodies, which has hampered the vaccine development.

PERSPECTIVE

Recent advances in our understanding of MV-H structures, combined with functional studies, have provided new insights into the mechanism of MV entry. Although the receptor-binding mode of MV-H is different from that of other paramyxovirus HN and G proteins, the overall entry process may be common among paramyxoviruses. MV-H forms tetramer (dimer of dimers), like other HN and G proteins, and we propose a model for fusion triggering, based on the presence of two forms of MV-H tetramer. However, further structural studies of MV-H and MV-F are required to completely understand the whole process of MV entry.

Crystal structures have also illuminated how a sugar-uncovered, exposed area of MV-H is targeted by receptors as well as by neutralizing antibodies. This nicely explains why only a single serotype occurs for MV and why measles vaccine, derived from one strain, has been effective for a long time. It is hoped that better understanding of the MV entry process will not only contribute to our measles eradication effort worldwide, but also allow us to develop effective vaccines for other challenging pathogens.

ACKNOWLEDGMENTS

We thank A. P. P. Zhang for discussion and reviewing the manuscript. Our work was supported by grants from the Ministry of Education, Culture, Sports, Science and Technology and the Ministry of Health, Labor and Welfare of Japan. Takao Hashiguchi is supported by the Japan Society for the Promotion of Science Research Fellowship for Young Scientists.

REFERENCES

Aguilar, H. C., Matreyek, K. A., Choi, D. Y., Filone, C. M., Young, S., and Lee, B. (2007). Polybasic KKR motif in the cytoplasmic tail of Nipah virus fusion protein modulates membrane fusion by inside-out signaling. *J. Virol.* 81, 4520–4532.

Aguilar, H. C., Matreyek, K. A., Filone, C. M., Hashimi, S. T., Levroney, E. L., Negrete, O. A., Bertolotti-Ciarlet, A., Choi, D. Y., Mchardy, I., Fulcher, J. A., Su, S. V., Wolf, M. C., Kohatsu, L., Baum, L. G., and Lee, B. (2006). N-glycans on Nipah virus fusion protein protect against neutralization but reduce membrane fusion and viral entry. *J. Virol.* 80, 4878–4889.

Bartz, R., Firsching, R., Rima, B., Ter Meulen, V., and Schneider-Schaulies, J. (1998). Differential receptor usage by measles virus strains. *J. Gen. Virol.* 79(Pt 5), 1015–1025.

Bellini, W. J., and Rota, P. A. (2011). Biological feasibility of measles eradication. *Virus Res.* 162, 72–79.

Bishop, K. A., Stantchev, T. S., Hickey, A. C., Khetawat, D., Bossart, K. N., Krasnoperov, V., Gill, P., Feng, Y. R., Wang, L., Eaton, B. T., Wang, L. F., and Broder, C. C. (2007). Identification of Hendra virus G glycoprotein residues that are critical for receptor binding. *J. Virol.* 81, 5893–5901.

Bonaparte, M. I., Dimitrov, A. S., Bossart, K. N., Crameri, G., Mungall, B. A., Bishop, K. A., Choudhry, V., Dimitrov, D. S., Wang, L. F., Eaton, B. T., and Broder, C. C. (2005). Ephrin-B2 ligand is a functional receptor for Hendra virus and Nipah virus. *Proc. Natl. Acad. Sci. U.S.A.* 102, 10652–10657.

Bose, S., Welch, B. D., Kors, C. A., Yuan, P., Jardetzky, T. S., and Lamb, R. A. (2011). Structure and mutagenesis of the parainfluenza virus 5 hemagglutinin-neuraminidase stalk domain reveals a four-helix bundle and the role of the stalk in fusion promotion. *J. Virol.* 85, 12855–12866.

Bowden, T. A., Aricescu, A. R., Gilbert, R. J., Grimes, J. M., Jones, E. Y., and Stuart, D. I. (2008). Structural basis of Nipah and Hendra virus attachment to their cell-surface receptor ephrin-B2. *Nat. Struct. Mol. Biol.* 15, 567–572.

Bowden, T. A., Crispin, M., Jones, E. Y., and Stuart, D. I. (2010). Shared paramyxoviral glycoprotein architecture is adapted for diverse attachment strategies. *Biochem. Soc. Trans.* 38, 1349–1355.

Burmeister, W. P., Ruigrok, R. W., and Cusack, S. (1992). The 2.2 A resolution crystal structure of influenza B neuraminidase and its complex with sialic acid. *EMBO J.* 11, 49–56.

Cocks, B. G., Chang, C.-C. J., Carballido, J. M., Yssel, H., De Vries, J. E., and Aversa, G. (1995). A novel receptor involved in T-cell activation. *Nature* 376, 260–263.

Cole, J. L., Housley, G. A. Jr., Dykman, T. R., Macdermott, R. P., and Atkinson, J. P. (1985). Identification of an additional class of C3-binding membrane proteins of human peripheral blood leukocytes and cell lines. *Proc. Natl. Acad. Sci. U.S.A.* 82, 859–863.

Colf, L. A., Juo, Z. S., and Garcia, K. C. (2007). Structure of the measles virus hemagglutinin. *Nat. Struct. Mol. Biol.* 14, 1227–1228.

Connolly, S. A., Leser, G. P., Jardetzky, T. S., and Lamb, R. A. (2009). Bimolecular complementation of paramyxovirus fusion and hemagglutinin-neuraminidase proteins enhances fusion: implications for the mechanism of fusion triggering. *J. Virol.* 83, 10857–10868.

Corey, E. A., and Iorio, R. M. (2009). Measles virus attachment proteins with impaired ability to bind CD46 interact more efficiently with the homologous fusion protein. *Virology* 383, 1–5.

Crennell, S., Takimoto, T., Portner, A., and Taylor, G. (2000). Crystal structure of the multifunctional paramyxovirus hemagglutinin-neuraminidase. *Nat. Struct. Biol.* 7, 1068–1074.

Dorig, R. E., Marcil, A., Chopra, A., and Richardson, C. D. (1993). The human CD46 molecule is a receptor for measles virus (Edmonston strain). *Cell* 75, 295–305.

Griffin, D. E. (2007). "Measles virus," in *Fields Virology*, 5th Edn, eds D. M. Knipe, P. M. Howley, D. E. Griffin, R. A. Lamb, M. A. Martin, B. Roizman, and S. E. Straus (Philadelphia: Lippincott Williams & Wilkins), 1551–1585.

Hashiguchi, T., Kajikawa, M., Maita, N., Takeda, M., Kuroki, K., Sasaki, K., Kohda, D., Yanagi, Y., and Maenaka, K. (2007). Crystal structure of measles virus hemagglutinin provides insight into effective vaccines. *Proc. Natl. Acad. Sci. U.S.A.* 104, 19535–19540.

Hashiguchi, T., Ose, T., Kubota, M., Maita, N., Kamishikiryo, J., Maenaka, K., and Yanagi, Y. (2011). Structure of the measles virus hemagglutinin bound to its cellular receptor SLAM. *Nat. Struct. Mol. Biol.* 18, 135–141.

Iorio, R. M., and Mahon, P. J. (2008). Paramyxoviruses: different receptors – different mechanisms of fusion. *Trends Microbiol.* 16, 135–137.

Katz, S. L. (2009). John F. Enders and measles virus vaccine – a reminiscence. *Curr. Top. Microbiol. Immunol.* 329, 3–11.

Kemper, C., and Atkinson, J. P. (2009). Measles virus and CD46. *Curr. Top. Microbiol. Immunol.* 329, 31–57.

Kobune, F., Sakata, H., and Sugiura, A. (1990). Marmoset lymphoblastoid cells as a sensitive host for isolation of measles virus. *J. Virol.* 64, 700–705.

Lamb, R. A., and Parks, G. D. (2007). "Paramyxoviridae: the viruses and their replication," in *Fields Virology*, 5th Edn, eds D. M. Knipe, P. M. Howley, D. E. Griffin, R. A. Lamb, M. A. Martin, B. Roizman, and S. E. Straus (Philadelphia: Lippincott Williams & Wilkins), 1449–1496.

Lawrence, M. C., Borg, N. A., Streltsov, V. A., Pilling, P. A., Epa, V. C., Varghese, J. N., Mckimm-Breschkin, J. L., and Colman, P. M. (2004). Structure of the haemagglutinin-neuraminidase from human parainfluenza virus type III. *J. Mol. Biol.* 335, 1343–1357.

Lecouturier, V., Fayolle, J., Caballero, M., Carabana, J., Celma, M. L., Fernandez-Munoz, R., Wild, T. F., and Buckland, R. (1996). Identification of two amino acids in the hemagglutinin glycoprotein of measles virus (MV) that govern hemadsorption, HeLa cell fusion, and CD46 downregulation: phenotypic markers that differentiate vaccine and wild-type MV strains. *J. Virol.* 70, 4200–4204.

Leonard, V. H., Sinn, P. L., Hodge, G., Miest, T., Devaux, P., Oezguen, N., Braun, W., Mccray, P. B. Jr., Mcchesney, M. B., and Cattaneo, R. (2008). Measles virus blind to its epithelial cell receptor remains virulent in rhesus monkeys but cannot cross the airway epithelium and is not shed. *J. Clin. Invest.* 118, 2448–2458.

Mahon, P. J., Mirza, A. M., Musich, T. A., and Iorio, R. M. (2008). Engineered intermonomeric disulfide bonds in the globular domain of Newcastle disease virus hemagglutinin-neuraminidase protein: implications for the mechanism of fusion promotion. *J. Virol.* 82, 10386–10396.

Muhlebach, M. D., Mateo, M., Sinn, P. L., Prufer, S., Uhlig, K. M., Leonard, V. H., Navaratnarajah, C. K., Frenzke, M., Wong, X. X., Sawatsky, B., Ramachandran, S., Mccray, P. B., Cichutek, K., Von Messling, V., Lopez, M., and Cattaneo, R. (2011). Adherens junction protein nectin-4 is the epithelial receptor for measles virus. *Nature*. doi: 10.1038/nature10639

Naniche, D., Varior-Krishnan, G., Cervoni, F., Wild, T. F., Rossi, B., Rabourdin-Combe, C., and Gerlier, D. (1993). Human membrane cofactor protein (CD46) acts as a cellular receptor for measles virus. *J. Virol.* 67, 6025–6032.

Navaratnarajah, C. K., Oezguen, N., Rupp, L., Kay, L., Leonard, V. H., Braun, W., and Cattaneo, R. (2011). The heads of the measles virus attachment protein move to transmit the fusion-triggering signal. *Nat. Struct. Mol. Biol.* 18, 128–134.

Negrete, O. A., Levroney, E. L., Aguilar, H. C., Bertolotti-Ciarlet, A., Nazarian, R., Tajyar, S., and Lee, B. (2005). EphrinB2 is the entry receptor for Nipah virus, an emergent deadly paramyxovirus. *Nature* 436, 401–405.

Negrete, O. A., Wolf, M. C., Aguilar, H. C., Enterlein, S., Wang, W., Muhlberger, E., Su, S. V., Bertolotti-Ciarlet, A., Flick, R., and Lee, B. (2006). Two key residues in ephrinB3 are critical for its use as an alternative receptor for Nipah virus. *PLoS Pathog.* 2, e7. doi:10.1371/journal.ppat.0020007

Noyce, R. S., Bondre, D. G., Ha, M. N., Lin, L. T., Sisson, G., Tsao, M. S., and Richardson, C. D. (2011). Tumor cell marker PVRL4 (Nectin 4) is an epithelial cell receptor for measles virus. *PLoS Pathog.* 7, e1002240. doi:10.1371/journal.ppat.1002240

Ono, N., Tatsuo, H., Tanaka, K., Minagawa, H., and Yanagi, Y. (2001). V domain of human SLAM (CDw150) is essential for its function as a measles virus receptor. *J. Virol.* 75, 1594–1600.

Paterson, R. G., Johnson, M. L., and Lamb, R. A. (1997). Paramyxovirus fusion (F) protein and hemagglutinin-neuraminidase (HN) protein interactions: intracellular retention of F and HN does not affect transport of the homotypic HN or F protein. *Virology* 237, 1–9.

Persson, B. D., Schmitz, N. B., Santiago, C., Zocher, G., Larvie, M., Scheu, U., Casasnovas, J. M., and Stehle, T. (2010). Structure of the extracellular portion of CD46 provides insights into its interactions with complement proteins and pathogens. *PLoS Pathog.* 6, e1001122. doi:10.1371/journal.ppat.1001122

Plemper, R. K., Brindley, M. A., and Iorio, R. M. (2011). Structural and mechanistic studies of measles virus illuminate paramyxovirus entry. *PLoS Pathog.* 7, e1002058. doi:10.1371/journal.ppat.1002058

Plemper, R. K., Hammond, A. L., and Cattaneo, R. (2001). Measles virus envelope glycoproteins hetero-oligomerize in the endoplasmic reticulum. *J. Biol. Chem.* 276, 44239–44246.

Plemper, R. K., Hammond, A. L., Gerlier, D., Fielding, A. K., and Cattaneo, R. (2002). Strength of envelope protein interaction modulates cytopathicity of measles virus. *J. Virol.* 76, 5051–5061.

Reymond, N., Fabre, S., Lecocq, E., Adelaide, J., Dubreuil, P., and Lopez, M. (2001). Nectin4/PRR4, a new afadin-associated member of the nectin family that trans-interacts with nectin1/PRR1 through V domain interaction. *J. Biol. Chem.* 276, 43205–43215.

Ruigrok, R. W., and Gerlier, D. (2007). Structure of the measles virus H glycoprotein sheds light on an efficient vaccine. *Proc. Natl. Acad. Sci. U.S.A.* 104, 20639–20640.

Santiago, C., Celma, M. L., Stehle, T., and Casasnovas, J. M. (2010). Structure of the measles virus hemagglutinin bound to the CD46 receptor. *Nat. Struct. Mol. Biol.* 17, 124–129.

Saphire, E. O., and Oldstone, M. B. (2011). Measles virus fusion shifts into gear. *Nat. Struct. Mol. Biol.* 18, 115–116.

Schneider-Schaulies, J., Schnorr, J.-J., Brinckmann, U., Dunster, L. M., Baczko, K., Liebert, U. G., Schneider-Schaulies, S., and Ter Meulen, V. (1995). Receptor usage and differential downregulation of CD46 by measles virus wild-type and vaccine strains. *Proc. Natl. Acad. Sci. U.S.A.* 92, 3943–3947.

Schwartzberg, P. L., Mueller, K. L., Qi, H., and Cannons, J. L. (2009). SLAM receptors and SAP influence lymphocyte interactions, development and function. *Nat. Rev. Immunol.* 9, 39–46.

Smith, E. C., Popa, A., Chang, A., Masante, C., and Dutch, R. E. (2009). Viral entry mechanisms: the increasing diversity of paramyxovirus entry. *FEBS J.* 276, 7217–7227.

Tahara, M., Takeda, M., Shirogane, Y., Hashiguchi, T., Ohno, S., and Yanagi, Y. (2008). Measles virus infects both polarized epithelial and immune cells by using distinctive receptor-binding sites on its hemagglutinin. *J. Virol.* 82, 4630–4637.

Takeda, M., Tahara, M., Hashiguchi, T., Sato, T. A., Jinnouchi, F., Ueki, S., Ohno, S., and Yanagi, Y. (2007). A human lung carcinoma cell line supports efficient measles virus growth and syncytium formation via a SLAM- and CD46-independent mechanism. *J. Virol.* 81, 12091–12096.

Tanaka, K., Xie, M., and Yanagi, Y. (1998). The hemagglutinin of recent measles virus isolates induces cell fusion in a marmoset cell line, but not in other CD46-positive human and monkey cell lines, when expressed together with the F protein. *Arch. Virol.* 143, 213–225.

Tatsuo, H., Ono, N., Tanaka, K., and Yanagi, Y. (2000). SLAM (CDw150) is a cellular receptor for measles virus. *Nature* 406, 893–897.

Xu, K., Rajashankar, K. R., Chan, Y. P., Himanen, J. P., Broder, C. C., and Nikolov, D. B. (2008). Host cell recognition by the henipaviruses: crystal structures of the Nipah G attachment glycoprotein and its complex with ephrin-B3. *Proc. Natl. Acad. Sci. U.S.A.* 105, 9953–9958.

Yanagi, Y., Takeda, M., Ohno, S., and Hashiguchi, T. (2009). Measles virus receptors. *Curr. Top. Microbiol. Immunol.* 329, 13–30.

Yuan, P., Swanson, K. A., Leser, G. P., Paterson, R. G., Lamb, R. A., and Jardetzky, T. S. (2011). Structure of the Newcastle disease virus hemagglutinin-neuraminidase (HN) ectodomain reveals a four-helix bundle stalk. *Proc. Natl. Acad. Sci. U.S.A.* 108, 14920–14925.

Yuan, P., Thompson, T. B., Wurzburg, B. A., Paterson, R. G., Lamb, R. A., and Jardetzky, T. S. (2005). Structural studies of the parainfluenza virus 5

hemagglutinin-neuraminidase tetramer in complex with its receptor, sialyllactose. *Structure* 13, 803–815.

Conflict of Interest Statement: The authors declare that the research was conducted in the absence of any commercial or financial relationships that could be construed as a potential conflict of interest.

Received: 14 November 2011; paper pending published: 17 November 2011; accepted: 23 November 2011; published online: 16 December 2011.

Citation: Hashiguchi T, Maenaka K and Yanagi Y (2011) Measles virus hemagglutinin: structural insights into cell entry and measles vaccine. Front. Microbio. ***2****:247. doi: 10.3389/fmicb.2011.00247*
This article was submitted to Frontiers in Virology, a specialty of Frontiers in Microbiology.

frontiers in
MICROBIOLOGY

ORIGINAL RESEARCH ARTICLE
published: 23 August 2011
doi: 10.3389/fmicb.2011.00173

Selective translation of the measles virus nucleocapsid mRNA by La protein

Yoshihisa Inoue[1], Hiroki Sato[1], Kentaro Fujita[1], Kyoko Tsukiyama-Kohara[2], Misako Yoneda[1] and Chieko Kai[1]*

[1] Laboratory Animal Research Center, Institute of Medical Science, The University of Tokyo, Tokyo, Japan
[2] Department of Experimental Phylaxiology, Faculty of Medical and Pharmaceutical Sciences, Kumamoto University, Kumamoto, Japan

Edited by:
Akio Adachi, The University of Tokushima Graduate School, Japan

Reviewed by:
Kaoru Takeuchi, University of Tsukuba, Japan
Hak Hotta, Kobe University Graduate School of Medicine, Japan

***Correspondence:**
Chieko Kai, Laboratory Animal Research Center, Institute of Medical Science, The University of Tokyo, 4-6-1 Shirokanedai, Minato-ku, Tokyo 108-8639, Japan.
e-mail: ckai@ims.u-tokyo.ac.jp

Measles, caused by measles virus (MeV) infection, is the leading cause of death in children because of secondary infections attributable to MeV-induced immune suppression. Recently, we have shown that wild-type MeVs induce the suppression of protein synthesis in host cells (referred to as "shutoff") and that viral mRNAs are preferentially translated under shutoff conditions in infected cells. To determine the mechanism behind the preferential translation of viral mRNA, we focused on the 5′ untranslated region (UTR) of nucleocapsid (N) mRNA. The La/SSB autoantigen (La) was found to specifically bind to an N-5′UTR probe. Recombinant La enhanced the translation of luciferase mRNA containing the N-5′UTR (N-fLuc), and RNA interference of La suppressed N-fLuc translation. Furthermore, recombinant MeV lacking the La-binding motif in the N-5′UTR displayed delayed viral protein synthesis and growth kinetics at an early phase of infection. These results suggest that La induced predominant translation of N mRNA via binding to its 5′UTR under shutoff conditions. This is the first report on a cellular factor that specifically regulates paramyxovirus mRNA translation.

Keywords: measles virus, 5′ untranslated region, La

INTRODUCTION

Measles virus (MeV) infection causes a maculopapular rash, fever, cough, and coryza (Griffin, 2007). Measles, caused by MeV, is the leading cause of death in children, particularly in developing countries, because of secondary bacterial or parasitic infections attributable to MeV-induced immune suppression (Moss and Griffine, 2006). MeV also causes neurological diseases such as subacute sclerosing panencephalitis (Griffin, 2007). Although many research studies have been conducted, many aspects of the pathogenesis of MeV remain unclear.

Measles virus (genus *Morbillivirus*, within the family Paramyxoviridae) possesses a single-stranded RNA genome with negative polarity. MeV has six genes on its genome [nucleocapsid (N), phospho (P), matrix (M), fusion (F), hemagglutinin (H), and large (L)] and produces eight proteins (V and C proteins are produced from the P gene). The L gene encodes the L protein, an RNA-dependent RNA polymerase that transcribes the template RNA into new genomic RNA and viral mRNAs, together with the N and P proteins (Griffin, 2007). MeV mRNAs are capped at the 5′ end by L protein (Yoshikawa et al., 1986; Hercyk et al., 1988) and are believed to be translated in a cap-dependent manner.

Recently, we have shown that wild-type MeVs induce the "shutoff" of host cellular protein synthesis in infected cells (Inoue et al., 2009). Furthermore, we clarified that the phosphorylation of eukaryotic initiation factor (eIF) 2α and the binding of MeV-N protein to eIF3-p40, which are cellular initiation factors required for cap-dependent translation, are involved in the induction of this shutoff (Sato et al., 2007; Inoue et al., 2009). Severe suppression of the cap-dependent translation of host proteins was observed in infected cells, however, translated MeV proteins were still clearly evident (Inoue et al., 2009). Thus, it is considered that MeV mRNAs might have other mechanism(s) that facilitate their specific translation under shutoff conditions.

Viruses have acquired various mechanisms for efficient mRNA translation. Specifically, picornaviruses inhibit mRNA translation of host cells at the initiation step, and viral mRNA undergoes selective translation via an internal ribosome entry site (IRES) in its 5′ untranslated region (UTR; Jang, 2006). Several cellular factors are reported to bind to the IRES and play roles in translation independent of the cap structure (Jang, 2006).

On the other hand, the 5′UTR of MeV mRNAs is short (20–60 nt), except for F mRNA (570 nt), and does not contain a functional structure similar to the IRES. However, based on the predicted secondary structure of N-5′UTR, a short hairpin may form at its 5′ end (**Figure 1A**). This implies that some specific cellular factors may bind to the N-5′UTR via its sequence or secondary structure and induce selective viral mRNA translation. To determine the mechanisms underlying the specific translation of MeV mRNAs, we analyzed the translational efficiency with the N-5′UTR and attempted to identify cellular factors mediating the specific translation of N mRNA.

MATERIALS AND METHODS

CONSTRUCTION OF TEMPLATE PLASMID AND *IN VITRO* TRANSCRIPTION OF REPORTER RNA

The DNA fragment containing the SP6 promoter followed by the N-5′UTR of the HL strain of MeV was amplified

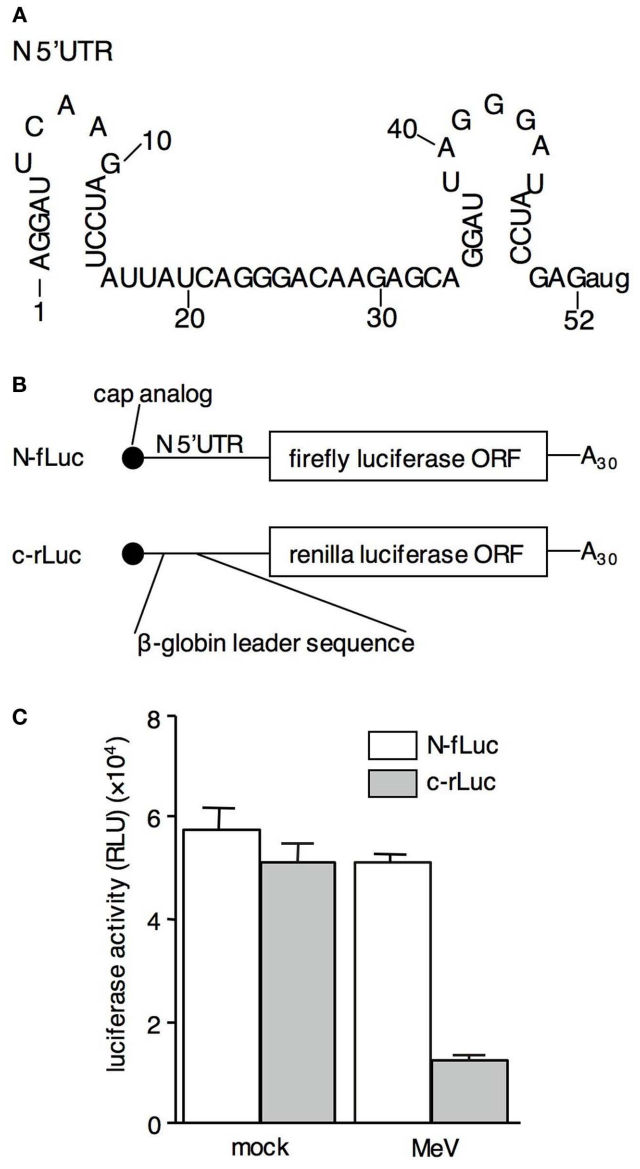

FIGURE 1 | RNA containing the N-5′UTR escapes the shutoff effect induced by MeVHL infection. (A) Sequence and computer-predicted structure of the wild-type N-5′UTR. **(B)** Structure of N-fLuc reporter RNA and c-rLuc reporter RNA. The 3′UTR and poly A tail of both types of RNAs, and the 5′UTR of c-rLuc RNA were derived from the pTNT vector. **(C)** Luciferase activity in mock- or MeV-infected B95a cells co-transfected with N-fLuc (white bar) and c-rLuc RNA (gray bar).

by PCR from the cDNA of the MeV genome, using primers 5′-ATTTAGGTGACACTATAGAGGATTCAAGATCCTATTATCAGGGACAAGAGC-3′ and 5′-CCATGGCTCGGATATCCCTAATCCTGCTCTTGTCCCTGAT-3′. The PCR fragment was subcloned into pCR2.1TOPO vector (Invitrogen, Carlsbad, CA, USA). After confirming the sequence, the SP6-N-5′UTR fragment was ligated to pGL3basic (Promega, Madison, WI, USA) at the *Kpn*I and *Nco*I sites. The "CC" residues in front of the AUG codon of the luciferase open reading frame (ORF) at the *Nco*I site was deleted using a QuikChange mutagenesis kit (Stratagene, La Jolla, CA, USA; pGL3 + NΔCC). The N-fLucΔCC fragment was digested with *Xho*I and *Xba*I and inserted to the pTNT vector (Promega) at the same site (pTNT-N-fLuc). N-fLuc with the polyA tail fragment was inserted to pCR2.1TOPO at the *Xho*I and *Bam*HI sites (N-fLuc template plasmid; pCR2.1-N-fLuc). Deletion of the N-5′UTR was performed with pGL3 + NΔCC using the QuikChange mutagenesis kit. After confirming the sequence, template plasmids were prepared in a similar way to pCR2.1-N-fLuc. The ORF of renilla luciferase, amplified from pRL-CMV (Promega) by PCR using primers containing the *Sal*I site at the 5′ end and the *Eco*RI site at the 3′ end was inserted into pTNT at the *Sal*I and *Eco*RI sites (pTNT-rLuc) as control RNA. The capped RNAs were transcribed from a linearized template with SP6 RNA polymerase using a RiboMAX Large Scale RNA production kit-SP6 (Promega) and cap analog (Promega). The capped RNA was purified by the method recommended by the manufacturer.

RNA TRANSFECTION

RNA was transfected into B95a cells (Kobune et al., 1990) derived from marmoset B cells which are highly susceptible to MeV infection, and grown in RPMI 1640 medium supplemented with 5% fetal calf serum (FCS) using Lipofectamine2000 (Invitrogen). After 4 h of incubation, the HL strain of MeV was infected into the B95a cells at a multiplicity of infection (moi) of 1. At 24 h post infection (hpi), the cells were harvested and luciferase activity was measured using a Dual Luciferase Assay kit (Promega).

ELECTROPHORESIS MOBILITY SHIFT ASSAY AND ULTRAVIOLET CROSS-LINK ASSAY

The fragment containing the SP6 promoter followed by the N-5′UTR containing the *Kpn*I site at the 3′ end was amplified by PCR from the pGL3-NΔCC plasmid and subcloned into pCR2.1TOPO (pCR2.1-N). After confirming the sequence, pCR2.1-N was linearized using *Kpn*I and blunted to delete a 3′ overhang at the 3′ end of 5′UTR using a blunting kit (TAKARA BIO INC., Shiga, Japan). The template of each deleted N-5′UTR probe was made from pCR2.1-N using a QuikChange mutagenesis kit. ^{32}P-labeled RNA probes were transcribed from the templates with a riboprobe kit-SP6 (Promega) and [α-^{32}P] UTP and purified by electrophoresis in an 8% polyacrylamide gel denatured by 8 M urea. The unlabeled probe was transcribed for competitor RNA. B95a extract was prepared from B95a cells that were frozen and thawed three times in buffer A [20 mM Tris-HCL (pH 7.5), 150 mM KCl, 1 mM DTT, and 1 mM EDTA]. His_6-tagged recombinant La protein (rLa) was synthesized using the RTS 500 Wheat Germ CECF kit and pIVEX1.4WG (Roche Applied Science, Basel, Switzerland) in which the ORF of human La was inserted at the *Nco*I and *Sma*I sites. rLa was purified using a Protino Ni 1000 prepacked column kit (MACHEREY-NAGEL, Düren, Germany). EMSA and a UV cross-link assay were performed as previously described by Park and Katze (1995). After electrophoresis, the gels were dried, exposed to imaging plates (FUJI FILM, Tokyo, Japan) and visualized with FLA5100 (FUJI FILM). Competitor RNA was added to the B95a extract and preincubated at 30°C for 10 min before

adding the probe. The antibody against La (Santa Cruz Biotechnology, Santa Cruz, CA, USA) was added to the B95a extract and preincubated on ice for 30 min prior to adding the probes.

IN VITRO TRANSLATION ASSAY

Cell-free translation S10 extracts from the suspension of COBL-a cells (derived from human umbilical cord cells and highly susceptible to MeV infection; Kobune et al., 2007) were prepared, and an *in vitro* translation assay was performed according to the method of Cuconati et al. (1998). After translation, luciferase activity was measured with PicaGene (Toyo Inki, Tokyo, Japan).

RNA INTERFERENCE

The La-small interfering RNA (siRNA) target sequence (5′-GUUGAACCGUCUAACAACAGA-3′) was designed using siDirect software and purchased from RNAi Co., Ltd (Tokyo, Japan). Silencer Negative Control #1 siRNA was purchased from Ambion (Austin, TX, USA). Transfection experiments were performed using X-tremeGENE siRNA Transfection Reagent (Roche Applied Science) according to the manufacturer's recommendation. After 48-h incubation, the cells were harvested and checked for the efficiency of RNAi by Western blotting with antibodies against La and β-actin (Santa Cruz Biotechnology). Reporter RNA was transfected into HepG2 cells after the 48-h incubation following siRNA transfection.

REVERSE GENETICS

To create recombinant MeV lacking the La-binding motif in the N-5′UTR, a previously established plasmid encoding the cDNA of the full-length genome of the HL strain of MeV was used (Terao-Muto et al., 2008). Deletion of six nucleotides was introduced into the N-5′UTR of the plasmid (genome position 66–71), and the resulting plasmid was designated pMeV-6del. The recombinant MeVHL-6del plasmid was generated from pMeV-6del. Briefly, 293 cells were placed in a six-well culture dish, inoculated with a recombinant vaccinia virus (MVA-T7) for 1 h, and then transfected with 1 μg of pMeV-6del, 1 μg of pKS-N1, 1 μg of pKS-P, and 0.3 μg of pGEM-L per well, which expressed N, P, and L proteins, respectively, under the control of a T7 promoter, using FuGENE6 (Roche Applied Science). After incubation for 3 days, the cells were co-cultivated with B95a cells at a concentration of 2×10^6 cells per well, and further incubated until extensive cytopathic effects were noted. The cells were collected and lysed by three cycles of freeze thawing. After sonication, samples were centrifuged at $1500 \times g$ for 10 min to remove the cell debris and stored as a crude virus stock at −80°C.

VIRUS GROWTH

B95a cells (1×10^6 cells) were infected with wild-type MeVHL or MeVHL-6del at an moi of 0.001 for 1 h. The inoculum was removed and the cells were washed once with medium and then incubated in medium containing 2.5% FCS. Cells and supernatants were harvested at the indicated times, and three cycles of freeze thawing were carried out. Infectivity was determined by tissue culture infective dose 50 ($TCID_{50}$) titration using the standard method. The experiment was repeated twice.

RESULTS

ANALYSIS OF N-5′UTR FUNCTION IN TRANSLATION

Measles virus mRNAs possess unknown mechanism(s) underlying their specific translation under shutoff conditions in MeV-infected cells. To determine whether the 5′UTR of N mRNA functions as the cis-element for translation in the MeV-infected cells, we constructed a reporter RNA (N-fLuc) that has the N-5′UTR in front of the ORF of the firefly luciferase gene (**Figure 1B**). As a control for cellular RNA translation, renilla luciferase RNA containing a leader sequence of β-globin mRNA in its 5′UTR was also constructed (c-rLuc). MeV was infected after the reporter RNAs were co-transfected into B95a cells. At 24 h postinfection, the cells were harvested, and luciferase activity was measured. The renilla luciferase activity derived from c-rLuc decreased (**Figure 1C**), confirming our previous results that MeV infection inhibited cap-dependent cellular mRNA translation (Inoue et al., 2009). In contrast, the firefly luciferase activity derived from N-fLuc was unaltered by MeV infection. This result suggests that N-5′UTR plays an important role in the specific translation of MeV-N mRNA in the shutoff conditions induced by MeV infection.

IDENTIFICATION OF CELLULAR PROTEINS THAT BIND TO N-5′UTR

To determine the presence of cellular proteins that specifically bind to the N-5′UTR, EMSA was performed using an N-5′UTR probe and B95a cell extracts (**Figure 2A**). The shift observed in the electrophoretic mobility of the N-5′UTR probe indicated the presence of a protein in the extract that interacted with the N-5′UTR probe (lane 1). Non-labeled RNA with the same sequence inhibited protein–RNA complex formation in a concentration-dependent manner (lanes 2–4). Since the protein–RNA interaction was not inhibited when yeast tRNA was used as the competitor RNA (lanes 5 and 6), the formation of this complex could be specific for N-5′UTR. A UV cross-link assay was performed to determine the molecular weight of proteins that bind to N-5′UTR. Several proteins that interacted with the N-5′UTR probe were observed (**Figure 2B**, lane 1). Among these, three proteins (of 52, 40, and 35 kDa) formed a specific complex with the N-5′UTR because their bands disappeared or the intensity of their bands decreased when non-labeled RNA was included in the reaction mixture (lane 2). The 52-kDa protein had the same molecular weight as that of the human La/SSB autoantigen (La). It has been reported that La binds to IRES in several viral-encoded RNAs, enhancing their translation (Jang, 2006). Although IRES is not present in MeV-N-5′UTR, we analyzed whether or not La bound to N-5′UTR. When an antibody against La was added to the EMSA reaction buffer prior to adding the probe, we observed that the specific complex (**Figure 2C**, lane 1) disappeared (lane 2). This was not observed with the antibody against the polypyrimidine tract binding protein (PTB; lane 3). To examine whether La specifically binds to N-5′UTR, rLa was constructed and subjected to EMSA along with N-5′UTR. When rLa was added, an rLa-probe complex was clearly observed (**Figure 2D**, lanes 2 and 3). Thus, several proteins in B95a cells specifically bind to N-5′UTR, one of which is La.

La-BINDING REGION OF N-5′UTR

To determine the sequence in N-5′UTR that interacts with La, deleted N-5′UTR probes (probes d1–d5) were constructed

(**Figure 3A**) and subjected to EMSA with rLa (**Figure 3B**). Each probe formed a complex with rLa, except the d2 probe that barely interacted with rLa (lane 3). Thus, nt 11–20 of N-5′UTR are required for the interaction with rLa. To evaluate the function of the deleted region in the N-5′UTR in translation, deletions similar to those in **Figure 3A** were introduced into N-fLuc (d1–d5-fLuc), and their luciferase activities were measured at 4 hpi in MeV-infected B95a cells co-transfected with mutant RNAs and c-rLuc. The luciferase activity from the translated d2-fLuc in the B95a cells was lower than that from other RNAs (**Figure 3C**). Because the observed decrease was by 30%, other region(s) than nt 11–20 may be involved in the interaction with La and the mRNA

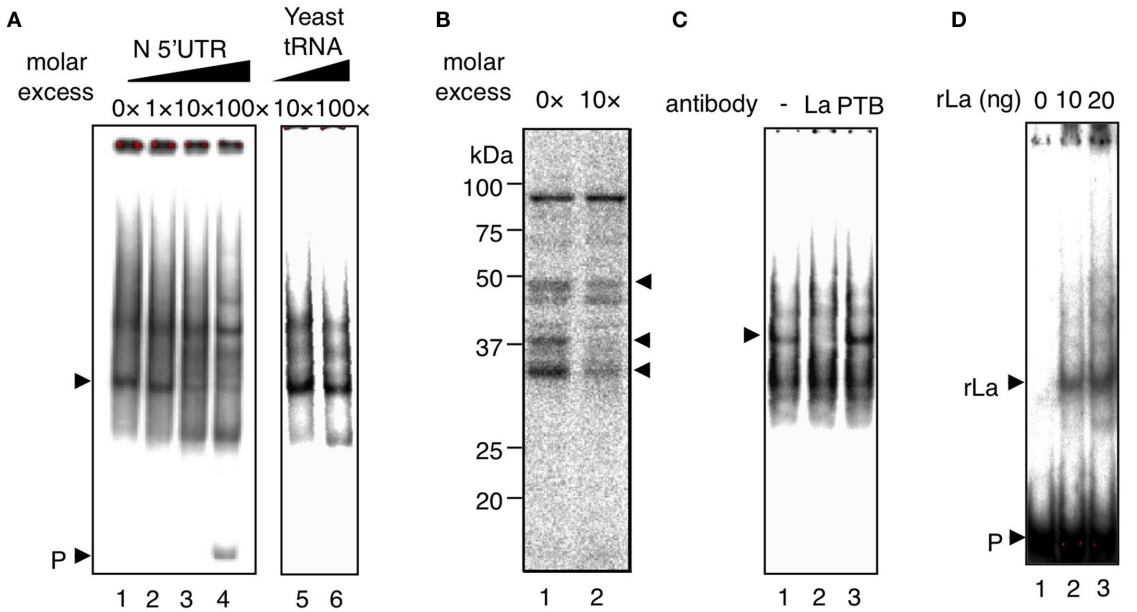

FIGURE 2 | La specifically interacts with N-5′UTR. (A) EMSA was performed with the N-5′UTR probe (P) and B95a cell extract. A specific competitor was added at the indicated molar excess ratio (lanes 2–4). Yeast tRNA was added at the indicated molar excess ratio as a non-specific competitor (lanes 5 and 6). The specific complex is indicated by an arrow. **(B)** The UV cross-link assay revealed that the molecular weight of specific-binding protein (which disappeared with the addition of a specific competitor RNA, lane 2) was approximately 35, 40, or 50 kDa (indicated by arrows). **(C)** The antibody against La inhibited the interaction of N-5′UTR and specific-binding protein (arrow; lane 2). As a control experiment, antibody against PTB was added (lane 3). **(D)** Recombinant La binds to the N-5′UTR probe. The probe (P) without rLa is shown in lane 1. rLa at the indicated dose was added to the reaction (lanes 2 and 3). The arrow indicates the complex derived from the rLa-probe.

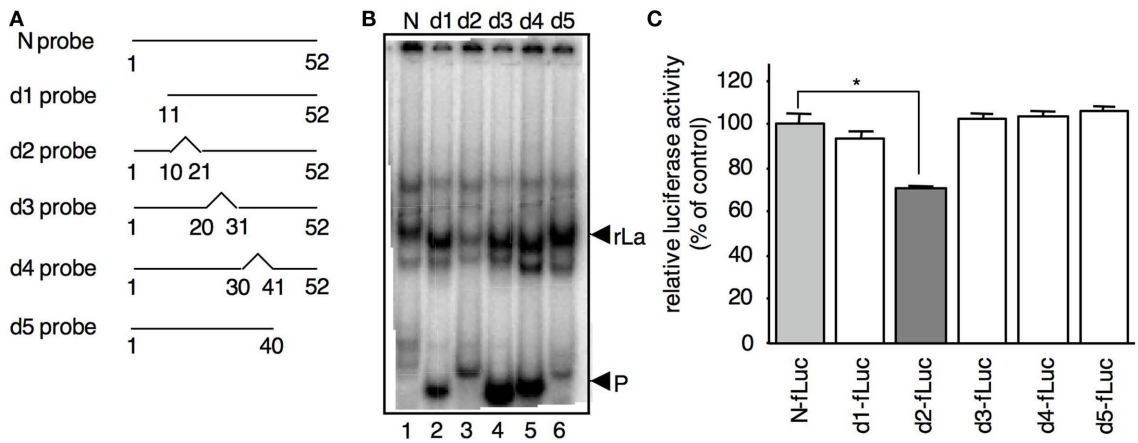

FIGURE 3 | The interaction of La with N-5′UTR requires a specific nt sequence in N (nt 11–20). (A) Outline of the deleted N-5′UTR probes used in the EMSA. The broken lines indicate the deleted regions. **(B)** The binding activity of rLa to the d2 probe was lower than that of other probes. The interactions of rLa with the probes (La) and the free probe (P) are indicated by arrows. **(C)** Luciferase activity of B95a cells transfected with the reporter RNA containing various N-5′UTRs. The deletions indicated in **(A)** were introduced into N-fLuc (d1–d5-fLuc). c-rLuc was co-transfected as an internal control. The N-fLuc value was arbitrarily set at 100%. Statistical analysis was performed using the Student's *t*-test; $*P < 0.01$.

translation. However, this result clearly indicated that nt 11–20 of N-5′UTR was required for the interaction with La and the optimum translation of N-fLuc RNA.

La ENHANCES *IN VITRO* N-fLuc REPORTER RNA TRANSLATION

To determine the role of La in translation via N-5′UTR, an *in vitro* translation assay was performed with a COBL-a S10 cell extract. N-fLuc or d2-fLuc RNA was translated in the COBL-a S10 extract containing rLa protein (**Figure 4A**). The luciferase activity translated from N-fLuc increased proportionally with the dose of rLa protein. The proportional increase was not observed for luciferase activity translated from d2-fLuc, indicating that La enhances N-fLuc translation via the N-5′UTR. The weak effect of the additional rLa on translation was probably due to the high amount of endogenous La in all extracts. La is a major mammalian cell component and its copy number reaches 2×10^7 copies/cell (Gottlieb and Steitz, 1989). In the case of the COBL-a S10 extract, a large amount of La was extracted (data not shown). To confirm the positive effect of La on translation, RNAi was performed to knock down La protein expression in HepG2 cells. Compared with the negative control siRNA-transfected cells, the La protein expression level decreased to 50% in La siRNA-transfected cells (**Figure 4B**). Under these conditions, N-fLuc or d2-fLuc RNA was transfected. Firefly luciferase activity decreased to 60% of the control cells following the knock down of La in the N-fLuc-transfected cells (**Figure 4C**). In contrast, the effect of La RNAi on the luciferase activity in d2-fLuc-transfected cells was less than that of N-fLuc (85% compared with the control cells). These results imply that La enhances N-fLuc translation by binding to the N-5′UTR *in vivo*.

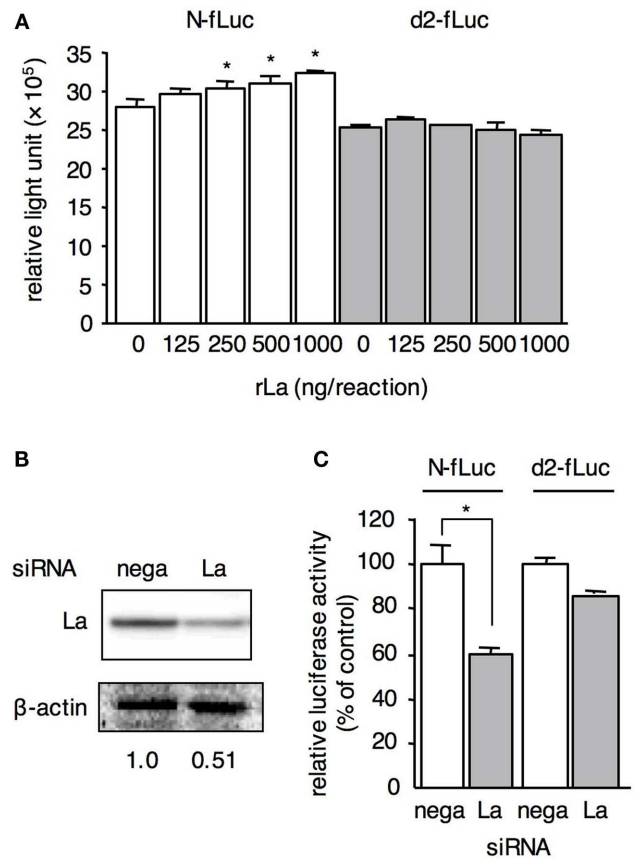

FIGURE 4 | La enhances N-fLuc translation. (A) N-fLuc and d2-fLuc were translated in COBLa S10 cell extracts with rLa at the indicated quantity. Statistical analysis was performed using the Student's *t*-test; $*P < 0.05$. **(B)** Expression level of La in HepG2 cells transfected with La siRNA (La) or negative control siRNA (nega). After 48-h incubation, the expression levels of La and actin on the same membrane were detected by western blotting. The relative value of the La expression level was measured and is provided under the panels. **(C)** The translation of N-fLuc in La siRNA-transfected HepG2 cells decreased more than that in d2-fLuc. The luciferase activity in HepG2 cells transfected with negative control siRNA was arbitrarily set at 100%.

INTERACTION OF La WITH N-5′UTR AFFECTS MV GROWTH EFFICIENCY AT AN EARLY PHASE OF INFECTION

We further investigated the effect of La on viral RNA in the replicating state using a recombinant MeV generated by reverse genetics (Terao-Muto et al., 2008). Because the genome length of *Morbilliviruses*, including MeV, is an integral of six (Kolakofsky et al., 1998), we synthesized a new deletion probe (6del-probe) by deleting nt 11–16 instead of nt 11–20 and tested the La interaction. La did not bind to the 6del-probe in EMSA, and a reporter RNA with the same deletion in the N-5′UTR showed low translation efficiency comparable to d2-fLuc (data not shown). Therefore, we performed reverse genetics using a plasmid encoding MeVHL full-length genome cDNA, which lacks 6 nt of the La-binding motif corresponding to the genome position 66–71, and generated the recombinant MeV (MeVHL-6del). Wild-type strain and MeVHL-6del were infected into B95a cells at an moi of 0.001 and harvested at each time point indicated. In cells infected with the 6del strain, the expression level of N protein lagged nearly 12 h behind that of wild-type infected cells (**Figure 5A**). Growth kinetics of the recombinant MeV indicated that production of infectious MeV particles in cells infected with MeVHL-6del was also delayed at an early phase of infection compared with the wild-type, and then recovered rapidly and reached similar levels to wild-type (**Figure 5B**). In MeV-infected cells, MeV-N is the first, most abundantly, and excessively synthesized among all viral proteins, and is necessary for viral genome replication and mRNA transcription, and therefore for virus growth. MeV-N synthesis was delayed in MeVHL-6del-infected cells approximately 12 h, and reached to the same amount as wild-type at 36 hpi (**Figure 5A**). Therefore, the virus growth kinetics was also delayed approximately 12 h, and increased rapidly between 24 and 36 hpi and reached the maximum titer at 48 hpi. Thus, the impaired La interaction with the N-5′UTR suppressed the translation efficiency of N mRNA and consequently virus replication at an early stage of infection. This result suggested that La contributes to synthesis of MeV proteins after infection.

DISCUSSION

We demonstrated that the 5′UTR of MeV-N mRNA possesses a function for selective translation under the shutoff conditions induced by MeV infection (**Figure 1**). Moreover, La binds to the N-5′UTR and plays an important role in the induction of specific translation of N-5′UTR-driven mRNA *in vitro* and *in vivo* (**Figures 2–4**).

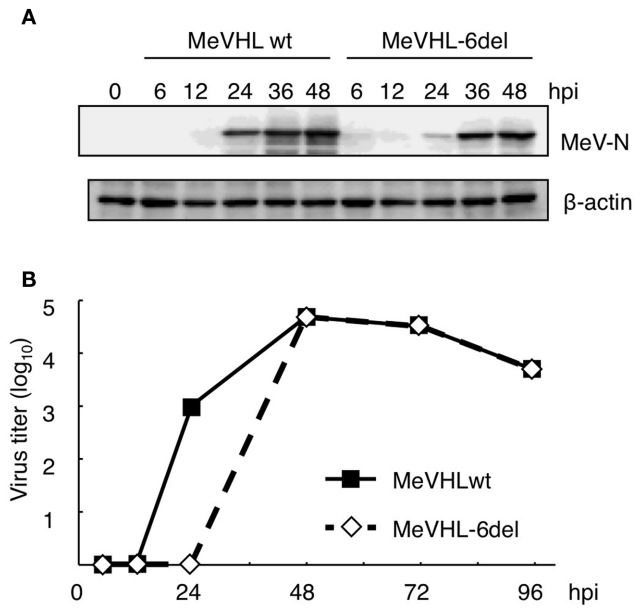

FIGURE 5 | La interaction with N-5′UTR affects the replication of MeV at an early phase of infection. (A) The expression levels of N protein in B95a cells infected with wild-type MeV or MeVHL-6del were determined by western blotting. As an internal control, β-actin protein was measured. **(B)** The growth kinetics of MeVHL-6del. Wild-type MeV (straight line) and MeVHL-6del (dotted line) were inoculated to B95a cells at an moi of 0.001, and harvested at the indicated time point. The average of two independent measurements is shown.

La was first described as an autoantigen in patients with the rheumatic diseases systemic lupus erythematosus and Sjogren's syndrome (Mattioli and Reichlin, 1974; Alspaugh et al., 1976). To date, it has been revealed that La possesses at least two major functions. First, La associates with various nascent RNAs transcribed by RNA polymerase III, such as pre-tRNAs and pre-5S rRNA, and plays a role in the regulation of RNA processing and nuclear export and retention (reviewed in Ref. Wolin and Cedervall, 2002). In this process, the La-binding motif (UUU-OH 3′) and the underlying molecular mechanisms have been well characterized. Many studies have indicated that the other major function of La protein is in the translation of specific viral and cellular mRNAs. For example, La binds to IRES in the 5′UTR of viral RNAs such as poliovirus (Meerovitch et al., 1993) and hepatitis C virus (HCV) RNA (Jang, 2006), as well as some eukaryotic mRNAs, namely, human immunoglobulin heavy chain binding protein mRNA (Kim et al., 2001). La also interacts with the 5′ end of HIV mRNAs which contain no IRES but have a *trans*-activation response (TAR) element (Chang et al., 1994; Svitkin et al., 1994). These interactions are proposed to enhance RNA translation (Ali and Siddiqui, 1995; Pudi et al., 2004). In addition, La has a negative effect on the translation of mRNAs of ribosomal proteins and translation elongation factors which contain the 5′ terminal oligopyrimidine tract sequence (Zhu et al., 2001). These data suggest that La has various functions in translation which maintain the optimal activity of interacting RNA. In this study, we showed that La has a positive effect on the translation of MeV-N-5′UTR-driven mRNA, although it contains neither an IRES nor a TAR element. The precise mechanism of upregulation of mRNA translation by La has not yet been elucidated, however, one possible role has been discussed on the basis of the reported function of La. La protein has been reported to function as a helicase that unwinds double-stranded RNA (Xiao et al., 1994; Hühu et al., 1997). The TAR element of HIV RNA is a stem-loop structure and suppresses the translation of the following RNA (Parkin et al., 1988), and La-binding enhances the translation of TAR-driven RNA (Chang et al., 1994; Svitkin et al., 1994). These reports imply that La functions as a helicase on the 5′UTR of mRNA and serves as an RNA chaperone. The MeV-N-5′UTR has a small stem-loop structure at its 5′ end consisting of nt 1–15 (**Figure 1A**), and the region responsible for La-binding is found in the stem region (**Figure 3**). In **Figure 3**, d2 probe showed low interaction with La, while d1 probe, which also lacks a part of the stem-loop structure at 5′ end (**Figure 1A**), bound to La comparable to N probe. Interestingly, d1 probe is estimated to form an alternative short hairpin structure at the 5′ end, which consists of nt 12–26, from a secondary structure prediction (data not shown). It suggests that La bound to d1 probe via the alternative stem structure at 5′ end. Thus, unwinding of the stem structure by La may result in the efficient translation of MeV-N mRNA. Alternatively, previous reports indicated that the binding of La to the stem-loop IV region of HCV IRES facilitates the formation of the 48S ribosomal complex on IRES (Costa-Mattioli et al., 2004; Pudi et al., 2004). Therefore, the binding of La to the N-5′UTR might facilitate formation of the ribosomal complex at the 5′ end. Interestingly, secondary structure predictions have indicated that not only N but also other MeV mRNAs, except for F, possess similar small stem-loop structures on their 5′UTR, and our preliminary experiments suggest that each 5′UTR can bind to La *in vitro* (data not shown). These findings indicate that efficient translation of other MeV mRNAs under shutoff conditions is also upregulated by similar mechanisms.

Recently, an additional function of La has been proposed in negative strand viruses, in which La binds to the leader RNA of viruses such as the human parainfluenza virus, vesicular stomatitis virus, rinderpest virus, and respiratory syncytial virus (Wilstz et al., 1983; De et al., 1996; Raha et al., 2004; Bitko et al., 2008). In particular, the leader RNA of rinderpest virus, which is closely related to MeV, specifically binds to La and this interaction enhances the replication/transcription of viral RNA (Raha et al., 2004). In addition, a more recent report indicated that La binds to the leader RNA of respiratory syncytial virus and shields it from RIG-I followed by abrogation of the early viral activation of type I interferon (Bitko et al., 2008). These results imply that La contributes to virus replication in multiple systems.

A previous study suggested that sufficient intracellular accumulation of N protein is required for viral genome replication (Lamb and Kolakofsky, 2001). Moreover, a recent report showed that a siRNA that specifically targets MeV-N represses the synthesis of viral mRNAs and genomic RNA (Reuter et al., 2006). These findings indicate that the efficient expression of N protein is important for virus replication. N protein binds to the viral genome and forms a ribonucleoprotein complex with P and L proteins, which acts as a template for viral genome replication

and transcription. Therefore, interference of N protein expression might result in the suppression of MeV transcription and replication. In this study, we demonstrated that the lack of La-binding to N-5′UTR, which elicits lower expression of N protein, caused a delay in N protein synthesis and virus replication at an early phase of infection (**Figure 5**). This suggests that the binding of La to N-5′UTR contributes to the rapid expression of N protein which in turn facilitates efficient virus growth.

In conclusion, our study revealed that a host protein, La autoantigen, enhances the translation of RNA containing N-5′UTR, and that La interaction can facilitate escape from the shutoff effect induced by MeV infection. This is the first report of a cellular factor that specifically regulates morbilliviral mRNA translation. Further studies are required to clarify the overall mechanism underlying the upregulation of mRNA translation and its implication in the pathogenesis of MeV.

ACKNOWLEDGMENTS

We thank Dr. K. Ito (Institute of Medical Science, The University of Tokyo) for providing valuable insights and for critical reading of this manuscript. This work was supported by grants from the Japanese Ministry of Education, Culture, Sports, Science and Technology, and the Bio-oriented Technology Research Advance Institution.

REFERENCES

Ali, N., and Siddiqui, A. (1995). The La antigen binds 5′ noncoding region of the hepatitis C virus RNA in the context of the initiator AUG codon and stimulates internal ribosome entry site-mediated translation. *Proc. Natl. Acad. Sci. U.S.A.* 94, 2249–2254.

Alspaugh, M. A., Talal, N., and Tan, E. M. (1976). Differentiation and characterization of autoantibodies and their antigens in Sjogren's syndrome. *Arthritis Rheum.* 19, 216–222.

Bitko, V., Musiyenko, A., Bayfield, M. A., Maraia, R. J., and Barik, S. (2008). Cellular La protein shields nonsegmented negative-strand RNA viral leader RNA from RIG-I and enhances virus growth by diverse mechanisms. *J. Virol.* 82, 7977–7987.

Chang, Y. N., Kenan, D. J., Keene, J. D., Gatignol, A., and Jeang, K. T. (1994). Direct interactions between autoantigen La and human immunodeficiency virus leader RNA. *J. Virol.* 68, 7008–7020.

Costa-Mattioli, M., Svitkin, Y., and Sonenberg, N. (2004). La autoantigen is necessary for optimal function of the poliovirus and hepatitis C virus internal ribosome entry site in vivo and in vitro. *Mol. Cell. Biol.* 24, 6861–6870.

Cuconati, A., Molla, A., and Wimmer, E. (1998). Brefeldin A inhibits cell-free, de novo synthesis of poliovirus. *J. Virol.* 72, 6456–6464.

De, B. P., Gupta, S., Zhao, H., Drazba, J. A., and Banerjee, A. (1996). Specific interaction in vitro and in vivo of glyceraldehyde-3-phosphate dehydrogenase and LA protein with cis-acting RNAs of human parainfluenza virus type 3. *J. Biol. Chem.* 271, 24728–24735.

Gottlieb, E., and Steitz, J. A. (1989). The RNA binding protein La influences both the accuracy and the efficiency of RNA polymerase II transcription in vitro. *EMBO J.* 8, 841–850.

Griffin, D. E. (2007). "Measles virus," in *Fields Virology*, 5th Edn, Vol. 2, eds D. M. Knipe and P. M. Howley (Philadelphia, PA: Lippincott Williams & Wilkins), 1551–1586.

Hercyk, N., Horikami, S. M., and Moyer, S. A. (1988). The vesicular stomatitis virus L protein possesses the mRNA methyltransferase activities. *Virology* 163, 222–225.

Hühu, P., Prujin, G. J. M., Van Venrooji, W. J., and Bachmann, M. (1997). Characterization of the autoantigen La (SS-B) as a dsRNA unwinding enzyme. *Nucleic Acids Res.* 25, 410–416.

Inoue, Y., Tsukiyama-Kohara, K., Yoneda, M., Sato, H., and Kai, C. (2009). Inhibition of host protein synthesis in B95a cells infected with the HL strain of measles virus. *Comp. Immunol. Microbiol. Infect. Dis.* 32, 29–41.

Jang, S. K. (2006). Internal initiation: IRES elements of picornaviruses and hepatitis c virus. *Virus Res.* 119, 2–15.

Kim, A. K., Back, S. H., Rho, J., Lee, S. H., and Jang, S. K. (2001). La autoantigen enhances translation of BiP mRNA. *Nucleic Acids Res.* 29, 5009–5016.

Kobune, F., Ami, Y., Katayama, M., Takahashi, M., Tuul, R., Korukluoglu, G., Kiyohara, T., Miura, R., Sato, H., Yoneda, M., and Kai, C. (2007). A novel monolayer cell line derived from human umbilical cord blood cells shows high sensitivity to measles virus. *J. Gen. Virol.* 88, 1565–1567.

Kobune, F., Sakata, H., and Sugiura, A. (1990). Marmoset lymphoblastoid cells as a sensitive host for isolation of measles virus. *J. Virol.* 64, 700–705.

Kolakofsky, D., Pelet, T., Garcin, D., Hausmann, S., Curran, J., and Roux, L. (1998). Paramyxovirus RNA synthesis and the requirement for hexamer genome length: the rule of six revisited. *J. Virol.* 72, 891–899.

Lamb, R. A., and Kolakofsky, D. (2001). *Fields virology*, 4th Edn, Vol. 1. Philadelphia, PA: Lippincott Williams & Wilkins, 1305–1340.

Mattioli, M., and Reichlin, M. (1974). Heterogeneity of RNA protein antigen reactive with sera of patients with systemic lupus arythematosus. Description of a cytoplasmic nonribosomal antigen. *Arthritis Rheum.* 17, 421–429.

Meerovitch, K. S., Svitkin, Y. V., Lee, H. S., Lejbkowicz, F., Kenan, D. J., Chan, E. K., Agol, V. I., Keene, J. D., and Sonenberg, N. (1993). La autoantigen enhances and corrects aberrant translation of poliovirus RNA in reticulocyte lysate. *J. Virol.* 67, 3798–3807.

Moss, W. J., and Griffine, D. E. (2006). Global measles elimination. *Nat. Rev. Microbiol.* 4, 900–908.

Park, Y. W., and Katze, M. G. (1995). Translational control by influenza virus. Identification of cis-acting sequence and trans-acting factors which may regulate selective viral mRNA translation. *J. Biol. Chem.* 270, 28433–28439.

Parkin, N. T., Cohen, E. A., Darveau, A., Rosen, C., Haseltine, W., and Sonenberg, N. (1988). Mutational analysis of the 5′non-coding region of human immunodeficiency virus type 1: effects of secondary structure on translation. *EMBO J.* 7, 2831–2837.

Pudi, R., Srivasan, P., and Das, S. (2004). La protein binding at the GCAC site near the initiator AUG facilitate the ribosomal assembly on the hepatitis c virus RNA to influence internal ribosomal entry site-mediated translation. *J. Biol. Chem.* 279, 29879–29888.

Raha, T., Pudi, R., Das, S., and Shaila, M. S. (2004). Leader RNA of rinderpest virus binds specifically with cellular La protein: a possible role in virus replication. *Virus Res.* 104, 101–109.

Reuter, T., Weissbrich, B., Schneider-Schaulies, S., and Schneider-Schaulies, J. (2006). RNA interference with measles virus N, P, and L mRNAs efficiently prevents and with matrix protein mRNA enhances viral transcription. *J. Virol.* 80, 5951–5957.

Sato, H., Masuda, M., Kanai, M., Tsukiyama-Kohara, K., Yoneda, M., and Kai, C. (2007). Measles virus N protein inhibits host translation by binding to eIF3-p40. *J. Virol.* 81, 11569–11576.

Svitkin, Y. V., Pause, A., and Sonenberg, N. (1994). Autoantigen alleviates translational repression by the 5′ leader sequence of the human immunodeficiency virus type 1 mRNA. *J. Virol.* 68, 7001–7007.

Terao-Muto, Y., Yoneda, M., Seki, T., Watanabe, A., Tsukiyama-Kohara, K., Fujita, K., and Kai, C. (2008). Heparin-like glycosaminoglycans prevent the infection of measles virus in SLAM-negative cell lines. *Antiviral Res.* 80, 370–376.

Wilstz, J., Kurilla, M. G., and Keene, J. D. (1983). A host protein (La) binds to a unique species of minus-sense leader RNA during replication of vesicular stomatitis virus. *Proc. Natl. Acad. Sci. U.S.A.* 80, 5827–5831.

Wolin, S. L., and Cedervall, T. (2002). The La protein. *Annu. Rev. Biochem.* 71, 375–403.

Xiao, Q., Sharp, T. V., Jeffrey, I. W., James, M. C., Prijin, G. J. M., Van Venrooji, W. J., and Clemens, M. J. (1994). The La antigen inhibits the activation of the interferon-inducible protein kinase PKR by sequestering and unwinding double-stranded RNA. *Nucleic Acids Res.* 22, 2512–2518.

Yoshikawa, Y., Mizumoto, K., and Yamanouchi, K. (1986). Characterization of messenger RNAs of measles virus. *J. Gen. Virol.* 67, 2807–2812.

Zhu, J., Hayakawa, A., Kakegawa, T., and Kasper, R. L. (2001). Binding of the

La autoantigen to the 5′ untranslated region of a chimeric human translation elongation factor 1A reporter mRNA inhibits translation in vitro. *Biochim. Biophys. Acta* 1521, 19–29.

Conflict of Interest Statement: The authors declare that the research was conducted in the absence of any commercial or financial relationships that could be construed as a potential conflict of interest.

Received: 02 June 2011; accepted: 02 August 2011; published online: 23 August 2011.

Citation: Inoue Y, Sato H, Fujita K, Tsukiyama-Kohara K, Yoneda M and Kai C (2011) Selective translation of the measles virus nucleocapsid mRNA by La protein. Front. Microbio. ***2****:173. doi: 10.3389/fmicb.2011.00173*
This article was submitted to Frontiers in Virology, a specialty of Frontiers in Microbiology.

frontiers in
MICROBIOLOGY

MINI REVIEW ARTICLE
published: 03 January 2012
doi: 10.3389/fmicb.2011.00269

Native morphology of influenza virions

Takeshi Noda*

Division of Virology, Department of Microbiology and Immunology, Institute of Medical Science, University of Tokyo, Tokyo, Japan

Edited by:
Akio Adachi, The University of Tokushima Graduate School, Japan

Reviewed by:
Kiyoko Iwatsuki-Horimoto, University of Tokyo, Japan
Fumitaka Momose, Kitasato University, Japan

****Correspondence:***
Takeshi Noda, Division of Virology, Department of Microbiology and Immunology, Institute of Medical Science, University of Tokyo, 4-6-1 Shirokanedai, Minatoku, Tokyo 108-8639, Japan.
e-mail: t-noda@ims.u-tokyo.ac.jp

Influenza A virus is an enveloped virus with a segmented, single-strand, negative-sense RNA genome. Its virions show spherical or filamentous shapes of about 100 nm in diameter and occasionally irregular morphology, which exemplifies the pleomorphic nature of these virions. Each viral RNA segment forms a ribonucleoprotein complex (RNP), along with an RNA-dependent RNA polymerase complex and multiple copies of nucleoproteins; the RNPs reside in the enveloped virions. Here, we focus on electron microscopic analyses of influenza virions and RNPs. Based on the morphological and structural observations obtained by using electron microscopic techniques, we present a model of the native morphology of the influenza virion.

Keywords: influenza virus, morphology, electron microscopy

INTRODUCTION

Influenza A, B, and C viruses are members of the *Orthomyxoviridae*, which is a family of enveloped viruses with segmented, single-stranded, negative-sense RNA genomes (Palese, 2007). They are classified according to antigenic differences in their nucleoprotein (NP) and matrix protein (M1), which are major structural components of their virions. Of the three members, Influenza A viruses, which are further classified into 16 hemagglutinin (HA) subtypes and 9 neuraminidase (NA) subtypes on the basis of their antigenic properties, cause annual epidemics in humans and recurring pandemics that spread globally with severe consequences for human health and the economy.

The genome of influenza A virus consists of eight single-stranded, negative-sense RNA segments that form ribonucleoprotein complexes (RNPs) together with the viral RNA (vRNA)-dependent RNA polymerase complex [basic polymerase 1 (PB1), basic polymerase 2 (PB2), and acidic polymerase (PA)] and many nucleoprotein (NP) molecules. The genome encodes at least 12 viral proteins, most of which are necessary for efficient virus replication in host cells and for virion formation. During virus infection, the virus attaches to receptors (i.e., sialic acid linked to galactose) on the cell surface via HA virion surface proteins and enters the cell by clathrin-mediated endocytosis. The RNPs within the virion are released into the cytoplasm by acidic pH-dependent membrane fusion, again via the HA proteins, and are transported to the nucleus of the infected cells. Unlike most negative-sense RNA viruses, transcription and replication of the influenza virus genome take place in the nucleus. After the RNPs are synthesized in the nucleus, they are exported to the cytoplasm with the help of two viral proteins, M1 (Bui et al., 1996, 2000) and nuclear export protein (NEP/NS2; O'Neill et al., 1998; Ye et al., 1999; Baudin et al., 2001), via the cellular chromosome region maintenance 1 (Crm1) protein-dependent pathway (Neumann et al., 2000; Elton et al., 2001; Ma et al., 2001; Watanabe et al., 2001; Akarsu et al., 2003; Iwatsuki-Horimoto et al., 2004). They are then transported to the budding site of the apical plasma membrane of polarized cells, through a Rab 11-dependent vesicular transport pathway (Amorim et al., 2011; Eisfeld et al., 2011; Momose et al., 2011). The transmembrane proteins HA, NA, and an ion channel protein (M2) are conveyed to the budding site by a standard exocytic pathway through the endoplasmic reticulum and Golgi apparatus. M1 is presumed to interact with both the RNPs and the cytoplasmic tails of HA, NA, and M2 and to act as a bridge between them at the budding site (Zhang et al., 2000; McCown and Pekosz, 2005). Eventually, all of the viral components, including the viral transmembrane proteins, M1, and RNPs, are orderly assembled into progeny virions. The progeny virions are released from the apical plasma membrane into the extracellular environment, where NA plays an important role in cleaving sialic acids bound to receptors on the cell surface and HA proteins on the progeny virions.

Although the morphology of influenza A virions, whether budding virions or purified virions, has been investigated extensively for many years by using various electron microscopic methods, knowledge of the virion structure remains limited, mainly due to pleomorphism, which complicates morphological and structural analyses and impedes investigators efforts to draw conclusions about the native structure of the virion. However, recent electron microscopic analyses have revealed several important morphological and structural features of influenza virions, which provide valuable information about the native morphology of these structures. This review summarizes the current progress in virion morphology studies and presents a model of the likely native morphology of influenza A virion.

THE MORPHOLOGY OF THE INFLUENZA A VIRION

Virions possess a lipid envelope that is derived from the host cellular membrane during the budding. They are generally spherical or elliptical in shape, ranging from approximately 80–120 nm in diameter and are occasionally filamentous, reaching more than 20 μm in length. Sometimes, however, they take on an irregular

shape. Virions are covered with numerous membrane-spanning glycoproteins, HA and NA, and small amounts of M2. The peripheral membrane protein, M1, which is one of the most abundant viral proteins in the virion, binds to the lipid envelope to maintain virion morphology. The segmented genome is enclosed in the virion in the form of the RNP. Although small amounts of NEP are present within the virion (Yasuda et al., 1993), its localization is unknown.

Most laboratory-adapted strains of influenza A virus are predominantly spherical or elliptical, whereas clinical isolates are predominantly filamentous and their adaptation in eggs results in the loss of this filamentous phenotype (Chu et al., 1949; Kilbourne and Murphy, 1960). The filamentous phenotype is thought to be a genetic trait, as shown by virus gene reassortment experiments (Smirnov et al., 1991) and reverse genetics studies (Bourmakina and Garcia-Sastre, 2003; Elleman and Barclay, 2004). Such studies have demonstrated that the M1 and M2 proteins are important determinants of filamentous virion formation (Hughey et al., 1995; Roberts et al., 1998; Bourmakina and Garcia-Sastre, 2003). In addition, the polarized cell phenotype and actin cytoskeleton network also play important roles in the formation of filamentous virions (Roberts and Compans, 1998), suggesting that several factors are involved in determining virion morphology. The significance of the filamentous morphology for virus replication and pathogenesis remains uncertain; however, the fact that clinical isolates, independent of HA and NA subtype, consistently form filamentous shapes strongly suggests that this filamentous phenotype is essential for virus survival in nature. The filamentous morphology may, for example, facilitate cell-to-cell transmission of progeny virions in the respiratory mucosa of infected individuals.

In addition to the spherical, elliptical, and filamentous virions, irregular-shaped virions are sometimes observed when using negative-staining electron microscopy (negative-staining EM) of purified virions (**Figure 1**; Stevenson and Biddle, 1966; Almeida and Waterson, 1967; Wrigley, 1979). Interestingly, such virions have never been reported when ultrathin-section transmission electron microscopy (ultrathin-section EM) or scanning electron microscopy (SEM) is used to view budding virions. This discrepancy is thought to be partially due to artifacts caused during sample preparation for negative-staining, since artifacts can be introduced into fragile biological specimens on air drying (Nermut and Frank, 1971; Ruigrok et al., 1992). However, other artifacts may also be included, because such irregular-shaped virions are also reported when using cryoelectron microscopy (cryoEM) of purified virions (Harris et al., 2006; Nayak et al., 2009), which does not involve air drying. Earlier reports suggested that the pleomorphism is introduced during the storage of virions at 4°C after they are harvested (Choppin et al., 1961; Nermut and Frank, 1971). More importantly, it was recently demonstrated that virion morphology is substantially affected by ultracentrifugation, which is often involved in the negative-staining process, resulting in the appearance of morphologically irregular virions (Sugita et al., 2011). When virions are chemically fixed with glutaraldehyde (GLA), which presumably creates cross-links among the membrane-bound M1 proteins that form the layer underneath the viral envelope as well as among M1 proteins and the cytoplasmic tails of the HA, NA, and M2 transmembrane proteins, the virion morphology is relatively conserved even after ultracentrifugation. This finding is consistent with observations made when using ultrathin-section TEM and SEM of budding virions, where morphologically irregular virions have never been found; sample processing of the ultrathin-section TEM and SEM usually begins with GLA fixation, and does not involve ultracentrifugation. Taken together, the pleomorphism of influenza virions observed when using negative-staining EM and cryoEM is an artifact that is mainly introduced during sample preparation procedures that involve ultracentrifugation and storage.

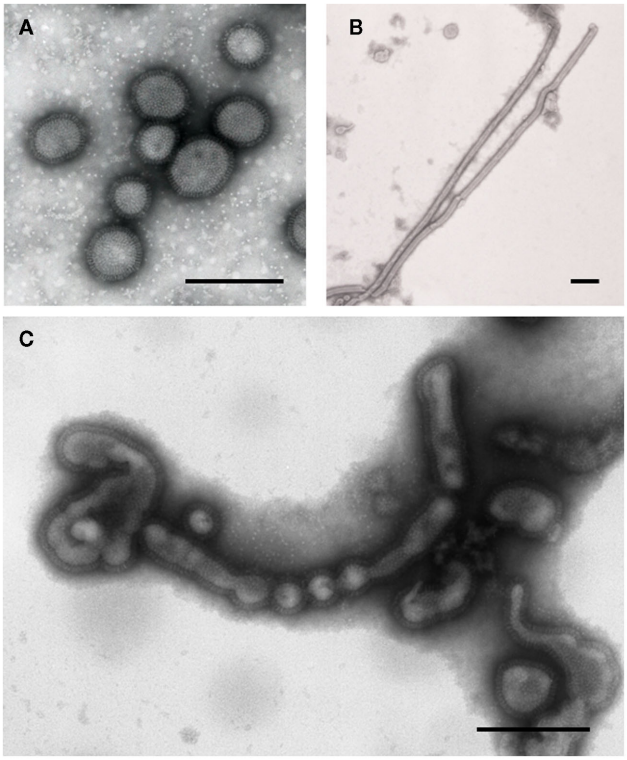

FIGURE 1 | Electron micrograph of influenza virions. The virions were purified by ultracentrifugation, and visualized by negative-staining EM. Bars, 200 nm. **(A)** Spherical virions [A/WSN/33 (H1N1)], **(B)** filamentous virions [A/Udorn/307/72 (H3N2)], and **(C)** irregular-shaped virions [A/Puerto Rico/8/34 (H1N1)].

RNPs WITHIN THE VIRION

The eight vRNA segments, which contain conserved sequences at their 3′ and 5′ ends that are partially complimentary to each other and form the core promoter (Skehel and Hay, 1978; Robertson, 1979; Desselberger et al., 1980), range in size from 890 to 2341 bases. Each vRNA segment is separately encapsidated by NP to form the RNP, which has a flexible, twisted rod-like structure that is folded back and coiled on itself. The rod-like RNPs are approximately 12 nm in diameter, but vary in length from approximately 30–110 nm (Pons et al., 1969; Compans et al., 1972). The length of each rod-like RNP correlates with the length of each vRNA segment (Compans et al., 1972).

Although the morphology of the purified RNPs has been well characterized, the conformation of RNPs inside virions had been largely unknown for a long time. When virions were examined by using negative-staining EM or cryoEM, a continuous strand of 7–8 nm in diameter, which was regularly packed in the form of a helix, was observed within disrupted virions (Hoyle et al., 1961; Apostolov and Flewett, 1965; Schulze, 1972; Almeida and Brand, 1975; Murti et al., 1980, 1992; Booy et al., 1985; Harris et al., 2006). Although the strands were observed only at a low frequency, they were the sole structure clearly visualized by using negative-staining EM and cryoEM. Therefore, it was proposed that RNPs exist as a single continuous helix, which would be fragmented into multiple rod-like RNPs during the purification process of RNPs (Almeida and Brand, 1975; Murti et al., 1980). Later, however, it was demonstrated by use of negative-staining EM (Ruigrok et al., 1989) and cryoEM (Calder et al., 2010), that the continuous helix found within disrupted virions was a layer of M1 proteins underneath the lipid envelope.

How, then, are the RNP fragments arranged within the virion? By using thin-section EM, it is shown that progeny virions budding from the plasma membrane of infected cells contain a distinct arrangement of RNPs (Oxford and Hockley, 1987; Noda et al., 2006). The RNPs are always suspended from the top of the budding virions and are oriented perpendicular to the budding tip. Many transversely sectioned budding virions contain eight RNPs, in which a central RNP is consistently surrounded by seven others. Serial transverse ultrathin-sections of whole budding virions have revealed that the eight RNPs within a virion differ in length, suggesting that the budding virion contains different kinds of vRNAs (Compans et al., 1972). Filamentous virions also contain eight RNPs arranged in this distinct pattern. Interestingly, the eight RNPs are confined to the top of the filamentous virion and the reminder of the filamentous virion is empty, indicating that such filamentous virions do not randomly incorporate multiple sets of eight RNPs (Noda et al., 2006). Recent cryoEM analyses of purified virions confirmed that they contain eight RNPs arranged in a distinct pattern (Harris et al., 2006; Calder et al., 2010). Furthermore, the RNPs are restricted to one end of the filamentous particles that are released from infected cells, which is consistent with the observations made by using ultrathin-section EM of budding virions (Noda et al., 2006). Thus, virions, regardless of their shape, incorporate an organized set of eight RNPs.

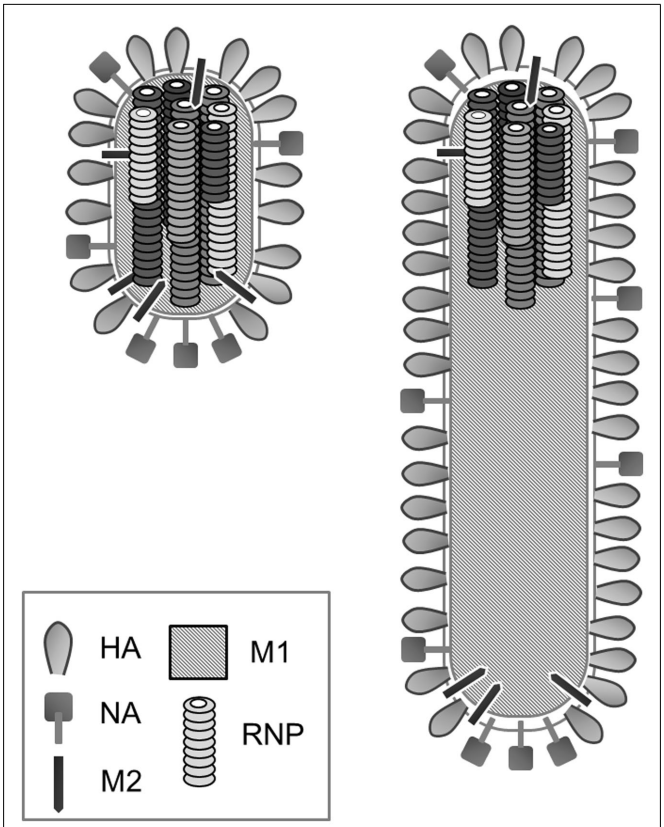

FIGURE 2 | Schematic diagram of influenza virions. Left, an elliptical virion; right, a filamentous virion. Note that both virions contain an organized set of eight RNPs at the end of the virion.

A MODEL OF A NATIVE INFLUENZA A VIRION

Based on recent microscopic analyses, a schematic diagram of a native influenza virion is depicted in **Figure 2**. Whether spherical, elliptical (**Figure 2** left), or filamentous (**Figure 2** right), the lipid-enveloped virions are regular in shape and covered with HA and NA glycoproteins and M2 proteins. Abundant HA proteins are distributed over the virion surface. Single NA proteins can be observed anywhere on the virion surface, whereas a cluster of NA proteins is also found at the end of the virion that is opposite to the end where the RNPs are located (Calder et al., 2010). Because the RNPs bind to the inner leaflet of the envelope at the distal end of budding virion (Noda et al., 2006; Calder et al., 2010), the NA cluster would play a role in release from the infected cell by destroying the HA binding to receptors on the cell surface. Given that membrane scission is caused by M2 proteins (Rossman et al., 2010), M2 proteins are likely located at the proximal end of the budding virion, on the same side as the NA cluster. In addition, the M2 protein plays an important role in RNP incorporation (McCown and Pekosz, 2005; Iwatsuki-Horimoto et al., 2006), suggesting that it should also be present at the distal end of the budding virion, where the M2 protein and RNPs could associate with each other. The M1 protein forms a matrix layer underneath the lipid envelope that is arranged as an ordered helix composed of multiple copies of M1 proteins that contribute to the virion morphology (Calder et al., 2010).

The eight rod-like RNPs, which differ in length, are arranged in a distinct pattern, in which seven peripheral RNPs surround a central RNP (Oxford and Hockley, 1987; Noda et al., 2006). Such an arrangement is observed not only in budding virions, but also in isolated virions (Harris et al., 2006; Calder et al., 2010), suggesting that there are interactions among the RNPs to maintain this organization. The eight RNPs are consistently associated with the inner envelope at the distal end of the budding virion and oriented almost perpendicular to the budding tip (Oxford and Hockley, 1987; Noda et al., 2006), indicating a polar organization of the virion.

CONCLUSION

Electron microscopic approaches are useful methods for investigating morphological and structural features of viruses. However, when fragile, lipid-enveloped viruses, including influenza viruses, are examined by using electron microscopy, artifactual effects such as ultracentrifugation, storage, and air drying should be considered. If not, misleading information can be visualized. Recent electron microscopic analyses of influenza virions clearly show that the native virion morphology is uniformly spherical, elliptical, or filamentous. Irregularly shaped virus particles are mainly artifacts caused during sample processing, indicating that such virus particles unlikely reflect the true virion structure. Accordingly, it is important to pay close attention to sample processing, when structurally examining influenza virions with electron microscopic techniques.

Despite the fact that various electron microscopic analyses have contributed to our knowledge of influenza virion morphology, much about the internal structure of the virion remains unknown. For instance, how do the RNPs associate with the envelope at the tip of the virion? How are the eight RNPs arranged in their distinct pattern? Do they interact with each other? If so, where and how do they interact? Although solving these issues by using conventional two-dimensional electron microscopic methods, such as thin-section EM and negative-staining EM would be difficult, if not impossible, they can be addressed by using three-dimensional analysis of RNPs within the virion by means of electron tomography, which provides higher resolution images.

ACKNOWLEDGMENTS

I thank Susan Watson for editing the manuscript. This work is supported by a Grant-in-Aid for Young Scientists from the Japan Society for the Promotion of Science.

REFERENCES

Akarsu, H., Burmeister, W. P., Petosa, C., Petit, I., Müller, C. W., Ruigrok, R. W., and Baudin, F. (2003). Crystal structure of the M1 protein-binding domain of the influenza A virus nuclear export protein (NEP/NS2). *EMBO J.* 22, 4646–4655.

Almeida, J. D., and Brand, C. M. A. (1975). Morphological study of the internal component of influenza virus. *J. Gen. Virol.* 27, 313–318.

Almeida, J. D., and Waterson, A. P. (1967). Some observations on the envelope of an influenza virus. *J. Gen. Microbiol.* 46, 107–110.

Amorim, M. J., Bruce, E. A., Reed, E. K., Foeglein, A., Mahen, R., Stuart, A. D., and Digard, P. (2011). A Rab11- and microtubule-dependent mechanism for cytoplasmic transport of influenza A virus viral RNA. *J. Virol.* 85, 4134–4156.

Apostolov, K., and Flewett, T. H. (1965). Internal structure of influenza virus. *Virology* 26, 506–508.

Baudin, F., Petit, I., Weissenhorn, W., and Ruigrok, R. W. (2001). In vitro dissection of the membrane and RNP binding activities of influenza virus M1 protein. *Virology* 281, 102–108.

Booy, F. P., Ruigrok, R. W., and van Bruggen, E. F. (1985). Electron microscopy of influenza virus. A comparison of negatively stained and ice-embedded particles. *J. Mol. Biol.* 184, 667–676.

Bourmakina, S. V., and Garcia-Sastre, A. (2003). Reverse genetics studies on the filamentous morphology of influenza A virus. *J. Gen. Virol.* 84, 517–527.

Bui, M., Whittaker, G., and Helenius, A. (1996). Effect of M1 protein and low pH on nuclear transport of influenza virus ribonucleoproteins. *J. Virol.* 70, 8391–8401.

Bui, M., Wills, E. G., Helenius, A., and Whittaker, G. R. (2000). Role of the influenza virus M1 protein in nuclear export of viral ribonucleoproteins. *J. Virol.* 74, 1781–1786.

Calder, L. J., Wasilewski, S., Berriman, J. A., and Rosenthal, P. B. (2010). Structural organization of a filamentous influenza A virus. *Proc. Natl. Acad. Sci. U.S.A.* 107, 10685–10690.

Choppin, P. W., Murphy, J. S., and Stoeckenius, W. (1961). The surface structure of influenza virus filaments. *Virology* 13, 548–550.

Chu, C. M., Dawson, L. M., and Elford, W. J. (1949). Filamentous forms associated with newly isolated influenza virus. *Lancet* 1, 602.

Compans, R. W., Content, J., and Duesberg, P. H. (1972). Structure of the ribonucleoprotein of influenza virus. *J. Virol.* 10, 795–800.

Desselberger, U., Racaniello, V. R., Zazra, J. J., and Palese, P. (1980). The 3′ and 5′-terminal sequences of influenza A, B and C virus RNA segments are highly conserved and show partial inverted complementarity. *Gene* 8, 315–328.

Eisfeld, A. J., Kawakami, E., Watanabe, T., Neumann, G., and Kawaoka, Y. (2011). RAB11A is essential for transport of the influenza virus genome to the plasma membrane. *J. Virol.* 85, 6117–6126.

Elleman, C. J., and Barclay, W. S. (2004). The M1 matrix protein controls the filamentous phenotype of influenza A virus. *Virology* 321, 144–153.

Elton, D., Simpson-Holley, M., Archer, K., Medcalf, L., Hallam, R., McCauley, J., and Digard, P. (2001). Interaction of the influenza virus nucleoprotein with the cellular CRM1-mediated nuclear export pathway. *J. Virol.* 75, 408–419.

Harris, A., Cardone, G., Winkler, D. C., Heymann, J. B., Brecher, M., White, J. M., and Steven, A. C. (2006). Influenza virus pleiomorphy characterized by cryoelectron tomography. *Proc. Natl. Acad. Sci. U.S.A.* 103, 19123–19127.

Hoyle, L., Horne, R. W., and Waterson, A. P. (1961). The structure and composition of the myxoviruses. II. Components released from the influenza virus particle by ether. *Virology* 13, 448–459.

Hughey, P. G., Roberts, P. C., Holsinger, L. J., Zebedee, S. L., Lamb, R. A., and Compans, R. W. (1995). Effects of antibody to the influenza A virus M2 protein on M2 surface expression and virus assembly. *Virology* 212, 411–421.

Iwatsuki-Horimoto, K., Horimoto, T., Fujii, Y., and Kawaoka, Y. (2004). Generation of influenza A virus NS2 (NEP) mutants with an altered nuclear export signal sequence. *J. Virol.* 78, 10149–10155.

Iwatsuki-Horimoto, K., Horimoto, T., Noda, T., Kiso, M., Maeda, J., Watanabe, S., Muramoto, Y., Fujii, K., and Kawaoka, Y. (2006). The cytoplasmic tail of the influenza A virus M2 protein plays a role in viral assembly. *J. Virol.* 80, 5233–5240.

Kilbourne, E. D., and Murphy, J. S. (1960). Genetic studies of influenza viruses. 1. Viral morphology and growth capacity as exchangeable genetic traits. Rapid in ovo adaptation of early passage Asian strain isolates by combination with PR8. *J. Exp. Med.* 111, 387–406.

Ma, K., Roy, A. M., and Whittaker, G. R. (2001). Nuclear export of influenza virus ribonucleoproteins: identification of an export intermediate at the nuclear periphery. *Virology* 282, 215–220.

McCown, M. F., and Pekosz, A. (2005). The influenza A virus M2 cytoplasmic tail is required for infectious virus production and efficient genome packaging. *J. Virol.* 79, 3595–3605.

Momose, F., Sekimoto, T., Ohkura, T., Jo, S., Kawaguchi, A., Nagata, K., and Morikawa, Y. (2011). Apical transport of influenza A virus ribonucleoprotein requires Rab11-positive recycling endosome. *PLoS ONE* 6, e21123. doi:10.1371/journal.pone.0021123

Murti, K. G., Bean, W. J. Jr., and Webster, R. G. (1980). Helical ribonucleoproteins of influenza virus: an electron microscopic analysis. *Virology* 104, 224–229.

Murti, K. G., Brown, P. S., Bean, W. J. Jr., and Webster, R. G. (1992). Composition of the helical internal components of influenza virus as revealed by immunogold labeling/electron microscopy. *Virology* 186, 294–299.

Nayak, D. P., Balogun, R. A., Yamada, H., Zhou, Z. H., and Barman, S. (2009). Influenza virus morphogenesis and budding. *Virus Res.* 143, 147–161.

Nermut, M. V., and Frank, H. (1971). Fine structure of influenza A2 (Singapore) as revealed by negative staining, freeze-drying and freeze-etching. *J. Gen. Virol.* 10, 37–51.

Neumann, G., Hughes, M. T., and Kawaoka, Y. (2000). Influenza A virus NS2 protein mediates vRNP nuclear export through NES-independent interaction with hCRM1. *EMBO J.* 19, 6751–6758.

Noda, T., Sagara, H., Yen, A., Takada, A., Kida, H., Cheng, R. H., and Kawaoka, Y. (2006). Architecture of ribonucleoprotein complexes in influenza A virus particles. *Nature* 439, 490–492.

O'Neill, R. E., Talon, J., and Palese, P. (1998). The influenza virus NEP (NS2 protein) mediates the nuclear export of viral ribonucleoproteins. *EMBO J.* 17, 288–296.

Oxford, J. S., and Hockley, D. J. (1987). *Orthomyxoviridae. Animal Virus Structure.* Amsterdam: Elsevier, 213–232.

Palese, P. (2007). "Orthomyxoviridae," in *Fields Virology*, 5th Edn, eds D. M. Knipe, P. M. Howley, D. E. Griffin, R. A. Lamb, M. A. Martin, B. Roizman, and S. E. Straus (Philadelphia: Lippincott Williams & Wilkins), 1647–1689.

Pons, M. W., Schulze, I. T., Hirst, G. K., and Hauser, R. (1969). Isolation and characterization of the ribonucleoprotein of influenza virus. *Virology* 39, 250–259.

Roberts, P. C., and Compans, R. W. (1998). Host cell dependence of viral morphology. *Proc. Natl. Acad. Sci. U.S.A.* 95, 5746–5751.

Roberts, P. C., Lamb, R. A., and Compans, R. W. (1998). The M1 and M2 proteins of influenza A virus are important determinants in filamentous particle formation. *Virology* 240, 127–137.

Robertson, J. S. (1979). 5′ and 3′ terminal nucleotide sequences of the RNA genome segments of influenza virus. *Nucleic Acids Res.* 6, 3745–3757.

Rossman, J. S., Jing, X., Leser, G. P., and Lamb, R. A. (2010). Influenza virus M2 protein mediates ESCRT-independent membrane scission. *Cell* 142, 902–913.

Ruigrok, R. W., Calder, L. J., and Wharton, S. A. (1989). Electron microscopy of the influenza virus submembranal structure. *Virology* 173, 311–316.

Ruigrok, R. W., Hewat, E. A., and Wade, R. H. (1992). Low pH deforms the influenza virus envelope. *J. Gen. Virol.* 73, 995–998.

Schulze, I. T. (1972). The structure of influenza virus. II. A model based on the morphology and composition of subviral particles. *Virology* 47, 181–196.

Skehel, J. J., and Hay, A. J. (1978). Nucleotide sequences at the 5′ termini of influenza virus RNAs and their transcripts. *Nucleic Acids Res.* 5, 1207–1219.

Smirnov, Y. U. A., Kuznetsova, M. A., and Kaverin, N. V. (1991). The genetic aspects of influenza virus filamentous particle formation. *Arch. Virol.* 118, 279–284.

Stevenson, J. P., and Biddle, F. (1966). Pleomorphism of influenza virus particles under the electron microscope. *Nature* 212, 619–621.

Sugita, Y., Noda, T., Sagara, H., and Kawaoka, Y. (2011). Ultracentrifugation deforms unfixed influenza A virions. *J. Gen. Virol.* 92, 2485–2493.

Watanabe, K., Takizawa, N., Katoh, M., Hoshida, K., Kobayashi, N., and Nagata, K. (2001). Inhibition of nuclear export of ribonucleoprotein complexes of influenza virus by leptomycin B. *Virus Res.* 77, 31–42.

Wrigley, N. G. (1979). Electron microscopy of influenza virus. *Br. Med. Bull.* 35, 35–38.

Yasuda, J., Nakada, S., Kato, A., Toyoda, T., and Ishihama, A. (1993). Molecular assembly of influenza virus: association of the NS2 protein with virion matrix. *Virology* 196, 249–255.

Ye, Z., Liu, T., Offringa, D. P., Mclnnis, J., and Levandowski, R. A. (1999). Association of influenza virus matrix protein with ribonucleoproteins. *J. Virol.* 73, 7467–7473.

Zhang, J., Leser, G. P., Pekosz, A., and Lamb, R. A. (2000). The cytoplasmic tails of the influenza virus spike glycoproteins are required for normal genome packaging. *Virology* 269, 325–334.

Conflict of Interest Statement: The author declares that the research was conducted in the absence of any commercial or financial relationships that could be construed as a potential conflict of interest.

Received: 02 December 2011; accepted: 17 December 2011; published online: 03 January 2012.

Citation: Noda T (2012) Native morphology of influenza virions. Front. Microbio. ***2****:269. doi: 10.3389/fmicb.2011.00269*

This article was submitted to Frontiers in Virology, a specialty of Frontiers in Microbiology.

frontiers in
MICROBIOLOGY

REVIEW ARTICLE
published: 07 February 2012
doi: 10.3389/fmicb.2012.00038

Morphogenesis of infectious hepatitis C virus particles

Tetsuro Suzuki*

Department of Infectious Diseases, Hamamatsu University School of Medicine, Hamamatsu, Japan

Edited by:
Akio Adachi, The University of Tokushima Graduate School, Japan

Reviewed by:
MinKyung Yi, University of Texas Medical Branch at Galveston, USA
Michael Schindler, Helmholtz Zentrum München – German Research Center for Environmental Health, Germany
Hideki Tani, National Institute of Infectious Diseases, Japan

***Correspondence:**
Tetsuro Suzuki, Department of Infectious Diseases, Hamamatsu University School of Medicine, 1-20-1 Handayama, Higashi-ku, Hamamatsu 431-3192, Japan.
e-mail: tesuzuki@hama-med.ac.jp

More than 170 million individuals are currently infected with hepatitis C virus (HCV) worldwide and are at continuous risk of developing chronic liver disease. Since a cell culture system enabling relatively efficient propagation of HCV has become available, an increasing number of viral and host factors involved in HCV particle formation have been identified. Association of the viral Core, which forms the capsid with lipid droplets appears to be prerequisite for early HCV morphogenesis. Maturation and release of HCV particles is tightly linked to very-low-density lipoprotein biogenesis. Although expression of Core as well as E1 and E2 envelope proteins produces virus-like particles in heterologous expression systems, there is increasing evidence that non-structural viral proteins and p7 are also required for the production of infectious particles, suggesting that HCV genome replication and virion assembly are closely linked. Advances in our understanding of the various molecular mechanisms by which infectious HCV particles are formed are summarized.

Keywords: hepatitis C virus, assembly, lipid droplet, VLDL

INTRODUCTION

Hepatitis C virus (HCV) infection is a major cause of chronic hepatitis, liver cirrhosis, and hepatocellular carcinoma. HCV is primarily transmitted by blood-borne routes, including shared needles and transfused blood products. The WHO estimates that a minimum of 2–3% of the world's population is chronically infected with HCV (Wasley and Alter, 2000). Despite the fact that HCV is targeted by innate, cellular, and humoral immune mechanisms, it establishes long-standing persistent infection in a majority of the people that it infects (Pawlotsky, 2006). HCV belongs to the genus *Hepacivirus* within the Flaviviridae family. The virus forms small round-shaped particles ranging from 50 to 80 nm in diameter. The mature HCV virion is thought to consist of a nucleocapsid, an outer envelope composed of E1 and E2 viral proteins, and a lipid membrane. HCV particles isolated from the sera of infected patients demonstrate heterogeneity in their density. Density gradient analyses have shown that viral RNA exists within both low- and high-density fractions (Andre et al., 2005), and that the low-density fractions contain lipoproteins that associate with apolipoprotein B (ApoB), apolipoprotein E (ApoE), triglycerides, and cholesterol, as well as viral structural proteins (Thomssen et al., 1992; Andre et al., 2002; Maillard et al., 2006; Nielsen et al., 2006). Only the low-density fraction derived from HCV-positive human serum exhibits high infectivity in chimpanzees (Bradley et al., 1991; Beach et al., 1992). Since the establishment of a robust tissue culture infection system using strain HCV JFH-1 (Lindenbach et al., 2005; Wakita et al., 2005; Zhong et al., 2005), the entire HCV lifecycle has been studied and the biophysical properties of the viral particles produced using the HCVcc cell culture system have been characterized. Most viral RNA-containing particles secreted from HCV-infected cells are poorly infectious and fractionate at high densities such as ∼1.14 g/mL, while highly infectious HCVcc are found within low-density fractions of ∼1.10 g/mL (Lindenbach et al., 2005).

Here, we provide a general account of our current understanding of the HCV lifecycle and a review of recent studies focusing on the morphogenesis of HCV particles within cell culture systems.

HCV GENOME ORGANIZATION AND PROTEIN SYNTHESIS

Hepatitis C virus is a positive-stranded RNA virus, and its ∼9.6-kb genome contains an open reading frame encoding a polyprotein of ∼3000 amino acids (aa) flanked by untranslated regions (UTRs) at both ends. Six genotypes have been reported based on HCV genome sequence variations (Simmonds, 1996). The UTRs are highly structured sequences encompassing critical cis-active RNA elements essential for genome replication and translation. The 5′ UTR, which is ∼341 nucleotides (nt) in length, contains an internal ribosomal entry site, which is a prerequisite for cap-independent translation of viral RNA, from which four highly structured domains (I–IV) are produced (Bukh et al., 1992; Tsukiyama-Kohara et al., 1992; Wang et al., 1993; Honda et al., 1996; Friebe et al., 2001). The 3′ UTR varies between 200 and 235 nt in length, including a short variable region, as well as a poly(U/UC) tract with an average length of 80 nt which is considered crucial for RNA replication, and a virtually invariant 98-nt X-tail region (Tanaka et al., 1995; Ito and Lai, 1999; Friebe and Bartenschlager, 2002; Yi and Lemon, 2003).

The genome is translated into a single precursor polyprotein, which is processed by cellular and viral proteases into 10 structural and non-structural proteins (Core, E1, E2, p7, NS2, NS3, NS4A, NS4B, NS5A, and NS5B; **Figure 1**). HCV proteins derived from the amino-terminal third of the precursor include Core, E1 and E2 structural proteins. A crucial function of Core protein is assembly of the viral nucleocapsid. The aa sequence of this protein is well conserved among different HCV strains compared to other HCV proteins. The non-structural (NS) proteins NS3-NS5B are thought to assemble into a membrane-associated HCV RNA replicase complex. NS3 functions as serine protease, RNA helicase, and NTPase.

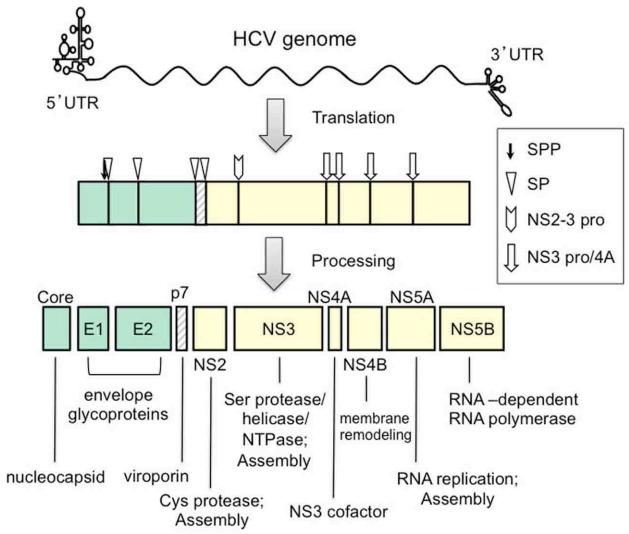

FIGURE 1 | The HCV genome and polyprotein. The RNA genome comprises a 9.6-kb RNA of plus strand polarity. Post-translational cleavages by SPP (signal peptide peptidase), SP (signal peptidase), NS2-3 pro (NS2–NS3 cysteine protease), and NS3 pro/4A (NS3 serine protease and NS4A complex) lead to the production of functional HCV proteins. Functions of each protein in the viral lifecycle are indicated below the open reading frame.

NS4A serves as a cofactor for NS3 and is involved in targeting NS3 to the ER membrane (Wolk et al., 2000). NS4B plays a role in the remodeling of host-cell membranes, probably to generate a site for replicase assembly. NS5A is also thought to play an important but undefined role in viral RNA replication. NS5B functions as an RNA-dependent RNA polymerase. The role of HCV NS proteins in assembly of the infectious virion is described below.

CORE PROTEIN AND NUCLEOCAPSID FORMATION

The Core is 191 aa in length and consists of three distinct predicted domains: an N-terminal domain that is two-thirds hydrophilic, a C-terminal domain that is one-third hydrophobic, and a short signal peptide sequence of the downstream protein E1. The precursor Core is cleaved between Core and E1 by a host signal peptidase. A C-terminal membrane-anchor of the Core is further cleaved by a signal peptide peptidase. The mature Core is estimated to be 177–179 aa (Ogino et al., 2004; Okamoto et al., 2004). Maturation of the Core by a signal peptide peptidase is required for virion production (Okamoto et al., 2008; Targett-Adams et al., 2008). Biophysical techniques have been used to demonstrate that the mature Core is a dimeric alpha-helical protein (Boulant et al., 2005). Its aa sequence is highly conserved among different HCV strains, compared with other HCV proteins. Thus, Core is used in most serologic assays since anti-core antibodies are highly prevalent among HCV-infected individuals.

Core has been detected in a number of subcellular compartments. Core protein is found on ER membranes, on the surface of lipid droplets (LDs), on the mitochondrial outer membrane, and to some extent, in the nucleus (Moradpour et al., 1996; Barba et al., 1997; Moriya et al., 1998; Yasui et al., 1998; Hope et al., 2002; Suzuki et al., 2005). Following is a proposed mechanism of translocation of Core to membranes within the ER network such as LDs (McLauchlan et al., 2002; Schwer et al., 2004). After being processed by a signal peptide peptidase, a large part of the Core remains within cytoplasmic leaflets of the ER membrane due to preservation of the original transmembrane domain. The cytoplasmic leaflets then swell as lipid accumulates between the two membrane leaflets. As a result, the Core is translocated along with part of the ER membrane to the surface of a nascent LD before the droplet buds off the ER. The proteasome-dependent degradation pathway then participates in post-translational modification of the Core (Suzuki et al., 2001, 2009; Moriishi et al., 2003, 2007, 2010; Shirakura et al., 2007). Ubiquitin ligase E6AP and proteasome activator PA28gamma are key regulators in determining the fate of the Core, and thereby play a role in virus production (Shirakura et al., 2007; Moriishi et al., 2010).

The ∼120 N-terminal residues of the Core protein (domain I) contain multiple positively charged residues that are implicated in RNA binding and homo-oligomerization. It is therefore likely that this domain is a prerequisite for assembly of the HCV nucleocapsid (Kunkel et al., 2001; Klein et al., 2004, 2005; Majeau et al., 2004). It has been shown that a region extending from aa 72 to 91 is responsible for auto-oligomerization of Core (Nakai et al., 2006). Although conclusive data for direct packaging of the HCV genome into the viral capsid is lacking, the viral RNA sequence of the Core protein through to the NS2 region appears not to contain a cis-acting packaging signal. A subgenomic replicon RNA carrying the NS3–NS5B region can be encapsidated in the viral trans-packaging system (Ishii et al., 2008; Steinmann et al., 2008; Adair et al., 2009; Masaki et al., 2010). In addition, the RNA sequence encoding the first 62 aa of Core contains highly conserved structures including two stem-loops that are important for RNA translation/replication (McMullan et al., 2007). Domain II (aa ∼120–170) is predicted to form two alpha-helices that enable Core to associate with membrane proteins and lipids. Domain II is involved in targeting of Core to LDs. It has been proposed that domain II folding occurs in a membrane environment and is critical for the folding of domain I (Boulant et al., 2005). In addition, a cysteine residue at aa 128 of domain II creates a disulfide bond to produce a Core protein dimer that is required for particle formation (Kushima et al., 2010). Domain III, pertaining to ∼20 residues at the C-terminal, is highly hydrophobic and serves as a signal sequence for E1. Although little is known about the molecular mechanisms governing assembly of Core into nucleocapsids, comprehensive mutagenesis studies have enabled identification of various aa residues which are essential for HCV morphogenesis (Murray et al., 2007; Alsaleh et al., 2010; Kopp et al., 2010).

INVOLVEMENT OF OTHER HCV PROTEINS IN ASSEMBLY

Two N-glycosylated envelope proteins E1 and E2 are exposed on the surface of the virus as a heterodimer that mediates viral attachment to host-cell receptors and facilitates virus entry (Op De Beeck et al., 2004; Vieyres et al., 2010). During their synthesis, E1 and E2 assemble as non-covalent heterodimers. Ectodomains of E1 and E2 are translocated inside the ER lumen and their transmembrane domains are inserted in the membrane of this compartment. E1 contains four to five N-linked glycans and E2

has 11 N-glycosylation sites. HCV glycans, which are thought to contain a mixture of complex and high mannose side-chain, play a role in envelope protein folding and formation of the E1/E2 complexes. The importance of incorporating N-linked glycans of the envelope proteins into infectious virions has been demonstrated (Helle et al., 2010). A recent study has shown that HCV infection activates the ER-associated degradation pathway, which in turn controls the fate of E1 and E2 and modulates virus production (Saeed et al., 2011).

A role of viral NS proteins in HCV production was first suggested following the observation that JFH-1-derived NS proteins are required to generate infectious virus from intra- and inter-genotype chimeric constructs (Lindenbach et al., 2005; Pietschmann et al., 2006). Evidence supporting a role of NS2, NS3, and NS5A in the assembly or release of infectious HCV has come from mutational analyses (Jones et al., 2007; Miyanari et al., 2007; Appel et al., 2008; Jirasko et al., 2008; Ma et al., 2008; Masaki et al., 2008; Tellinghuisen et al., 2008).

NS5A is a hydrophilic phosphoprotein which plays a key role in viral RNA replication and is involved in modulation of cell signaling pathways and the interferon response (Huang et al., 2007). NS5A is associated with membrane mediated by a unique amphipathic alpha helix which is located at its N-terminus (Moradpour et al., 2005), and part of NS5A localizes to LDs when expressed alone or as the viral polyprotein (Shi et al., 2002). Experiments based on HCV genomes containing mutated NS5A have shown that some mutants result in failure of association of NS5A with LDs and failure of production of infectious particles (Miyanari et al., 2007). Further studies have revealed that the C-terminal region of NS5A plays a key role in HCV production (Appel et al., 2008; Masaki et al., 2008; Tellinghuisen et al., 2008). Substitutions at a serine cluster of the NS5A C-terminus (aa 2428, 2430, and 2433) which have no impact on viral RNA replication, have been observed to inhibit the interaction between NS5A and Core, thereby suggesting that an association between NS5A and Core might be involved in virus production (Masaki et al., 2008). Structural analyses have shown that the N-terminal region of NS5A forms a "claw-like" dimer, which might accommodate RNA and interact with viral and cellular proteins and membranes (Huang et al., 2005; Tellinghuisen et al., 2005). It appears that recruitment of NS5A to LDs, thereby enabling interaction with the Core, is crucial for virion assembly. One can imagine that newly synthesized HCV RNA bound to NS5A is released from the replication complex-containing membrane compartment and can then be captured by Core through interaction with the C-terminal region of NS5A at the surface of LDs or LD-associated membranes. Consequently, viral RNA becomes encapsidated and virion assembly proceeds (**Figure 2**). In this regard, a study has revealed an interaction between NS5A and ApoE, suggesting that recruitment of ApoE by NS5A is important for the assembly and release of HCV particles (Benga et al., 2010).

NS3–NS4A is another component of the viral replication complex that exhibits serine protease, as well as RNA helicase and RNA-stimulated NTPase activity, necessary for viral RNA replication. It is now apparent that NS3–NS4A also contributes to viral assembly (Yi et al., 2007; Ma et al., 2008; Han et al., 2009; Phan et al., 2011). A previous study has provided genetic evidence that

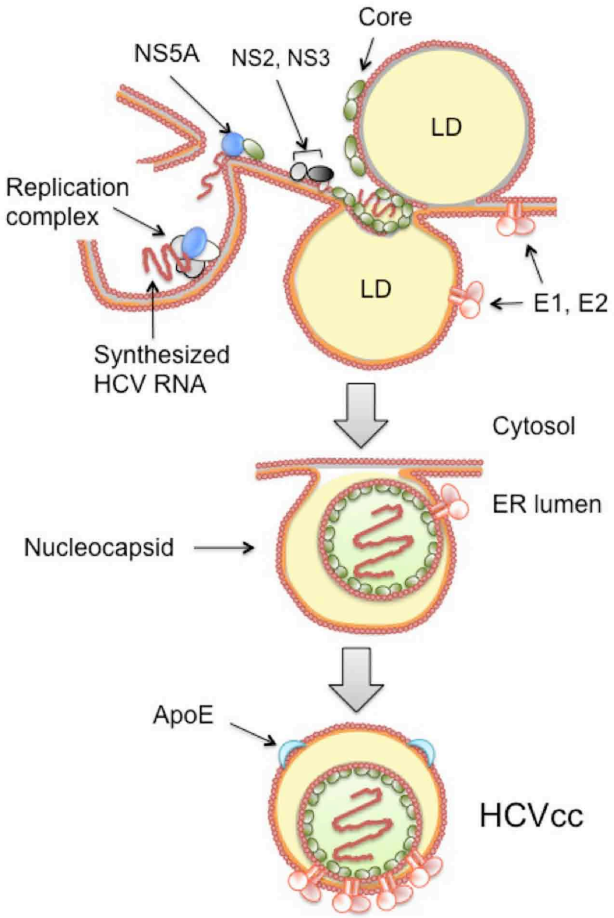

FIGURE 2 | Proposed model for assembly of HCV particles. After accumulation of synthesized genome RNA and the viral proteins, the HCV particles are assembled in an ER-related compartment in close connection with the VLDL pathway. The viral replication complex, which is composed of NS3–NS5B and host factors, is a specialized structure protected by cellular membrane. Newly synthesized viral RNAs are recruited to surfaces of lipid droplet (LD), where ER membrane is associated, possibly via interaction between NS5A and Core. Thus, the RNAs enable to associate with Core, thereby proceeding encapsidation and nucleocapsid formation. The nucleocapsid is presumably inserted into the lipid core of the luminal LD and buds into the ER lumen with incorporation of E1 and E2. HCV–lipoprotein particle formed is then released from the cells.

two major subdomains of the NS3 helicase, one demonstrating NTPase activity and the other associated with RNA binding, are involved in the early stages of virion assembly, independent of their roles as enzymes (Ma et al., 2008). A separate investigation has revealed a contribution of the acidic domain of NS4A to both RNA replication and virus assembly (Phan et al., 2011).

NS2 is a cysteine protease composed of a highly hydrophobic N-terminal membrane binding domain which forms either three or four transmembrane helices that insert into the ER membrane. NS2 also contains a C-terminal globular and cytosolic protease subdomain, that produce zinc-stimulated NS2/3 autoprotease activity together with the N-terminal one-third of NS3.

Mutagenesis of NS2 has identified regions or residues that are important for infectious virus production (Jones et al., 2007; Yi et al., 2007, 2009; Jirasko et al., 2008, 2010; Dentzer et al., 2009; Phan et al., 2009; Ma et al., 2011; Popescu et al., 2011). For example, mutations involving the dimer interface of the protease region or the C-terminus of NS2 impair the production of infectious HCV, while the catalytic activity of NS2 is not required for viral assembly. Genetic and biochemical data demonstrate that NS2 is possibly involved in multiple interactions with both HCV structural and NS proteins including E1–E2, p7, NS3, and NS5A, suggesting that NS2 has a role in recruiting these viral proteins to sites in close proximity with LDs. Alternatively, it may act as a scaffold promoting virus assembly (Jirasko et al., 2010; Ma et al., 2011; Stapleford and Lindenbach, 2011).

p7 is a 63-aa polypeptide located between E2 and NS2, and is a membrane-spanning protein localized within the ER. p7 belongs to a class of viral permeability-altering proteins termed "viroporins." It behaves as an ion channel when reconstituted into artificial lipid membranes. Although p7 is not required for viral RNA replication in cell culture, the protein is essential for HCV infectivity in chimpanzees (Sakai et al., 2003). Subsequent analyses in HCVcc systems have demonstrated that p7 is important for virion production since the introduction of p7 mutations, such as mutations in the basic residues required for its ion channel activity, impair virus production (Jones et al., 2007; Steinmann et al., 2007; Brohm et al., 2009). Although it is not yet clear whether the ion channel function of the protein is needed for virus assembly, a recent study has demonstrated that p7 functions as an H^+ channel in native intracellular membranes and links p7-induced pH changes to the production of infectious intracellular virions (Wozniak et al., 2010).

ROLE OF LIPID METABOLISM IN HCV ASSEMBLY

HCVcc contained within low-density fractions from the culture supernatant of virus-producing cells displays greater specific infectivity than virus in high-density fractions (Lindenbach et al., 2005; Ogawa et al., 2009). Looking also at the behavior of HCV circulating within the sera of infected hosts, it may be that low-density virus associates with lipid and very-low-density lipoprotein (VLDL) and/or low-density lipoprotein (LDL). Furthermore, HCV particles obtained from virus-infected animals, such as chimpanzees and chimeric mice transplanted with human hepatocytes, demonstrate greater infectivity than virus produced in cell cultures. The virus populations derived from these infected animals have been observed to fractionate into lower density fractions than a major population of HCVcc (Lindenbach et al., 2006). Interestingly, the association of cholesterol and sphingolipid with HCV virions has been shown to play a critical role in viral infectivity (Kapadia et al., 2007; Aizaki et al., 2008; Voisset et al., 2008). Depletion of cholesterol and sphingomyelin from HCV virions inhibits the infectivity of HCVcc (Aizaki et al., 2008). The structural requirement of virion-associated cholesterol for infectivity, as well as its influence on buoyant density, and the association of apolipoprotein with HCV, has been further demonstrated by Yamamoto et al. (2011).

There is accumulating evidence that assembly and secretion of HCV particles are associated with the VLDL assembly pathway. Lipoproteins can be differentiated on the basis of their density, which is affected by lipid content and the types of apolipoprotein they contain. VLDLs are large triglyceride-rich lipoproteins (30–80 nm in diameter) containing cholesterol, cholesteryl esters, ApoB, and other minor apolipoprotein(s). VLDLs carry triglyceride from the liver to peripheral tissue for storage and to provide a source of energy. Triglyceride availability and the size of intracellular triglyceride pools are important regulatory factors in the regulation of VLDL production. In addition, the microsomal triglyceride transfer protein (MTP), which is responsible for the transport of triglyceride and cholesteryl esters across ER membranes, is required for VLDL assembly. Purified membrane vesicles containing the HCV replication complex are enriched with ApoB, MTP, and ApoE (Huang et al., 2007). Moreover, agents that inhibit VLDL assembly also inhibit HCV secretion from cells producing infectious virus (Chang et al., 2007; Huang et al., 2007; Gastaminza et al., 2008). ApoB, ApoC1, and ApoE have been observed to associate with HCV particles during viral morphogenesis in the HCVcc system (Chang et al., 2007; Meunier et al., 2008; Jiang and Luo, 2009; Owen et al., 2009; Benga et al., 2010). Furthermore, ApoE depletion suppresses the production of infectious HCV (Chang et al., 2007; Jiang and Luo, 2009; Owen et al., 2009; Benga et al., 2010; Hishiki et al., 2010). These findings demonstrate that ApoE is important for HCV infectivity, suggesting that HCV virions are assembled as ApoE-enriched lipoprotein particles. A study in which virion-associated cholesterol was depleted and replenished with exogenous sterol analogs has provided evidence that virion-associated cholesterol contributes to the interaction between HCV and ApoE (Yamamoto et al., 2011). ApoE is a polymorphic protein with three major isoforms: ApoE2, ApoE3, and ApoE4. Differential roles of ApoE isoforms on infectious HCV production have been revealed: ectopic expression of ApoE3 or ApoE4 enables recovery of infectious HCV, while ApoE2 has little influence on virus production (Hishiki et al., 2010). Not surprisingly, ApoE2 demonstrates significantly less LDL receptor binding activity than ApoE3 and ApoE4 (Davignon et al., 1988).

Hepatitis C virus may utilize the assembly and secretion of VLDL to exit cells. In fact, secretion of E1 and E2 within the culture supernatant is reduced by treatment with MTP inhibitors (Icard et al., 2009). VLDL maturation occurs by acquisition of lipids from LDs either in the ER lumen or in the Golgi apparatus. It is likely that HCV envelopment takes place in a lipid-enriched microdomain at the ER membrane where luminal LDs or VLDL precursors are generated (**Figure 2**), in keeping with evidence of increased cholesterol content among HCV particles compared to host-cell membranes (Aizaki et al., 2008).

Neutral lipids such as triglycerides and cholesterol esters are stored within cytosolic LD in cells. LD is thought to be a source of neutral lipid for metabolism and membrane synthesis. Neutral lipids form the LD core and are surrounded by an outer layer of amphipathic lipids such as phospholipids and cholesterol. LD is thought to be surrounded by a lipid monolayer. Prior to the availability of a tissue culture system for virion production, HCV Core was shown to associate with ER membranes and on the surface of LDs in heterologous expression systems in mammalian cells (Moradpour et al., 1996; Barba et al., 1997). Early studies of cells infected with HCV JFH-1 indicate that Core is detectable at the ER

and on the surface of LDs in association with the ER (Rouille et al., 2006). Core associates with LDs in a time-dependent manner and disruption of this process coincides with a loss of virion production (Boulant et al., 2007). It has subsequently been demonstrated that LDs are directly involved in the production of infectious HCV and that Core recruits viral non-structural proteins as well as the replication complex to the LD-associated membranes, suggesting that the association between Core and LDs is required at a certain stage of HCV morphogenesis (Miyanari et al., 2007). Fluorescent labeling and functional imaging of Core in living cells has recently been used to visualize Core during HCV assembly (Counihan et al., 2011). Core has been observed to move to the surface of large, immobile LDs soon after protein translation. Core has also been observed in motile puncta that travel along microtubules. Diacylglycerol acyltransferases (DGATs) catalyze the final step of triglyceride synthesis and are crucial for LD biogenesis. A study has revealed that DGAT1 interacts with Core and is required for trafficking of the Core to LD. Disrupting translocation of the Core to LD by inhibiting DGAT1 activity or through knockdown of the DGAT1 gene impairs virus production (Herker et al., 2010). Thus, there is now increasing evidence that LDs play a central role in the production of infectious HCV and participate in virus assembly. However, one study has demonstrated that, while Core derived from HCV JFH-1 is strongly associated with cytoplasmic LDs, minimal Core from a HCV clone with higher assembly efficiency is detectable on LDs (Shavinskaya et al., 2007). Thus, it remains debatable whether HCV assembly is initiated on the surface of LDs or at sites where ER cisternae are in contact with LDs. Based on the current evidence, a model for nucleocapsid formation following the initial phase of assembly is demonstrated in **Figure 2**. Two potential models to explain HCV nucleocapsid formation, including the model shown in **Figure 2**, have been proposed by Bartenschlager et al. (2011).

FUTURE PERSPECTIVES

Evidence regarding the assembly of infectious HCV particles has accumulated over the past several years since the availability of HCVcc systems. A variety of key factors in HCV morphogenesis have been identified, including the requirement for components of the VLDL biosynthetic machinery and viral NS proteins. However, there are still essential questions to be answered. Detailed mechanisms pertaining to nucleotide formation, genome packaging, and the way in which HCV interacts with the lipoprotein/VLDL pathway, as well as the precise role of various NS proteins and p7 in HCV assembly, remain unclear. Structural studies will be important to clarify the exact composition of the HCV virion, as well as similarities and differences between HCVcc generated in Huh-7-derived cells and the "lipoviroparticles" produced by circulating virus within infected individuals.

ACKNOWLEDGMENTS

The author is grateful to Masayoshi Fukasawa (National Institute of Infectious Diseases, Department of Biochemistry and Cell Biology) for his helpful discussion. The author would also like to thank all members of the National Institute of Infectious Diseases, Department of Virology II, as well as the Hamamatsu University School of Medicine, Department of Infectious Diseases, for their technical support and valuable discussion and advice. This work was supported in part by a Grant-in-Aid from the Ministry of Health, Labor, and Welfare of Japan, and by a Grant-in-Aid from the Ministry of Education, Culture, Sports, Science, and Technology of Japan.

REFERENCES

Adair, R., Patel, A. H., Corless, L., Griffin, S., Rowlands, D. J., and Mccormick, C. J. (2009). Expression of hepatitis C virus (HCV) structural proteins in trans facilitates encapsidation and transmission of HCV subgenomic RNA. *J. Gen. Virol.* 90, 833–842.

Aizaki, H., Morikawa, K., Fukasawa, M., Hara, H., Inoue, Y., Tani, H., Saito, K., Nishijima, M., Hanada, K., Matsuura, Y., Lai, M. M. C., Miyamura, T., Wakita, T., and Suzuki, T. (2008). Critical role of virion-associated cholesterol and sphingolipid in hepatitis C virus infection. *J. Virol.* 82, 5715–5724.

Alsaleh, K., Delavalle, P.-Y., Pillez, A., Duverlie, G., Descamps, V., Rouille, Y., Dubuisson, J., and Wychowski, C. (2010). Identification of basic amino acids at the N-terminal end of the core protein that are crucial for hepatitis C virus infectivity. *J. Virol.* 84, 12515–12528.

Andre, P., Komurian-Pradel, F., Deforges, S., Perret, M., Berland, J. L., Sodoyer, M., Pol, S., Brechot, C., Paranhos-Baccala, G., and Lotteau, V. (2002). Characterization of low- and very-low-density hepatitis C virus RNA-containing particles. *J. Virol.* 76, 6919–6928.

Andre, P., Perlemuter, G., Budkowska, A., Brechot, C., and Lotteau, V. (2005). Hepatitis C virus particles and lipoprotein metabolism. *Semin. Liver Dis.* 25, 93–104.

Appel, N., Zayas, M., Miller, S., Krijnse-Locker, J., Schaller, T., Friebe, P., Kallis, S., Engel, U., and Bartenschlager, R. (2008). Essential role of domain III of nonstructural protein 5A for hepatitis C virus infectious particle assembly. *PLoS Pathog.* 4, e1000035. doi:10.1371/journal.ppat.1000035

Barba, G., Harper, F., Harada, T., Kohara, M., Goulinet, S., Matsuura, Y., Eder, G., Schaff, Z., Chapman, M. J., Miyamura, T., and Brechot, C. (1997). Hepatitis C virus core protein shows a cytoplasmic localization and associates to cellular lipid storage droplets. *Proc. Natl. Acad. Sci. U.S.A.* 94, 1200–1205.

Bartenschlager, R., Penin, F., Lohmann, V., and Andre, P. (2011). Assembly of infectious hepatitis C virus particles. *Trends Microbiol.* 19, 95–103.

Beach, M. J., Meeks, E. L., Mimms, L. T., Vallari, D., Ducharme, L., Spelbring, J., Taskar, S., Schleicher, J. B., Krawczynski, K., and Bradley, D. W. (1992). Temporal relationships of hepatitis C virus RNA and antibody responses following experimental infection of chimpanzees. *J. Med. Virol.* 36, 226–237.

Benga, W. J. A., Krieger, S. E., Dimitrova, M., Zeisel, M. B., Parnot, M., Lupberger, J., Hildt, E., Luo, G., Mclauchlan, J., Baumert, T. F., and Schuster, C. (2010). Apolipoprotein E interacts with hepatitis C virus nonstructural protein 5A and determines assembly of infectious particles. *Hepatology* 51, 43–53.

Boulant, S., Targett-Adams, P., and Mclauchlan, J. (2007). Disrupting the association of hepatitis C virus core protein with lipid droplets correlates with a loss in production of infectious virus. *J. Gen. Virol.* 88, 2204–2213.

Boulant, S., Vanbelle, C., Ebel, C., Penin, F., and Lavergne, J.-P. (2005). Hepatitis C virus core protein is a dimeric alpha-helical protein exhibiting membrane protein features. *J. Virol.* 79, 11353–11365.

Bradley, D., Mccaustland, K., Krawczynski, K., Spelbring, J., Humphrey, C., and Cook, E. H. (1991). Hepatitis C virus: buoyant density of the factor VIII-derived isolate in sucrose. *J. Med. Virol.* 34, 206–208.

Brohm, C., Steinmann, E., Friesland, M., Lorenz, I. C., Patel, A., Penin, F., Bartenschlager, R., and Pietschmann, T. (2009). Characterization of determinants important for hepatitis C virus p7 function in morphogenesis by using trans-complementation. *J. Virol.* 83, 11682–11693.

Bukh, J., Purcell, R. H., and Miller, R. H. (1992). Sequence analysis of the 5' noncoding region of hepatitis C virus. *Proc. Natl. Acad. Sci. U.S.A.* 89, 4942–4946.

Chang, K.-S., Jiang, J., Cai, Z., and Luo, G. (2007). Human apolipoprotein e is required for infectivity and production of hepatitis C virus in cell culture. *J. Virol.* 81, 13783–13793.

Counihan, N. A., Rawlinson, S. M., and Lindenbach, B. D. (2011). Trafficking of hepatitis C virus core protein during virus particle assembly. *PLoS Pathog.* 7, e1002302. doi:10.1371/journal.ppat.1002302

Davignon, J., Gregg, R. E., and Sing, C. F. (1988). Apolipoprotein E polymorphism and atherosclerosis. *Arteriosclerosis* 8, 1–21.

Dentzer, T. G., Lorenz, I. C., Evans, M. J., and Rice, C. M. (2009). Determinants of the hepatitis C virus nonstructural protein 2 protease domain required for production of infectious virus. *J. Virol.* 83, 12702–12713.

Friebe, P., and Bartenschlager, R. (2002). Genetic analysis of sequences in the 3' nontranslated region of hepatitis C virus that are important for RNA replication. *J. Virol.* 76, 5326–5338.

Friebe, P., Lohmann, V., Krieger, N., and Bartenschlager, R. (2001). Sequences in the 5' nontranslated region of hepatitis C virus required for RNA replication. *J. Virol.* 75, 12047–12057.

Gastaminza, P., Cheng, G., Wieland, S., Zhong, J., Liao, W., and Chisari, F. V. (2008). Cellular determinants of hepatitis C virus assembly, maturation, degradation, and secretion. *J. Virol.* 82, 2120–2129.

Han, Q., Xu, C., Wu, C., Zhu, W., Yang, R., and Chen, X. (2009). Compensatory mutations in NS3 and NS5A proteins enhance the virus production capability of hepatitis C reporter virus. *Virus Res.* 145, 63–73.

Helle, F., Vieyres, G., Elkrief, L., Popescu, C.-I., Wychowski, C., Descamps, V., Castelain, S., Roingeard, P., Duverlie, G., and Dubuisson, J. (2010). Role of N-linked glycans in the functions of hepatitis C virus envelope proteins incorporated into infectious virions. *J. Virol.* 84, 11905–11915.

Herker, E., Harris, C., Hernandez, C., Carpentier, A., Kaehlcke, K., Rosenberg, A. R., Farese, R. V. Jr., and Ott, M. (2010). Efficient hepatitis C virus particle formation requires diacylglycerol acyltransferase-1. *Nat. Med.* 16, 1295–1298.

Hishiki, T., Shimizu, Y., Tobita, R., Sugiyama, K., Ogawa, K., Funami, K., Ohsaki, Y., Fujimoto, T., Takaku, H., Wakita, T., Baumert, T. F., Miyanari, Y., and Shimotohno, K. (2010). Infectivity of hepatitis C virus is influenced by association with apolipoprotein E isoforms. *J. Virol.* 84, 12048–12057.

Honda, M., Brown, E. A., and Lemon, S. M. (1996). Stability of a stem-loop involving the initiator AUG controls the efficiency of internal initiation of translation on hepatitis C virus RNA. *RNA* 2, 955–968.

Hope, R. G., Murphy, D. J., and Mclauchlan, J. (2002). The domains required to direct core proteins of hepatitis C virus and GB virus-B to lipid droplets share common features with plant oleosin proteins. *J. Biol. Chem.* 277, 4261–4270.

Huang, H., Sun, F., Owen, D. M., Li, W., Chen, Y., Gale, M. Jr., and Ye, J. (2007). Hepatitis C virus production by human hepatocytes dependent on assembly and secretion of very low-density lipoproteins. *Proc. Natl. Acad. Sci. U.S.A.* 104, 5848–5853.

Huang, L., Hwang, J., Sharma, S. D., Hargittai, M. R. S., Chen, Y., Arnold, J. J., Raney, K. D., and Cameron, C. E. (2005). Hepatitis C virus nonstructural protein 5A (NS5A) is an RNA-binding protein. *J. Biol. Chem.* 280, 36417–36428.

Icard, V., Diaz, O., Scholtes, C., Perrin-Cocon, L., Ramiere, C., Bartenschlager, R., Penin, F., Lotteau, V., and Andre, P. (2009). Secretion of hepatitis C virus envelope glycoproteins depends on assembly of apolipoprotein B positive lipoproteins. *PLoS ONE* 4, e4233. doi:10.1371/journal.pone.0004233

Ishii, K., Murakami, K., Hmwe, S. S., Zhang, B., Li, J., Shirakura, M., Morikawa, K., Suzuki, R., Miyamura, T., Wakita, T., and Suzuki, T. (2008). Trans-encapsidation of hepatitis C virus subgenomic replicon RNA with viral structure proteins. *Biochem. Biophys. Res. Commun.* 371, 446–450.

Ito, T., and Lai, M. M. (1999). An internal polypyrimidine-tract-binding protein-binding site in the hepatitis C virus RNA attenuates translation, which is relieved by the 3'-untranslated sequence. *Virology* 254, 288–296.

Jiang, J., and Luo, G. (2009). Apolipoprotein E but not B is required for the formation of infectious hepatitis C virus particles. *J. Virol.* 83, 12680–12691.

Jirasko, V., Montserret, R., Appel, N., Janvier, A., Eustachi, L., Brohm, C., Steinmann, E., Pietschmann, T., Penin, F., and Bartenschlager, R. (2008). Structural and functional characterization of nonstructural protein 2 for its role in hepatitis C virus assembly. *J. Biol. Chem.* 283, 28546–28562.

Jirasko, V., Montserret, R., Lee, J. Y., Gouttenoire, J., Moradpour, D., Penin, F., and Bartenschlager, R. (2010). Structural and functional studies of nonstructural protein 2 of the hepatitis C virus reveal its key role as organizer of virion assembly. *PLoS Pathog.* 6, e1001233. doi:10.1371/journal.ppat.1001233

Jones, C. T., Murray, C. L., Eastman, D. K., Tassello, J., and Rice, C. M. (2007). Hepatitis C virus p7 and NS2 proteins are essential for production of infectious virus. *J. Virol.* 81, 8374–8383.

Kapadia, S. B., Barth, H., Baumert, T., Mckeating, J. A., and Chisari, F. V. (2007). Initiation of hepatitis C virus infection is dependent on cholesterol and cooperativity between CD81 and scavenger receptor B type I. *J. Virol.* 81, 374–383.

Klein, K. C., Dellos, S. R., and Lingappa, J. R. (2005). Identification of residues in the hepatitis C virus core protein that are critical for capsid assembly in a cell-free system. *J. Virol.* 79, 6814–6826.

Klein, K. C., Polyak, S. J., and Lingappa, J. R. (2004). Unique features of hepatitis C virus capsid formation revealed by de novo cell-free assembly. *J. Virol.* 78, 9257–9269.

Kopp, M., Murray, C. L., Jones, C. T., and Rice, C. M. (2010). Genetic analysis of the carboxy-terminal region of the hepatitis C virus core protein. *J. Virol.* 84, 1666–1673.

Kunkel, M., Lorinczi, M., Rijnbrand, R., Lemon, S. M., and Watowich, S. J. (2001). Self-assembly of nucleocapsid-like particles from recombinant hepatitis C virus core protein. *J. Virol.* 75, 2119–2129.

Kushima, Y., Wakita, T., and Hijikata, M. (2010). A disulfide-bonded dimer of the core protein of hepatitis C virus is important for virus-like particle production. *J. Virol.* 84, 9118–9127.

Lindenbach, B. D., Evans, M. J., Syder, A. J., Wolk, B., Tellinghuisen, T. L., Liu, C. C., Maruyama, T., Hynes, R. O., Burton, D. R., Mckeating, J. A., and Rice, C. M. (2005). Complete replication of hepatitis C virus in cell culture. *Science* 309, 623–626.

Lindenbach, B. D., Meuleman, P., Ploss, A., Vanwolleghem, T., Syder, A. J., Mckeating, J. A., Lanford, R. E., Feinstone, S. M., Major, M. E., Leroux-Roels, G., and Rice, C. M. (2006). Cell culture-grown hepatitis C virus is infectious in vivo and can be recultured in vitro. *Proc. Natl. Acad. Sci. U.S.A.* 103, 3805–3809.

Ma, Y., Anantpadma, M., Timpe, J. M., Shanmugam, S., Singh, S. M., Lemon, S. M., and Yi, M. (2011). Hepatitis C virus NS2 protein serves as a scaffold for virus assembly by interacting with both structural and nonstructural proteins. *J. Virol.* 85, 86–97.

Ma, Y., Yates, J., Liang, Y., Lemon, S. M., and Yi, M. (2008). NS3 helicase domains involved in infectious intracellular hepatitis C virus particle assembly. *J. Virol.* 82, 7624–7639.

Maillard, P., Huby, T., Andreo, U., Moreau, M., Chapman, J., and Budkowska, A. (2006). The interaction of natural hepatitis C virus with human scavenger receptor SR-BI/Cla1 is mediated by ApoB-containing lipoproteins. *FASEB J.* 20, 735–737.

Majeau, N., Gagne, V., Boivin, A., Bolduc, M., Majeau, J.-A., Ouellet, D., and Leclerc, D. (2004). The N-terminal half of the core protein of hepatitis C virus is sufficient for nucleocapsid formation. *J. Gen. Virol.* 85, 971–981.

Masaki, T., Suzuki, R., Murakami, K., Aizaki, H., Ishii, K., Murayama, A., Date, T., Matsuura, Y., Miyamura, T., Wakita, T., and Suzuki, T. (2008). Interaction of hepatitis C virus nonstructural protein 5A with core protein is critical for the production of infectious virus particles. *J. Virol.* 82, 7964–7976.

Masaki, T., Suzuki, R., Saeed, M., Mori, K.-I., Matsuda, M., Aizaki, H., Ishii, K., Maki, N., Miyamura, T., Matsuura, Y., Wakita, T., and Suzuki, T. (2010). Production of infectious hepatitis C virus by using RNA polymerase I-mediated transcription. *J. Virol.* 84, 5824–5835.

McLauchlan, J., Lemberg, M. K., Hope, G., and Martoglio, B. (2002). Intramembrane proteolysis promotes trafficking of hepatitis C virus core protein to lipid droplets. *EMBO J.* 21, 3980–3988.

McMullan, L. K., Grakoui, A., Evans, M. J., Mihalik, K., Puig, M., Branch, A. D., Feinstone, S. M., and Rice, C. M. (2007). Evidence for a functional RNA element in the hepatitis C virus core gene. *Proc. Natl. Acad. Sci. U.S.A.* 104, 2879–2884.

Meunier, J.-C., Russell, R. S., Engle, R. E., Faulk, K. N., Purcell, R. H., and Emerson, S. U. (2008). Apolipoprotein c1 association with hepatitis C virus. *J. Virol.* 82, 9647–9656.

Miyanari, Y., Atsuzawa, K., Usuda, N., Watashi, K., Hishiki, T., Zayas, M., Bartenschlager, R., Wakita, T., Hijikata, M., and Shimotohno, K. (2007). The lipid droplet is an important organelle for hepatitis C virus production. *Nat. Cell Biol.* 9, 1089–1097.

Moradpour, D., Brass, V., and Penin, F. (2005). Function follows form: the structure of the N-terminal domain of HCV NS5A. *Hepatology* 42, 732–735.

Moradpour, D., Wakita, T., Tokushige, K., Carlson, R. I., Krawczynski, K., and Wands, J. R. (1996). Characterization of three novel monoclonal antibodies against hepatitis C virus core protein. *J. Med. Virol.* 48, 234–241.

Moriishi, K., Mochizuki, R., Moriya, K., Miyamoto, H., Mori, Y., Abe, T., Murata, S., Tanaka, K., Miyamura, T., Suzuki, T., Koike, K., and Matsuura, Y. (2007). Critical role of PA28gamma in hepatitis C virus-associated steatogenesis and hepatocarcinogenesis. *Proc. Natl. Acad. Sci. U.S.A.* 104, 1661–1666.

Moriishi, K., Okabayashi, T., Nakai, K., Moriya, K., Koike, K., Murata, S., Chiba, T., Tanaka, K., Suzuki, R., Suzuki, T., Miyamura, T., and Matsuura, Y. (2003). Proteasome activator PA28gamma-dependent nuclear retention and degradation of hepatitis C virus core protein. *J. Virol.* 77, 10237–10249.

Moriishi, K., Shoji, I., Mori, Y., Suzuki, R., Suzuki, T., Kataoka, C., and Matsuura, Y. (2010). Involvement of PA28gamma in the propagation of hepatitis C virus. *Hepatology* 52, 411–420.

Moriya, K., Fujie, H., Shintani, Y., Yotsuyanagi, H., Tsutsumi, T., Ishibashi, K., Matsuura, Y., Kimura, S., Miyamura, T., and Koike, K. (1998). The core protein of hepatitis C virus induces hepatocellular carcinoma in transgenic mice. *Nat. Med.* 4, 1065–1067.

Murray, C. L., Jones, C. T., Tassello, J., and Rice, C. M. (2007). Alanine scanning of the hepatitis C virus core protein reveals numerous residues essential for production of infectious virus. *J. Virol.* 81, 10220–10231.

Nakai, K., Okamoto, T., Kimura-Someya, T., Ishii, K., Lim, C. K., Tani, H., Matsuo, E., Abe, T., Mori, Y., Suzuki, T., Miyamura, T., Nunberg, J. H., Moriishi, K., and Matsuura, Y. (2006). Oligomerization of hepatitis C virus core protein is crucial for interaction with the cytoplasmic domain of E1 envelope protein. *J. Virol.* 80, 11265–11273.

Nielsen, S. U., Bassendine, M. F., Burt, A. D., Martin, C., Pumeechockchai, W., and Toms, G. L. (2006). Association between hepatitis C virus and very-low-density lipoprotein (VLDL)/LDL analyzed in iodixanol density gradients. *J. Virol.* 80, 2418–2428.

Ogawa, K., Hishiki, T., Shimizu, Y., Funami, K., Sugiyama, K., Miyanari, Y., and Shimotohno, K. (2009). Hepatitis C virus utilizes lipid droplet for production of infectious virus. *Proc. Jpn. Acad. Ser. B Phys. Biol. Sci.* 85, 217–228.

Ogino, T., Fukuda, H., Imajoh-Ohmi, S., Kohara, M., and Nomoto, A. (2004). Membrane binding properties and terminal residues of the mature hepatitis C virus capsid protein in insect cells. *J. Virol.* 78, 11766–11777.

Okamoto, K., Mori, Y., Komoda, Y., Okamoto, T., Okochi, M., Takeda, M., Suzuki, T., Moriishi, K., and Matsuura, Y. (2008). Intramembrane processing by signal peptide peptidase regulates the membrane localization of hepatitis C virus core protein and viral propagation. *J. Virol.* 82, 8349–8361.

Okamoto, K., Moriishi, K., Miyamura, T., and Matsuura, Y. (2004). Intramembrane proteolysis and endoplasmic reticulum retention of hepatitis C virus core protein. *J. Virol.* 78, 6370–6380.

Op De Beeck, A., Voisset, C., Bartosch, B., Ciczora, Y., Cocquerel, L., Keck, Z., Foung, S., Cosset, F.-L., and Dubuisson, J. (2004). Characterization of functional hepatitis C virus envelope glycoproteins. *J. Virol.* 78, 2994–3002.

Owen, D. M., Huang, H., Ye, J., and Gale, M. Jr. (2009). Apolipoprotein E on hepatitis C virion facilitates infection through interaction with low-density lipoprotein receptor. *Virology* 394, 99–108.

Pawlotsky, J. M. (2006). Hepatitis C virus population dynamics during infection. *Curr. Top. Microbiol. Immunol.* 299, 261–284.

Phan, T., Beran, R. K. F., Peters, C., Lorenz, I. C., and Lindenbach, B. D. (2009). Hepatitis C virus NS2 protein contributes to virus particle assembly via opposing epistatic interactions with the E1-E2 glycoprotein and NS3-NS4A enzyme complexes. *J. Virol.* 83, 8379–8395.

Phan, T., Kohlway, A., Dimberu, P., Pyle, A. M., and Lindenbach, B. D. (2011). The acidic domain of hepatitis C virus NS4A contributes to RNA replication and virus particle assembly. *J. Virol.* 85, 1193–1204.

Pietschmann, T., Kaul, A., Koutsoudakis, G., Shavinskaya, A., Kallis, S., Steinmann, E., Abid, K., Negro, F., Dreux, M., Cosset, F.-L., and Bartenschlager, R. (2006). Construction and characterization of infectious intragenotypic and intergenotypic hepatitis C virus chimeras. *Proc. Natl. Acad. Sci. U.S.A.* 103, 7408–7413.

Popescu, C.-I., Callens, N., Trinel, D., Roingeard, P., Moradpour, D., Descamps, V., Duverlie, G., Penin, F., Heliot, L., Rouille, Y., and Dubuisson, J. (2011). NS2 protein of hepatitis C virus interacts with structural and non-structural proteins towards virus assembly. *PLoS Pathog.* 7, e1001278. doi:10.1371/journal.ppat.1001278

Rouille, Y., Helle, F., Delgrange, D., Roingeard, P., Voisset, C., Blanchard, E., Belouzard, S., Mckeating, J., Patel, A. H., Maertens, G., Wakita, T., Wychowski, C., and Dubuisson, J. (2006). Subcellular localization of hepatitis C virus structural proteins in a cell culture system that efficiently replicates the virus. *J. Virol.* 80, 2832–2841.

Saeed, M., Suzuki, R., Watanabe, N., Masaki, T., Tomonaga, M., Muhammad, A., Kato, T., Matsuura, Y., Watanabe, H., Wakita, T., and Suzuki, T. (2011). Role of the endoplasmic reticulum-associated degradation (ERAD) pathway in degradation of hepatitis C virus envelope proteins and production of virus particles. *J. Biol. Chem.* 286, 37264–37273.

Sakai, A., Claire, M. S., Faulk, K., Govindarajan, S., Emerson, S. U., Purcell, R. H., and Bukh, J. (2003). The p7 polypeptide of hepatitis C virus is critical for infectivity and contains functionally important genotype-specific sequences. *Proc. Natl. Acad. Sci. U.S.A.* 100, 11646–11651.

Schwer, B., Ren, S., Pietschmann, T., Kartenbeck, J., Kaehlcke, K., Bartenschlager, R., Yen, T. S. B., and Ott, M. (2004). Targeting of hepatitis C virus core protein to mitochondria through a novel C-terminal localization motif. *J. Virol.* 78, 7958–7968.

Shavinskaya, A., Boulant, S., Penin, F., Mclauchlan, J., and Bartenschlager, R. (2007). The lipid droplet binding domain of hepatitis C virus core protein is a major determinant for efficient virus assembly. *J. Biol. Chem.* 282, 37158–37169.

Shi, S. T., Polyak, S. J., Tu, H., Taylor, D. R., Gretch, D. R., and Lai, M. M. C. (2002). Hepatitis C virus NS5A colocalizes with the core protein on lipid droplets and interacts with apolipoproteins. *Virology* 292, 198–210.

Shirakura, M., Murakami, K., Ichimura, T., Suzuki, R., Shimoji, T., Fukuda, K., Abe, K., Sato, S., Fukasawa, M., Yamakawa, Y., Nishijima, M., Moriishi, K., Matsuura, Y., Wakita, T., Suzuki, T., Howley, P. M., Miyamura, T., and Shoji, I. (2007). E6AP ubiquitin ligase mediates ubiquitylation and degradation of hepatitis C virus core protein. *J. Virol.* 81, 1174–1185.

Simmonds, P. (1996). Virology of hepatitis C virus. *Clin. Ther.* 18 Suppl B, 9–36.

Stapleford, K. A., and Lindenbach, B. D. (2011). Hepatitis C virus NS2 coordinates virus particle assembly through physical interactions with the E1-E2 glycoprotein and NS3-NS4A enzyme complexes. *J. Virol.* 85, 1706–1717.

Steinmann, E., Brohm, C., Kallis, S., Bartenschlager, R., and Pietschmann, T. (2008). Efficient trans-encapsidation of hepatitis C virus RNAs into infectious virus-like particles. *J. Virol.* 82, 7034–7046.

Steinmann, E., Penin, F., Kallis, S., Patel, A. H., Bartenschlager, R., and Pietschmann, T. (2007). Hepatitis C virus p7 protein is crucial for assembly and release of infectious virions. *PLoS Pathog.* 3, e103. doi:10.1371/journal.ppat.0030103

Suzuki, R., Moriishi, K., Fukuda, K., Shirakura, M., Ishii, K., Shoji, I., Wakita, T., Miyamura, T., Matsuura, Y., and Suzuki, T. (2009). Proteasomal turnover of hepatitis C virus core protein is regulated by two distinct mechanisms: a ubiquitin-dependent mechanism and a ubiquitin-independent but PA28gamma-dependent mechanism. *J. Virol.* 83, 2389–2392.

Suzuki, R., Sakamoto, S., Tsutsumi, T., Rikimaru, A., Tanaka, K., Shimoike, T., Moriishi, K., Iwasaki, T., Mizumoto, K., Matsuura, Y., Miyamura, T., and Suzuki, T. (2005). Molecular determinants for subcellular localization of hepatitis C virus core protein. *J. Virol.* 79, 1271–1281.

Suzuki, R., Tamura, K., Li, J., Ishii, K., Matsuura, Y., Miyamura, T., and Suzuki, T. (2001). Ubiquitin-mediated degradation of hepatitis C virus core protein is regulated by processing at its carboxyl terminus. *Virology* 280, 301–309.

Tanaka, T., Kato, N., Cho, M. J., and Shimotohno, K. (1995). A novel sequence found at the 3' terminus of hepatitis C virus genome. *Biochem. Biophys. Res. Commun.* 215, 744–749.

Targett-Adams, P., Hope, G., Boulant, S., and Mclauchlan, J. (2008). Maturation of hepatitis C virus core protein by signal peptide peptidase is required for virus production. *J. Biol. Chem.* 283, 16850–16859.

Tellinghuisen, T. L., Foss, K. L., and Treadaway, J. (2008). Regulation of hepatitis C virion production via phosphorylation of the NS5A protein. *PLoS Pathog.* 4, e1000032. doi:10.1371/journal.ppat.1000032

Tellinghuisen, T. L., Marcotrigiano, J., and Rice, C. M. (2005). Structure of the zinc-binding domain of an essential component of the hepatitis C virus replicase. *Nature* 435, 374–379.

Thomssen, R., Bonk, S., Propfe, C., Heermann, K. H., Kochel, H. G., and Uy, A. (1992). Association of hepatitis C virus in human sera with beta-lipoprotein. *Med. Microbiol. Immunol.* 181, 293–300.

Tsukiyama-Kohara, K., Iizuka, N., Kohara, M., and Nomoto, A. (1992). Internal ribosome entry site within hepatitis C virus RNA. *J. Virol.* 66, 1476–1483.

Vieyres, G., Thomas, X., Descamps, V., Duverlie, G., Patel, A. H., and Dubuisson, J. (2010). Characterization of the envelope glycoproteins associated with infectious hepatitis C virus. *J. Virol.* 84, 10159–10168.

Voisset, C., Lavie, M., Helle, F., Op De Beeck, A., Bilheu, A., Bertrand-Michel, J., Terce, F., Cocquerel, L., Wychowski, C., Vu-Dac, N., and Dubuisson, J. (2008). Ceramide enrichment of the plasma membrane induces CD81 internalization and inhibits hepatitis C virus entry. *Cell. Microbiol.* 10, 606–617.

Wakita, T., Pietschmann, T., Kato, T., Date, T., Miyamoto, M., Zhao, Z., Murthy, K., Habermann, A., Krausslich, H.-G., Mizokami, M., Bartenschlager, R., and Liang, T. J. (2005). Production of infectious hepatitis C virus in tissue culture from a cloned viral genome. *Nat. Med.* 11, 791–796.

Wang, C., Sarnow, P., and Siddiqui, A. (1993). Translation of human hepatitis C virus RNA in cultured cells is mediated by an internal ribosome-binding mechanism. *J. Virol.* 67, 3338–3344.

Wasley, A., and Alter, M. J. (2000). Epidemiology of hepatitis C: geographic differences and temporal trends. *Semin. Liver Dis.* 20, 1–16.

Wolk, B., Sansonno, D., Krausslich, H. G., Dammacco, F., Rice, C. M., Blum, H. E., and Moradpour, D. (2000). Subcellular localization, stability, and trans-cleavage competence of the hepatitis C virus NS3-NS4A complex expressed in tetracycline-regulated cell lines. *J. Virol.* 74, 2293–2304.

Wozniak, A. L., Griffin, S., Rowlands, D., Harris, M., Yi, M., Lemon, S. M., and Weinman, S. A. (2010). Intracellular proton conductance of the hepatitis C virus p7 protein and its contribution to infectious virus production. *PLoS Pathog.* 6, e1001087. doi:10.1371/journal.ppat.1001087

Yamamoto, M., Aizaki, H., Fukasawa, M., Teraoka, T., Miyamura, T., Wakita, T., and Suzuki, T. (2011). Structural requirements of virion-associated cholesterol for infectivity, buoyant density and apolipoprotein association of hepatitis C virus. *J. Gen. Virol.* 92, 2082–2087.

Yasui, K., Wakita, T., Tsukiyama-Kohara, K., Funahashi, S. I., Ichikawa, M., Kajita, T., Moradpour, D., Wands, J. R., and Kohara, M. (1998). The native form and maturation process of hepatitis C virus core protein. *J. Virol.* 72, 6048–6055.

Yi, M., and Lemon, S. M. (2003). 3' Nontranslated RNA signals required for replication of hepatitis C virus RNA. *J. Virol.* 77, 3557–3568.

Yi, M., Ma, Y., Yates, J., and Lemon, S. M. (2007). Compensatory mutations in E1, p7, NS2, and NS3 enhance yields of cell culture-infectious intergenotypic chimeric hepatitis C virus. *J. Virol.* 81, 629–638.

Yi, M., Ma, Y., Yates, J., and Lemon, S. M. (2009). Trans-complementation of an NS2 defect in a late step in hepatitis C virus (HCV) particle assembly and maturation. *PLoS Pathog.* 5, e1000403. doi:10.1371/journal.ppat.1000403

Zhong, J., Gastaminza, P., Cheng, G., Kapadia, S., Kato, T., Burton, D. R., Wieland, S. F., Uprichard, S. L., Wakita, T., and Chisari, F. V. (2005). Robust hepatitis C virus infection in vitro. *Proc. Natl. Acad. Sci. U.S.A.* 102, 9294–9299.

Conflict of Interest Statement: The author declares that the research was conducted in the absence of any commercial or financial relationships that could be construed as a potential conflict of interest.

Received: 16 December 2011; accepted: 23 January 2012; published online: 07 February 2012.

Citation: Suzuki T (2012) Morphogenesis of infectious hepatitis C virus particles. Front. Microbio. ***3****:38. doi: 10.3389/fmicb.2012.00038*

This article was submitted to Frontiers in Virology, a specialty of Frontiers in Microbiology.

frontiers in
MICROBIOLOGY

ORIGINAL RESEARCH ARTICLE
published: 21 December 2011
doi: 10.3389/fmicb.2011.00251

The structure of the hantavirus zinc finger domain is conserved and represents the only natively folded region of the Gn cytoplasmic tail

D. Fernando Estrada[1], Michael Conner[1], Stephen C. St. Jeor[2] and Roberto N. De Guzman[1]*

[1] *Department of Molecular Biosciences, University of Kansas, Lawrence, KS, USA*
[2] *Department of Microbiology and Immunology, University of Nevada, Reno, NV, USA*

Edited by:
Akio Adachi, The University of Tokushima Graduate School, Japan

Reviewed by:
Yasuyuki Miyazaki, The University of Tokushima Graduate School, Japan
Masayuki Saijo, National Institute of Infectious Diseases, Japan

***Correspondence:**
Roberto N. De Guzman, Department of Molecular Biosciences, University of Kansas, 1200 Sunnyside Avenue, Lawrence, KS 66047, USA.
e-mail: rdguzman@ku.edu

Hantaviruses, of the family Bunyaviridae, are present throughout the world and cause a variety of infections ranging from the asymptomatic to mild and severe hemorrhagic fevers. Hantaviruses are enveloped anti-sense RNA viruses that contain three genomic segments that encode for a nucleocapsid protein, two membrane glycoproteins (Gn and Gc), and an RNA polymerase. Recently, the pathogenicity of hantaviruses has been mapped to the carboxyl end of the 150 residue Gn cytoplasmic tail. The Gn tail has also been shown to play a role in binding the ribonucleoprotein (RNP), a step critical for virus assembly. In this study, we use NMR spectroscopy to compare the structure of a Gn tail zinc finger domain of both a pathogenic (Andes) and a non-pathogenic (Prospect Hill) hantavirus. We demonstrate that despite a stark difference in the virulence of both of these viruses, the structure of the Gn core zinc finger domain is largely conserved in both strains. We also use NMR backbone relaxation studies to demonstrate that the regions of the Andes virus Gn tail immediately outside the zinc finger domain, sites known to bind the RNP, are disordered and flexible, thus intimating that the zinc finger domain is the only structured region of the Gn tail. These structural observations provide further insight into the role of the Gn tail during viral assembly as well as its role in pathogenesis.

Keywords: hantavirus, andes virus, Prospect Hill virus, zinc finger, glycoprotein

INTRODUCTION

Infection by a hantavirus can occur by inhalation of aerosolized urine or excrement from an infected rodent, thus leading a wide range of hemorrhagic fevers. European and Asian strains, for example, cause hemorrhagic fever with renal syndrome (HFRS), which is fatal in 1–15% of patients (Khaiboullina et al., 2005). The American strains, by contrast, cause the more severe hantavirus cardiopulmonary syndrome (HCPS), which is more aggressive and carries up to 40% mortality rate (Khaiboullina et al., 2005). Perhaps even more interesting are the two well known hantaviruses non-pathogenic to humans: Tula virus (present in European common voles) and the Prospect Hill virus (PHV; present in the American meadow vole; Mackow and Gavrilovskaya, 2009). In general, pathogenic and non-pathogenic hantaviruses appear to have a similar organization. They are enveloped and contain an anti-sense segmented RNA genome composed of a small (S) segment, medium (M) segment, and large (L) segment (Elliott et al., 2000). These in turn encode for the viral nucleocapsid protein, a glycoprotein polyprotein (subsequently processed into Gn and Gc proteins), and the RNA polymerase, respectively. RNA segments are bound to repeating trimers of the nucleocapsid protein into an assembled ribonucleocapsid (RNP) particle (Elliott et al., 2000).

As do most of the hantavirus structural proteins, the Gn glycoprotein has multiple functions in the viral replication cycle. As part of the virus envelope, it forms the structural core of a spike complex that consists of a multimeric arrangement of Gn and Gc glycoproteins, with a Gn tetramer at the center of the complex (Hepojoki et al., 2010a). On the cytoplasmic side of this complex, the inward facing 150 residue Gn cytoplasmic tail associates with the RNP during viral assembly (Hepojoki et al., 2010b,c; Wang et al., 2010; Battisti et al., 2011). Previously, we reported that a conserved array of cysteine and histidine residues (the dual CCHC motifs) within the Andes virus Gn tail folds into a compact dual ββα-type zinc fingers (Estrada et al., 2009a; Estrada and De Guzman, 2011). While ββα-type zinc fingers are primarily known for binding nucleic acids, the core zinc finger domain formed by 57-residues of the Andes virus Gn tail (residues 543–599) did not bind RNA *in vitro* (Estrada et al., 2009a), thus suggesting a role in protein–protein binding during the Gn–RNP interaction. Recently, Hepojoki et al. (2010c) showed that the Gn tail does bind the nucleocapsid (N) protein, the principal component of the RNP. Specifically, they showed that residues flanking the core zinc finger domain contain three binding sites (Binding sites 1, 2, and 3, **Figure 1**) for the N-protein (Hepojoki et al., 2010c). Others showed that the proper folding of the zinc finger domain was required for the ability of the Gn cytoplasmic tail to interact with the N-protein (Wang et al., 2010). These data strongly suggest a role for Gn tail in mediating an interaction with the N-protein.

Additionally, the Gn tails of hantaviruses also participate in determination of virulence, specifically by helping to modulate the host cell immune response to infection (Geimonen et al., 2003b; Alff et al., 2006, 2008). The non-pathogenic PHV tail fails

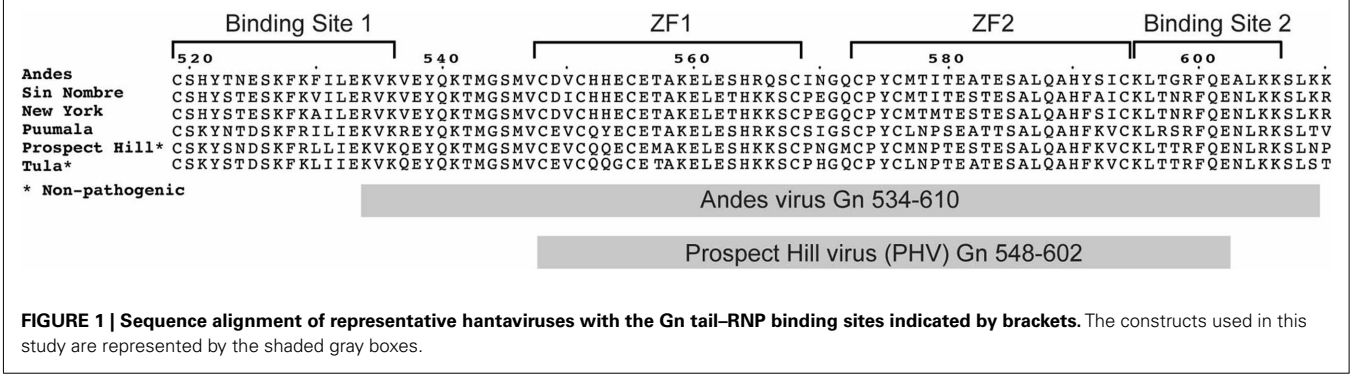

FIGURE 1 | Sequence alignment of representative hantaviruses with the Gn tail–RNP binding sites indicated by brackets. The constructs used in this study are represented by the shaded gray boxes.

to co-precipitate tumor necrosis factor receptor-associated factor 3 (TRAF3), as is the case for the New York hantavirus (Alff et al., 2008). TRAF3 is a key component of the host cell's interferon response to viral infection. In addition, the Gn tail of PHV was found not to be degraded, as is the case for typical pathogenic hantaviruses (Sen et al., 2007). However, the mutations of four residues at the carboxyl terminus of the Gn tail effectively targeted the PHV tail for proteasomal degradation (Sen et al., 2007). The observation of a virulence contribution by the Gn tail raises the possibility of potentially important differences between the predicted dual CCHC-type zinc finger domain of PHV and the structure determined for the pathogenic Andes virus (Estrada et al., 2009a). The two Gn tails overall are highly conserved between both viruses (75% identity, 84% similarity for the entire tail; 70% identity, 77% similarity for the zinc finger domain alone; **Figure 1**).

In this study, we used 2D and 3D NMR spectroscopy to compare the structures of two constructs representing segments of the cytoplasmic Gn tail for both a pathogenic (Andes virus) and a non-pathogenic hantavirus (PHV). Our NMR data suggests that, similar to the Andes virus, the dual CCHC motif of PHV forms an independently folded zinc binding domain. The Cα secondary chemical shifts of the PHV zinc finger domain are remarkably similar to those of the Andes structure, suggesting there is no appreciable difference in the two structures. These findings further support reports that the virulence determinants are located further toward the C-terminal end of the Gn tails. Furthermore, we also report the backbone assignment of an extended form of the Andes virus Gn tail (76 residues, from residues 534–610) that includes all of RNP Binding site 2 and part of RNP Binding site 1 (**Figure 1**). We demonstrate that Binding site 2 includes a short helix, while Binding site 1 appears to be largely disordered. Our results of NMR backbone dynamics indicate that both binding sites are flexible and undergo motion on a faster timescale than that of the core zinc finger domain. This enhanced motion may confer some degree of modularity in binding a crowded RNP complex. Taken together, these results provide novel structural insight into both the structural and immunogenic functions of the hantavirus Gn cytoplasmic tail.

MATERIALS AND METHODS

PROTEIN EXPRESSION AND PURIFICATION

For NMR data collection, the soluble Gn construct spanning residues 534–610 of the Andes virus Gn cytoplasmic tail (GenBank #AF291703) and residues 548–602 of the PHV Gn tails (GenBank #X55129) were expressed as fusion proteins with the *Streptococcal* GB1 domain linked with a tobacco etch virus (TEV) protease cleavage site (Estrada et al., 2009b). The fusion proteins were expressed and purified under native conditions following closely the method reported previously for the Andes virus zinc finger domain (Estrada et al., 2009b). Briefly, ^{15}N- and ^{15}N/^{13}C-labeled proteins were expressed in *E. coli* BL21(DE3) grown in 1 L M9 minimal media supplemented with 0.1 mM $ZnSO_4$ before and after induction. Cells were grown at 37°C, induced with 1 mM isopropyl-β-D-thiogalactopyranoside at $A_{600} \sim 0.8$, and cell growth was continued in a 15°C shaker overnight (to a final $A_{600} \sim 2.0$). Cells were centrifuged, resuspended in nickel column binding buffer (20 mM Tris–HCl pH 8.0, 500 mM NaCl, 5 mM imidazole, 0.1 mM $ZnSO_4$), and lysed by sonication. Cellular debris was removed by centrifugation, and to the supernatant was added $^1/_{10}$ volume of 1% polyethyleneimine (pH 8) to precipitate the nucleic acids. Following centrifugation, the supernatant was bound to a charged 10 mL nickel-affinity column and eluted with buffer (20 mM Tris–HCl pH 8.0, 500 mM NaCl, 250 mM imidazole, 0.1 mM $ZnSO_4$). For TEV protease digestion, fractions containing the fusion protein were pooled and dialyzed at 25°C overnight in buffer (50 mM Tris–HCl pH 8.0, 20 mM NaCl, 1 mM DTT, 1 mM $ZnSO_4$) with 0.16 mg recombinant TEV protease (Geisbrecht et al., 2006) per 10 mL of fusion protein. The TEV digestion mixture was dialyzed back into the nickel column binding buffer and passed again through a charged 10 mL nickel resin. The His-tagged GB1 protein was retained on the column while hantavirus Gn tail constructs were present in the flow-through. The flow-through fractions were analyzed by SDS-PAGE and key fractions pooled and concentrated using Ultra-15 centrifugal filters (Amicon) and dialyzed into NMR buffer (20 mM $NaPO_4$ pH 7.0, 20 mM NaCl, 1 mM DTT, 0.1 mM $ZnSO_4$). Both proteins retained two residues (Gly–His) cloning artifacts at the N-terminus.

Notably, approximately half of the expressed Andes virus Gn 534–610 remained in the insoluble portion upon lysis. This fraction was solubilized in 6 M urea and 10 mM DTT, then refolded by step-wise dialysis to remove the denaturant and digested with TEV protease as described above. While the ^{1}H–^{15}N HSQC spectrum of the refolded protein showed a similar peak pattern for the core zinc finger domain (residues 543–599), several of the additional peaks corresponding to the binding sites had

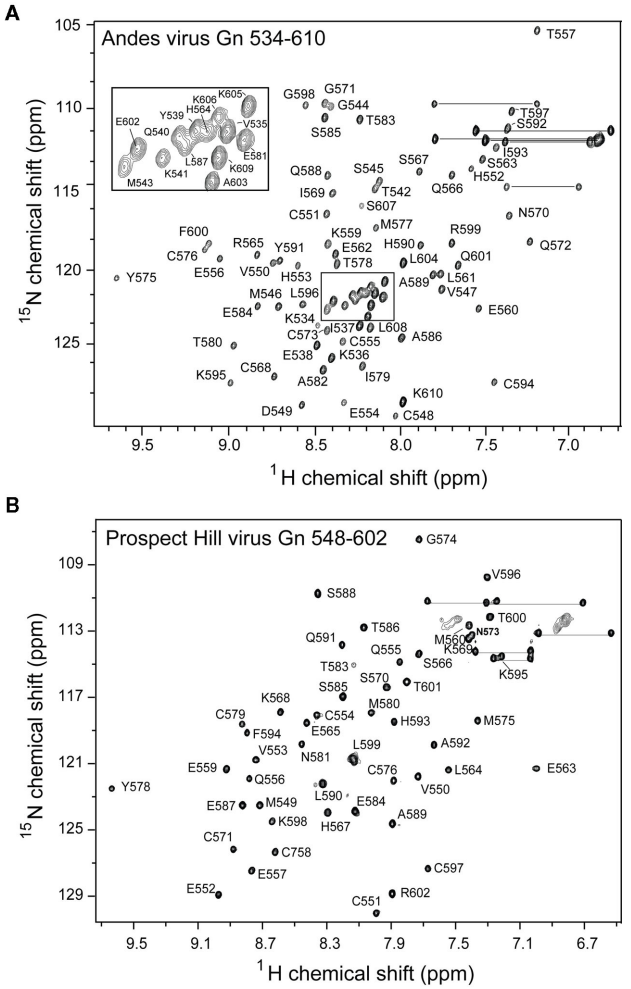

FIGURE 2 | Assigned 2D ^{1}H–^{15}N HSQC spectra for (A) the Andes Gn 534–610 and (B) the Prospect Hill virus Gn 548–602. Well-dispersed and resolved spectra for both constructs allowed complete assignment of the protein backbone.

different chemical shifts compared to the natively expressed protein (**Figure 2**). Therefore, the 3D NMR data used for analysis was collected exclusively on the natively expressed Andes virus Gn 534–610.

NMR SPECTROSCOPY

NMR data were acquired at 25˚C using a Bruker Avance 800 MHz spectrometer equipped with a cryoprobe, processed with NMRPipe (Delaglio et al., 1995), and analyzed with NMRView (Johnson, 2004). Backbone assignments for PHV Gn 548–602 were obtained from 2D ^{1}H–^{15}N HSQC (Grzesiek and Bax, 1993), 3D HNCA (Grzesiek et al., 1992), and HNCACB (Wittekind and Mueller, 1993) while assignments for Andes virus Gn 534–610 were obtained from the 2D ^{1}H–^{15}N HSQC and 3D HNCA alone. Secondary structures were identified from the Cα chemical shifts (Wishart and Nip, 1998). The heteronuclear {^{1}H}–^{15}N NOE for Andes virus Gn 534–610 was acquired as described (Stone et al., 1992) with 2048 (^{1}H) × 128 (^{15}N) complex points, 32 scans per point, and a 5-s recycle delay. Error bars were estimated using the SD of the background signal of each spectrum.

CD SPECTROSCOPY

CD spectra were collected in triplicate at 25˚ on a JASCO J-815 Spectropolarimeter using a scanning speed of 50 nm/min. Protein concentrations were kept at 5 μM in buffer (10 μM $NaPO_4$, 10 μM NaCl, 0.1 mM $ZnSO_4$). EDTA and $ZnSO_4$ titrations were applied to the same sample.

PHV ZF STRUCTURAL MODELING

Modeling of the structure of PHV Gn 548–602 was achieved by using the Andes dual zinc finger domain (PDB ID: 2K9H) as a template for the I-TASSER structure prediction software (Zhang, 2008). The model backbone was aligned with the backbone of the Andes virus Gn zinc finger structure using TM-Align (Zhang and Skolnick, 2005). Surface electrostatics were calculated using APBS (Baker et al., 2001) and visualized using Pymol (DeLano, 2002).

RESULTS

PROTEIN EXPRESSION

The PHV Gn tail construct was designed similarly to the previously published structure of the Andes virus core zinc finger domain (Estrada et al., 2009a), yielding a construct of residues 548–602. The Andes virus Gn tail construct used in this study include as much of the reported binding sites as possible, yielding a protein containing residues 534–610. Both proteins expressed well in *E. coli* as N-terminal GB1 fusion recombinant proteins and were purified under native conditions via ion exchange chromatography. Our attempts to express longer full-length Gn tail in Andes virus and other hantaviruses have been unsuccessful. However, the Andes virus Gn tail construct used for this study (76 residues) does represent the longest piece of the hantavirus Gn tail that is structurally characterized at atomic resolution. Incidentally, expression of the Andes virus Gn 548–602 construct yielded approximately half of the protein in inclusion bodies. Upon removal of the GB1 tag via cleavage by treatment with TEV protease, the Andes virus Gn 548–602 protein that was purified from the inclusion body and the natively purified fraction gave well resolved and well-dispersed ^{1}H–^{15}N HSQC spectra (**Figure 3**).

PHV GN TAIL RELIES ON Zn^{2+} FOR PROPER REFOLDING

As expected, treatment of the ^{15}N labeled PHV Gn 548–602 NMR sample with excess EDTA resulted in a near complete collapse of the 2D ^{1}H–^{15}N HSQC spectrum (**Figure 4A**), suggesting a loss of tertiary structure. Similarly, the CD trace of the PHV Gn 548–602 was also affected by the presence of EDTA (**Figure 4B**). The addition of Zn^{2+} back into the sample was only partially able to recover the original helical trace. This behavior of the PHV domain resembled that of the Andes protein (Estrada et al., 2009a), suggesting the confirmed cysteines and histidines in Gn tails were required for metal coordination.

NMR DATA AND BACKBONE ASSIGNMENTS

Prospect Hill virus Gn 548–602 and Andes virus Gn 534–610 both show a well-dispersed two-dimensional (2D) ^{1}H–^{15}N HSQC (**Figure 2**). However, an interesting feature of the natively folded

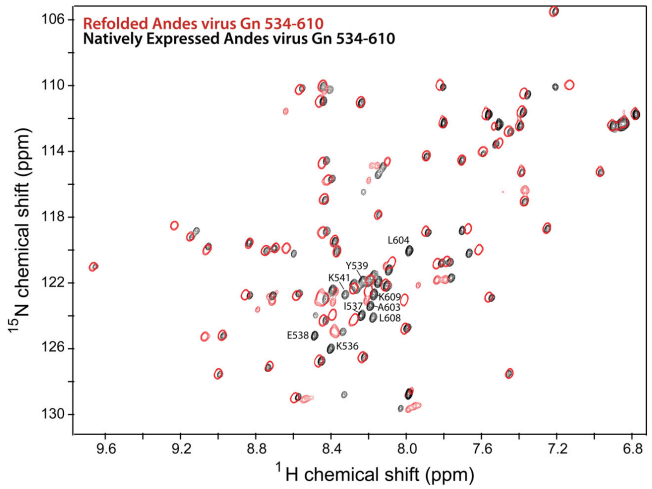

FIGURE 3 | Overlay of 2D ^{1}H–^{15}N HSQC spectra of the Andes virus Gn (534–610) that has been refolded from insoluble inclusion bodies (red) and that was natively expressed in the soluble fraction (black). Notably, the chemical shift values for the flanking sequences are different for each spectra, indication two conformations for these sequences.

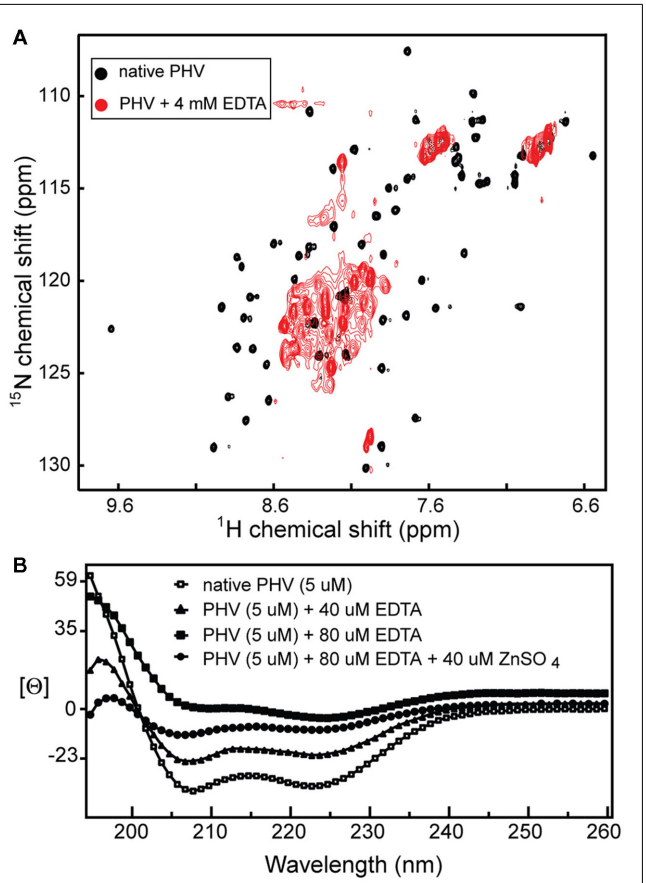

FIGURE 4 | (A) EDTA titration of the 2D ^{1}H–^{15}N HSQC spectrum of PHV Gn 548–602 causes a dramatic narrowing of the spectrum, suggesting a loss of tertiary structure and **(B)** the same effect on the protein CD trace [Θ is mean molar residue ellipticity (×107, degree·cm2/dmol·residue)].

Andes virus Gn 534–610 spectrum is that it differed from the spectrum of protein refolded from inclusion bodies. An overlay of the ^{1}H–^{15}N HSQC spectra of the refolded and natively expressed Andes virus Gn 534–610 confirmed that the majority of peaks are in identical positions and that the core zinc finger domain (residues 543–599; Estrada et al., 2009a) was properly folded (**Figure 3**). However, all subsequent data and assignments were conducted on the natively Andes virus Gn 534–610 expressed protein. Nearly complete backbone assignments were obtained from 2D and 3D NMR datasets for PHV Gn 548–620 and Andes virus Gn 534–610. Analysis of the Cα secondary chemical shifts for the PHV protein indicated the presence of two short α-helices and two random coil regions flanking the central domain (**Figure 5A**; Wishart and Nip, 1998). This pattern closely resembles that of the Andes virus Gn zinc finger domain (**Figure 5A**). Given the high degree of secondary structural similarity between the zinc binding domains in both structures (77% similarity) and the remarkable similarity of the Cα secondary chemical shift profile, full side chain assignments and structure determination of PHV Gn 548–620 was not continued.

SECONDARY CHEMICAL SHIFT PROFILE OF THE RNP BINDING SITES

Based on the HNCA-derived assignments of the Andes virus Gn 534–610 backbone, we constructed the secondary Cα chemical shift profile of both the core zinc finger domain (residues 543–599) along with the flanking sequences (**Figure 5B**). Notably, analysis of the profile suggested the N-terminal sequence (Lys^{534}–Met^{543}) was disordered. However, the C-terminus contained an intact helix between residues Arg^{599} and Lys^{606}. Another interesting feature was that the intervening sequence corresponding to the core zinc finger domain appeared largely unchanged from that of the protein without the flanking sequences, indicating that the presence of the binding sites reported by Hepojoki et al. (2010c) did not affect the local environment and had minimal contact with the core zinc finger domain.

BACKBONE DYNAMICS OF THE RNP BINDING SITES

Heteronuclear {^{1}H}–^{15}N NOE analysis of Andes virus Gn 534–610, which provides a probe on protein backbone dynamics, suggests that the core zinc finger domain is largely a rigid structure (**Figure 6A**). However, the flanking sequences are considerably more flexible. The disordered N-terminus is almost entirely flexible relative to the core structure as evident by the heteronuclear {^{1}H}–^{15}N NOE values below 0.2 in this region (**Figure 6A**). Notably, gradually increasing flexibility at the C-terminus corresponds to the tapering of helix α3, with greatest flexibility at the disordered five terminal residues. Backbone R_1 and R_2 relaxation results also indicate that the flanking sequences undergo motion on a faster time scale than the core zinc finger, with ZF1 and ZF2 both reflecting R_1 values of approximately 2.0, while the flanking sequences having R_1 values of approximately 4.0 (**Figure 6B**).

MODELING THE PHV GN ZINC FINGER STRUCTURE

The similarity between the secondary chemical shift profiles of the PHV and the Andes virus zinc binding domains suggest the two

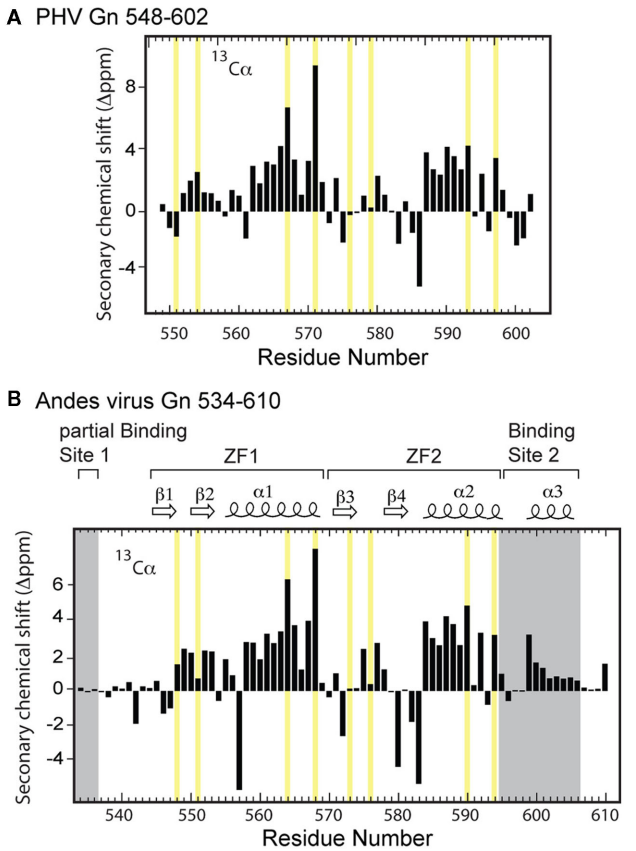

FIGURE 5 | Secondary Cα chemical shift profile for (A) PHV Gn 548–602 and (B) Andes virus Gn 534–610 zinc finger structures. The zinc coordinating residues are highlighted in yellow.

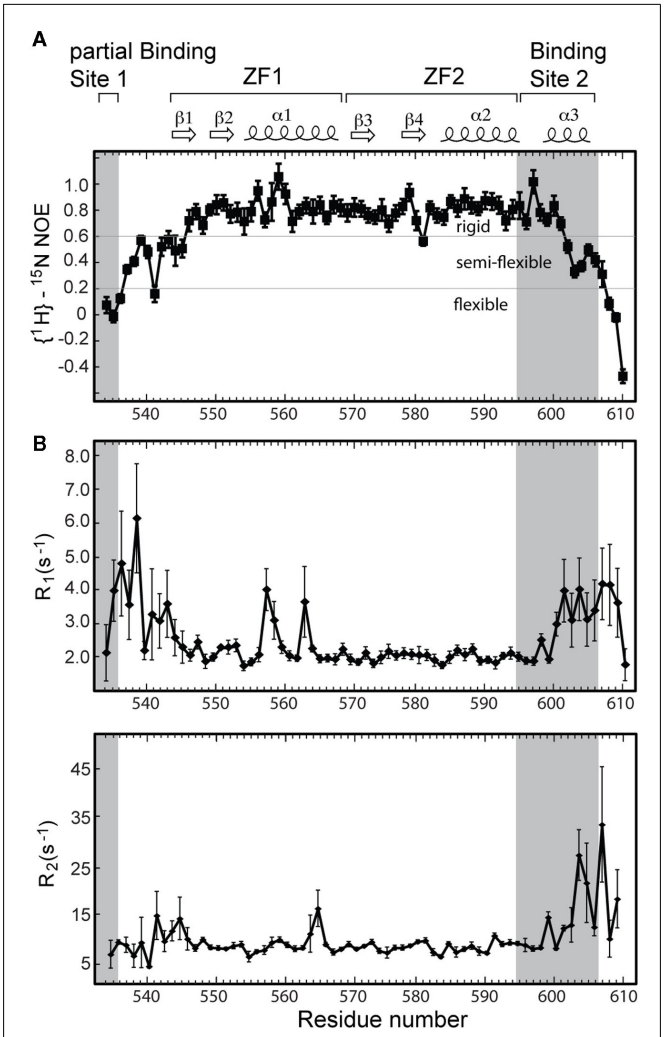

FIGURE 6 | (A) Heteronuclear {^{1}H}–^{15}N NOE values for the Andes virus zinc finger protein indicate enhanced flexibility corresponding to both binding sites. **(B)** The relative motions of each binding site are quantified with R_1 and R_2 relaxation rates. The spin–lattice relaxation rates R_1 suggest each binding site undergoes motions at least twice as fast as the rigid core zinc finger domain.

proteins have similar folds. Therefore, the structure of the Andes virus core zinc finger domain (residues 543–599, PDB ID 2K9H; Estrada et al., 2009a) was used as a template for the structural modeling of the PHV structure. The program I-TASSER (Zhang, 2008) was used to thread the PHV sequence onto the structure. The resulting structure is shown in **Figure 7A**. It closely resembles that of the Andes structure, with a backbone rmsd of 0.68 between the two (**Figure 7B**). Notably, the surface electrostatics of the PHV model closely resemble those of the Andes virus structure (**Figures 7C,D**) in that neither exhibit extensive clustering of charges.

DISCUSSION

Studies into the virulence of hantaviruses reveal several notable differences in cells infected by pathogenic and non-pathogenic hantaviruses. For example, while the non-pathogenic PHV still manages to infect endothelial cells, the virus apparently does not successfully replicate in humans (Mackow and Gavrilovskaya, 2009). This suggests PHV does not manage to evade the host immunogenic response. This notion is supported by evidence that early infection by PHV causes the induction of up to 24 early interferon genes, as opposed to only three by the pathogenic New York and Hantaan viruses (Geimonen et al., 2002; Spiropoulou et al., 2007).

Recent studies have begun to map virulence in hantaviruses to the Gn cytoplasmic tail (Geimonen et al., 2003a,b; Alff et al., 2006, 2008). In light of these findings, our structural studies were conducted on the predicted Gn tail zinc finger domain of the non-pathogenic PHV for the purpose of comparing the structure to that of the pathogenic Andes virus (**Figure 1**). Additionally, due to the recent report of the presence of Gn tail–RNP binding sites located proximal and on either side of the zinc finger domain of the Andes virus, the Andes protein used in this study represents a larger construct design to contain as much of the reported binding sites as possible. Due to the toxicity of the full-length Gn tail in bacteria, this latter construct (76 residues) represents the largest soluble segment of the Gn tail that we have been able to produce.

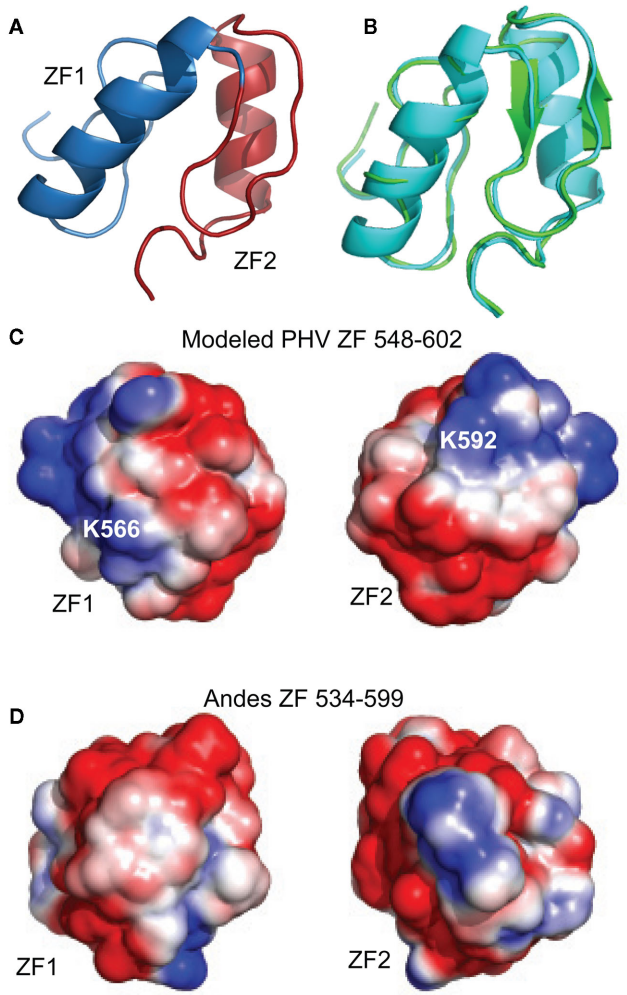

FIGURE 7 | Model of (A) PHV Gn 548–602 superimposed on the (B) Andes virus zinc finger structure. The PHV model (cyan) matched the Andes structure (green) with a backbone rmsd of 0.68 for all Cα's. The PHV model was constructed using I-TASSER (Zhang, 2008) using the Andes structure as a template. Structural alignment was carried out using I-TASSER TM-align (Zhang and Skolnick, 2005). Surface electrostatic comparison between the **(C)** PHV model (residues 548–602) and **(D)** the Andes virus zinc finger domain (residues 534–599). Despite the presence of two charges (K566 and K592), the net distribution of charges in the PHV model is not appreciably different from that of the pathogenic.

With respect to the PHV zinc finger domain, the CD data and the spectrum of the protein in the presence of chelator (**Figure 4A**) confirmed the presence of a metal binding domain. Specifically, the fact that titration of zinc sulfate back into the CD sample (**Figure 4B**) partially recovers the original spectrum indicates the domain binds zinc. These results compare favorably with the behavior of the core zinc finger domain in the Andes virus (Estrada et al., 2009a).

The 2D ^{1}H–^{15}N HSQC of the PHV Gn tail consisting of residues 548–602 showed a well-dispersed spectrum (**Figure 4A**), suggesting a monomeric and independently folded protein. Likewise, the ^{1}H–^{15}N HSQC spectrum of the extended Andes virus Gn 534–610 also showed well-dispersed and resolvable peaks (**Figure 2**). The high quality of the NMR data facilitated assignment of the backbone resonances, yielding the Cα chemical shift profile for both proteins. The profile of the PHV zinc finger domain is compared to that of the Andes virus in **Figure 5**. Given the high degree of sequence conservation, as well as conservation in the spacing of the dual CCHC motif (**Figure 1**), it is not surprising to find that the profiles of the core domain are remarkably similar. The only notable differences occur in the first and final coordinating cysteines (Cys^{551} and Cys^{597}, respectively). These differences may be due to the presence of two non-conserved residues, Glu^{552} and Lys^{598}, immediately following each cysteine.

One interesting feature of the PHV Gn amino acid sequence is the presence of a proline (Pro^{572}) in the linker. The proline is somewhat conserved; it is present in Tula and Hantaan viruses but absent in the Andes virus, which has an isoleucine in the same position. Interestingly, a residue with a rigid peptide bond in this position has little effect on the Cα secondary chemical shift of Cys^{571}. The secondary chemical shift profile for this part of the ZF1 array is virtually identical to that of the ZF1 array in the Andes virus structure (**Figure 5**), suggesting the tight turn between the β hairpin and helix of ZF1 is maintained despite the difference in residues in this region. This observation was an early indicator that the dual zinc finger fold is preserved despite large differences in chemical composition (**Figure 1**).

Due to the apparent similarity of the structures, we did not solve the three-dimensional (3D) structure of the PHV zinc finger domain. However, a model using I-TASSER (Zhang, 2008) and the Andes structure as a template was constructed to check the surface electrostatics of the protein which could then influence the molecular interactions of this protein. The modeled PHV zinc finger domain contains two similar short α-helices in a relative orientation as seen in the Andes structure (**Figure 7**). Previously, we have reported that the core zinc finger domain of a related Bunyavirus, the Crimean Congo Hemorrhagic Fever virus, contains a vastly different arrangement of basic charged residues on its surface when compared to the Andes virus structure (Estrada and De Guzman, 2011). With respect to the PHV model, we find that the surface electrostatics resemblance those of the Andes virus structure, with dispersed charges covering the zinc fingers. Only two non-conserved basic charges, K^{566} and K^{592}, are present which are not on the Andes virus structure. Despite these, the PHV structure is also acidic, with a theoretical isoelectric point of approximately 6.0, thus suggesting that differences in electrostatics of the core zinc finger domain are not likely to play a role in pathogenicity.

Overall, the PHV Gn zinc finger domain appears to adopt the same dual zinc finger fold to that of the pathogenic Andes virus. There were no obvious differences in either the secondary chemical shift profile or the predicted surface electrostatics. Based on this data we conclude that, given the widespread nature of the dual zinc finger fold in hantaviruses, its role is likely general in nature and apparently does not play a role in the determination of virulence. These conclusions are consistent with studies mapping virulence to the C-terminus of the Gn tails (Sen et al., 2007; Spiropoulou et al., 2007).

With respect to the role of the Gn tail in virus assembly, the amino acid sequences flanking the hantavirus zinc finger domain

have been shown to be important for Gn–N protein interaction (Hepojoki et al., 2010b). Specifically, short peptides representing these regions of the Gn tail disrupted the Gn–N protein interaction as detected using a SPOT peptide array (Hepojoki et al., 2010b). Generation of the extended zinc finger domain (534–610) in the Andes virus allowed us to characterize one full RNP binding site (Lys^{595}–Lys^{610}) and a portion of a second (Lys^{534} and Lys^{536}).

The reported Binding site 2 (Hepojoki et al., 2010c) contains the short helix α3 located near the carboxyl terminus. Helix α3 contains three conserved basic residues. Arg^{599} is located at the beginning turn of the helix, while the lysine pair located at positions 605 and 606 approximate the end of the helix. A helical wheel projection suggests that Arg^{599} and Lys^{606} are likely oriented in the same direction and may form a conserved basic patch. Notably, the surface opposite these charges contains the two conserved hydrophobic residues Phe^{600} and Leu^{604}, suggesting the helix is amphipathic. Despite this, the helix does not appear to form part of the independently folded core zinc finger domain.

Significantly, half of the protein expressed for this larger segment was insoluble. The solubilized and refolded fraction appeared to have a normal core zinc finger fold, as measured by an overlay of the previously published spectrum and that of the refolded Andes virus Gn (534–610). However, comparison of the spectrum of the refolded protein with that of the native protein revealed two distinct set of chemical shift values for the flanking sequences, thus indicating two separate conformations (**Figure 3**). While this was likely an artifact of refolding, it suggested the arms can be arranged independent of the core zinc finger structure. This notion is supported by the heteronuclear $\{^1H\}$–^{15}N NOE plot (**Figure 6A**), which suggests that much of the flanking sequence is either somewhat or fully flexible.

The presence of a Gn tetramer in the hantavirus spike complex suggests that four Gn cytoplasmic tails may participate in binding the RNP (Hepojoki et al., 2010a). Meanwhile, the RNP itself consists primarily of an N-protein trimer complexed with RNA (Alfadhli et al., 2001; Kaukinen et al., 2004; Mir and Panganiban, 2004) thus making the Gn–N protein binding site a crowded space where the important intra-molecular contacts may be complex and multivalent. Our NMR results indicate that the Gn tail consists of a structured core zinc finger domain that is flanked by flexible regions where the reported N-protein binding sites are located (Hepojoki et al., 2010c). The flexibility in Binding site 2 and part of Binding site 1 as described here may contribute to modularity of the Gn tail in binding at multiple sites. Thus, our NMR results, together with the results of others (Hepojoki et al., 2010c; Wang et al., 2010) suggest that backbone flexibility may be important in the molecular recognition of the Gn tail.

In summary, the work presented here strongly indicates that the conserved dual CCHC motif of hantavirus Gn cytoplasmic tails correlates to a structurally conserved dual zinc finger domain that likely represents the only structured region of the tail. The widespread nature of this domain within *Bunyaviridae* and the high degree of structural conservation both suggest an important role in viral assembly, possibly by helping to mediate inter-molecular contacts with the RNP. The RNP binding sites characterized here were shown to be flexible and move independently of the core Andes domain, thus suggesting some degree of modularity in the function of the Gn tail.

ACKNOWLEDGMENTS

We acknowledge funding from the American Heart Association 0755724Z (Roberto N. De Guzman), K-INBRE NIH P20 RR016475 (Roberto N. De Guzman), NIH AI065359 (Stephen C. St. Jeor), and the Madison and Lila Self Graduate Fellowship (D. Fernando Estrada). We are grateful to Gerard Kroon (Scripps Research Institute) and Asokan Anbanandam (University of Kansas) for helpful discussions.

REFERENCES

Alfadhli, A., Love, Z., Arvidson, B., Seeds, J., Willey, J., and Barklis, E. (2001). Hantavirus nucleocapsid protein oligomerization. *J. Virol.* 75, 2019–2023.

Alff, P. J., Gavrilovskaya, I. N., Gorbunova, E., Endriss, K., Chong, Y., Geimonen, E., Sen, N., Reich, N. C., and Mackow, E. R. (2006). The pathogenic NY-1 hantavirus G1 cytoplasmic tail inhibits RIG-I- and TBK-1-directed interferon responses. *J. Virol.* 80, 9676–9686.

Alff, P. J., Sen, N., Gorbunova, E., Gavrilovskaya, I. N., and Mackow, E. R. (2008). The NY-1 hantavirus Gn cytoplasmic tail coprecipitates TRAF3 and inhibits cellular interferon responses by disrupting TBK1-TRAF3 complex formation. *J. Virol.* 82, 9115–9122.

Baker, N. A., Sept, D., Joseph, S., Holst, M. J., and Mccammon, J. A. (2001). Electrostatics of nanosystems: application to microtubules and the ribosome. *Proc. Natl. Acad. Sci. U.S.A.* 98, 10037–10041.

Battisti, A. J., Chu, Y. K., Chipman, P. R., Kaufmann, B., Jonsson, C. B., and Rossmann, M. G. (2011). Structural studies of Hantaan virus. *J. Virol.* 85, 835–841.

Delaglio, F., Grzesiek, S., Vuister, G. W., Zhu, G., Pfeifer, J., and Bax, A. (1995). NMRPipe: a multidimensional spectral processing system based on UNIX pipes. *J. Biomol. NMR* 6, 277–293.

DeLano, W. L. (2002). *The PyMOL Molecular Graphics System.* San Carlos, CA: DeLano Scientific.

Elliott, R. M., Bouloy, M., Calisher, C. H., Goldbach, R., Moyer, J. T., Nichol, S. T., Pettersson, R., Plyusnin, A., and Schmaljohn, C. (2000). "Bunyaviridae," in *Virus Taxonomy: The classification and Nomenclature of Viruses. The Seventh Report of the International Committee on Taxonomy of Viruses*, eds M. H. V. Van Regenmortel, C. M. Fauquet, D. H. L. Bishop, E. B. Carsten, M. K. Estes, S. M. Lemon, J. Maniloff, M. A. Mayo, D. J. Mcgeoch, C. R. Pringle and R. B. Wickner (San Diego: Academic Press), 599–621.

Estrada, D. F., Boudreaux, D. M., Zhong, D., St Jeor, S. C., and De Guzman, R. N. (2009a). The hantavirus glycoprotein G1 tail contains dual CCHC-type classical zinc fingers. *J. Biol. Chem.* 284, 8654–8660.

Estrada, D. F., Boudreaux, D. M., Zhong, D., St. Jeor, S. C., and De Guzman, R. N. (2009b). The hantavirus glycoprotein G1 tail contains dual CCHC-type classical zinc fingers. *J. Biol. Chem.* 284, 8654–8660.

Estrada, D. F., and De Guzman, R. N. (2011). Structural characterization of the Crimean-Congo hemorrhagic fever virus Gn tail provides insight into virus assembly. *J. Biol. Chem.* 286, 21678–21686.

Geimonen, E., Fernandez, I., Gavrilovskaya, I. N., and Mackow, E. R. (2003a). Tyrosine residues direct the ubiquitination and degradation of the NY-1 hantavirus G1 cytoplasmic tail. *J. Virol.* 77, 10760–10868.

Geimonen, E., Lamonica, R., Springer, K., Farooqui, Y., Gavrilovskaya, I. N., and Mackow, E. R. (2003b). Hantavirus pulmonary syndrome-associated hantaviruses contain conserved and functional ITAM signaling elements. *J. Virol.* 77, 1638–1643.

Geimonen, E., Neff, S., Raymond, T., Kocer, S. S., Gavrilovskaya, I. N., and Mackow, E. R. (2002). Pathogenic and nonpathogenic hantaviruses differentially regulate endothelial cell responses. *Proc. Natl. Acad. Sci. U.S.A.* 99, 13837–13842.

Geisbrecht, B. V., Bouyain, S., and Pop, M. (2006). An optimized system for expression and purification of secreted bacterial proteins. *Protein Expr. Purif.* 46, 23–32.

Grzesiek, S., and Bax, A. (1993). The importance of not saturating H2O in protein NMR. Application to sensitivity enhancement and NOE measurements. *J. Am. Chem. Soc.* 115, 12593–12594.

Grzesiek, S., Dobeli, H., Gentz, R., Garotta, G., Labhardt, A. M., and Bax, A. (1992). 1H, 13C, and 15N NMR backbone assignments and secondary structure of human interferon-gamma. *Biochemistry* 31, 8180–8190.

Hepojoki, J., Strandin, T., Vaheri, A., and Lankinen, H. (2010a). Interactions and oligomerization of hantavirus glycoproteins. *J. Virol.* 84, 227–242.

Hepojoki, J., Strandin, T., Wang, H., Vapalahti, O., Vaheri, A., and Lankinen, H. (2010b). Cytoplasmic tails of hantavirus glycoproteins interact with the nucleocapsid protein. *J. Gen. Virol.* 91, 2341–2350.

Hepojoki, J. M., Strandin, T., Wang, H., Vapalahti, O., Vaheri, A., and Lankinen, H. (2010c). The cytoplasmic tails of hantavirus glycoproteins interact with the nucleocapsid protein. *J. Gen. Virol.* 91, 2341–2350.

Johnson, B. A. (2004). Using NMRView to visualize and analyze the NMR spectra of macromolecules. *Methods Mol. Biol.* 278, 313–352.

Kaukinen, P., Kumar, V., Tulimaki, K., Engelhardt, P., Vaheri, A., and Plyusnin, A. (2004). Oligomerization of hantavirus N protein: C-terminal alpha-helices interact to form a shared hydrophobic space. *J. Virol.* 78, 13669–13677.

Khaiboullina, S. F., Morzunov, S. P., and St Jeor, S. C. (2005). Hantaviruses: molecular biology, evolution and pathogenesis. *Curr. Mol. Med.* 5, 773–790.

Mackow, E. R., and Gavrilovskaya, I. N. (2009). Hantavirus regulation of endothelial cell functions. *Thromb. Haemost.* 102, 1030–1041.

Mir, M. A., and Panganiban, A. T. (2004). Trimeric hantavirus nucleocapsid protein binds specifically to the viral RNA panhandle. *J. Virol.* 78, 8281–8288.

Sen, N., Sen, A., and Mackow, E. R. (2007). Degrons at the C terminus of the pathogenic but not the nonpathogenic hantavirus G1 tail direct proteasomal degradation. *J. Virol.* 81, 4323–4330.

Spiropoulou, C. F., Albarino, C. G., Ksiazek, T. G., and Rollin, P. E. (2007). Andes and Prospect Hill hantaviruses differ in early induction of interferon although both can downregulate interferon signaling. *J. Virol.* 81, 2769–2776.

Stone, M. J., Fairbrother, W. J., Palmer, A. G., Iii, Reizer, J., Saier, M. H. Jr., and Wright, P. E. (1992). Backbone dynamics of the *Bacillus subtilis* glucose permease IIA domain determined from 15N NMR relaxation measurements. *Biochemistry* 31, 4394–4406.

Wang, H., Alminaite, A., Vaheri, A., and Plyusnin, A. (2010). Interaction between hantaviral nucleocapsid protein and the cytoplasmic tail of surface glycoprotein Gn. *Virus Res.* 151, 205–212.

Wishart, D. S., and Nip, A. M. (1998). Protein chemical shift analysis: a practical guide. *Biochem. Cell Biol.* 76, 153–163.

Wittekind, M., and Mueller, L. (1993). HNCACB, a high sensitivity 3D NMR experiment to correlate amide proton and nitrogen resonances with the alpha-carbon and beta-carbon resonances in proteins. *J. Magn. Reson.* 101B, 201–205.

Zhang, Y. (2008). I-TASSER server for protein 3D structure prediction. *BMC Bioinformatics* 9, 40. doi:10.1186/1471-2105-9-40

Zhang, Y., and Skolnick, J. (2005). TM-align: a protein structure alignment algorithm based on the TM-score. *Nucleic Acids Res.* 33, 2302–2309.

Conflict of Interest Statement: The authors declare that the research was conducted in the absence of any commercial or financial relationships that could be construed as a potential conflict of interest.

Received: 09 November 2011; paper pending published: 21 November 2011; accepted: 27 November 2011; published online: 21 December 2011.

Citation: Estrada DF, Conner M, Jeor SCS and Guzman RND (2011) The structure of the hantavirus zinc finger domain is conserved and represents the only natively folded region of the Gn cytoplasmic tail. Front. Microbio. ***2****:251. doi: 10.3389/fmicb.2011.00251*

This article was submitted to Frontiers in Virology, a specialty of Frontiers in Microbiology.

frontiers in
MICROBIOLOGY

REVIEW ARTICLE
published: 17 February 2012
doi: 10.3389/fmicb.2012.00055

Role of the HIV-1 matrix protein in Gag intracellular trafficking and targeting to the plasma membrane for virus assembly

Ruba H. Ghanam, Alexandra B. Samal, Timothy F. Fernandez and Jamil S. Saad*

Department of Microbiology, University of Alabama at Birmingham, Birmingham, AL, USA

Edited by:
Akio Adachi, The University of Tokushima Graduate School, Japan

Reviewed by:
Eric O. Freed, National Cancer Institute at Frederick, USA
Yasuyuki Miyazaki, The University of Tokushima Graduate School, Japan
Hironori Sato, National Institute of Infectious Diseases, Japan

***Correspondence:**
Jamil S. Saad, Department of Microbiology, University of Alabama at Birmingham, 845 19th Street South, Birmingham, AL 35294, USA.
e-mail: saad@uab.edu

Human immunodeficiency virus type-1 (HIV-1) encodes a polypeptide called Gag that is able to form virus-like particles *in vitro* in the absence of any cellular or viral constituents. During the late phase of the HIV-1 infection, Gag polyproteins are transported to the plasma membrane (PM) for assembly. In the past two decades, *in vivo*, *in vitro*, and structural studies have shown that Gag trafficking and targeting to the PM are orchestrated events that are dependent on multiple factors including cellular proteins and specific membrane lipids. The matrix (MA) domain of Gag has been the focus of these studies as it appears to be engaged in multiple intracellular interactions that are suggested to be critical for virus assembly and replication. The interaction between Gag and the PM is perhaps the most understood. It is now established that the ultimate localization of Gag on punctate sites on the PM is mediated by specific interactions between the MA domain of Gag and phosphatidylinositol-4,5-bisphosphate [PI(4,5)P_2], a minor lipid localized on the inner leaflet of the PM. Structure-based studies revealed that binding of PI(4,5)P_2 to MA induces minor conformational changes, leading to exposure of the myristyl (myr) group. Exposure of the myr group is also triggered by binding of calmodulin, enhanced by factors that promote protein self-association like the capsid domain of Gag, and is modulated by pH. Despite the steady progress in defining both the viral and cellular determinants of retroviral assembly and release, Gag's intracellular interactions and trafficking to its assembly sites in the infected cell are poorly understood. In this review, we summarize the current understanding of the structural and functional role of MA in HIV replication.

Keywords: assembly, Gag, matrix, myristyl, NMR, trafficking, plasma membrane

Human immunodeficiency virus type-1 (HIV-1), the causative agent of AIDS, is blamed for over 34 million deaths and is poised to claim over two million lives a year in the absence of efficient therapeutic intervention (UNAIDS report 2011). HIV-1 replication is strongly dependent on the cellular machinery to produce progeny virus. Since its discovery, efforts have focused on the development of effective vaccines and drugs that target different stages of the HIV lifecycle. Combinations of drugs that target protease, reverse transcriptase, integrase, or virus fusion form the basis of current antiretroviral therapy (ART; Greene et al., 2008). However, the genetic diversity and the ability of the virus to mutate to evade drug treatment remains a threat to the future success of ART. The discovery of cellular factors that participate in HIV-1 replication pathways has provided new insights into the molecular basis of virus–host cell interactions. Recent studies have identified hundreds of cellular factors that are involved in HIV replication (Brass et al., 2008; König et al., 2008; Zhou et al., 2008; Jäger et al., 2011; Lever and Jeang, 2011). Drugs that target the essential interactions of viral factors with host-proteins have the potential to not only complement current therapy, but may also overcome the problem of viral escape. As host-factors are stable and not diverse, the mutational capacity of the virus that usually allows for drug escape is thus restricted by the requirement to remain compatible to an invariant host-factor. Elucidation of the molecular interactions between the host cell and HIV are important for understanding the virus replication and the subsequent cytopathogenesis in the infected cell, which will aid in the development of more efficient antiviral drugs.

Retroviral genomes encode a polyprotein called Gag (**Figure 1**) that contains all the viral elements required for virus assembly and is capable of forming virus-like particles (VLPs) *in vitro* in the absence of viral and cellular constituents (Gheysen et al., 1989; Campbell and Rein, 1999; Campbell et al., 2001a). Subsequent to their synthesis, Gag proteins are targeted to the plasma membrane (PM) for assembly and budding (Adamson and Freed, 2007; Chu et al., 2010). During or shortly after budding, the virally encoded protease cleaves off Gag proteins at five positions into matrix (MA), capsid (CA), nucleocapsid (NC), spacer peptide 1 (SP1), spacer peptide 2 (SP2), and P6, which rearrange to form mature and infectious virions (**Figure 1**; Turner and Summers, 1999; Adamson and Freed, 2007; Ganser-Pornillos et al., 2008; Briggs and Kräusslich, 2011).

It is widely accepted that HIV-1 Gag budding and assembly occur predominantly on the PM (**Figure 1**; Hermida-Matsumoto and Resh, 2000; Jouvenet et al., 2006, 2008; Finzi et al., 2007; Li et al., 2007; Welsch et al., 2007; Gousset et al., 2008; Joshi

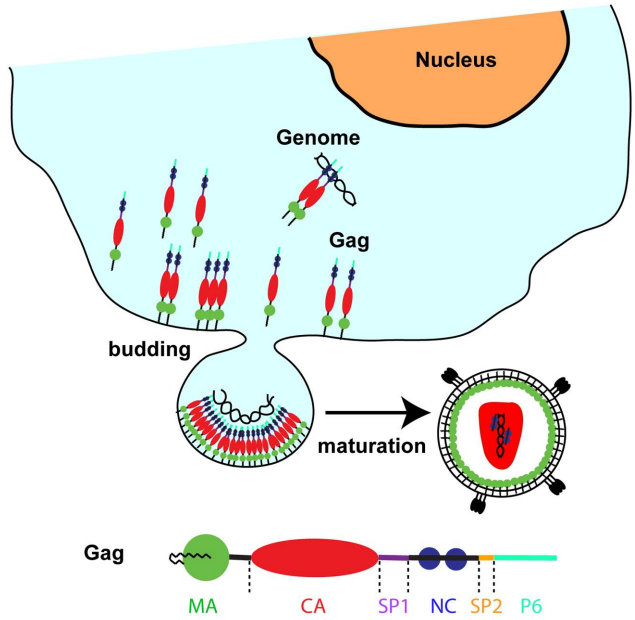

FIGURE 1 | Schematic representation showing the late phase of HIV replication involving Gag targeting and assembly on the plasma membrane.

et al., 2009a; Ono, 2009, 2010). Membrane binding is mediated by Gag's N-terminal myristoylated MA domain [myr(+)MA; Adamson and Freed, 2007; Ganser-Pornillos et al., 2008; Ono, 2009; Chukkapalli and Ono, 2011; Hamard-Peron and Muriaux, 2011]. The myristyl (myr) group functions in concert with a group of conserved basic residues to facilitate membrane anchoring and assembly of Gag. Mutations that either block myristoylation or disrupt the basic patch lead to inefficient Gag targeting to the PM, resulting in dramatically reduced virus production (Bryant and Ratner, 1990; Freed et al., 1994; Spearman et al., 1997; Hermida-Matsumoto and Resh, 2000; Ono et al., 2000b).

Role of the MA protein in HIV replication has been extensively examined. In this review, we focus on the functional role of MA in the late phase of infection. In the last few years, efforts have been focused on the identification of structural requirements that enable efficient Gag-membrane association. Success in producing the first retroviral matrix myristoylated protein for structural studies (Tang et al., 2004) afforded invaluable insight into understanding specific factors that regulate the myr switch and the potential implication in virus assembly.

INTRINSIC FACTORS THAT MODULATE THE myr SWITCH IN HIV-1 MA

In vitro studies have established that Gag binds membranes more efficiently than the isolated MA protein (Zhou and Resh, 1996; Spearman et al., 1997; Hermida-Matsumoto and Resh, 1999; Ono and Freed, 1999; Paillart and Gottlinger, 1999; Bouamr et al., 2003). This led to the hypothesis that the myr group is exposed in HIV-1 Gag and sequestered in the MA protein, which has come to be known the "myristyl switch mechanism" (Spearman et al., 1997; Hermida-Matsumoto and Resh, 1999; Ono and Freed, 1999; Bouamr et al., 2003). However, pioneering NMR structural studies by the Summers lab confirmed that the myr group can adopt sequestered [myr(s)] and exposed [myr(e)] conformations even in the isolated MA protein (Tang et al., 2004). Equilibrium data revealed that while myr(+)MA resides in monomer–trimer equilibrium, the myr(−)MA protein maintains the monomeric character in solution under all conditions (Tang et al., 2004). In addition, exposure of the myr group is coupled with protein trimerization (Tang et al., 2004). The myr switch was found to be sensitive to protein concentration, which led to the proposition of the "entropic switch mechanism" (Tang et al., 2004). Additionally, inclusion of the CA domain increases exposure of the myr group, which indicates that exposure of the myr group is dependent on Gag multimerization (Tang et al., 2004). Most recently, we have shown that myr exposure is also modulated by pH (Fledderman et al., 2010). Since these factors (protein concentration, multimerization, and pH) are intrinsically confined to the MA protein, we call them the "internal modulators."

Gag MULTIMERIZATION, A TRIGGER FOR myr EXPOSURE AND A REQUIREMENT FOR EFFICIENT MEMBRANE ASSOCIATION

As mentioned above, previous studies revealed that exposure of the myr group is coupled with protein trimerization and is enhanced by factors that promote protein self-association, such as increasing protein concentration or inclusion of the CA domain (Tang et al., 2004). HIV-1 Gag multimerization is directly linked to efficient membrane binding and is required for particle formation and viral infectivity (Burniston et al., 1999; Ono et al., 2000a; Lindwasser and Resh, 2001; Li et al., 2007). The oligomerization properties of HIV-1 Gag, MA, and MACA constructs have been extensively studied (Morikawa et al., 1998, 2000; Tang et al., 2004; Alfadhli et al., 2007, 2009a,b; Dalton et al., 2007; Datta et al., 2007b; Li et al., 2007; Saad et al., 2007a,b; Dou et al., 2009; Hogue et al., 2009). The CA domain contains a dimerization site in the C terminus and is known to play a central role in mediating Gag–Gag interactions (Li et al., 2000; Joshi et al., 2006; Ganser-Pornillos et al., 2007, 2008; Wright et al., 2007; Briggs et al., 2009; Hogue et al., 2009; Chukkapalli and Ono, 2011). Other domains such as SP1 and NC also play important roles in Gag multimerization and assembly (Dawson and Yu, 1998; Burniston et al., 1999; Campbell and Rein, 1999; Cimarelli et al., 2000; Morikawa et al., 2000; Muriaux et al., 2001; Wright et al., 2007; Briggs et al., 2009). Altogether, despite the lack of a detailed structural mechanism these findings indicate that myr exposure is enhanced through synergistic intermolecular interactions between Gag subdomains that cooperatively promote assembly.

MYRISTYL EXPOSURE IS MODULATED BY pH

One of the key characteristics of the HIV-1 myr(+)MA is the presence of the myr group in two energetically stable states: exposed and sequestered (Tang et al., 2004). In solution, these two states are at equilibrium. However, it seems that subtle changes in sample conditions such as protein concentration can perturb the equilibrium state (Tang et al., 2004). Analysis of the HIV-1 myr(+)MA structure revealed that the imidazole ring of His-89, which is highly conserved among all strains of HIV-1, HIV-2, and simian immunodeficiency virus (SIV; Los Alamos National Laboratory,

http://www.hiv.lanl.gov), forms a salt bridge with Glu-12(COO−) in HIV-1 myr(−)MA but not in the myr(+)MA protein. Histidine residues play important roles in biological activity as they are frequently included in the active sites of enzymes and contribute to protein stability and function. The intrinsic pK_a of the histidine imidazole group, which varies depending on the degree of burial or exposure within proteins (Edgcomb and Murphy, 2002), typically lies between 6.0 and 7.0 (Liu et al., 1997; Edgcomb and Murphy, 2002). Previous studies have shown that mutation of His-89 led to targeting of Gag to intracellular compartments and severely reduced virus production (Freed et al., 1994). We have recently shown that deprotonation of the His-89 imidazole ring in myr(+)MA destabilizes the salt bridge formed between His-89(Hδ2) and Glu-12(COO−; **Figure 2**), leading to tight sequestration of the myr group and a shift in the equilibrium from trimer to monomer (Fledderman et al., 2010). By using NMR methods, we calculated the pK_a of the histidine imidazole group in both myr(−)MA and myr(+)MA to be 6.5 (Fledderman et al., 2010). Furthermore, we have shown that oligomerization of a Gag-like construct containing MACA is also pH-dependent. Increasing the pH to 8 inhibited the formation of trimers for MA and MACA (**Figure 3**; Fledderman et al., 2010). These findings indicate that trimerization of Gag *in vitro*, although enhanced by CA, is solely driven by the MA domain and tightly regulated by pH. Based on these findings, we suggested that changes in pH might have an effect on the affinity of MA and Gag binding to membranes.

Earlier studies have also shown that mutation of His-89 and other residues in the vicinity led to targeting of Gag to intracellular compartments and severely reduced virus production (Freed et al., 1994). We recently found that the internal Gag puncta observed with H89G mutation colocalized extensively with CD63, indicating multivesicular bodies (MVB) localization (Fledderman et al., 2010). These results indicate that His-89 is essential for proper targeting of Gag to the PM and efficient particle formation in HeLa cells. Structural studies have shown that substitution of His-89 destabilized the tertiary structure, triggering myr exposure, and promoting high-order protein self-association (Fledderman et al., 2010).

Altogether, structural studies revealed that MA acts as a "pH sensor" and that, at least *in vitro*, myr exposure is regulated by pH. A potential role of pH variations in subcellular localization and targeting of Gag has not yet been established. Intracellular pH often fluctuates (6.3–7.8) in response to cell growth, development, and apoptosis (Schuldiner and Rozengurt, 1982; Moolenaar et al., 1983; Gottlieb et al., 1995). Alterations in the PM function can also be induced by cytopathic viruses including HIV-1 (Makutonina et al., 1996). A significant decrease in pH from 7.2 to as low as 6.0 was observed in cells infected by HIV-1 (Makutonina et al., 1996). Despite the *in vitro* evidence for pH effect on the myr switch, it has yet to be established whether manipulation of intracellular pH can alter kinetic pathways and sites or efficiency of Gag assembly.

MA RESIDUES THAT REGULATE THE myr SWITCH MECHANISM AND/OR Gag ASSEMBLY SITES

Mutagenesis studies in the past two decades have identified several residues in the MA domain that can alter Gag targeting and assembly (Bryant and Ratner, 1990; Freed et al., 1994; Zhou et al., 1994; Ono et al., 1997, 2000b; Ono and Freed, 1999, 2004; Paillart and Gottlinger, 1999; Joshi et al., 2009a; Chukkapalli et al., 2010). Several of these residues are located in the N-terminus of MA and are considered critical for proper membrane selection (Freed et al., 1994; Ono et al., 1997; Ono and Freed, 1999; Paillart and Gottlinger, 1999). More specifically, V7R, L8A, and L8I mutations give rise to a phenotype similar to that observed for the unmyristoylated protein without blocking myristoylation. These mutants, which display a hazy, non-punctate staining pattern typical of HIV-1 Gag mutants that are defective in membrane binding, cause a significant increase in cytosolic localization of Gag and severely inhibit virus assembly and release (Freed et al., 1994; Ono et al., 1997; Ono and Freed, 1999; Paillart and Gottlinger, 1999). In order to identify the structural basis for weak membrane association and diminished assembly of Gag V7R, L8A and L8I mutants, NMR, and analytical centrifugation studies have been performed on MA V7R, L8A, and L8I mutants (Saad et al., 2007b). NMR structures revealed that the backbone atoms of these mutants are very similar to the coordinates of the wild-type MA protein, indicating that single mutations in the N-terminal loop had no effect on the globular fold of the protein (Saad et al., 2007b). These studies, however, have shown that these mutations shut off the myr switch and lead to complete sequestration of the myr group (Saad et al.,

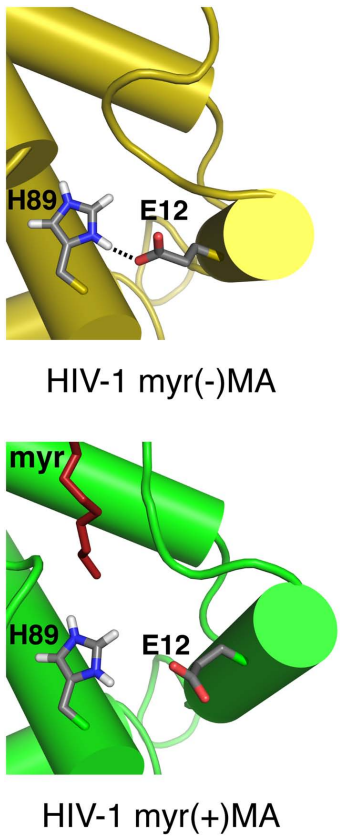

FIGURE 2 | The imidazole ring of His-89 forms a salt bridge with Glu-12(COO−) in HIV-1 myr(−)MA but not in myr(+)MA.

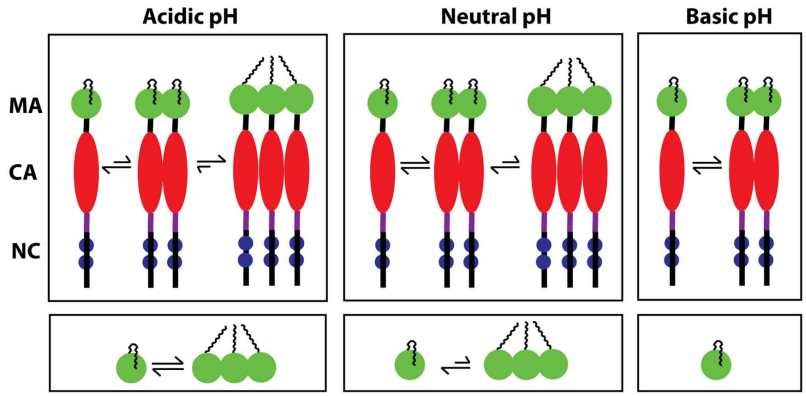

FIGURE 3 | Schematic representation showing multimerization events of Gag and MA proteins as a function of pH. Reprinted with permission from (Fledderman et al., 2010). Copyright {2010} American Chemical Society.

2007b). The main differences between the structures are localized within the disordered loop formed by residues Gly-2–Ser-9. For example, in the V7R MA structure the side chain of Arg-7 makes a salt bridge with the side chain of Glu-52, and the methylene groups of Arg-7 contribute to the hydrophobic interactions with the methylene groups of the myristate (Saad et al., 2007b). For L8A, the less bulky methyl group of Ala-8 creates a better cavity for the myristate group, which packs closer to Trp-16. Thus, structural changes involve only residues located near the mutation site, which may have only average intrinsic conformational mobility. The sensitivity of the myristyl switch equilibrium to subtle molecular changes is evident in the conservative substitution of Leu-8 by Ile, which is sufficient to block myristate exposure under conditions in which exposure is normally highly favored (Saad et al., 2007b). Altogether, *in vivo*, biochemical, and structural studies confirm that even conserved structural changes in the N-terminus of MA can lead to major effects on the myr switch, which in turn abrogate Gag binding to the PM and inhibit virus assembly.

Interestingly, the phenotype observed for mutants in the N-terminus is very different from that observed for mutants in the basic domain (e.g., K30E and K32E) or between residues 85 and 89, which have been shown to associate specifically with intracellular compartments like MVBs (Freed et al., 1994; Ono et al., 1997, 2000b; Ono and Freed, 2004; Joshi et al., 2009a). While the structural effect of K30E and K32E mutations on the myr switch is not yet known, we predict that substitutions between residues 85 and 89 may directly perturb the myr switch equilibrium. As mentioned above, H89G substitution in myr(+)MA led to formation of protein aggregates as a result of exposure of the myr group (Fledderman et al., 2010). Thus, it appears that sequestration or lack of myr group favors cytosolic localization rather than MVB association. Although targeting of Gag K30E/K32E mutant to MVB compartments led to severely defective virus particle production in HeLa cells (Ono et al., 2000b; Ono and Freed, 2004), recent evidence revealed that it can still support highly efficient assembly and release in T cells (Joshi et al., 2009a). It was suggested that under some circumstances, late endosomal compartments serve as productive sites for HIV assembly in some cell types (Joshi et al., 2009a).

ROLE OF PHOSPHATIDYLINOSITOL-4,5-BISPHOSPHATE [PI(4,5)P_2] IN HIV-1 Gag TARGETING, MEMBRANE BINDING, AND VIRUS ASSEMBLY

It is well established that assembly of retroviral Gag proteins occur predominantly on the PM (Hermida-Matsumoto and Resh, 2000; Jouvenet et al., 2006, 2008; Finzi et al., 2007; Li et al., 2007; Welsch et al., 2007; Gousset et al., 2008; Joshi et al., 2009a; Ono, 2009, 2010). Membrane selection appears to be critical for productive virus production. Rein and co-workers have shown that Gag constructs assemble *in vitro* into VLPs with diameters significantly smaller (25–30 nm) than those of authentic particles, whereas particles assembled in the presence of reticulocyte lysates exhibit normal diameters (∼100 nm; Campbell et al., 2001a). Further studies identified inositol pentaphosphate (IP5) as the active agent that promotes normal particle morphology and is capable of conferring resistance to disassembly in RNase, NaCl, and trypsin assays. Other inositol phosphates and IP derivatives, including inositol hexakisphosphate (IP6) and PI(4,5)P_2 (**Figure 4A**) had similar influence on *in vitro* Gag assembly, and mutagenesis studies suggested that they promote HIV-1 particle assembly by interacting with the MA domain of Gag (Campbell et al., 2001a; Crist et al., 2009). A Gag protein lacking residues 16–99 in its MA domain lost the requirement for inositol phosphates in assembly *in vitro*. Further exploration of the binding properties of IP6 to a Gag construct lacking the myr group and the p6 domain [myr(−)GagΔp6] revealed that both MA and NC domains of Gag contribute to IP6 binding (Datta et al., 2007b). Equilibrium studies have shown that myr(−)GagΔp6 undergoes an equilibrium switch from monomer–dimer in the absence of IP6 to monomer–trimer upon binding to IP6. However, myr(−)GagΔp6 with a mutation in the dimer interface of CA is monomeric in the presence of IP6, suggesting that the "dimer interface" is essential for the trimeric interaction (Datta et al., 2007b). These findings supported by hydrodynamic and small-angle neutron scattering (SANS) data led to the suggestion that the participation of both MA and NC domains of Gag in IP6 interaction is evidence for a folded conformation of Gag in solution, with its ends close to each other in the three-dimensional space (Datta et al., 2007a).

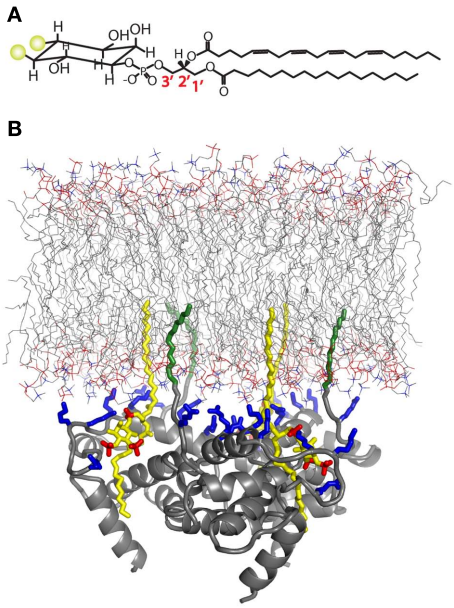

FIGURE 4 | (A) Representation of the PI(4,5)P_2 molecule (phosphate groups are shown as yellow balls), and **(B)** membrane binding model predicted from the structural studies; the exposed 1′-fatty acid chains (yellow) and myristyl groups (green) project from a highly basic surface (basic side chains shown in blue) in a manner expected to synergistically promote membrane binding. [**(B)** is reprinted from Saad et al., 2006; Copyright, Michael F. Summers, used with permission)].

Studies by Freed, Ono, and co-workers thereafter have provided compelling evidence that the ultimate localization of HIV-1 Gag on the PM is critically dependent on PI(4,5)P_2 (Ono et al., 2004; Chukkapalli et al., 2008, 2010; Chukkapalli and Ono, 2011). PI(4,5)P_2 is a membrane marker for proteins that are specifically targeted to the PM (Behnia and Munro, 2005; McLaughlin and Murray, 2005). Depletion of PI(4,5)P_2 by overexpression of 5-phosphatase IV (5ptase IV) led to accumulation of Gag at the membranes of late endosomes and MVBs, inhibited HIV assembly, and severely reduced virus production (Ono et al., 2004). Likewise, overexpression of a constitutively active form of Arf6 (Arf6/Q67L), which induces the formation of PI(4,5)P_2-enriched endosomal structures led to retargeting of Gag to these vesicles and severely reduced virus production. Sensitivity of Gag localization and assembly to PI(4,5)P_2 manipulation was lost upon substitution of the MA domain with the N-terminus of Fyn kinase [Fyn(10)ΔMA/delNC], which is not affected by 5ptaseIV overexpression. Altogether, these findings supported the hypothesis that interactions between MA and PI(4,5)P_2 are essential for proper Gag targeting and membrane binding.

NMR studies have been utilized to identify how MA interacts with PI(4,5)P_2 (Saad et al., 2006). NMR chemical shift perturbation data obtained for the MA protein revealed that residues Arg-22, Lys-26, Lys-27, His-33, Glu-73, Leu-75, and Ser-77 were the most affected upon binding of soluble analogs of PI(4,5)P_2 (Saad et al., 2006). These residues reside on a cleft formed by helices II and V, and a β hairpin (β-II-V cleft). Although these studies marked the first structural evidence for direct interactions between HIV-1 MA and a cellular constituent, the two most intriguing observations were the PI(4,5)P_2 binding mode and the effect of binding on the myr switch. The three-dimensional structure of the MA-PI(4,5)P_2 complex revealed that the acyl chain attached to the 2′-position of the glycerol packs within the β-II–V cleft against the side chains of Leu-21, Lys-27, Tyr-29, His-33, Trp-36, and Ser-77, while the phosphoinositide head group packs against Leu-21 and Lys-27, burying the 2′-fatty acid chain (**Figure 4A**). The 1′-acyl chain, however, is exposed to solvent with PI(4,5)P_2 molecule adopting an "extended lipid" conformation. Binding of PI(4,5)P_2 to MA induces a minor conformational change entailing a repositioning of helix I and destabilization of the hydrophobic cavity, leading to myr exposure. These results indicate that PI(4,5)P_2 acts as both a trigger of the myr switch and as a membrane anchor and suggest a potential mechanism for targeting Gag to membrane rafts (**Figure 4B**; Saad et al., 2006). Interestingly, the proposed membrane binding mode is very similar to the "extended lipid" conformation predicted in the phospholipid–cytochrome *c* model (Kinnunen et al., 1994; Rytömaa and Kinnunen, 1995; Tuominen et al., 2002).

Of particular note, our studies represent the first evidence that PI(4,5)P_2 can adopt an extended conformation. The hydrophobic cleft that interacts with the 2′-acyl chain of PI(4,5)P_2 analogs with short chains (four- and eight-carbon atoms) is also capable of accommodating longer fatty acids without inducing any major changes in the protein structure. A model of the trimeric PI(4,5)P_2:myr(+)MA–membrane complex constructed by using 18- and 20-carbon 1′- and 2′-acyl chains is shown in **Figure 4B**. Native PI(4,5)P_2 forms micelles in aqueous solution, making it virtually impossible to study its interaction with MA by NMR methods (Janmey et al., 1987). Difficulties in characterizing the binding of native PI(4,5)P_2 with the MA protein have only been overcome upon encapsulating the protein in reverse micelles (Valentine et al., 2010). Titration of MA with native PI(4,5)P_2 in reverse micelles has led to significant chemical shift changes in a subset of amide signals. Mapping of the chemical shift changes on the MA surface indicates a binding mode similar to that of the soluble analogs with short chains.

Binding of native PI(4,5)P_2 to myr(−)GagΔp6 has been characterized by mass spectrometric protein footprinting (Shkriabai et al., 2006). NHS-biotin modification approach was used to identify lysine residues in Gag that are exposed to solvent or those that are protected from biotinylation due to direct Gag-PI(4,5)P_2 contacts. Data revealed that among 21 surface Lys residues readily modified in free Gag, only MA K30 and K32 are protected in the Gag-PI(4,5)P_2 complex. Although NMR and mass spectrometry methods provide evidence for direct binding of native PI(4,5)P_2 to MA, the exact binding interface, and a high-resolution structural model have yet to be determined. Based on the NMR data obtained for MA in reverse micelles, our best guess is that the 20-carbon 2′-acyl chain of PI(4,5)P_2 is sequestered by the protein.

Confocal microscopy data revealed that Gag molecules assemble at punctate sites on the PM (Hermida-Matsumoto and Resh, 2000). What are these punctate sites and why does Gag select these sites? To address these questions, we recall a few previous observations that could support the structural studies and the MA–PI(4,5)P_2 binding mode as well as the overall association

with the PM. First, there is evidence that punctate sites comprise lipid raft microdomains (Aloia et al., 1993; Nguyen and Hildreth, 2000; Campbell et al., 2001b; Ono and Freed, 2001, 2005; Ding et al., 2003; Holm et al., 2003; Waheed and Freed, 2009). Lipid rafts are typically liquid-ordered membrane structures that contain elevated levels of cholesterol and sphingolipids with saturated fatty acids (Brown and London, 1997, 1998; Melkonian et al., 1999; Zacharias et al., 2002; Ono and Freed, 2005; Waheed and Freed, 2009). Proteins that associate with lipid rafts generally contain two saturated acyl chains or are anchored by adaptor molecules that contain two saturated chains (for example, glycosylphosphatidylinositol-anchored proteins; Brown and London, 2000; Ono and Freed, 2005). Because PI(4,5)P_2 contains stearate (18-carbon saturated acyl chain) at the 1′-position and arachidonate (20-carbon acyl chain with four non-conjugated double bonds) at the 2′-position, sequestration of the 2′-chain is likely to reduce the affinity of PI(4,5)P_2 for fluid regions of the membrane and promote its association with rafts. Since previous studies also suggest that PI(4,5)P_2 molecules are homogeneously dispersed within the PM of quiescent cells but they can colocalize with lipid rafts upon stimulation (Golub and Caroni, 2005), sequestration of the 2′-acyl chain by MA may suggest a potential mechanism for the lateral targeting of PI(4,5)P_2:Gag complexes to lipid raft microdomains (Saad et al., 2006). Second, the proposed mechanism for Gag binding to membrane is supported by the finding that substitution of the saturated myr group of HIV-1 Gag by unsaturated lipids reduces the affinity of Gag for rafts and inhibits particle assembly (Lindwasser and Resh, 2002).

Gag-PI(4,5)P_2 INTERACTIONS IN OTHER RETROVIRUSES

In the past few years, efforts have been focused on whether Gag targeting and virus assembly in other retroviruses are also dependent on PI(4,5)P_2. Subsequent to our studies on HIV-1, we discovered that HIV-2 MA binds specifically to PI(4,5)P_2 in a manner identical to that of HIV-1 (Saad et al., 2008). However, in HIV-2 MA the myr switch is less sensitive to PI(4,5)P_2 binding as the myr group is found to be sequestered in the complex. The subcellular site of HIV-2 Gag assembly is also regulated by PI(4,5)P_2. Like HIV-1, overexpression of 5ptaseIV or Arf6/Q67L also significantly reduced levels of released HIV-2 virions, indicating that the production of HIV-2 particles is inhibited by PI(4,5)P_2 perturbation (Saad et al., 2008).

In most retroviruses, membrane anchoring is strongly dependent on the myr group. However, Gag proteins of some retroviruses, notably alpha retroviruses [the prototype of which is Rous sarcoma virus (RSV)] and the lentivirus equine infectious anemia virus (EIAV), lack myr modification, and Gag targeting and binding to the PM is mainly mediated by electrostatic interactions (Erdie and Wills, 1990; Provitera et al., 2000; Dalton et al., 2005). For example, the association of RSV MA protein with liposomes of defined composition is electrostatic in nature and is dependent on the presence of a biologically relevant concentration of negatively charged lipids like phosphatidylserine (Dalton et al., 2005). In addition, MA-PI(4,5)P_2 interactions have been detected in Moloney murine leukemia virus (MMLV) and Mason-Pfizer monkey virus (MPMV; Stansell et al., 2007; Chan et al., 2008; Chen et al., 2008; Hamard-Peron et al., 2010). As has been observed for HIV-1 and HIV-2 MA, NMR-based studies have shown that a soluble analog of PI(4,5)P_2 interacts directly with EIAV MA, suggesting a potential role of this lipid in EIAV Gag assembly (Chen et al., 2008). However, a most recent study investigating the role of PI(4,5)P_2 in assembly of EIAV show that Gag was detected on the PM and in compartments enriched in phosphatidylinositol 3,5-biphosphate [PI(3,5)P_2; Fernandes et al., 2011]. NMR studies have shown that EIAV MA binds to phosphatidylinositol 3-phosphate [PI(3)P] with a higher affinity than that of PI(4,5)P_2 (Fernandes et al., 2011). Treatment of cells with YM201636, a kinase inhibitor that blocks production of PI(3,5)P_2 from PI(3)P led to Gag colocalization with aberrant compartments and inhibited VLP release (Fernandes et al., 2011). In contrast to HIV-1, release of EIAV VLPs was not significantly diminished by coexpression with 5ptase IV. Taken together, these results indicate that membrane targeting in EIAV proceeds via a mechanism that is probably distinct from that in HIV-1 or HIV-2. On the other hand, when compared to HIV-1 and HIV-2 recent studies have shown that human T-lymphotropic virus type (HTLV-1) and RSV Gag proteins have either lower or no requirement for PI(4,5)P_2 for membrane association (Chan et al., 2011; Inlora et al., 2011).

ROLE OF Gag IN ENVELOPE (Env) INCORPORATION

Retroviral Env protein is a glycosylated polyprotein synthesized as intact gp160 precursor that is subsequently cleaved by cellular proteases to form a complex of a surface unit (gp120) and transmembrane domain (gp41). During virus assembly, the gp120/gp41 complex is incorporated in the lipid bilayer of the nascent virions. Despite the progress made in understanding the structural details of Env and its components as well as the trafficking pathway of Env polyprotein, the mechanism by which Env is incorporated into virus particles is not completely understood. The Gag protein has long been implicated in Env incorporation based on the proposed interaction between the MA domain and the cytoplasmic (CT) domain of gp41 (Yu et al., 1992; Dorfman et al., 1994; Freed and Martin, 1995, 1996; Mammano et al., 1995). However, importance of this interaction is controversial since in many cell lines (HeLa, 293T, CV-1, and COS), deletion of the CT domain has virtually no effect on Env incorporation (Wilk et al., 1992; Freed and Martin, 1995, 1996; Murakami and Freed, 2000). Checkley et al. (2011) have recently reviewed the current understanding of HIV-1 Env trafficking and incorporation into virions. Several models have been proposed to explain Env incorporation into virus particles (Checkley et al., 2011):

(i) *"Passive" model*: Env is expressed on the host PM and subsequently incorporated into budding virions. Support of this model stems from the observation that host membrane proteins are abundantly incorporated into retrovirus particles (Lusso et al., 1990; Arthur et al., 1992; Ott, 2008).

(ii) *Direct Gag–Env interaction*: Genetic data revealed that the MA domain of Gag is required for Env incorporation (Yu et al., 1992; Dorfman et al., 1994; Freed and Martin, 1995, 1996). Mutations in or deletion of the MA domain of Gag decreased Env incorporation (Freed and Martin, 1995, 1996; Mammano et al., 1995; Reil et al., 1998; Brandano and Stevenson, 2012), while deletion of the gp41 CT domain reversed the Env incorporation defect dictated by MA mutations (Freed

and Martin, 1995, 1996; Mammano et al., 1995), or MA deletion (Reil et al., 1998). Altogether, these studies suggest that MA is required for full-length Env incorporation whereas Env–MA interaction is apparently not required for incorporation of truncated Env. The requirement of the MA and CT domains for Gag–gp41 interactions appears to be supported by a few studies albeit evidence for direct interactions is still weak. For example, previous studies have shown that HIV-1 Env is localized to the basolateral surface of polarized epithelial cells (Owens and Compans, 1989). Gag has been shown to bud in a non-polarized manner in these cells when Env was not expressed. Budding, however, was restricted to the basolateral surface upon coexpression of Gag and Env (Owens et al., 1991). Mutations in MA or CT truncation undermined the ability of Env to direct basolateral budding of Gag (Lodge et al., 1994). Although these studies suggest a cross-talk between the MA and CT domains, they do not necessarily indicate a direct interaction (Checkley et al., 2011).

(iii) *Gag–Env cotargeting*: As mentioned above, the absence of compelling evidence for direct interactions between Gag and gp41 may suggest that a cellular constituent like a protein or membrane acts as a bridge or a docking platform for the Gag–Env complex. A role of a cellular factor(s) in Env incorporation is perhaps supported by the results showing that the requirement of CT domain is strongly dependent on the cell type (permissive cells like HeLa, COS, and 293T; Wilk et al., 1992; Akari et al., 2000; Murakami and Freed, 2000). In non-permissive cell lines (e.g., T cells and macrophages), removal of gp41 CT led to ∼10-fold decrease in Env incorporation (Murakami and Freed, 2000). The identity of cellular factors required for Env incorporation in permissive and non-permissive cells have yet to be determined.

(iv) *Indirect Gag–Env interaction*: Since it is not clear whether there is a direct interaction between the MA domain of Gag and gp41 CT, it is conceivable that the interaction is mediated by cellular protein(s). Among the gp41 CT-interacting proteins are the adaptor protein complexes AP-1 and AP-2. The AP complexes are heterotetramers that mediate both the recruitment of clathrin to membranes and the recognition of sorting signals within the cytosolic tails of transmembrane cargo molecules (Robinson and Bonifacino, 2001; Boehm and Bonifacino, 2002; Nakatsu and Ohno, 2003). While AP-1 has been shown to regulate the subcellular localization of Env via binding to a dileucine motif in gp41 CT (Berlioz-Torrent et al., 1999; Byland et al., 2007; Wyss et al., 2011), AP-2 has been shown to bind to the gp41 CT domain and drive clathrin-mediated endocytosis of Env from the PM (Ohno et al., 1997; Boge et al., 1998). Interestingly, AP-1 and AP-2 has been shown to bind to the MA domain of Gag (see below; Batonick et al., 2005; Camus et al., 2007). Other proteins like the 47-kDa tail interacting protein (TIP47) and calmodulin (CaM) have been proposed to play some role in Env incorporation (discussed in more details below).

POTENTIAL ROLE OF MA IN GENOMIC RNA PACKAGING

Although MA's role in HIV-1 Gag targeting and assembly on the PM is the best understood, there is mounting evidence that it also plays a role in retroviral genome packaging. A recent review has shed light on the current understanding of the functional role of MA in genome packaging (Parent and Gudleski, 2011). Since the MA protein is usually associated to the lipid bilayer and on the opposite end from the NC domain, the biological importance for the proposed MA–RNA interactions is controversial and has been under scrutiny for a long time. Interest in assessing the functional role of MA in genome packaging stems from earlier studies on the interactions between HIV-1 MA and other retroviruses (e.g., RSV and bovine leukemia virus) with single-stranded and double-stranded DNA and RNA (Leis et al., 1978; Darlix and Spahr, 1982; Méric and Spahr, 1986; Steeg and Vogt, 1990; Katoh et al., 1991; Ott et al., 2005; Alfadhli et al., 2009b; Cai et al., 2010; Ramalingam et al., 2011). It has been shown that MA binds directly to an RNA molecule that is highly homologous to a fragment of the *pol* domain (Purohit et al., 2001). The interaction interface of MA is confined to the basic domain; substitutions in the basic residues led to weakened affinity to RNA *in vitro* and a delay in virus replication *in vivo* (Purohit et al., 2001). However, it has yet to be established whether MA binds directly to the packaging signal (ψ) of the RNA genome.

Most recent studies by Akira Ono and co-workers revealed that the highly basic region (HBR) in the N-terminus of MA not only contributes to binding of $PI(4,5)P_2$ to Gag, but is also capable of binding to RNA (Chukkapalli et al., 2010). These results are consistent with *in vitro* and NMR studies (Purohit et al., 2001; Hearps et al., 2008; Alfadhli et al., 2011). Interestingly, binding of RNA to HBR was found to inhibit association of Gag to membrane liposomes in the absence of $PI(4,5)P_2$ (Chukkapalli et al., 2010). As a consequence, RNA was considered as a negative regulator of Gag-membrane binding. Thus, the interplay between Gag, $PI(4,5)P_2$, and RNA appears to be an important aspect of Gag assembly that has to be examined further.

THE MISSING LINK: HIV-1 Gag *EN ROUTE* TO THE PLASMA MEMBRANE?

Great progress has been made in defining both the viral and cellular determinants of HIV-1 assembly and release (Chu et al., 2010). However, the trafficking pathway used by Gag to reach its assembly sites in the infected cell is poorly understood. There is mounting evidence that HIV-1 Gag interacts with several cellular proteins during the replication cycle. These include CaM (Radding et al., 2000), the human adaptor protein complexes AP-1, AP-2, and AP-3 (Batonick et al., 2005; Dong et al., 2005; Camus et al., 2007), TIP47 (Lopez-Vergès et al., 2006), Golgi-localized gammaear containing Arf-binding protein (GGA; Joshi et al., 2008, 2009b), ADP ribosylation factor (Arf; Joshi et al., 2008), the suppressor of cytokine signaling 1 (SOCS1; Ryo et al., 2008; Nishi et al., 2009), a lymphoid specific Src kinase (Lck; Strasner et al., 2008), *N*-ethylmaleimide-sensitive factor attachment protein receptor (SNARE; Joshi et al., 2011), Filamin A (Cooper et al., 2011), vacuolar protein sorting-associated protein 18 (Vps18; Tomita et al., 2011), Mon2 (Tomita et al., 2011), and Lyric (Engeland et al., 2011). The majority of these proteins have been implicated in retroviral assembly. Since we are focusing on the MA protein, we will summarize the current understanding of the proposed interactions between the MA domain of Gag and a small selection of the proteins described above including CaM, AP-3, TIP47, SOCS1, and Lyric.

POTENTIAL ROLE OF CaM IN HIV REPLICATION

CaM is a ubiquitous calcium-binding protein expressed in all eukaryotic cells. It binds to and regulates different protein targets, thereby affecting many different cellular functions (Osawa et al., 1999; Chin and Means, 2000; Hoeflich and Ikura, 2002; Vetter and Leclerc, 2003; Yamniuk and Vogel, 2004; Ishida and Vogel, 2006). It binds more than 100 proteins "specifically" (Rogers and Strehler, 1996) and is found in different subcellular locations, including the cytoplasm, within organelles, or associated with the plasma or organelle membranes (Osawa et al., 1999; Chin and Means, 2000; Hoeflich and Ikura, 2002; Vetter and Leclerc, 2003; Yamniuk and Vogel, 2004; Ishida and Vogel, 2006). CaM is perhaps one of the most characterized cellular proteins and its interactions with proteins have been extensively studied (Chattopadhyaya et al., 1992; Finn et al., 1995; Chin and Means, 2000; Fallon and Quiocho, 2003). Binding of calcium to CaM triggers a major conformational change and helical rearrangement, enabling it to bind to specific proteins for a specific response.

Subcellular distribution of CaM in HIV-infected cells has been shown to be distinct from that observed in uninfected cells (Radding et al., 1996). *In vivo* and *in vitro* studies revealed that CaM interacts with HIV-1 Gag, Nef, and gp160 proteins (Towler et al., 1988; Srinivas et al., 1993; Radding et al., 2000; Hayashi et al., 2002; Matsubara et al., 2005). Pioneering studies by Hunter and co-workers have shown that HIV-1 Gag can interact with CaM in a calcium-dependent manner (Radding et al., 2000). Gag and CaM colocalize in a diffuse pattern in the cytoplasm. Investigation of the underlying mechanism of Gag–CaM interactions has gained some momentum recently. Our lab (Ghanam et al., 2010) and others (Chow et al., 2010) have shown that CaM binds directly to the MA protein with 1:1 stoichiometry in a Ca^{2+}-dependent manner. We have also established that: (i) CaM-binding to myr(+)MA induces a structural change that triggers myr exposure (**Figure 5**), (ii) the myr group is not involved in CaM-binding, and (iii) CaM–MA interaction is hydrophobic and entropically driven, while electrostatic interactions appear to be inconsequential (Ghanam et al., 2010).

Radding et al. (2000) have shown that peptides from the N-terminus of MA bind to CaM with variable affinities and in different modes. These studies have prompted others to conduct SAXS experiments to elucidate the global features of CaM bound to short peptides derived from the MA protein (Izumi et al., 2008). SAXS studies conducted on CaM complexed with full-length MA shed light on the global features of the complex (Chow et al., 2010). However, SAXS methods cannot provide details on the complex interface and cannot identify specific residues that are important for the formation and stabilization of the complex. We have utilized NMR, biochemical, and biophysical methods to elucidate the precise molecular mechanism of MA–CaM interactions (Samal et al., 2011). In this work, we have (i) identified the interaction interface of CaM bound to short peptides derived from the MA protein, (ii) shown that MA peptides bind to CaM with variable affinities and diverse modes, and (iii) identified the minimal CaM-binding domain of MA as residues 8–43 (MA-8–43).

A typical CaM-binding peptide is 15–30 residues long with amphipathic character and a propensity to form an α-helix (Ishida and Vogel, 2006), features that helices I and II of MA possess

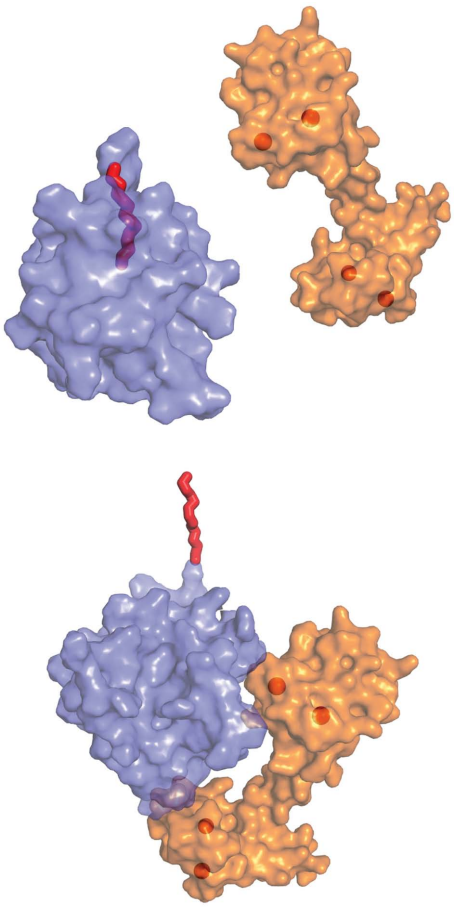

FIGURE 5 | CaM-binding to MA triggers myr exposure. Surface representation of CaM (orange) and myr(+)MA (slate) with the myr group (red) sequestered and exposed in the free and bound states, respectively. Spheres represent Ca^{2+} ions.

(**Figure 6**). The 36-residue long MA-8–43 peptide is perhaps one of the largest CaM-binding motifs to be discovered. The fact that MA-8–43 forms two helices is another striking feature of this peptide since almost all known CaM-target proteins usually possess a domain that forms only one α-helix. In many of the classical CaM-binding targets, hydrophobic residues usually occupy conserved positions at 1–5–10 or 1–8–14, which point to one face of the helix (Ishida and Vogel, 2006). Although these patterns are typically found in many CaM-binding proteins, numerous unclassified examples were also identified (Ishida and Vogel, 2006). By using a web-based tool to identify a sequence pattern with potential CaM-binding sites (Yap et al., 2000), the region between Arg22 and Glu40 (**Figure 6**) scored the highest. Scores are based on several criteria including hydropathy, α-helical propensity, residue weight and charge, hydrophobic residue content, helical class, and occurrence of particular residues. Arg22–Glu40 represents the majority of helix II. However, this peptide does not contain a motif that matches any of the known patterns of CaM-binding sites. Thus, MA-8–43 is considered a novel and unclassified CaM-binding sequence that is substantially different (in length and composition)

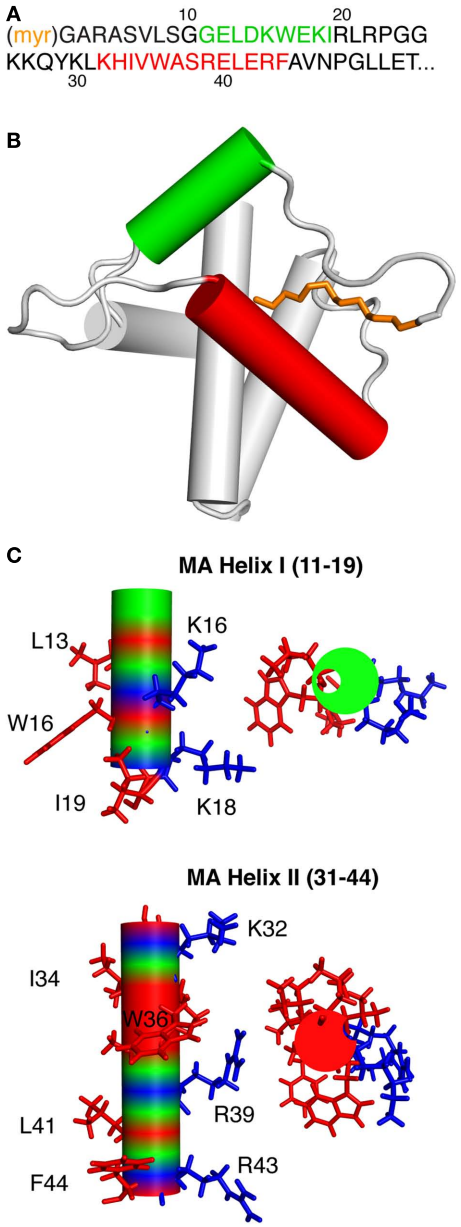

FIGURE 6 | (A) Amino acid sequence of the N-terminus of MA. **(B)** Cartoon representation of the NMR structure (2H3I) of myr(+)MA highlighting helices I and II in green and red, respectively. Myr group is shown in orange. **(C)** Amphipathic character of helices I and II with hydrophobic and basic residues shown in red and blue, respectively, "A modified version of this figure was published in the Journal of Biological Chemistry. Samal et al., 2011; The American Society for Biochemistry and Molecular Biology."

from all known CaM-binding domains. These findings confirm the enormous versatility of CaM-target complex formation and suggest a novel CaM-binding mode that requires engagement of hydrophobic residues from both helices I and II of MA (Ghanam et al., 2010; Samal et al., 2011).

The exact functional role of CaM in HIV replication is not known. The observation that CaM colocalized with Gag in the cytoplasm of the infected cell may suggest a role of CaM in the (pre)assembly stage. Could it be that CaM facilitates Gag transport to the PM? This is a reasonable hypothesis given the fact that one of the major functions of CaM is shuttling proteins to the PM. However, this hypothesis has yet to be tested. One interesting characteristic of CaM is its preferential binding to myristoylated proteins. Membrane association and dissociation of myristoylated proteins are often regulated by intracellular Ca^{2+} signaling through a "Ca^{2+}-myr switch" such as recoverin (Tanaka et al., 1995), neurocalcin (Faurobert et al., 1996), and S-modulin (Matsuda et al., 1998). As a consequence, intracellular localization from the cytosol to the membrane is dependent on Ca^{2+} binding (Braunewell and Gundelfinger, 1999). Other myristoylated proteins including myristoylated alanine-rich C kinase substrate (MARCKS), brain-specific protein kinase C substrate (CAP-23/NAP-22) and HIV-1 Nef interact with CaM via the myr group to facilitate their intracellular localization and membrane targeting (Matsubara et al., 2003, 2004, 2005). Our structural studies were the first of their kind to be conducted on binding of CaM to a native myristoylated protein and the first to show the subsequent exposure of the myr group (**Figure 5**). The finding that the myr group is not "grabbed" by CaM may suggest a novel functional role of CaM in the trafficking and/or targeting of Gag to the PM for assembly.

The functional role of CaM in the HIV replication cycle could be rather complex since interactions with gp160 and Nef have also been detected. Expression of the HIV-1 gp160 protein has led to a marked increase in CaM distribution (Radding et al., 1996). The CaM-binding region in gp160 was identified to be a helical peptide in gp41. Deletion of this region led to diminished virus infectivity (Srinivas et al., 1993; Radding et al., 1996). On the other hand, mutations in the cytoplasmic domain of gp41 eliminated co-immunoprecipitation of Env with calmodulin but had no significant effect on viral production or Env expression (Micoli et al., 2006). Confocal microscopy data confirmed the elevated level of CaM distribution and also showed that CaM colocalizes with the gp160 protein (Radding et al., 1996). Thus, the interplay between gp160, CaM, and Gag could be important in HIV replication. Although it is reasonable to hypothesize that HIV–CaM protein interactions may lead to disruption of CaM-dependent cell-signaling pathways and contribute to immune dysfunction during HIV pathogenesis, the exact functional role of CaM in HIV replication has yet to be examined.

ROLE OF THE ADAPTOR PROTEIN COMPLEXES IN Gag TRAFFICKING

To understand the critical steps of the molecular mechanism of HIV assembly, it is vital to identify the cellular machinery, its components, and how these components interact with each other and/or the HIV proteins. Although it is widely accepted that in most cell types HIV-1 Gag budding and assembly occur on the PM (Hermida-Matsumoto and Resh, 2000; Jouvenet et al., 2006, 2008; Finzi et al., 2007; Li et al., 2007; Welsch et al., 2007; Gousset et al., 2008; Joshi et al., 2009a; Ono, 2009, 2010), several research groups have shown that late endosomal compartments can serve as major assembly sites (Nguyen et al., 2003; Nydegger et al., 2003; Pelchen-Matthews et al., 2003; Sherer et al., 2003; Grigorov et al.,

2006). To further explore the assembly pathway in late endosomal compartments, efforts focused on cellular proteins and protein complexes that typically play roles in protein sorting to and from the endosomal pathway. Several of these factors, which are implicated in Gag trafficking and assembly have been discovered. These include AP-1, AP-2, and AP-3 (Batonick et al., 2005; Dong et al., 2005; Camus et al., 2007). AP-3 appears to be involved in the sorting of a subset of transmembrane proteins targeted to lysosomes and lysosome-related organelles. Studies by Spearman et al. (1997) indicate that HIV-1 Gag binds to the δ subunit of the AP-3 complex (Dong et al., 2005). The AP-3 binding domain in Gag is suggested to be within the N-terminal region of MA (helix I; **Figure 6**). Gag constructs lacking the MA domain failed to bind and recruit the AP-3 complex. In addition, particle formation by WT Gag was severely diminished by a dominant negative AP-3 δ fragment and by siRNA depletion of AP-3, indicating that interaction between Gag and AP-3 is essential for normal productive trafficking pathway of Gag in the cell (Dong et al., 2005). The trafficking of Gag to CD63-positive intracellular compartments was also eliminated when Gag–AP-3 interaction was disrupted.

In addition to binding to Gag, the cytoplasmic tail of gp41 contains a tyrosine-based signal that has been shown to be active in promoting clathrin-mediated endocytosis through interactions with the μ subunit of AP-2 (Boge et al., 1998; Berlioz-Torrent et al., 1999). This observation has led to the hypothesis that the Env protein is internalized to sorting/recycling endosome compartment where it becomes associated with Gag (Dong et al., 2005). The dual role of AP complexes in Env and Gag trafficking pathways and compelling evidence for direct physical interactions between MA and AP-3 have yet to be determined.

TIP47: ROLE IN Gag LOCALIZATION AND Env INCORPORATION

TIP47 is an essential protein for endosome-to-TGN retrograde transport of mannose-6-phosphate receptors, has been shown to form a ternary complex by bridging between the Env and Gag proteins (Lopez-Vergès et al., 2006). The interaction between Gag and TIP47 is mediated by the MA domain. Mutations in the MA domain of Gag that abrogate TIP47 binding were found to inhibit Env incorporation, Env–Gag colocalization, and virus infectivity (Lopez-Vergès et al., 2006). Silencing of TIP47 was found to impair Env incorporation and infectivity and abolished co-immunoprecipitation of Gag and Env. Based on these findings, it was suggested that TIP47 acts as a connector between Gag and Env during assembly (Lopez-Vergès et al., 2006). Interestingly, several point mutations and deletions within the first 23 residues of MA resulted in loss of TIP47 binding and thus Env incorporation. Among these mutations were W16A and E17A. Mutations in helix I of MA (L13, W16, E17, and K18) have been shown to block Env incorporation (Dorfman et al., 1994; Freed and Martin, 1996; Davis et al., 2006), which led to the suggestion that MA interacts directly with the Env protein. Altogether, studies on TIP47 suggest a functional role of this protein in Env incorporation and colocalization of Gag and Env. However, role of TIP47 in HIV biology remains unclear as studies conducted in other laboratories have failed to support any role of TIP47 in particle production or virus replication (Checkley et al., 2011).

Gag–SOCS1 INTERACTIONS

SOCS1, a member of negative regulators of cytokine signaling (Yoshimura et al., 2007) has been recently shown to be an inducible host-factor during HIV-1 infection and to regulate the late stages of the virus replication pathway (Ryo et al., 2008; Nishi et al., 2009). SOCS1 interacts with the MA and NC regions of Gag to facilitate its intracellular trafficking and stability. The depletion of SOCS1 caused a severe reduction in Gag trafficking and assembly (Ryo et al., 2008). It has been also shown that SOCS1 is involved in regulating Gag trafficking via the microtubule-dependent cellular machinery (Nishi et al., 2009).

Genetically, SOCS family members have a central SH2 domain and a conserved SOCS box (Yoshimura et al., 2007). Structure–function analyses revealed that the SH2 domain is critical for efficient binding to its substrates (Narazaki et al., 1998). Ryo et al. (2008) reinforced these findings by showing that a mutant lacking the SH2 domain does not bind HIV-1 Gag, whereas an N-terminus or a SOCS1 box deletion did not affect binding to Gag in 293T cells. Thus, elucidation of the structural requirements of Gag–SOCS1 interactions will provide insights into the functional role of SOCS1 in Gag trafficking and stability throughout the HIV replication cycle.

LYRIC–Gag INTERACTIONS

Lyric is a ubiquitously expressed 64 kDa protein with several isoforms due to differential splicing, which differ in their intracellular localization, and is normally involved in various signaling pathways (Thirkettle et al., 2009). Previous studies have shown that Lyric is an HIV-inducible gene that is involved in various signaling pathways and acts in a positive-feedback loop promoting HIV replication (Thirkettle et al., 2009). A recent study has identified Lyric as an HIV-1 Gag-interacting protein. Endogenous Lyric has been shown to be incorporated in HIV-1 virions (Engeland et al., 2011). Both MA and NC appear to be required for Lyric binding. However, deleting NC and fusing MA with a GCN4 motif to drive trimerization led to the same binding affinity to Lyric. Thus, it is possible that Lyric binding to Gag is mostly dependent on the MA protein but also requires multimerization. Gag-interacting region in the Lyric protein has been mapped to a region spanning residues 101–289. Expression of this region increased Gag expression and viral infectivity. Interestingly, the observation of Gag–Lyric interactions in MMLV and EIAV (Engeland et al., 2011) suggests that Lyric's role in the replication cycle is probably a conserved feature among retroviruses. Despite the experimental evidence for Gag–Lyric interaction, the precise functional role for Lyric has yet to be established.

SUMMARY

Several cellular factors have been proposed to interact directly with the MA domain to facilitate Gag trafficking and assembly. However, molecular interactions have yet to be validated and characterized in most cases. Despite the tremendous progress achieved in understanding the structural properties of Gag and its domains, high-resolution structures of their complexes with cellular partners are very limited. The discovery of new cellular factors that bind to Gag or Gag components (Brass et al., 2008; Jäger et al., 2011) should pave the way for further structural investigation and

hopefully will lead to identification of novel mechanisms and/or pathways critical for virus assembly. Such knowledge should facilitate the development of better approaches for the treatment of HIV.

NOMENCLATURE

MA mutants are named based on the myr group being designated as residue 1. In contrast, studies that performed the characterization of the mutants discussed here considered the N-terminal Gly of the myristoylated protein as residue 1 (Freed et al., 1994; Ono and Freed, 1999, 2004; Ono et al., 2000a; Joshi et al., 2009a; Chukkapalli et al., 2010). Thus, the mutant names are offset by one residue.

ACKNOWLEDGMENTS

Thanks to our laboratory members for the invaluable comments on the manuscript. Work from our laboratory described in this article is supported by the National Institutes of Health (1R01AI087101) and intramural funding from the Center for AIDS Research and Comprehensive Cancer Center at the University of Alabama at Birmingham.

REFERENCES

Adamson, C. S., and Freed, E. O. (2007). Human immunodeficiency virus type 1 assembly, release and maturation. *Adv. Pharmacol.* 55, 347–387.

Akari, H., Fukumori, T., and Adachi, A. (2000). Cell-dependent requirement of human immunodeficiency virus type 1 gp41 cytoplasmic tail for Env incorporation into virions. *J. Virol.* 74, 4891–4893.

Alfadhli, A., Barklis, R. L., and Barklis, E. (2009a). HIV-1 matrix organizes as a hexamer of trimers on membranes containing phosphatidylinositol-(4,5)-bisphosphate. *Virology* 387, 466–472.

Alfadhli, A., Still, A., and Barklis, E. (2009b). Analysis of human immunodeficiency virus type 1 matrix binding to membranes and nucleic acids. *J. Virol.* 83, 12196–12203.

Alfadhli, A., Huseby, D., Kapit, E., Colman, D., and Barklis, E. (2007). Human immunodeficiency virus type 1 matrix protein assembles on membranes as a hexamer. *J. Virol.* 81, 1472–1478.

Alfadhli, A., McNett, H., Tsagli, S., Bächinger, H. P., Peyton, D. H., and Barklis, E. (2011). HIV-1 matrix protein binding to RNA. *J. Mol. Biol.* 410, 653–666.

Aloia, R. C., Tian, H., and Jensen, F. C. (1993). Lipid composition and fluidity of the human immunodeficiency virus envelope and host cell plasma membranes. *Proc. Natl. Acad. Sci. U.S.A.* 90, 5181–5185.

Arthur, L. O., Bess, J. W. Jr., Sowder, R. C. I., Benveniste, R. E., Mann, D. L., Chermann, J.-C., and Henderson, L. E. (1992). Cellular proteins bound to immunodeficiency virus: implications for pathogenesis and vaccines. *Science* 258, 1935–1938.

Batonick, M., Favre, M., Boge, M., Spearman, P., Höning, S., and Thali, M. (2005). Interaction of HIV-1 Gag with the clathrin-associated adaptor AP-2. *Virology* 342, 190–200.

Behnia, R., and Munro, S. (2005). Organelle identity and the signposts for membrane traffic. *Nature* 438, 597–604.

Berlioz-Torrent, C., Shacklett, B. L., Erdtmann, L., Delamarre, L., Bouchaert, I., Sonigo, P., Dokhelar, M. C., and Benarous, R. (1999). Interactions of the cytoplasmic domains of human and simian retroviral transmembrane proteins with components of the clathrin adaptor complexes modulate intracellular and cell surface expression of envelope glycoproteins. *J. Virol.* 73, 1350–1361.

Boehm, M., and Bonifacino, J. S. (2002). Genetic analyses of adaptin function from yeast to mammals. *Gene* 286, 175–186.

Boge, M., Wyss, S., Bonifacino, J. S., and Thali, M. (1998). A membrane-proximal tyrosine-based signal mediates internalization of the HIV-1 envelope glycoprotein via interaction with the AP-2 clathrin adaptor. *J. Biol. Chem.* 273, 15773–15778.

Bouamr, F., Scarlata, S., and Carter, C. A. (2003). Role of myristylation in HIV-1 Gag assembly. *Biochemistry* 42, 6408–6417.

Brandano, L., and Stevenson, M. (2012). A highly conserved residue in the C-terminal helix of HIV-1 matrix is required for envelope incorporation into virus particles. *J. Virol.* 86, 2347–2359.

Brass, A. L., Dykxhoorn, D. M., Benita, Y., Yan, N., Engelman, A., Xavier, R. J., Lieberman, J., and Elledge, S. J. (2008). Identification of host proteins required for HIV infection through a functional genomic screen. *Science* 319, 921–926.

Braunewell, K. H., and Gundelfinger, E. D. (1999). Intracellular neuronal calcium sensor proteins: a family of EF-hand calcium-binding proteins in search of a function. *Cell Tissue Res.* 295, 1–12.

Briggs, J. A. G., and Kräusslich, H.-G. (2011). The molecular architecture of HIV. *J. Mol. Biol.* 410, 491–500.

Briggs, J. A. G., Riches, J. D., Glass, B., Bartonova, V., Zanetti, G., and Kräusslich, H.-G. (2009). Structure and assembly of immature HIV. *Proc. Natl. Acad. Sci. U.S.A.* 106, 11090–11095.

Brown, D. A., and London, E. (1997). Structure of detergent-resistant membrane domains: does phase separation occur in biological membranes? *Biochem. Biophys. Res. Commun.* 240, 1–7.

Brown, D. A., and London, E. (1998). Structure and origin of ordered lipid domains in biological membranes. *J. Membr. Biol.* 164, 103–114.

Brown, D. A., and London, E. (2000). Structure and function of sphingolipid- and cholesterol-rich membrane rafts. *J. Biol. Chem.* 275, 17221–17224.

Bryant, M., and Ratner, L. (1990). Myristoylation-dependent replication and assembly of human immunodeficiency virus 1. *Proc. Natl. Acad. Sci. U.S.A.* 87, 523–527.

Burniston, M. T., Cimarelli, A., Colgan, J., Curtis, S. P., and Luban, J. (1999). Human immunodeficiency virus type 1 Gag polyprotein multimerization requires the nucleocapsid domain and RNA and is promoted by the capsid-dimer interface and the basic region of matrix protein. *J. Virol.* 73, 8527–8540.

Byland, R., Vance, P. J., Hoxie, J. A., and Marsh, M. (2007). A conserved dileucine motif mediates clathrin and AP-2-dependent endocytosis of the HIV-1 envelope protein. *Mol. Biol. Cell* 18, 414–425.

Cai, M., Huang, Y., Craigie, R., and Clore, G. M. (2010). Structural basis of the association of HIV-1 matrix protein with DNA. *PLoS ONE* 5, e15675. doi:10.1371/journal.pone.0015675

Campbell, S., Fisher, R. J., Towler, E. M., Fox, S., Issaq, H. J., Wolfe, T., Phillips, L. R., and Rein, A. (2001a). Modulation of HIV-like particle assembly in vitro by inositol phosphates. *Proc. Natl. Acad. Sci. U.S.A.* 98, 10875–10879.

Campbell, S. M., Crowe, S. M., and Mak, J. (2001b). Lipid rafts and HIV-1: from viral entry to assembly of progeny virions. *J. Clin. Virol.* 22, 217–227.

Campbell, S., and Rein, A. (1999). In vitro assembly properties of human immunodeficiency virus type 1 Gag protein lacking the p6 domain. *J. Virol.* 73, 2270–2279.

Camus, G., Segura-Morales, C., Molle, D., Lopez-Vergès, S., Begon-Pescia, C., Cazevieille, C., Schu, P., Bertrand, E., Berlioz-Torrent, C., and Basyuk, E. (2007). The clathrin adaptor complex AP-1 binds HIV-1 and MLV Gag and facilitates their budding. *Mol. Biol. Cell* 18, 3193–3203.

Chan, J., Dick, R. A., and Vogt, V. M. (2011). Rous sarcoma virus Gag has no specific requirement for phosphatidylinositol-(4,5)-bisphosphate for plasma membrane association in vivo or for liposome interaction in vitro. *J. Virol.* 85, 10851–10860.

Chan, R., Uchil, P. D., Jin, J., Shui, G., Ott, D. E., Mothes, W., and Wenk, M. R. (2008). Retroviruses human immunodeficiency virus and murine leukemia virus are enriched in phosphoinositides. *J. Virol.* 82, 11228–11238.

Chattopadhyaya, R., Meador, W. E., Means, A. R., and Quiocho, F. A. (1992). Calmodulin structure refined at 1.7 Å resolution. *J. Mol. Biol.* 228, 1177–1192.

Checkley, M. A., Luttge, B. G., and Freed, E. O. (2011). HIV-1 envelope glycoprotein biosynthesis, trafficking, and incorporation. *J. Mol. Biol.* 410, 582–608.

Chen, K., Bachtiar, I., Piszczek, G., Bouamr, F., Carter, C., and Tjandra, N. (2008). Solution NMR characterization of oligomerization and dynamics of equine infectious anemia virus matrix protein and its interaction with PIP2. *Biochemistry* 47, 1928–1937.

Chin, D., and Means, A. R. (2000). Calmodulin: a prototypical calcium sensor. *Trends Cell Biol.* 10, 322–328.

Chow, J. Y. H., Jeffries, C. M., Kwan, A. H., Guss, J. M., and Trewhella, J. (2010). Calmodulin disrupts the structure of the HIV-1 MA protein. *J. Mol. Biol.* 400, 702–714.

Chu, H., Wang, J. J., and Spearman, P. (2010). Human immunodeficiency virus type-1 Gag and host vesicular trafficking pathways. *Curr. Top. Microbiol. Immunol.* 339, 67–84.

Chukkapalli, V., Hogue, I. B., Boyko, V., Hu, W.-S., and Ono, A. (2008). Interaction between HIV-1 Gag matrix domain and phosphatidylinositol-(4,5)-bisphosphate is essential for efficient Gag-membrane binding. *J. Virol.* 82, 2405–2417.

Chukkapalli, V., Oh, S. J., and Ono, A. (2010). Opposing mechanisms involving RNA and lipids regulate HIV-1 Gag membrane binding through the highly basic region of the matrix domain. *Proc. Natl. Acad. Sci. U.S.A.* 107, 1600–1605.

Chukkapalli, V., and Ono, A. (2011). Molecular determinants that regulate plasma membrane association of HIV-1 Gag. *J. Mol. Biol.* 410, 512–524.

Cimarelli, A., Sandin, S., Hoglund, S., and Luban, J. (2000). Basic residues in human immunodeficiency virus type 1 nucleocapsid promote virion assembly via interaction with RNA. *J. Virol.* 74, 3046–3057.

Cooper, J., Liu, L., Woodruff, E. A., Taylor, H. E., Goodwin, J. S., D'Aquila, R. T., Spearman, P., Hildreth, J. E. K., and Dong, X. (2011). Filamin A protein interacts with human immunodeficiency virus type 1 Gag protein and contributes to productive particle assembly. *J. Biol. Chem.* 286, 28498–28510.

Crist, R. M., Datta, S. A. K., Stephen, A. G., Soheilian, F., Mirro, J., Fisher, R. J., Nagashima, K., and Rein, A. (2009). Assembly properties of human immunodeficiency virus type 1 Gag-leucine zipper chimeras: implications for retrovirus assembly. *J. Virol.* 83, 2216–2225.

Dalton, A. K., Ako-Adjei, D., Murray, P. S., Murray, D., and Vogt, M. V. (2007). Electrostatic interactions drive membrane association of the human immunodeficiency virus type 1 Gag MA domain. *J. Virol.* 81, 6434–6445.

Dalton, A. K., Murray, P. S., Murray, D., and Vogt, V. M. (2005). Biochemical characterization of Rous sarcoma virus MA protein interaction with membranes. *J. Virol.* 79, 6227–6238.

Darlix, J. L., and Spahr, P. F. (1982). Binding sites of viral protein P19 onto Rous sarcoma virus RNA and possible controls of viral functions. *J. Mol. Biol.* 160, 147–161.

Datta, S. A. K., Curtis, J. E., Ratcliff, W., Clark, P. K., Crist, R. M., Lebowitz, J., Krueger, S., and Rein, A. (2007a). Conformation of the HIV-1 Gag protein in solution. *J. Mol. Biol.* 365, 812–824.

Datta, S. A. K., Zhao, Z., Clark, P. K., Tarasov, S., Alexandratos, J. N., Campbell, S. J., Kvaratskhelia, M., Lebowitz, J., and Rein, A. (2007b). Interactions between HIV-1 Gag molecules in solution: an inositol phosphate-mediated switch. *J. Mol. Biol.* 365, 799–811.

Davis, M. R., Jiang, J., Zhou, J., Freed, E. O., and Aiken, C. (2006). A mutation in the human immunodeficiency virus type 1 Gag protein destabilizes the interaction of the envelope protein subunits gp120 and gp41. *J. Virol.* 80, 2405–2417.

Dawson, L., and Yu, X. F. (1998). The role of nucleocapsid of HIV-1 in virus assembly. *Virology* 251, 141–157.

Ding, L., Derdowski, A., Wang, J.-J., and Spearman, P. (2003). Independent segregation of human immunodeficiency virus type 1 Gag protein complexes and lipid rafts. *J. Virol.* 77, 1916–1926.

Dong, X., Li, H., Derdowski, A., Ding, L., Burnett, A., Chen, X., Peters, T. R., Dermody, T. S., Woodruff, E., Wang, J.-J., and Spearman, P. (2005). AP-3 directs the intracellular trafficking of HIV-1 Gag and plays a key role in particle assembly. *Cell* 120, 663–674.

Dorfman, T., Mammano, F., Haseltine, W. A., and Göttlinger, H. G. (1994). Role of the matrix protein in the virion association of the human immunodeficiency virus type 1 envelope glycoprotein. *J. Virol.* 68, 1689–1696.

Dou, J., Wang, J.-J., Chen, X., Li, H., Ding, L., and Spearman, P. (2009). Characterization of a myristoylated, monomeric HIV Gag protein. *Virology* 387, 341–352.

Edgcomb, S. P., and Murphy, K. P. (2002). Variability in the pKa of histidine side-chains correlates with burial within proteins. *Proteins* 49, 1–6.

Engeland, C. E., Oberwinkler, H., Schümann, M., Krause, E., Müller, G. A., and Kräusslich, H.-G. (2011). The cellular protein lyric interacts with HIV-1 Gag. *J. Virol.* 85, 13322–13332.

Erdie, C. R., and Wills, J. W. (1990). Myristoylation of Rous sarcoma virus Gag protein does not prevent replication in avian cells. *J. Virol.* 64, 5204–5208.

Fallon, J. L., and Quiocho, F. A. (2003). A closed compact structure of native Ca^{+} 2-calmodulin. *Structure* 11, 1303–1307.

Faurobert, E., Chen, C.-K., Hurley, J. B., and Teng, D. H.-F. (1996). Drosophila neurocalcin, a fatty acylated, Ca-binding protein that associates with membranes and inhibits in vitro phosphorylation of bovine rhodopsin. *J. Biol. Chem.* 271, 10256–10262.

Fernandes, F., Chen, K., Ehrlich, L. S., Jin, J., Chen, M. H., Medina, G. N., Symons, M., Montelaro, R., Donaldson, J., Tjandra, N., and Carter, C. A. (2011). Phosphoinositides direct equine infectious anemia virus Gag trafficking and release. *Traffic* 12, 438–451.

Finn, B. E., Evenäs, J., Drakenberg, T., Waltho, J. P., Thulin, E., and Forsén, S. (1995). Calcium-induced structural changes and domain autonomy in calmodulin. *Nat. Struct. Biol.* 2, 777–783.

Finzi, A., Orthwein, A., Mercier, J., and Cohen, E. A. (2007). Productive human immunodeficiency virus type 1 assembly takes place at the plasma membrane. *J. Virol.* 81, 7476–7490.

Fledderman, E. L., Fujii, K., Ghanam, R. H., Waki, K., Prevelige, P. E., Freed, E. O., and Saad, J. S. (2010). Myristate exposure in the HIV-1 matrix protein is modulated by ph. *Biochemistry* 49, 9551–9562.

Freed, E. O., and Martin, A. M. (1996). Domains of the human immonodeficiency virus type 1 matrix and gp41 cytoplasmic tail required for envelope incorporation into virions. *J. Virol.* 70, 341–351.

Freed, E. O., Orenstein, J. M., Buckler-White, A. J., and Martin, M. A. (1994). Single amino acid changes in the human immunodeficiency virus type 1 matrix protein block virus particle production. *J. Virol.* 68, 5311–5320.

Freed, O. E., and Martin, A. M. (1995). Virion incorporation of envelope glycoproteins with long but not short cytoplasmic tails is blocked by specific, single amino acid substitutions in the human immunodeficiency virus type 1 matrix. *J. Virol.* 69, 1984–1989.

Ganser-Pornillos, B. K., Cheng, A., and Yeager, M. (2007). Structure of full-length HIV-1 CA: a model for the mature capsid lattice. *Cell* 131, 70–79.

Ganser-Pornillos, B. K., Yeager, M., and Sundquist, W. I. (2008). The structural biology of HIV assembly. *Curr. Opin. Struct. Biol.* 18, 203–217.

Ghanam, R. H., Fernandez, T. F., Fledderman, E. L., and Saad, J. S. (2010). Binding of calmodulin to the HIV-1 matrix protein triggers myristate exposure. *J. Biol. Chem.* 285, 41911–41920.

Gheysen, D., Jacobs, E., De Foresta, F., Thiriart, C., Francotte, M., Thines, D., and De Wilde, M. (1989). Assembly and release of HIV-1 precursor Pr55gag virus-like particles from recombinant baculovirus-infected insect cells. *Cell* 59, 103–112.

Golub, T., and Caroni, P. (2005). PI(4,5)P2-dependent microdomain assemblies capture microtubules to promote and control leading edge motility. *J. Cell Biol.* 169, 151–162.

Gottlieb, R. A., Giesing, H. A., Zhu, J. Y., Engler, R. L., and Babior, B. M. (1995). Cell acidification in apoptosis: granulocyte colony-stimulating factor delays programmed cell death in neutrophils by up-regulating the vacuolar H^{+}-ATPase. *Proc. Natl. Acad. Sci. U.S.A.* 92, 5965–5968.

Gousset, K., Ablan, S. D., Coren, L. V., Ono, A., Soheilian, F., Nagashima, K., Ott, D. E., and Freed, E. O. (2008). Real-time visualization of HIV-1 GAG trafficking in infected macrophages. *PLoS Pathog.* 4, e1000015. doi:10.1371/journal.ppat.1000015

Greene, W. C., Debyser, Z., Ikeda, Y., Freed, E. O., Stephens, E., Yonemoto, W., Buckheit, R. W., Esté, J. A., and Cihlar, T. (2008). Novel targets for HIV therapy. *Antiviral Res.* 80, 251–265.

Grigorov, B., Arcanger, F., Roingeard, P., Darlix, J. L., and Muriaux, D. (2006). Assembly of infectious HIV-1 in human epithelial and T-lymphoblastic cell lines. *J. Mol. Biol.* 359, 848–862.

Hamard-Peron, E., Juilliard, F., Saad, J. S., Roy, C., Roingeard, P., Summers, M. F., Darlix, J. L., Picart, C., and Muriaux, D. (2010). Targeting of MuLV Gag to the plasma membrane is mediated by PI(4,5)P2/PS and a polybasic region in the Matrix. *J. Virol.* 84, 503–515.

Hamard-Peron, E., and Muriaux, D. (2011). Retroviral matrix and lipids, the intimate interactions. *Retrovirology* 8, 15.

Hayashi, N., Matsubara, M., Jinbo, Y., Titani, K., Izumi, Y., and Matsushima, N. (2002). Nef of HIV-1 interacts directly with calcium-bound calmodulin. *Protein Sci.* 11, 529–537.

Hearps, A. C., Wagstaff, K. M., Piller, S. C., and Jans, D. A. (2008). The N-terminal basic domain of the HIV-1 matrix protein does not contain a conventional nuclear localization sequence but is required for DNA binding and protein self-association. *Biochemistry* 47, 2199–2210.

Hermida-Matsumoto, L., and Resh, M. D. (1999). Human immunodeficiency virus type 1 protease triggers a myristoyl switch that modulates membrane binding fo Pr55gag and p17MA. *J. Virol.* 73, 1902–1908.

Hermida-Matsumoto, L., and Resh, M. D. (2000). Localization of human immunodeficiency virus type 1 Gag and Env at the plasma membrane by confocal imagine. *J. Virol.* 74, 8670–8679.

Hoeflich, K. P., and Ikura, M. (2002). Calmodulin in action: diversity in target recognition and activation mechanisms. *Cell* 108, 739–742.

Hogue, I. B., Hoppe, A., and Ono, A. (2009). Quantitative FRET microscopy analysis of HIV-1 Gag-Gag interaction: the relative contributions of CA and NC domains, and membrane binding. *J. Virol.* 83, 7322–7336.

Holm, K., Weclewicz, K., Hewson, R., and Suomalainen, M. (2003). Human immunodeficiency virus type 1 assembly and lipid rafts: Pr55gag associates with membrane domains that are largely resistant to Brij98 but sensitive to Triton X-100. *J. Virol.* 77, 4805–4817.

Inlora, J., Chukkapalli, V., Derse, D., and Ono, A. (2011). Gag localization and virus-like particle release mediated by the matrix domain of human T-lymphotropic virus type 1 Gag are less dependent on phosphatidylinositol-(4,5)-bisphosphate than those mediated by the matrix domain of HIV-1 Gag. *J. Virol.* 85, 3802–3810.

Ishida, H., and Vogel, H. J. (2006). Protein-peptide interaction studies demonstrate the versatility of calmodulin target protein binding. *Protein Pept. Lett.* 13, 455–465.

Izumi, Y., Watanabe, H., Watanabe, N., Aoyama, A., Jinbo, J., and Hayashi, N. (2008). Solution X-ray scattering reveals a novel structure of calmodulin complexed with a binding domain peptide from the HIV-1 matrix protein p17. *Biochemistry* 47, 7158–7166.

Jäger, S., Cimermancic, P., Gulbahce, N., Johnson, J. R., McGovern, K. E., Clarke, S. C., Shales, M., Mercenne, G., Pache, L., Li, K., Hernandez, H., Jang, G. M., Roth, S. L., Akiva, E., Marlett, J., Stephens, M., D'Orso, I., Fernandes, J., Fahey, M., Mahon, C., O'Donoghue, A. J., Todorovic, A., Morris, J. H., Maltby, D. A., Alber, T., Cagney, G., Bushman, F. D., Young, J. A., Chanda, S. K., Sundquist, W. I., Kortemme, T., Hernandez, R. D., Craik, C. S., Burlingame, A., Sali, A., Frankel, A. D., and Krogan, N. J. (2011). Global landscape of HIV-human protein complexes. *Nature* 481, 365–370.

Janmey, P. A., Iida, K., Yin, H. L., and Stossel, T. P. (1987). Polyphosphoinositide micelles and polyphosphoinositide-containing vesicles dissociate endogenous gelsolin-actin complexes and promote actin assembly from the fast-growing end of actin filaments blocked by gelsolin. *J. Biol. Chem.* 262, 12228–12236.

Joshi, A., Ablan, S. D., Soheilian, F., Nagashima, K., and Freed, E. O. (2009a). Evidence that productive human immunodeficiency virus type 1 assembly can occur in an intracellular compartment. *J. Virol.* 83, 5375–5387.

Joshi, A., Nagashima, K., and Freed, E. O. (2009b). Defects in cellular sorting and retroviral assembly induced by GGA overexpression. *BMC Cell Biol.* 10, 72. doi:10.1186/1471-2121-10-72

Joshi, A., Garg, H., Ablan, S. D., and Freed, E. O. (2011). Evidence of a role for soluble N-ethylmaleimide-sensitive factor attachment protein receptor (SNARE) machinery in HIV-1 assembly and release. *J. Biol. Chem.* 286, 29861–28971.

Joshi, A., Garg, H., Nagashima, K., Bonifacino, J. S., and Freed, E. O. (2008). GGA and Arf proteins modulate retrovirus assembly and release. *Mol. Cell* 30, 227–238.

Joshi, A., Nagashima, K., and Freed, E. O. (2006). Mutation of dileucine-like motifs in the human immunodeficiency virus type 1 capsid disrupts virus assembly, Gag-Gag interactions, Gag-membrane binding, and virion maturation. *J. Virol.* 80, 7939–7951.

Jouvenet, N., Bieniasz, P. D., and Simon, S. M. (2008). Imaging the biogenesis of individual HIV-1 virions in live cells. *Nature* 454, 236–240.

Jouvenet, N., Neil, S. J. D., Bess, C., Johnson, M. C., Virgen, C. A., Simon, S. M., and Bieniasz, P. D. (2006). Plasma membrane is the site of productive HIV-1 particle assembly. *PLoS Biol.* 4, e435. doi:10.1371/journal.pbio.0040435

Katoh, I., Kyushiki, H., Sakamoto, Y., Ikawa, Y., and Yoshinaka, Y. (1991). Bovine leukemia virus matrix-associated protein MA(p15): further processing and formation of a specific complex with the dimer of the 5′-terminal genomic rna fragment. *J. Virol.* 65, 6845–6855.

Kinnunen, P. K., Kõiv, A., Lehtonen, J. Y., Rytömaa, M., and Mustonen, P. (1994). Lipid dynamics and peripheral interactions of proteins with membrane surfaces. *Chem. Phys. Lipids* 73, 181–207.

König, R., Zhou, Y., Elleder, D., Diamond, T. L., Bonamy, G. M. C., Irelan, J. T., Chiang, C.-Y., Tu, B. P., De Jesus, P. D., Lilley, C. E., Seidel, S., Opaluch, A. M., Caldwell, J. S., Weitzman, M. D., Kuhen, K. L., Bandyopadhyay, S., Ideker, T., Orth, A. P., Miraglia, L. J., Bushman, F. D., Young, J. A., and Chanda, S. K. (2008). Global analysis of host-pathogen interactions that regulate early-stage HIV-1 replication. *Cell* 135, 49–60.

Leis, J. P., McGinnis, J., and Green, R. W. (1978). Rous sarcoma virus p19 binds to specific double-stranded regions of viral RNA: effect of p19 on cleavage of viral RNA by RNase III. *Virology* 84, 87–98.

Lever, A. M. L., and Jeang, K.-T. (2011). Insights into cellular factors that regulate HIV-1 replication in human cells. *Biochemistry* 50, 920–931.

Li, H., Dou, J., Ding, L., and Spearman, P. (2007). Myristoylation is required for human immunodeficiency virus type 1 Gag-Gag multimerization in mammalian cells. *J. Virol.* 81, 12899–12910.

Li, S., Hill, C. P., Sundquist, W. I., and Finch, J. T. (2000). Image reconstructions of helical assemblies of the HIV-1 CA protein. *Nature* 407, 409–413.

Lindwasser, O. W., and Resh, M. D. (2001). Multimerization of human immunodeficiency virus type 1 Gag promotes its localization to barges, raft-like membrane microdomains. *J. Virol.* 75, 7913–7924.

Lindwasser, O. W., and Resh, M. D. (2002). Myristoylation as a target for inhibiting HIV assembly: unsaturated fatty acids block viral budding. *Proc. Natl. Acad. Sci. U.S.A.* 99, 13037–13042.

Liu, T., Ryan, M., Dahlquist, F. W., and Griffith, O. H. (1997). Determination of pKa values of the histidine side chains of phosphatidylinositol-specific phospholipase C from *Bacillus cereus* by NMR spectroscopy and site-directed mutagenesis. *Protein Sci.* 6, 1937–1944.

Lodge, R., Gottlinger, H., Gabuzda, D., Cohen, E. A., and Lemay, G. (1994). The intracytoplasmic domain of gp41 mediates polarized budding of human immunodeficiency virus type 1 in MDCK cells. *J. Virol.* 68, 4857–4861.

Lopez-Vergès, S., Camus, G., Blot, G., Beauvoir, R., Benarous, R., and Berlioz-Torrent, C. (2006). Tail-interacting protein TIP47 is a connector between Gag and Env and is required for Env incorporation into HIV-1 virions. *Proc. Natl. Acad. Sci. U.S.A.* 103, 14947–14952.

Lusso, P., Di Marzo Veronese, F., Ensoli, B., Franchini, G., Jemma, C., Derocco, S. E., Kalyanaraman, V. S., and Gallo, R. C. (1990). Expanded HIV-1 cellular tropism by phenotypic mixing with murine endogenous retroviruses. *Science* 247, 848–852.

Makutonina, A., Voss, T. G., Plymale, D. R., Fermin, C. D., Norris, C. H., Vigh, S., and Garry, R. F. (1996). Human immunodeficiency virus infection of T-lymphoblastoid cells reduces intracellular pH. *J. Virol.* 70, 7049–7055.

Mammano, F., Kondo, E., Sodroski, J., Bukovsky, A., and Gottlinger, H. G. (1995). Rescue of human immunodeficiency virus type I matrix protein mutants by envelope glycoproteins with short cytoplasmic domains. *J. Virol.* 69, 3824–3830.

Matsubara, M., Jing, T., Kawamura, K., Shimojo, N., Titani, K., Hashimoto, K., and Hayashi, N. (2005). Myristoyl moiety of HIV Nef is involved in regulation of the interaction with calmodulin in vivo. *Protein Sci.* 14, 494–503.

Matsubara, M., Nakatsu, T., Kato, H., and Taniguchi, H. (2004). Crystal structure of a myristoylated CAP-23/NAP-22 N-terminal domain complexed with Ca^{2+}/calmodulin. *EMBO J.* 23, 712–718.

Matsubara, M., Titani, K., Taniguchi, H., and Hayashi, N. (2003). Direct involvement of protein myristoylation in myristoylated alanine-rich C kinase substrate (MARCKS)-calmodulin interaction. *J. Biol. Chem.* 278, 48898–48902.

Matsuda, S., Hisatomi, O., Ishino, T., Kobayashi, Y., and Tokunaga, F. (1998). The role of calcium-binding sites in S-modulin function. *J. Biol. Chem.* 273, 20223–20227.

McLaughlin, S., and Murray, D. (2005). Plasma membrane phosphoinositide organization by protein electrostatics. *Nature* 438, 605–611.

Melkonian, K. A., Ostermeyer, A. G., Chen, J. Z., Roth, M. G., and Brown, D. A. (1999). Role of lipid modifications in targeting proteins to

detergent-resistant membrane rafts. *J. Biol. Chem.* 274, 3910–3917.

Méric, C., and Spahr, P.-F. (1986). Rous sarcoma virus nucleic acid-binding protein p12 is necessary for viral 70S RNA dimer formation and packaging. *J. Virol.* 60, 450–459.

Micoli, K. J., Mamaeva, O., Piller, S. C., Barker, J. L., Pan, G., Hunter, E., and McDonald, J. M. (2006). Point mutations in the C-terminus of HIV-1 gp160 reduce apoptosis and calmodulin binding without affecting viral replication. *Virology* 344, 468–479.

Moolenaar, W. H., Tsien, R. Y., Van Der Saag, P. T., and De Laat, S. W. (1983). Na^+/H^+ exchange and cytoplasmic pH in the action of growth factors in human fibroblasts. *Nature* 304, 645–648.

Morikawa, Y., Hockley, D. J., Nermut, M. V., and Jones, I. M. (2000). Roles of matrix, p2, and N-terminal myristoylation in human immunodeficiency virus type 1 Gag assembly. *J. Virol.* 74, 16–23.

Morikawa, Y., Zhang, W.-H., Hockley, D. J., Nermut, M. V., and Jones, I. M. (1998). Detection of a trimeric human immunodeficiency virus type 1 Gag intermediate is dependent on sequences in the matrix protein, p17. *J. Virol.* 72, 7659–7663.

Murakami, T., and Freed, E. O. (2000). The long cytoplasmic tail of gp41 is required in a cell type-dependent manner for HIV-1 envelope glycoprotein incorporation into virions. *Proc. Natl. Acad. Sci. U.S.A.* 97, 343–348.

Muriaux, D., Mirro, J., Harvin, D., and Rein, A. (2001). RNA is a structural element in retrovirus particles. *Proc. Natl. Acad. Sci. U.S.A.* 98, 5246–5251.

Nakatsu, F., and Ohno, H. (2003). Adaptor protein complexes as the key regulators of protein sorting in the post-Golgi network. *Cell Struct. Funct.* 28, 419–429.

Narazaki, M., Fujimoto, M., Matsumoto, T., Morita, Y., Saito, H., Kajita, T., Yoshizaki, K., Naka, T., and Kishimoto, T. (1998). Three distinct domains of SSI-1/SOCS-1/JAB protein are required for its suppression of interleukin 6 signaling. *Proc. Natl. Acad. Sci. U.S.A.* 95, 13130–13134.

Nguyen, D. G., Booth, A., Gould, S. J., and Hildreth, J. E. (2003). Evidence that HIV budding in primary macrophages occurs through the exosome release pathway. *J. Biol. Chem.* 278, 52347–52354.

Nguyen, D. H., and Hildreth, J. E. (2000). Evidence for budding of human immunodeficiency virus type 1 selectively from glycolipid-enriched membrane lipid rafts. *J. Virol.* 74, 3264–3272.

Nishi, M., Ryo, A., Tsurutani, N., Ohba, K., Sawasaki, T., Morishita, R., Perrem, K., Aoki, I., Morikawa, Y., and Yamamoto, N. (2009). Requirement for microtubule integrity in the SOCS1-mediated intracellular dynamics of HIV-1 Gag. *FEBS Lett.* 583, 1243–1250.

Nydegger, S., Foti, M., Derdowski, A., Spearman, P., and Thali, M. (2003). HIV-1 egress is gated through late endosomal membranes. *Traffic* 4, 902–910.

Ohno, H., Aguilar, R. C., Fournier, M. C., Hennecke, S., Cosson, P., and Bonifacino, J. S. (1997). Interaction of endocytic signals from the HIV-1 envelope glycoprotein complex with members of the adaptor medium chain family. *Virology* 238, 305–315.

Ono, A. (2009). HIV-1 assembly at the plasma membrane: Gag trafficking and localization. *Future Virol.* 4, 241–257.

Ono, A. (2010). Relationships between plasma membrane microdomains and HIV-1 assembly. *Biol. Cell* 102, 335–350.

Ono, A., Ablan, S. D., Lockett, S. J., Nagashima, K., and Freed, E. O. (2004). Phosphatidylinositol (4,5) bisphosphate regulates HIV-1 Gag targeting to the plasma membrane. *Proc. Natl. Acad. Sci. U.S.A.* 101, 14889–14894.

Ono, A., Demirov, D., and Freed, E. O. (2000a). Relationship between human immunodeficiency virus type-1 Gag multimerization and membrane binding. *J. Virol.* 74, 5142–5150.

Ono, A., Orenstein, J. M., and Freed, E. O. (2000b). Role of the Gag matrix domain in targeting human immunodeficiency virus type 1 assembly. *J. Virol.* 74, 2855–2866.

Ono, A., and Freed, E. O. (1999). Binding of human immunodeficiency virus type 1 Gag to membrane: role of the matrix amino terminus. *J. Virol.* 73, 4136–4144.

Ono, A., and Freed, E. O. (2001). Plasma membrane rafts play a critical role in HIV-1 assembly and release. *Proc. Natl. Acad. Sci. U.S.A.* 98, 13925–13930.

Ono, A., and Freed, E. O. (2004). Cell-type-dependent tageting of human immunodeficiency virus type 1 assembly to the plasma membrane and the multivesicular body. *J. Virol.* 78, 1552–1563.

Ono, A., and Freed, E. O. (2005). Role of lipid rafts in virus replication. *Adv. Virus Res.* 64, 311–358.

Ono, A., Huang, M., and Freed, E. O. (1997). Characterization of human immunodeficiency virus type 1 matrix revertants: effects on virus assembly, Gag processing, and Env incorporation into virions. *J. Virol.* 71, 4409–4418.

Osawa, M., Tokumitsu, H., Swindells, M. B., Kurihara, H., Orita, M., Shibanuma, T., Furuya, T., and Ikura, M. (1999). A novel target recognition revealed by calmodulin in complex with Ca^{2+}-calmodulin-dependent kinase kinase. *Nat. Struct. Biol.* 6, 819–824.

Ott, D. E. (2008). Cellular proteins detected in HIV-1. *Rev. Med. Virol.* 18, 159–175.

Ott, D. E., Coren, L. V., and Gagliardi, T. D. (2005). Redundant roles for nucleocapsid and matrix RNA-binding sequences in human immunodeficiency virus type 1 assembly. *J. Virol.* 79, 13839–13847.

Owens, R. J., and Compans, R. W. (1989). Expression of the human immunodeficiency virus envelope glycoprotein is restricted to basolateral surfaces of polarized epithelial cells. *J. Virol.* 63, 978–982.

Owens, R. J., Dubay, J. W., Hunter, E., and Compans, R. W. (1991). Human immunodeficiency virus envelope protein determines the site of virus release in polarized epithelial cells. *Proc. Natl. Acad. Sci. U.S.A.* 88, 3987–3991.

Paillart, J.-C., and Gottlinger, H. G. (1999). Opposing effects of human immunodeficiency virus type 1 matrix mutations support a myristyl switch model of Gag membrane targeting. *J. Virol.* 73, 2604–2612.

Parent, L. J., and Gudleski, N. (2011). Beyond plasma membrane targeting: role of the MA domain of Gag in retroviral genome encapsidation. *J. Mol. Biol.* 410, 553–564.

Pelchen-Matthews, A., Krameer, B., and Marsh, M. (2003). Infectious HIV-1 assembles in late endosomes in primary macrophages. *J. Cell Biol.* 162, 443–445.

Provitera, P., Bouamr, F., Murray, D., Carter, C., and Scarlata, S. (2000). Binding of equine infectious anemia virus matrix protein to membrane bilayers involves multiple interactions. *J. Mol. Biol.* 296, 887–898.

Purohit, P., Dupont, S., Stevenson, M., and Green, M. R. (2001). Sequence-specific interaction between HIV-1 matrix protein and viral genomic RNA revealed by in vitro genetic selection. *RNA* 7, 576–584.

Radding, W., Pan, Z. Q., Hunter, E., Johnston, P., Williams, J. P., and McDonald, J. M. (1996). Expression of HIV-1 envelope glycoprotein alters cellular calmodulin. *Biochem. Biophys. Res. Commun.* 218, 192–197.

Radding, W., Williams, J. P., McKenna, M. A., Tummala, R., Hunter, E., Tytler, E. M., and McDonald, J. M. (2000). Calmodulin and HIV type 1: interactions with Gag and Gag products. *AIDS Res. Hum. Retroviruses* 16, 1519–1525.

Ramalingam, D., Duclair, S., Datta, S. A., Ellington, A., Rein, A., and Prasad, V. R. (2011). RNA aptamers directed to human immunodeficiency virus type 1 Gag polyprotein bind to the matrix and nucleocapsid domains and inhibit virus production. *J. Virol.* 85, 305–314.

Reil, H., Bukovsky, A. A., Gelderblom, H. R., and Gottlinger, H. G. (1998). Efficient HIV-1 replication can occur in the absence of the viral matrix protein. *EMBO J.* 17, 2699–2708.

Robinson, M. S., and Bonifacino, J. S. (2001). Adaptor-related proteins. *Curr. Opin. Cell Biol.* 13, 444–453.

Rogers, M. S., and Strehler, E. E. (1996). "Calmodulin-like proteins," in *Guidebook to the Calcium-Binding Proteins,* eds M. R. Celio, T. Pauls, and B. Schwaller (Oxford: Oxford University Press), 34–40.

Ryo, A., Tsurutani, N., Obha, K., Kimura, R., Komano, J., Nishi, M., Soeda, H., Hattori, S., Perrem, K., Yamamoto, M., Chiba, J., Mimaya, J.-I., Yoshimura, K., Matsushita, S., Honda, M., Yoshimura, A., Sawasaki, T., Aoki, I., Morikawa, Y., and Yamamoto, N. (2008). SOCS1 is an inducible host factor during HIV-1 infection and regulates the intracellular trafficking and stability of HIV-1 Gag. *Proc. Natl. Acad. Sci. U.S.A.* 105, 294–299.

Rytömaa, M., and Kinnunen, P. K. (1995). Reversibility of the binding of cytochrome c to liposomes. Implications for lipid-protein interactions. *J. Biol. Chem.* 270, 3197–3202.

Saad, J. S., Ablan, S. D., Ghanam, R. H., Kim, A., Andrews, K., Nagashima, K., Soheilian, F., Freed, E. O., and Summers, M. F. (2008). Structure of the myristylated HIV-2 MA protein and the role of phosphatidylinositol-(4,5)-bisphosphate in membrane targeting. *J. Mol. Biol.* 382, 434–447.

Saad, J. S., Kim, A., Ghanam, R. H., Dalton, A. K., Vogt, M. V., Wu, Z., Lu, W., and Summers, M. F. (2007a). Mutations that mimic phosphorylation of the HIV-1 matrix protein do not perturb the myristyl switch. *Protein Sci.* 16, 1793–1797.

Saad, J. S., Loeliger, E., Luncsford, P., Liriano, M., Tai, J., Kim, A., Miller, J., Joshi, A., Freed, E. O., and Summers, M. F. (2007b). Point mutations in the HIV-1 matrix protein turn off the myristyl switch. *J. Mol. Biol.* 366, 574–585.

Saad, J. S., Miller, J., Tai, J., Kim, A., Ghanam, R. H., and Summers, M. F. (2006). Structural basis for targeting HIV-1 Gag to virus assembly sites on the plasma membrane. *Proc. Natl. Acad. Sci. U.S.A.* 103, 11364–11369.

Samal, A. B., Ghanam, R. H., Fernandez, T. F., Monroe, E. B., and Saad, J. S. (2011). NMR, biophysical and biochemical studies reveal the minimal calmodulin-binding domain of the HIV-1 matrix protein. *J. Biol. Chem.* 286, 33533–33543.

Schuldiner, S., and Rozengurt, E. (1982). Na^+/H^+ antiport in Swiss 3T3 cells: mitogenic stimulation leads to cytoplasmic alkalinization. *Proc. Natl. Acad. Sci. U.S.A.* 79, 7778–7782.

Sherer, N. M., Lehmann, M. J., Jimenez-Soto, L. F., Ingmundson, A., Horner, S. M., Cicchetti, G., Allen, P. G., Pypaert, M., Cunningham, J. M., and Mothes, W. (2003). Visualization of retroviral replication in living cells reveals budding into multivesicular bodies. *Traffic* 4, 785–801.

Shkriabai, N., Datta, S. A., Zhao, Z., Hess, S., Rein, A., and Kvaratskhelia, M. (2006). Interactions of HIV-1 Gag with assembly cofactors. *Biochemistry* 45, 4077–4083.

Spearman, P., Horton, R., Ratner, L., and Kuli-Zade, I. (1997). Membrane binding of human immunodeficiency virus type 1 matrix protein in vivo supports a conformational myristyl switch mechanism. *J. Virol.* 71, 6582–6592.

Srinivas, S. K., Srinivas, R. V., Anantharamaiah, G. M., Compans, R. W., and Segrest, J. P. (1993). Cytosolic domain of the human immunodeficiency virus envelope glycoproteins binds to calmodulin and inhibits calmodulin-regulated proteins. *J. Biol. Chem.* 268, 22895–22899.

Stansell, E., Apkarian, R., Haubova, S., Diehl, W. E., Tytler, E. M., and Hunter, E. (2007). Basic residues in the Mason-Pfizer monkey virus Gag matrix domain regulate intracellular trafficking and capsid-membrane interactions. *J. Virol.* 81, 8977–8988.

Steeg, C. M., and Vogt, V. M. (1990). RNA-binding properties of the matrix protein (p19gag) of avian sarcoma and leukemia viruses. *J. Virol.* 64, 847–855.

Strasner, A. B., Natarajan, M., Doman, T., Key, D., August, A., and Henderson, A. J. (2008). The Src kinase Lck facilitates assembly of HIV-1 at the plasma membrane. *J. Immunol.* 181, 3706–3713.

Tanaka, T., Ames, J. B., Harvey, T. S., Stryer, L., and Ikura, M. (1995). Sequestration of the membrane-targeting myristoyl group of recoverin in the calcium-free state. *Nature* 376, 444–447.

Tang, C., Loeliger, E., Luncsford, P., Kinde, I., Beckett, D., and Summers, M. F. (2004). Entropic switch regulates myristate exposure in the HIV-1 matrix protein. *Proc. Natl. Acad. Sci. U.S.A.* 101, 517–522.

Thirkettle, H. J., Girling, J., Warren, A. Y., Mills, I. G., Sahadevan, K., Leung, H., Hamdy, F., Whitaker, H. C., and Neal, D. E. (2009). LYRIC/AEG-1 is targeted to different subcellular compartments by ubiquitinylation and intrinsic nuclear localization signals. *Clin. Cancer Res.* 15, 3003–3013.

Tomita, Y., Noda, T., Fujii, K., Watanabe, T., Morikawa, Y., and Kawaoka, Y. (2011). The cellular factors Vps18 and Mon2 are required for efficient production of infectious HIV-1 particles. *J. Virol.* 85, 5618–5627.

Towler, D. A., Adams, S. P., Eubanks, S. R., Towery, D. S., Jackson-Machelski, E., Glaser, L., and Gordon, J. I. (1988). Myristyl CoA:protein N-myristoyltransferase activities from rat liver and yeast possess overlapping yet distinct peptide substrate specificities. *J. Biol. Chem.* 263, 1784–1790.

Tuominen, E. K., Wallace, C. J., and Kinnunen, P. K. (2002). Phospholipid-cytochrome c interaction: evidence for the extended lipid anchorage. *J. Biol. Chem.* 277, 8822–8826.

Turner, B. G., and Summers, M. F. (1999). Structural biology of HIV. *J. Mol. Biol.* 285, 1–32.

Valentine, K. G., Peterson, R., Saad, J. S., Summers, M. F., Xu, X., Ames, J. B., and Wand, A. J. (2010). Reverse micelle encapsulation of membrane anchored proteins for solution NMR studies. *Structure* 18, 9–16.

Vetter, S. W., and Leclerc, E. (2003). Novel aspects of calmodulin target recognition and activation. *Eur. J. Biochem.* 270, 404–414.

Waheed, A. A., and Freed, E. O. (2009). Lipids and membrane microdomains in HIV-1 replication. *Virus Res.* 143, 162–176.

Welsch, S., Keppler, O. T., Habermann, A., Allespach, I., Krijnse-Locker, J., and Kräusslich, H.-G. (2007). HIV-1 buds predominantly at the plasma membrane of primary human macrophages. *PLoS Pathog.* 3, e36.

Wilk, T., Pfeiffer, T., and Bosch, V. (1992). Retained in vitro infectivity and cytopathogenicity of HIV-1 despite truncation of the C-terminal tail of the env gene product. *Virology* 189, 167–177.

Wright, E. R., Schooler, J. B., Ding, H. J., Kieffer, C., Fillmore, C., Sundquist, W. I., and Jensen, G. J. (2007). Electron crytomography of immature HIV-1 virions reveals the structure of the CA and SP1 Gag shells. *EMBO J.* 26, 2218–2226.

Wyss, S., Berlioz-Torrent, C., Boge, M., Blot, G., Höning, S., Benarous, R., and Thali, M. (2011). The highly conserved C-terminal dileucine motif in the cytosolic domain of the human immunodeficiency virus type 1 envelope glycoprotein is critical for its association with the AP-1 clathrin adaptor [correction of adapter]. *J. Virol.* 75, 2982–2992.

Yamniuk, A. P., and Vogel, H. J. (2004). Calmodulin's flexibility allows for promiscuity in its interactions with target proteins and peptides. *Mol. Biotechnol.* 27, 33–57.

Yap, K. L., Kim, J., Truong, K., Sherman, M., Yuan, T., and Ikura, M. (2000). Calmodulin target database. *J. Struct. Funct. Genomics* 1, 8–14.

Yoshimura, A., Naka, T., and Kubo, M. (2007). SOCS proteins, cytokine signalling and immune regulation. *Nat. Rev. Immunol.* 7, 454–465.

Yu, X., Yuan, X., Matsuda, Z., Lee, T.-H., and Essex, M. (1992). The matrix protein of human immunodeficiency virus type I is required for incorporation of viral envelope protein into mature virions. *J. Virol.* 66, 4966–4971.

Zacharias, D. A., Violin, J. D., Newton, A. C., and Tsien, R. Y. (2002). Partitioning of lipid-modified monomeric GFPs into membrane microdomains of live cells. *Science* 296, 913–916.

Zhou, H., Xu, M., Huang, Q., Gates, A. T., Zhang, X. D., Castle, J. C., Stec, E., Ferrer, M., Strulovici, B., Hazuda, D. J., and Espeseth, A. S. (2008). Genome-scale RNAi screen for host factors required for HIV replication. *Cell Host Microbe* 4, 495–504.

Zhou, W., Parent, L. J., Wills, J. W., and Resh, M. D. (1994). Identification of a membrane-binding domain within the amino-terminal region of human immunodeficiency virus type 1 Gag protein which interacts with acidic phospholipids. *J. Virol.* 68, 2556–2569.

Zhou, W., and Resh, M. D. (1996). Differential membrane binding of the human immunodeficiency virus type 1 matrix protein. *J. Virol.* 70, 8540–8548.

Conflict of Interest Statement: The authors declare that the research was conducted in the absence of any commercial or financial relationships that could be construed as a potential conflict of interest.

Received: 27 December 2011; paper pending published: 09 January 2012; accepted: 01 February 2012; published online: 17 February 2012.

*Citation: Ghanam RH, Samal AB, Fernandez TF and Saad JS (2012) Role of the HIV-1 matrix protein in Gag intracellular trafficking and targeting to the plasma membrane for virus assembly. Front. Microbio. **3**:55. doi: 10.3389/fmicb.2012.00055*

This article was submitted to Frontiers in Virology, a specialty of Frontiers in Microbiology.

frontiers in
MICROBIOLOGY

MINI REVIEW ARTICLE
published: 13 October 2011
doi: 10.3389/fmicb.2011.00210

Non-enzymatic functions of retroviral integrase: the next target for novel anti-HIV drug development

Takao Masuda*

Department of Immunotherapeutics, Tokyo Medical and Dental University, Tokyo, Japan

Edited by:
Akio Adachi, The University of Tokushima Graduate School, Japan

Reviewed by:
Mikako Fujita, Kumamoto University, Japan
Yasuyuki Miyazaki, The University of Tokushima Graduate School, Japan

****Correspondence:***
Takao Masuda, Department of Immunotherapeutics, Graduate School of Medicine and Dentistry, Tokyo Medical and Dental University, 1-5-45 Yushima, Bunkyo-ku, Tokyo 113-8519, Japan.
e-mail: tmasu.impt@tmd.ac.jp

Integrase (IN) is a retroviral enzyme that catalyzes the insertion of viral DNA (vDNA) into host chromosomal DNA, which is necessary for efficient viral replication. The crystal structure of prototype foamy virus IN bound to cognate vDNA ends, a complex referred to as the intasome, has recently been resolved. Structure analysis of the intasome revealed a tetramer structure of IN that was required for its catalytic function, and also showed the inhibitory mechanism of the IN inhibitor. Genetic analysis of IN has revealed additional non-enzymatic roles during viral replication cycles at several steps other than integration. However, the higher order structure of IN that is required for its non-enzymatic functions remains to be delineated. This is the next major challenge in the field of IN structural biology hoping to be a platform for the development of novel IN inhibitors to treat human immunodeficiency virus type 1 infectious disease.

Keywords: HIV-1, integrase, reverse transcriptase, *pol*, reverse transcription, intasome, Gemin2

INTRODUCTION

Reverse transcription of viral RNA into double-stranded (ds) DNA, and the subsequent insertion of the synthesized viral DNA (vDNA) into a host chromosome, are characteristic features of retroviruses including human immunodeficiency virus type 1 (HIV-1). The reverse transcription and integration of the viral genome is sequentially catalyzed by the enzymes reverse transcriptase (RT) and integrase (IN), respectively. These retroviral enzymes are originally packaged in the viral particle along with the viral genomic RNA. After synthesis of vDNA by RT, IN acts on the termini of vDNA and catalyzes insertion of the vDNA into the host chromosome through two sequential enzymatic reactions: 3′-end processing and strand-transfer (Katz and Skalka, 1994). Currently, a clinically approved IN inhibitor specifically targets strand-transfer activity but not 3′-end processing activity (Summa et al., 2008). Therefore, the IN inhibitor is referred to as a strand-transfer inhibitor (STI). The STI shows very potent antiviral activity; however, emergence of STI-resistant variants is inevitable (Metifiot et al., 2010), as seen in patients treated with a combination of inhibitors against RT and protease activities. Efforts to develop novel drugs with distinct inhibitory mechanisms must continue so that we can effectively treat HIV-1 infections. For development of novel IN inhibitors, in addition to its enzymatic action, other non-enzymatic functions of IN, as described below, might be the next target(s) (Luo and Muesing, 2010).

STRUCTURE OF HIV-1 IN

Human immunodeficiency virus type 1 IN is composed of 288 amino acids with three structurally distinct domains (Li et al., 2011): an N-terminal domain (NTD), a central catalytic core domain (CCD), and a C-terminal domain (CTD; **Figure 1**). The NTD contains a highly conserved (His-His-Cys-Cys, HHCC) motif, which binds to zinc ions (Zn^{2+}) and folds a helix-turn-helix (HTH) structure. Through a tetrahedral attachment to the HHCC motif, Zn^{2+} enhances both multimerization and enzymatic activities of HIV-1 IN *in vitro* (Burke et al., 1992; Ellison et al., 1995; Cai et al., 1997). The CCD contains the highly conserved Asp, Asp, and Glu (DDE) residues directly involved in the catalytic activities of IN (Engelman and Craigie, 1992; Kulkosky et al., 1992; LaFemina et al., 1992; Bushman et al., 1993). Overall topology of the CCD is similar to those of ribonuclease H (RNaseH), the Holliday junction resolvase RuvC, and bacteriophage transposase Mu. Despite lack of sequence similarity between the CCD and RNaseH, there is remarkable similarity in the positioning of the two Asp catalytic residues (Dyda et al., 1994). The CTD, consisting of a structure that closely resembles Src homology 3 domains (SH3-like), possesses sequence- and metal ion-independent DNA binding activity (Eijkelenboom et al., 1995; Lodi et al., 1995). Each domain has been demonstrated to form a dimer and higher multimerization states (Dyda et al., 1994; Eijkelenboom et al., 1995; Cai et al., 1997), which might be required for all the enzymatic functions of IN.

Recently, the entire prototype foamy virus (PFV) IN in a complex with its cognate vDNA ends, referred to as the intasome, has been successfully crystallized (Hare et al., 2010). The crystal structure analysis of the PFV intasome revealed an unprecedented tetramer structure for IN (see Cherepanov et al., 2011; Li et al., 2011 for recent review). The IN tetramer structure observed in the PFV intasome demonstrated that two sets of IN dimer acts on each vDNA end (**Figure 2**). The inner subunits of each IN dimer contact with vDNA and form a tetramer. The outer subunits of each IN dimer might be speculated to have supportive or other functions, such as engagement of target DNA or interaction with host factors. Several models for the IN tetramer have been proposed from previous structure analysis using partial IN fragments possessing the NTD–CCD or CCD–CTD (Chen et al., 2000; Wang et al., 2001;

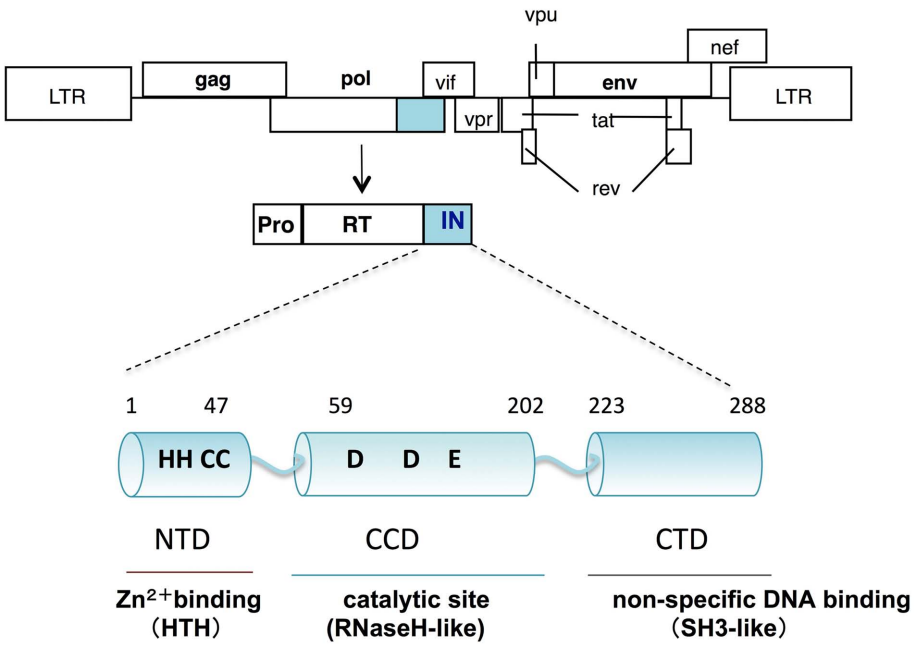

FIGURE 1 | Schematic diagram of HIV-1 IN. The genetic organization of HIV-1 is shown at the top. HIV-1 IN is encoded by the pol region and composed of 288 amino acids with three structurally distinct domains: an N-terminal domain (NTD); a central catalytic core domain (CCD); and a C-terminal domain (CTD). The CCD contains the highly conserved DDE motif, which is directly involved in the catalytic activities of IN. Overall topology of the CCD is similar to that of ribonuclease H (RNaseH). The NTD, contains a highly conserved HHCC motif, which binds to zinc and folds a helix-turn-helix (HTH) structure. The CTD, consisting of a structure that closely resembles Src homology 3 domains (SH3), possesses sequence- and metal ion-independent DNA binding activity.

Hare et al., 2009a). However, these IN tetramer models are different from those observed in the active PFV intasome (Craigie, 2010). Stable interaction of IN with 3′-end processed vDNA in the intasome might be a plausible explanation for the difference. The stable IN tetramer formation observed in the intasome reflects the IN-DNA complex required for proper concerted integration of both vDNA ends into the proximal sites of the target host chromosomal DNA. Furthermore, analysis of the PFV intasome interacting with the STI elucidated its inhibitory mechanism. Based on the PFV intasome structure as a template, structural modeling of the HIV-1 intasome has also been reported (Krishnan et al., 2010). Structural analysis of this intasome revealed numerous details of retroviral integration and will contribute to the design of the next generation of HIV-1 IN catalytic inhibitors. The functional significance of the DNA-independent IN tetramer as observed by analysis of partial IN fragments (Chen et al., 2000; Wang et al., 2001; Hare et al., 2009a) remains unclear (Cherepanov et al., 2011).

NON-ENZYMATIC FUNCTIONS OF IN

Originally, we found that introduction of amino acid substitutions at conserved HHCC residues in the NTD of HIV-1 IN resulted in almost complete abrogation of proviral DNA formation, concomitant with a severe reduction in vDNA synthesis. This suggests the mutations in the IN affected the viral life cycle at steps prior to integration (Masuda et al., 1995). Further genetic analysis of HIV-1 IN revealed that the pleiotropic effects of IN mutations affected uncoating (Masuda et al., 1995; Leavitt et al., 1996; Nakamura et al., 1997; Briones et al., 2010), reverse transcription (Engelman et al., 1995; Masuda et al., 1995; Wu et al., 1999; Tsurutani et al., 2000; Nishitsuji et al., 2009) nuclear import of vDNA (Gallay et al., 1997; Tsurutani et al., 2000; Ikeda et al., 2004), and protein processing during viral particle assembly and maturation (Mohammed et al., 2011). Importantly, HIV-1 carrying point mutations at the catalytic sites of IN (DDE) affected the integration step, but not vDNA synthesis (Masuda et al., 1995). Thus, the pleiotropic effects of IN mutations might not be directly related to the loss of its catalytic function. These experiments suggest that IN may possess non-enzymatic roles throughout the viral replication cycle (**Figure 2**).

Among the possible non-enzymatic roles of IN, there has been an accumulation of evidence to suggest involvement of retroviral IN during reverse transcription (Engelman et al., 1995; Masuda et al., 1995; Tsurutani et al., 2000; Lu et al., 2005; Dobard et al., 2007). The contribution of IN during reverse transcription has also been noticed in a retrovirus-like element of *Saccharomyces cerevisiae*, Ty3 (Nymark-McMahon and Sandmeyer, 1999; Nymark-McMahon et al., 2002). A previous study from our laboratory showed that reverse transcription of HIV-1 was abrogated by knocking down a host factor, survival motor neuron (SMN)-interacting protein 1 (SIP1/Gemin2), which binds to HIV-1 IN (Hamamoto et al., 2006). Gemin 2 is a component of the SMN complex that mediates the assembly of spliceosomal small nuclear ribonucleoproteins and nucleolar ribonucleoproteins (Fischer et al., 1997; Liu et al., 1997; Buhler et al., 1999; Jablonka et al., 2001; Meister et al., 2001). In a subsequent study, we demonstrated that HIV-1 IN and Gemin2 synergistically stimulate

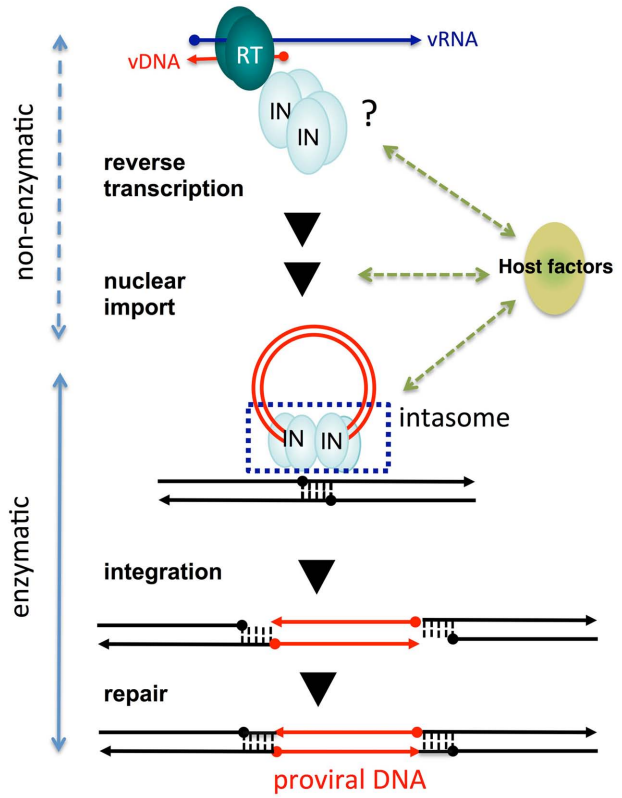

FIGURE 2 | Non-enzymatic and enzymatic roles of HIV-1 IN that help establish proviral DNA. After entry into cells, retroviral genomic RNA (vRNA) is reverse transcribed into DNA (vDNA) by RT. Then, vDNA is transported into the nucleus (nuclear import) and finally integrated into host chromosomal DNA (black lines). IN forms a functional tetramer with vDNA ends (intasome) to assist with integration. Subsequent repair processes by host DNA repair machinery establishes the proviral DNA, in which retrovirus DNA is stably integrated into host chromosomal DNA. IN tetramer structures for its enzymatic (integration) and non-enzymatic functions (reverse transcription and nuclear import) and possible involvement of host factors are schematically depicted. The vRNA, vDNA, and host DNA are shown as blue, red, and black lines, respectively. An arrowhead shows the direction of each genome from the 5′- to the 3′-end.

RT activity by enhancing the assembly of RT on viral RNA *in vitro* (Nishitsuji et al., 2009). Chow and colleagues have also reported that HIV-1 IN stimulates RT activity through physical interactions with RT (Zhu et al., 2004). Thus, IN might possess a direct function to support efficient reverse transcription by RT.

INSIGHT ON PUTATIVE STRUCTURE OF IN FOR ITS NON-ENZYMATIC FUNCTION

Delineation of the IN mutant structure could provide clues for depicting the IN conformation required for non-enzymatic functions. Nuclear magnetic resonance (NMR) analysis of an isolated NTD has shown that the NTD exists in two conformational states, the E and D forms (Cai et al., 1997). A previous study using NMR spectroscopy indicated that the NTD mutant protein, in which the Tyr 15 residue was replaced with Ala (Y15A), folds correctly but only as the E form (Nomura et al., 2006). The IN tetramer structure was formed through interaction of NTD–CCD between the inner subunits in the intasome (Hare et al., 2010). The residues 13–26 and 40–45 in the NTD interact extensively with residues 150–196 in the CCD of the other subunit. The importance of the NTD–CCD interaction to form the IN tetramer has been proposed from previous crystal structure analysis using the NTD–CCD IN fragments (Wang et al., 2001; Hare et al., 2009b). As observed in these previous analyses, the hydrogen-bond contacts between the side chains of CCD residues Gln164 and Arg187 and the backbones of the NTD residues Lys14 and Tyr15 also persist in the recent structure-based model of the HIV-1 IN intasome (Krishnan et al., 2010). HIV-1 carrying IN mutations at the Lys186, Arg187, and Lys188 residues exhibited a reverse transcription-defective phenotype (Tsurutani et al., 2000) as found in the NTD mutants including Y15A. These experimental data suggest that the functional tetramer form, stabilized with the NTD–CCD interaction, might be critical for the non-enzymatic function of IN during reverse transcription.

IMPACT OF HOST FACTORS ON IN STRUCTURE AND NON-ENZYMATIC FUNCTION

Numerous host factors that interact with HIV-1 IN have been reported (Al-Mawsawi and Neamati, 2007). The best characterized factor is lens epithelium-derived growth factor/transcription co-activator p75 (LEDGF/p75; Cherepanov et al., 2003) for chromosomal targeting of HIV-1 IN (Maertens et al., 2003, 2004; Shun et al., 2007). The crystal structure analysis of the PFV intasome (Hare et al., 2010) together with results from previous studies (Li et al., 2006; Hare et al., 2009a) suggest that synapsis formation with DNA ends of the virus through tetramerization of IN might be critical for proper assembly and/or a stable and functionally active intasome. Importantly, LEDGF/p75 stabilizes the functional tetramer of IN for its enzymatic function. Meanwhile, a reduction of the tetramer form of IN was reproduced when wild-type IN was expressed in cells in which endogenous Gemin2 was knocked down by RNA interference (Nishitsuji et al., 2009). We also noticed that the intracellular stability and multimer formation of IN, especially the tetramer formation of IN, were dramatically reduced by IN mutations that led to a reverse transcription-defective phenotype. Thus, in the absence of vDNA, host factors might be involved in forming or maintaining highly ordered structures of IN, which is critical for non-enzymatic function. Therefore, inhibition of the interaction between IN and host factors could be a novel therapeutic approach for the design and development of new classes of IN inhibitors targeting non-enzymatic functions.

CONCLUSION

It is obvious that IN must be closely associated with the viral genome complex to form an active intasome upon the completion of reverse transcription. Physical interaction of IN with RT (Zhu et al., 2004; Wilkinson et al., 2009) could contribute to keeping IN close to the viral genome complex. How is the IN structure in the absence of vDNA before and during reverse transcription maintained? What is the contribution of host factors to

IN conformation that is required for non-enzymatic functions? The highly ordered IN structure and/or its interface structure for interaction with host factors required for non-enzymatic IN function(s) should be determined.

Finally, it should be emphasized that IN mutations affecting non-enzymatic function resulted in severe deleterious affects to HIV-1 replication compared with IN mutations that specifically affected catalytic activity. Clinical efficacy of the STI that blocks IN catalytic activity guarantees that a greater impact on HIV-1 control would be achieved with a novel inhibitor that blocks the non-enzymatic function of IN.

ACKNOWLEDGMENTS

This work was supported by a Grant-in-Aid for Scientific Research on Priority Areas from the Ministry of Education, Culture, Sports, Science, and Technology (MEXT) of Japan and a grant for HIV/AIDS research from the Ministry of Health, Labor, and Welfare of Japan.

REFERENCES

Al-Mawsawi, L. Q., and Neamati, N. (2007). Blocking interactions between HIV-1 integrase and cellular cofactors: an emerging anti-retroviral strategy. *Trends Pharmacol. Sci.* 28, 526–535.

Briones, M. S., Dobard, C. W., and Chow, S. A. (2010). Role of human immunodeficiency virus type 1 integrase in uncoating of the viral core. *J. Virol.* 84, 5181–5190.

Buhler, D., Raker, V., Luhrmann, R., and Fischer, U. (1999). Essential role for the tudor domain of SMN in spliceosomal U snRNP assembly: implications for spinal muscular atrophy. *Hum. Mol. Genet.* 8, 2351–2357.

Burke, C. J., Sanyal, G., Bruner, M. W., Ryan, J. A., Lafemina, R. L., Robbins, H. L., Zeft, A. S., Middaugh, C. R., and Cordingley, M. G. (1992). Structural implications of spectroscopic characterization of a putative zinc finger peptide from HIV-1 integrase. *J. Biol. Chem.* 267, 9639–9644.

Bushman, F. D., Engelman, A., Palmer, I., Wingfield, P., and Craigie, R. (1993). Domains of the integrase protein of human immunodeficiency virus type 1 responsible for polynucleotidyl transfer and zinc binding. *Proc. Natl. Acad. Sci. U.S.A.* 90, 3428–3432.

Cai, M., Zheng, R., Caffrey, M., Craigie, R., Clore, G. M., and Gronenborn, A. M. (1997). Solution structure of the N-terminal zinc binding domain of HIV-1 integrase. *Nat. Struct. Biol.* 4, 567–577.

Chen, J. C., Krucinski, J., Miercke, L. J., Finer-Moore, J. S., Tang, A. H., Leavitt, A. D., and Stroud, R. M. (2000). Crystal structure of the HIV-1 integrase catalytic core and C-terminal domains: a model for viral DNA binding. *Proc. Natl. Acad. Sci. U.S.A.* 97, 8233–8238.

Cherepanov, P., Maertens, G., Proost, P., Devreese, B., Van Beeumen, J., Engelborghs, Y., De Clercq, E., and Debyser, Z. (2003). HIV-1 integrase forms stable tetramers and associates with LEDGF/p75 protein in human cells. *J. Biol. Chem.* 278, 372–381.

Cherepanov, P., Maertens, G. N., and Hare, S. (2011). Structural insights into the retroviral DNA integration apparatus. *Curr. Opin. Struct. Biol.* 21, 249–256.

Craigie, R. (2010). Structural biology: when four become one. *Nature* 464, 167–168.

Dobard, C. W., Briones, M. S., and Chow, S. A. (2007). Molecular mechanisms by which human immunodeficiency virus type 1 integrase stimulates the early steps of reverse transcription. *J. Virol.* 81, 10037–10046.

Dyda, F., Hickman, A. B., Jenkins, T. M., Engelman, A., Craigie, R., and Davies, D. R. (1994). Crystal structure of the catalytic domain of HIV-1 integrase: similarity to other polynucleotidyl transferases. *Science* 266, 1981–1986.

Eijkelenboom, A. P., Lutzke, R. A., Boelens, R., Plasterk, R. H., Kaptein, R., and Hard, K. (1995). The DNA-binding domain of HIV-1 integrase has an SH3-like fold. *Nat. Struct. Biol.* 2, 807–810.

Ellison, V., Gerton, J., Vincent, K. A., and Brown, P. O. (1995). An essential interaction between distinct domains of HIV-1 integrase mediates assembly of the active multimer. *J. Biol. Chem.* 270, 3320–3326.

Engelman, A., and Craigie, R. (1992). Identification of conserved amino acid residues critical for human immunodeficiency virus type 1 integrase function in vitro. *J. Virol.* 66, 6361–6369.

Engelman, A., Englund, G., Orenstein, J. M., Martin, M. A., and Craigie, R. (1995). Multiple effects of mutations in human immunodeficiency virus type 1 integrase on viral replication. *J. Virol.* 69, 2729–2736.

Fischer, U., Liu, Q., and Dreyfuss, G. (1997). The SMN-SIP1 complex has an essential role in spliceosomal snRNP biogenesis. *Cell* 90, 1023–1029.

Gallay, P., Hope, T., Chin, D., and Trono, D. (1997). HIV-1 infection of nondividing cells through the recognition of integrase by the importin/karyopherin pathway. *Proc. Natl. Acad. Sci. U.S.A.* 94, 9825–9830.

Hamamoto, S., Nishitsuji, H., Amagasa, T., Kannagi, M., and Masuda, T. (2006). Identification of a novel human immunodeficiency virus type 1 integrase interactor, Gemin2, that facilitates efficient viral cDNA synthesis in vivo. *J. Virol.* 80, 5670–5677.

Hare, S., Di Nunzio, F., Labeja, A., Wang, J., Engelman, A., and Cherepanov, P. (2009a). Structural basis for functional tetramerization of lentiviral integrase. *PLoS Pathog.* 5, e1000515. doi:10.1371/journal.ppat.1000515

Hare, S., Shun, M. C., Gupta, S. S., Valkov, E., Engelman, A., and Cherepanov, P. (2009b). A novel co-crystal structure affords the design of gain-of-function lentiviral integrase mutants in the presence of modified PSIP1/LEDGF/p75. *PLoS Pathog.* 5, e1000259. doi:10.1371/journal.ppat.1000259

Hare, S., Gupta, S. S., Valkov, E., Engelman, A., and Cherepanov, P. (2010). Retroviral intasome assembly and inhibition of DNA strand transfer. *Nature* 464, 232–236.

Ikeda, T., Nishitsuji, H., Zhou, X., Nara, N., Ohashi, T., Kannagi, M., and Masuda, T. (2004). Evaluation of the functional involvement of human immunodeficiency virus type 1 integrase in nuclear import of viral cDNA during acute infection. *J. Virol.* 78, 11563–11573.

Jablonka, S., Bandilla, M., Wiese, S., Buhler, D., Wirth, B., Sendtner, M., and Fischer, U. (2001). Co-regulation of survival of motor neuron (SMN) protein and its interactor SIP1 during development and in spinal muscular atrophy. *Hum. Mol. Genet.* 10, 497–505.

Katz, R. A., and Skalka, A. M. (1994). The retroviral enzymes. *Annu. Rev. Biochem.* 63, 133–173.

Krishnan, L., Li, X., Naraharisetty, H. L., Hare, S., Cherepanov, P., and Engelman, A. (2010). Structure-based modeling of the functional HIV-1 intasome and its inhibition. *Proc. Natl. Acad. Sci. U.S.A.* 107, 15910–15915.

Kulkosky, J., Jones, K. S., Katz, R. A., Mack, J. P., and Skalka, A. M. (1992). Residues critical for retroviral integrative recombination in a region that is highly conserved among retroviral/retrotransposon integrases and bacterial insertion sequence transposases. *Mol. Cell. Biol.* 12, 2331–2338.

LaFemina, R. L., Schneider, C. L., Robbins, H. L., Callahan, P. L., Legrow, K., Roth, E., Schleif, W. A., and Emini, E. A. (1992). Requirement of active human immunodeficiency virus type 1 integrase enzyme for productive infection of human T-lymphoid cells. *J. Virol.* 66, 7414–7419.

Leavitt, A. D., Robles, G., Alesandro, N., and Varmus, H. E. (1996). Human immunodeficiency virus type 1 integrase mutants retain in vitro integrase activity yet fail to integrate viral DNA efficiently during infection. *J. Virol.* 70, 721–728.

Li, M., Mizuuchi, M., Burke, T. R. Jr., and Craigie, R. (2006). Retroviral DNA integration: reaction pathway and critical intermediates. *EMBO J.* 25, 1295–1304.

Li, X., Krishnan, L., Cherepanov, P., and Engelman, A. (2011). Structural biology of retroviral DNA integration. *Virology* 411, 194–205.

Liu, Q., Fischer, U., Wang, F., and Dreyfuss, G. (1997). The spinal muscular atrophy disease gene product, SMN, and its associated protein SIP1 are in a complex with spliceosomal snRNP proteins. *Cell* 90, 1013–1021.

Lodi, P. J., Ernst, J. A., Kuszewski, J., Hickman, A. B., Engelman, A., Craigie, R., Clore, G. M., and Gronenborn, A. M. (1995). Solution structure of the DNA binding domain of HIV-1 integrase. *Biochemistry* 34, 9826–9833.

Lu, R., Ghory, H. Z., and Engelman, A. (2005). Genetic analyses of conserved residues in the carboxyl-terminal domain of human immunodeficiency virus type 1 integrase. *J. Virol.* 79, 10356–10368.

Luo, Y., and Muesing, M. A. (2010). Prospective strategies for targeting HIV-1 integrase function. *Future Med. Chem.* 2, 1055–1060.

Maertens, G., Cherepanov, P., Debyser, Z., Engelborghs, Y., and Engelman, A. (2004). Identification and characterization of a functional nuclear localization signal in the HIV-1 integrase interactor LEDGF/p75. *J. Biol. Chem.* 279, 33421–33429.

Maertens, G., Cherepanov, P., Pluymers, W., Busschots, K., De Clercq, E., Debyser, Z., and Engelborghs, Y. (2003). LEDGF/p75 is essential for nuclear and chromosomal targeting of HIV-1 integrase in human cells. *J. Biol. Chem.* 278, 33528–33539.

Masuda, T., Planelles, V., Krogstad, P., and Chen, I. S. (1995). Genetic analysis of human immunodeficiency virus type 1 integrase and the U3 att site: unusual phenotype of mutants in the zinc finger-like domain. *J. Virol.* 69, 6687–6696.

Meister, G., Buhler, D., Pillai, R., Lottspeich, F., and Fischer, U. (2001). A multiprotein complex mediates the ATP-dependent assembly of spliceosomal U snRNPs. *Nat. Cell Biol.* 3, 945–949.

Metifiot, M., Marchand, C., Maddali, K., and Pommier, Y. (2010). Resistance to integrase inhibitors. *Viruses* 2, 1347–1366.

Mohammed, K. D., Topper, M. B., and Muesing, M. A. (2011). Sequential deletion of the integrase (Gag-Pol) carboxyl terminus reveals distinct phenotypic classes of defective HIV-1. *J. Virol.* 85, 4654–4666.

Nakamura, T., Masuda, T., Goto, T., Sano, K., Nakai, M., and Harada, S. (1997). Lack of infectivity of HIV-1 integrase zinc finger-like domain mutant with morphologically normal maturation. *Biochem. Biophys. Res. Commun.* 239, 715–722.

Nishitsuji, H., Hayashi, T., Takahashi, T., Miyano, M., Kannagi, M., and Masuda, T. (2009). Augmentation of reverse transcription by integrase through an interaction with host factor, SIP1/Gemin2 Is critical for HIV-1 infection. *PLoS ONE* 4, e7825. doi:10.1371/journal.pone.0007825

Nomura, Y., Masuda, T., and Kawai, G. (2006). Structural analysis of a mutant of the HIV-1 integrase zinc finger domain that forms a single conformation. *J. Biochem.* 139, 753–759.

Nymark-McMahon, M. H., Beliakova-Bethell, N. S., Darlix, J. L., Le Grice, S. F., and Sandmeyer, S. B. (2002). Ty3 integrase is required for initiation of reverse transcription. *J. Virol.* 76, 2804–2816.

Nymark-McMahon, M. H., and Sandmeyer, S. B. (1999). Mutations in nonconserved domains of Ty3 integrase affect multiple stages of the Ty3 life cycle. *J. Virol.* 73, 453–465.

Shun, M. C., Raghavendra, N. K., Vandegraaff, N., Daigle, J. E., Hughes, S., Kellam, P., Cherepanov, P., and Engelman, A. (2007). LEDGF/p75 functions downstream from preintegration complex formation to effect gene-specific HIV-1 integration. *Genes Dev.* 21, 1767–1778.

Summa, V., Petrocchi, A., Bonelli, F., Crescenzi, B., Donghi, M., Ferrara, M., Fiore, F., Gardelli, C., Gonzalez Paz, O., Hazuda, D. J., Jones, P., Kinzel, O., Laufer, R., Monteagudo, E., Muraglia, E., Nizi, E., Orvieto, F., Pace, P., Pescatore, G., Scarpelli, R., Stillmock, K., Witmer, M. V., and Rowley, M. (2008). Discovery of raltegravir, a potent, selective orally bioavailable HIV-integrase inhibitor for the treatment of HIV-AIDS infection. *J. Med. Chem.* 51, 5843–5855.

Tsurutani, N., Kubo, M., Maeda, Y., Ohashi, T., Yamamoto, N., Kannagi, M., and Masuda, T. (2000). Identification of critical amino acid residues in human immunodeficiency virus type 1 IN required for efficient proviral DNA formation at steps prior to integration in dividing and nondividing cells. *J. Virol.* 74, 4795–4806.

Wang, J. Y., Ling, H., Yang, W., and Craigie, R. (2001). Structure of a two-domain fragment of HIV-1 integrase: implications for domain organization in the intact protein. *EMBO J.* 20, 7333–7343.

Wilkinson, T. A., Januszyk, K., Phillips, M. L., Tekeste, S. S., Zhang, M., Miller, J. T., Le Grice, S. F., Clubb, R. T., and Chow, S. A. (2009). Identifying and characterizing a functional HIV-1 reverse transcriptase-binding site on integrase. *J. Biol. Chem.* 284, 7931–7939.

Wu, X., Liu, H., Xiao, H., Conway, J. A., Hehl, E., Kalpana, G. V., Prasad, V., and Kappes, J. C. (1999). Human immunodeficiency virus type 1 integrase protein promotes reverse transcription through specific interactions with the nucleoprotein reverse transcription complex. *J. Virol.* 73, 2126–2135.

Zhu, K., Dobard, C., and Chow, S. A. (2004). Requirement for integrase during reverse transcription of human immunodeficiency virus type 1 and the effect of cysteine mutations of integrase on its interactions with reverse transcriptase. *J. Virol.* 78, 5045–5055.

Conflict of Interest Statement: The author declares that the research was conducted in the absence of any commercial or financial relationships that could be construed as a potential conflict of interest.

Received: 14 September 2011; paper pending published: 24 September 2011; accepted: 26 September 2011; published online: 13 October 2011.

*Citation: Masuda T (2011) Non-enzymatic functions of retroviral integrase: the next target for novel anti-HIV drug development. Front. Microbio. **2**:210. doi: 10.3389/fmicb.2011.00210*

This article was submitted to Frontiers in Virology, a specialty of Frontiers in Microbiology.

frontiers in
MICROBIOLOGY

MINI REVIEW ARTICLE
published: 09 December 2011
doi: 10.3389/fmicb.2011.00242

Morphogenesis of the infectious HIV-1 virion

Jun-ichi Sakuragi*

Department of Viral Infections, Research Institute for Microbial Diseases, Osaka University, Osaka, Japan

Edited by:
Akio Adachi, The University of Tokushima Graduate School, Japan

Reviewed by:
Masako Nomaguchi, The University of Tokushima Graduate School, Japan
Mikako Fujita, Kumamoto University, Japan

Correspondence:
Jun-ichi Sakuragi, Department of Viral Infections, Research Institute for Microbial Diseases, Osaka University, 3-1 Yamadaoka, Suita, Osaka 565-0871, Japan.
e-mail: sakuragi@biken.osaka-u.ac.jp

The virion of HIV-1 is spherical and viral glycoprotein spikes (gp120, gp41) protrude from its envelope. The characteristic cone-shaped core exists within the virion, caging the ribonucleoprotein (RNP) complex, which is comprised of viral RNA, nucleocapsid (NC), and viral enzymes. The HIV-1 virion is budded and released from the infected cell as an immature donut-shaped particle. During or immediately after release, viral protease (PR) is activated and subsequently processes the viral structural protein Gag. Through this maturation process, virions acquire infectivity, but its mechanism and transition of morphology largely remain unclear. Recent technological advances in experimental devices and techniques have made it possible to closely dissect the viral production site on the cell, the exterior – or even the interior – of an individual virion, and many new aspects on virion morphology and maturation. In this manuscript, I review the morphogenesis of HIV-1 virions. I focus on several studies, including some of our recent findings, which examined virion formation and/or maturation processes. The story of novel compound, which inhibits virion maturation, and the importance of maturation research are also discussed.

Keywords: HIV-1, virion, maturation, Gag, RNA, morphology

INTRODUCTION

The infectious particle of virus (virion) is a very sophisticated device since it needs to be durable enough to protect the packaged viral genome from extracellular nucleases and other obstructions; where it has to be subsequently dissociated appropriately in the target cell to initiate infection.

The virion of the retrovirus, including Human Immunodeficiency Virus type 1 (HIV-1), is spherical with a diameter of about 120 nm and viral glycoprotein spikes protrude from its envelope. HIV-1 dynamically converts the interior morphology of its particle during particle release, termed *maturation*. Maturation changes the virion morphology from an immature particle, called the donut-shaped particle, to the mature virion; a particle that is (1) lined with viral matrix proteins (MA), (2) containing a condensed cone-shaped core composed of a viral capsid (CA) which finally encapsidates the (3) RNP complex, comprised of viral RNA, NC, and viral enzymes such as reverse transcriptase (RT) and integrase (IN) (Frankel and Young, 1998). After the maturation, the virus acquires ability to infect adjacent host cells and, thus, the maturation is inevitably essential for particle infectivity. Although much about how the process of virion maturation contributes to achieving infectivity remain unclear, it is a well-accepted concept that viral infectivity is fully acquired only after complete virion maturation (Bukrinskaya, 2004). Here, I review the morphogenesis of HIV-1 virions, focusing on studies, including our own studies, which have examined the virion formation and/or maturation processes. The mutual relationship between protein processing and virion structure are discussed for a further understanding of how virion morphology plays a key role in the HIV-1 life cycle.

HIV-1 VIRION MATURATION PROCESS

The construction of the spherical virion of HIV-1 solely driven by the viral gag proteins. The precursor proteins of gag (Pr55) and gag–pol (Pr160) are expressed from an unspliced full-length viral RNA, which is targeted to the plasma membrane by their N-terminal myristoylation and the adequate accumulation of precursor proteins drive virion assembly beneath the host cell membrane (Ganser-Pornillos et al., 2008). Many features of the virion assembly, budding, and release processes are largely unknown, but many host cell factors are suggested to support and/or actively contribute to these processes (Martin-Serrano and Neil, 2011). Several thousands of gag precursors are required to construct the normal virion (Briggs et al., 2004), but budded particle is not fully infectious at its current state. To acquire infectivity, the virion must undergo a maturation process, which is mediated by the precursor protein processing by virally encoded PR (Briggs and Krausslich, 2011). Virion maturation is believed to initiate and complete during or immediately after particle release (Kaplan et al., 1994; Bukrinskaya, 2004), although it still remains unclear what triggers viral PR activation.

The Pr55 polypeptide is composed of four protein domains – MA, CA, NC, and p6 – and two spacer peptides, p2 and p1. The N-to-C terminal order of the six proteins and peptides are MA–CA–p2–NC–p1–p6, thus containing five proteolytic cleavage sites to be processed by PR. It was previously demonstrated that the processing rates of the five cleavage sites were not equal (Pettit et al., 1994), where the processing rate of the cleavage site between p2 and NC (p2/NC) is the fastest, while p1/p6 and MA/CA are the second and the third, respectively. The processing rates of the two remaining sites (CA/p2 and NC/p1) are much slower than

those of the three aforementioned sites. As virion maturation is suggested to occur during particle production, it is very difficult to observe the exact maturation process over a time series. Therefore, we recently constructed four sequential HIV-1 Gag mutants in an attempt to generate a sequential series of Gag maturation intermediates and effectively snapshoot the process of virion maturation (Ohishi et al., 2011). We examined the physical states of the RNA viral genome, including dimerization and stability, the ability of endogenous reverse transcription and overall infectivity of particles generated with these mutants. The results are summarized in **Figure 1**. During the virion maturation process, stabilization of the RNA dimer primes during the primary cleavage (p2–NC) of Pr55 Gag. However, the primary cleavage alone is insufficient and the ensuing cleavages are required for complete the uniform dimerization of viral RNA. Although endogenous virion RT activity was fully acquired at the initial step of maturation, the following processes were necessary for viral DNA production in the infected cell, suggesting that viral RNA/protein maturation plays a critical role for viral infectivity outside the RT process.

MORPHOLOGICAL STUDIES OF VIRION

It is well-accepted that HIV-1 virion morphology dramatically changes during Pr55 processing. To investigate whether the morphological changes of the virion are correlated with maturation, we examined virion morphological features generated from the four sequential step mutants via electron microscopy (Ohishi et al., 2011). We classified the virion morphologies into four main groups (A, B, C, and D) based on structure of viral core and membrane features (**Figure 1**). The morphology of all ΔPR virions were typical immature particles (Group A) as demonstrated by many previous reports (e.g., Peng et al., 1989). As expected, virions from the Step0 mutant were very similar to those of ΔPR, containing a thick electron-dense ring devoid of a conical-shaped core, termed a donut-shaped morphology. The morphologies of the WT were classified into two major groups. One was the typical mature particle (Group D), with a conical core surrounded by an envelope. The second was an enveloped particle containing some amorphous structures rather than an obvious core (Group C). Most of the virions from Step1 to 1.1 were immature (Group B), but did not have an apparent

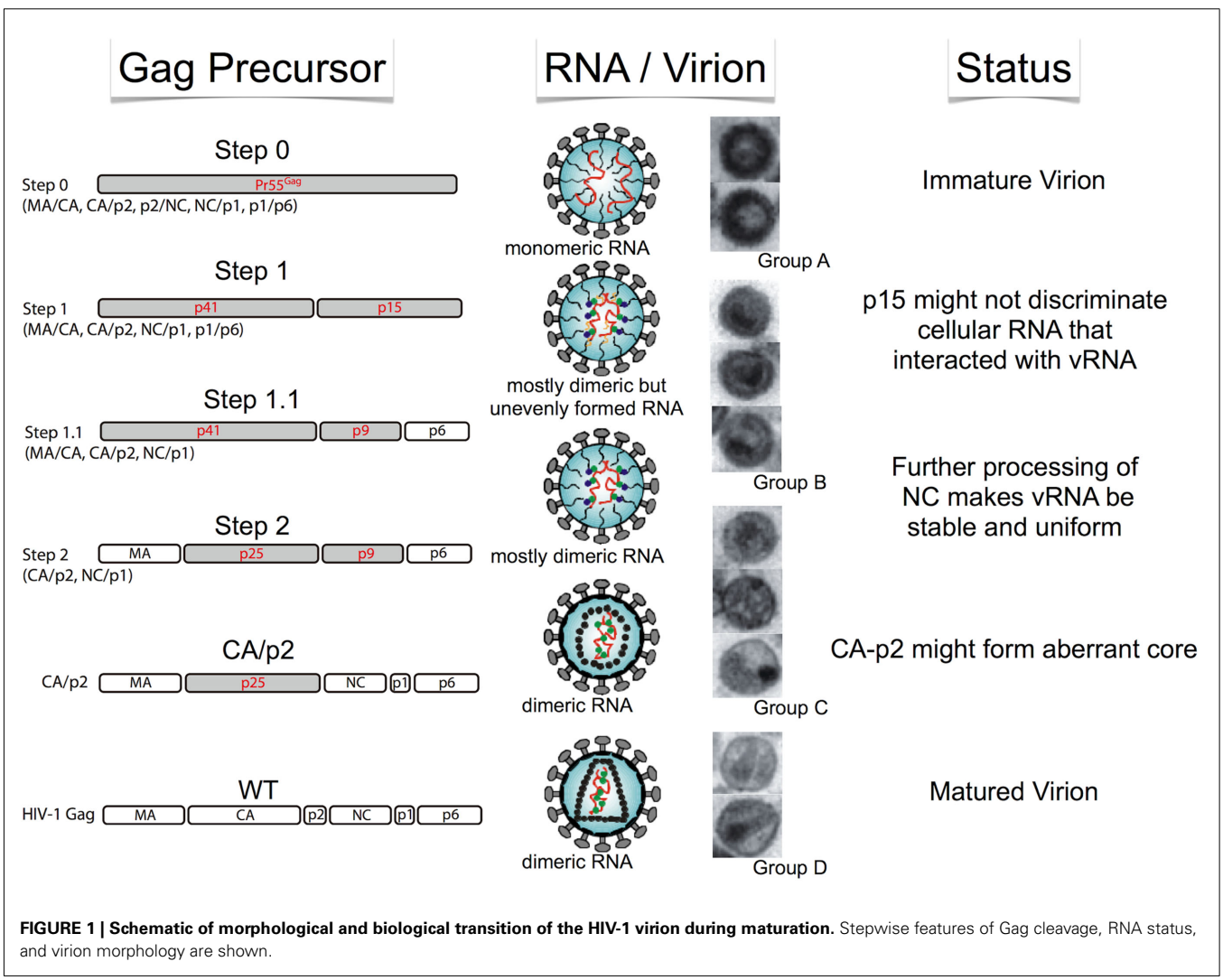

FIGURE 1 | Schematic of morphological and biological transition of the HIV-1 virion during maturation. Stepwise features of Gag cleavage, RNA status, and virion morphology are shown.

electron-dense ring observed in Group A particles, along with envelopes that were thicker than those of Group C. The virions from Step2 contained both Group B and C particles. **Figure 1** represents the schematic of morphological transition of the HIV-1 virion during maturation. As the change from Group A to B was characterized by the disappearance of an electron-dense ring inside the viral membrane, the observed ring is likely composed by the p15 (NC–p1–p6) region within Pr55. After the cleavage at p2–NC position, the ordered array of the p15 region would be lost and p15 would be released from inner viral membrane. This transition was synchronous with initial dimeric RNA stabilization, suggesting the release of genome RNA from a perimembrane localization to a space inside the virion where p15 could trigger dimer maturation. The thin-membraned virions (Group C) became abundant after the third proteolytic processing at the MA/CA region, represented by the Step2 mutant. Viral membranes of Group B may appear to be thick because of the fusion between the Pr55 CA and MA, which lines the inner membrane.

Recent advances in analytical technology, particularly electron microscopy, enabled researchers to study the structure of intact virions and even within the virion itself (Liu et al., 2010), and several morphological studies about HIV-1 virion were reported (Carlson et al., 2010; de Marco et al., 2010; Zhang et al., 2011). Of particular note, a cryoelectron tomography study examined the maturation process of the HIV-1 virion (de Marco et al., 2010). Several stepwise mutants of Gag cleavage were constructed and the changes in virion structure that occurred during maturation were observed. They visualized the arrangement of Gag in three-dimensions (3D) using cryoelectron tomography and sub-tomogram averaging. The condensation of the RNP complex with RNA genome and viral proteins were detected at the initial cleavage event. This inner RNA/protein structure appears to maintain a link with the remaining Gag lattice. Processing on both sides of CA–p2 – the main structural module of Gag – is required for disassembly of the immature Gag lattice. The results provided structural correlates of the ordered processing events during HIV-1 maturation and were also consistent in principle with our observations (Ohishi et al., 2011).

Another report studied the budding process of HIV-1 (Carlson et al., 2010). They established experimental systems to study HIV-1 budding sites by cryoelectron tomography and observed variable 3D structures within HIV-1 virions and budding sites. By analyzing these images they showed that the organization of released immature virions is not altered to a large degree from the state of its intracellular assembly. They also identified a novel Gag lattice structure present at viral budding sites. It seemed to be caused by the premature processing of Gag precursors and resulted in the production of dead-end particles. The structures were abundant at viral budding sites in some HIV-1 infected T-cells, suggesting that a crucial control step during virus maturation was lost. They suggested this loss of control might be caused by the host cell environment and a host factor, but the significance of this phenomena was unclear. The actin filaments were often observed around and at the budding sites, and sometimes they appeared stuck to the budding virions.

Although it is not clear whether actin actively contributes to the HIV-1 budding process or not, a recent report denied the effect of HIV-1 replication on the coherency of the actin cytoskeleton (Weichsel et al., 2010). On the other hand, clathrin, a major player in the formation of coated vesicles (Pearse, 1976), was reported to facilitate the morphogenesis of retrovirus particles (Zhang et al., 2011). Clathrin was previously thought to be only passively incorporated into retroviral virions (Hammarstedt and Garoff, 2004). However in this report, abundant amounts of clathrin was shown to be actively and specifically incorporated into retrovirus particles. In several cases, retroviral proteins contain peptide motifs for clathrin recruitment. HIV, SIV, and other murine and simian retroviruses actively packaged clathrin and the prevention of clathrin incorporation caused a variety of defects in the generation of infectious virions, evidenced by viral protein destabilization, inhibition of particle assembly/release, and reduction in virion infectivity. The virion morphology of an SIV mutant lacking the PTAP motif showed grossly abnormal clathrin incorporation. Virus-producing-cells exhibited hemispherical protrusions from their surfaces, but complete spherical particles were hardly observed via scanning electron microscopy. In case of MLV, the virion's ability to saturate the TRIM5alpha (T5a) restriction factor was examined. For efficient elimination of T5a activity, the presence of an unmodified capsid lattice was reported to be required (Pertel et al., 2011). As expected, mutant particles lacking clathrin were approximately 10-fold less active in the T5a saturation assay to that of the WT. The finding suggested that their cores were not properly formed, or unstable, therefore suggesting that clathrin is important for correct MLV particle morphogenesis. These studies suggested that clathrin might be frequently recruited by retroviruses to assist the correct assembly of infectious virions.

ANTI-VIRAL DRUGS TARGETING FOR VIRION MATURATION

As the virion maturation process is essential for acquiring viral infectivity, it is a reasonable target for developing anti-viral drugs (Adamson and Freed, 2011). The principal anti-viral target of HIV-1 maturation for many effective drugs was viral PR, (Perno, 2011) however, the emergence of drug-resistant strains in patients undergoing drug treatments appear inevitable. In addition, multiple drug targeting a single protein such as PR often induces the emergence of cross-resistant strains, which have very serious implications for infection dissemination and control (Lefebvre and Schiffer, 2008). Thus, the development of drugs using alternative strategies and targets may be required. An alternative target for a maturation inhibitor is Pr55, which is the substrate of PR (Adamson et al., 2009). The small molecule 3-*O*-(3′, 3′-dimethylsuccinyl)-betulinic acid (DSB), also known as bevirimat (BVM), PA-457, or MPC-4326, is the first maturation inhibitor, which potently inhibits HIV-1 replication by blocking a late step of the Gag cleavage pathway, preventing scission at the CA–p2 junction (Li et al., 2003). Although the structural study is still ongoing, it has been demonstrated that BVM is incorporated into assembling virus particles in a Gag-dependent manner (Zhou et al., 2005) and is able to prevent cleavage of CA from p2 in the context of premature Gag used in virion assembly assembled into virions, but not in free Gag in solution (Li et al., 2003; Sakalian et al., 2006). These data have led to a model where the BVM binding site

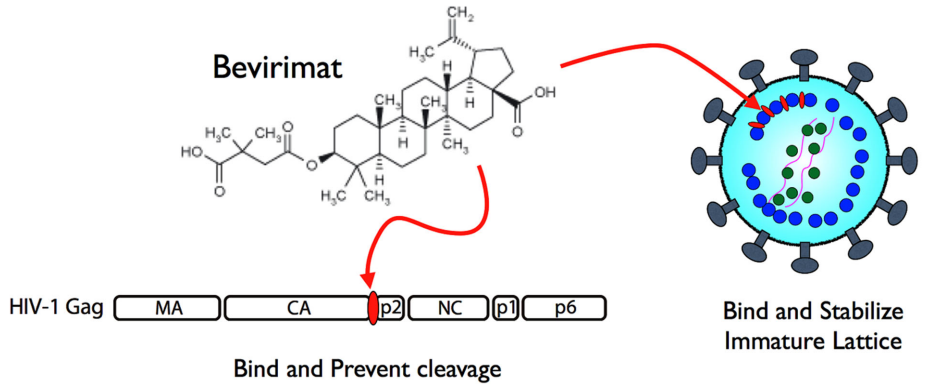

FIGURE 2 | Mechanism of action of bevirimat. It binds to CA/p2 cleavage site of HIV-1 Pr55 to prevent processing by PR (left) and also to stabilize viral core formation in immature status (right).

is present during Gag assembly, at or nearby the CA–p2 cleavage site, and binding of BVM blocks PR from accessing the cleavage site (**Figure 2**). When virions isolated from BVM-treated cells were observed, the drug disrupted virion production as particles contained an incomplete shell of protein density – with a structure similar to the Gag lattice of an immature HIV-1 particle. Similar to the CA–p2 fusion mutant, BVM binding was suggested to stabilize the immature lattice and prevent capsid maturation, effectively suppressing particle infectivity (Keller et al., 2011). Although BVM was in Phase II clinical trial to determine its use as a treatment against HIV-1, several reports suggested that there was a very low genetic barrier for resistance against BVM (Seclen et al., 2010; Verheyen et al., 2010), eliciting concern for the continuation of its clinical development and subsequently the pharmaceutical company has recently halted BVM development (Wainberg and Albert, 2010). Nonetheless, other pharmaceutical companies still express strong interests in developing a second generation of maturation inhibitor drugs, indicating a compelling demand and promising future for these novel drugs.

CONCLUSION

The HIV-1 virion structure, as well as the processes involved in their generation, are not fully elucidated. The virion maturation process is one of the most challenging events to be completely understood. It completely changes the morphology and conditions within the virion and primes viral infectivity by properly arranging the core, which contains the viral RNA and enzymes. Recent advancements of tools and methodologies for experimentation enables scientists to unveil many features of virion morphology and its architecture. Many observations pertaining to virion formation are waiting to be discovered and further structural studies alongside technological improvements would be valuable to resolve these issues. The morphological studies of the virion will not only elucidate the lifecycle of virus replication, but will further the understanding of drug efficacy mechanisms. In fact, cryoelectron tomography studies provided structural correlates of the ordered processing events during HIV-1 maturation and shed light on the mechanism of action of BVM (de Marco et al., 2010). Although current maturation inhibitors seem to be concentrated on the CA–p2 cleavage site (Salzwedel et al., 2007), there remain four additional cleavage sites which may serve as potential drug targets, thus underscoring the importance of studies involving virion morphology and these study cannot be overlooked in the future.

ACKNOWLEDGMENTS

I appreciate Prof. Tatsuo Shioda and Dr. Seiga Ohmine for critically reading the manuscript. This work was supported by a Grant-in-Aid for Scientific Research on Priority Areas from the Ministry of Education, Culture, Sports, Science, and Technology (MEXT) of Japan and a grant for HIV/AIDS research from the Ministry of Health, Labor, and Welfare of Japan.

REFERENCES

Adamson, C. S., and Freed, E. O. (2011). Novel approaches to inhibiting HIV-1 replication. *Antiviral Res.* 85, 119–141.

Adamson, C. S., Salzwedel, K., and Freed, E. O. (2009). Virus maturation as a new HIV-1 therapeutic target. *Expert Opin. Ther. Targets* 13, 895–908.

Briggs, J. A., and Krausslich, H. G. (2011). The molecular architecture of HIV. *J. Mol. Biol.* 410, 491–500.

Briggs, J. A., Simon, M. N., Gross, I., Krausslich, H. G., Fuller, S. D., Vogt, V. M., and Johnson, M. C. (2004). The stoichiometry of Gag protein in HIV-1. *Nat. Struct. Mol. Biol.* 11, 672–675.

Bukrinskaya, A. G. (2004). HIV-1 assembly and maturation. *Arch. Virol.* 149, 1067–1082.

Carlson, L. A., de Marco, A., Oberwinkler, H., Habermann, A., Briggs, J. A., Krausslich, H. G., and Grunewald, K. (2010). Cryo electron tomography of native HIV-1 budding sites. *PLoS Pathog.* 6, e1001173. doi:10.1371/journal.ppat.1001173

de Marco, A., Muller, B., Glass, B., Riches, J. D., Krausslich, H. G., and Briggs, J. A. (2010). Structural analysis of HIV-1 maturation using cryo-electron tomography. *PLoS Pathog.* 6, e1001215. doi:10.1371/journal.ppat.1001215

Frankel, A. D., and Young, J. A. (1998). HIV-1: fifteen proteins and an RNA. *Annu. Rev. Biochem.* 67, 1–25.

Ganser-Pornillos, B. K., Yeager, M., and Sundquist, W. I. (2008). The structural biology of HIV assembly. *Curr. Opin. Struct. Biol.* 18, 203–217.

Hammarstedt, M., and Garoff, H. (2004). Passive and active inclusion of host proteins in human immunodeficiency virus type 1 gag particles during budding at the plasma membrane. *J. Virol.* 78, 5686–5697.

Kaplan, A. H., Manchester, M., and Swanstrom, R. (1994). The activity of the protease of human immunodeficiency virus type 1 is initiated at the membrane of infected cells before the release of viral proteins and is required for release to occur with maximum efficiency. *J. Virol.* 68, 6782–6786.

Keller, P. W., Adamson, C. S., Heymann, J. B., Freed, E. O., and Steven, A. C. (2011). HIV-1 maturation inhibitor bevirimat stabilizes the immature Gag lattice. *J. Virol.* 85, 1420–1428.

Lefebvre, E., and Schiffer, C. A. (2008). Resilience to resistance of HIV-1 protease inhibitors: profile of darunavir. *AIDS Rev.* 10, 131–142.

Li, F., Goila-Gaur, R., Salzwedel, K., Kilgore, N. R., Reddick, M., Matallana, C., Castillo, A., Zoumplis, D., Martin, D. E., Orenstein, J. M., Allaway, G. P., Freed, E. O., and Wild, C. T. (2003). PA-457: a potent HIV inhibitor that disrupts core condensation by targeting a late step in Gag processing. *Proc. Natl. Acad. Sci. U.S.A.* 100, 13555–13560.

Liu, J., Wright, E. R., and Winkler, H. (2010). 3D visualization of HIV virions by cryoelectron tomography. *Meth. Enzymol.* 483, 267–290.

Martin-Serrano, J., and Neil, S. J. (2011). Host factors involved in retroviral budding and release. *Nat. Rev. Microbiol.* 9, 519–531.

Ohishi, M., Nakano, T., Sakuragi, S., Shioda, T., Sano, K., and Sakuragi, J. I. (2011). The relationship between HIV-1 genome RNA dimerization, virion maturation and infectivity. *Nucleic Acids Res.* 39, 3404–3017.

Pearse, B. M. (1976). Clathrin: a unique protein associated with intracellular transfer of membrane by coated vesicles. *Proc. Natl. Acad. Sci. U.S.A.* 73, 1255–1259.

Peng, C., Ho, B. K., Chang, T. W., and Chang, N. T. (1989). Role of human immunodeficiency virus type 1-specific protease in core protein maturation and viral infectivity. *J. Virol.* 63, 2550–2556.

Perno, C. F. (2011). The discovery and development of HIV therapy: the new challenges. *Ann. Ist. Super. Sanita* 47, 41–43.

Pertel, T., Hausmann, S., Morger, D., Zuger, S., Guerra, J., Lascano, J., Reinhard, C., Santoni, F. A., Uchil, P. D., Chatel, L., Bisiaux, A., Albert, M. L., Strambio-De-Castillia, C., Mothes, W., Pizzato, M., Grutter, M. G., and Luban, J. (2011). TRIM5 is an innate immune sensor for the retrovirus capsid lattice. *Nature* 472, 361–365.

Pettit, S. C., Moody, M. D., Wehbie, R. S., Kaplan, A. H., Nantermet, P. V., Klein, C. A., and Swanstrom, R. (1994). The p2 domain of human immunodeficiency virus type 1 Gag regulates sequential proteolytic processing and is required to produce fully infectious virions. *J. Virol.* 68, 8017–8027.

Sakalian, M., McMurtrey, C. P., Deeg, F. J., Maloy, C. W., Li, F., Wild, C. T., and Salzwedel, K. (2006). 3-O-(3′,3′-dimethysuccinyl) betulinic acid inhibits maturation of the human immunodeficiency virus type 1 Gag precursor assembled in vitro. *J. Virol.* 80, 5716–5722.

Salzwedel, K., Martin, D. E., and Sakalian, M. (2007). Maturation inhibitors: a new therapeutic class targets the virus structure. *AIDS Rev.* 9, 162–172.

Seclen, E., Gonzalez Mdel, M., Corral, A., de Mendoza, C., Soriano, V., and Poveda, E. (2010). High prevalence of natural polymorphisms in Gag (CA-SP1) associated with reduced response to Bevirimat, an HIV-1 maturation inhibitor. *AIDS* 24, 467–469.

Verheyen, J., Verhofstede, C., Knops, E., Vandekerckhove, L., Fun, A., Brunen, D., Dauwe, K., Wensing, A. M., Pfister, H., Kaiser, R., and Nijhuis, M. (2010). High prevalence of bevirimat resistance mutations in protease inhibitor-resistant HIV isolates. *AIDS* 24, 669–673.

Wainberg, M. A., and Albert, J. (2010). Can the further clinical development of bevirimat be justified? *AIDS* 24, 773–774.

Weichsel, J., Herold, N., Lehmann, M. J., Krausslich, H. G., and Schwarz, U. S. (2010). A quantitative measure for alterations in the actin cytoskeleton investigated with automated high-throughput microscopy. *Cytometry A* 77, 52–63.

Zhang, F., Zang, T., Wilson, S. J., Johnson, M. C., and Bieniasz, P. D. (2011). Clathrin facilitates the morphogenesis of retrovirus particles. *PLoS Pathog.* 7, e1002119. doi:10.1371/journal.ppat.1002119

Zhou, J., Huang, L., Hachey, D. L., Chen, C. H., and Aiken, C. (2005). Inhibition of HIV-1 maturation via drug association with the viral Gag protein in immature HIV-1 particles. *J. Biol. Chem.* 280, 42149–42155.

Conflict of Interest Statement: The author declares that the research was conducted in the absence of any commercial or financial relationships that could be construed as a potential conflict of interest.

Received: 15 November 2011; paper pending published: 20 November 2011; accepted: 21 November 2011; published online: 09 December 2011.

Citation: Sakuragi J-i (2011) Morphogenesis of the infectious HIV-1 virion. Front. Microbio. ***2****:242. doi: 10.3389/fmicb.2011.00242*

This article was submitted to Frontiers in Virology, a specialty of Frontiers in Microbiology.

frontiers in
MICROBIOLOGY

MINI REVIEW ARTICLE
published: 21 December 2011
doi: 10.3389/fmicb.2011.00258

Structural features of antiviral APOBEC3 proteins are linked to their functional activities

Shingo Kitamura*[1,2], *Hirotaka Ode*[1] *and Yasumasa Iwatani*[1,3]

[1] *Laboratory of Infectious Diseases, Department of Infectious Diseases and Immunology, Clinical Research Center, National Hospital Organization Nagoya Medical Center, Nagoya, Japan*
[2] *Department of Biotechnology, Graduate School of Engineering, Nagoya University, Nagoya, Japan*
[3] *Department of AIDS Research, Graduate School of Medicine, Nagoya University, Nagoya, Japan*

Edited by:
Akio Adachi, The University of Tokushima Graduate School, Japan

Reviewed by:
Youichi Suzuki, National University of Singapore, Singapore
Kenzo Tokunaga, National Institute of Infectious Diseases, Japan

Correspondence:
Yasumasa Iwatani, Department of Infectious Diseases and Immunology, Clinical Research Center, National Hospital Organization Nagoya Medical Center, 4-1-1 San-no-Maru, Naka-ku, Nagoya, Japan.
e-mail: iwataniy@nnh.hosp.go.jp

Human APOBEC3 (A3) proteins are cellular cytidine deaminases that potently restrict the replication of retroviruses by hypermutating viral cDNA and/or inhibiting reverse transcription. There are seven members of this family including A3A, B, C, DE, F, G, and H, all encoded in a tandem array on human chromosome 22. A3F and A3G are the most potent inhibitors of HIV-1, but only in the absence of the virus-encoded protein, Vif. HIV-1 utilizes Vif to abrogate A3 functions in the producer cells. More specifically, Vif, serving as a substrate receptor, facilitates ubiquitination of A3 proteins by forming a Cullin5 (Cul5)-based E3 ubiquitin ligase complex, which targets A3 proteins for rapid proteasomal degradation. The specificity of A3 degradation is determined by the ability of Vif to bind to the target. Several lines of evidence have suggested that three distinct regions of A3 proteins are involved in the interaction with Vif. Here, we review the biological functions of A3 family members with special focus on A3G and base our analysis on the available structural information.

Keywords: APOBEC3, Vif, APOBEC3G, HIV, retrovirus, ubiquitin, cytidine deaminase, structure

INTRODUCTION

During coevolution of mammalian organisms and retroelements, the hosts have developed defense systems to restrict replication of these elements. The restriction factors include the A3 family of DNA cytidine deaminases, which is characterized by the presence of one or two Zn clusters consisting of $(H/C)XE(X)_{23–28}CXXC$ motifs (reviewed in Wedekind et al., 2003). In humans, there are seven members of the A3 family (A3A, B, C, DE, F, G, and H), each encoded in a tandem array on chromosome 22 (Jarmuz et al., 2002; **Figure 1A**). Each protein has been found to have different inhibitory effects on various retroelements that are mediated by cytidine deamination and other mechanisms (reviewed in Goila-Gaur and Strebel, 2008; Albin and Harris, 2010). In order to overcome A3 antiviral activity, the viruses have acquired their own strategies (Yu, 2006). HIV-1 encodes the Vif protein to counteract the most potent inhibitors, human A3G (hA3G) and A3F (Sheehy et al., 2002; Wiegand et al., 2004; Zheng et al., 2004; Simon et al., 2005; Miyagi et al., 2010). Vif binds the A3 proteins and serves as a substrate receptor to recruit the Cul5-based E3 ubiquitin (Ub) ligase complex, which facilitates the polyubiquitination and subsequent proteasome-mediated degradation (Yu et al., 2003). The elimination of A3 during virus production prevents its encapsidation into progeny viruses. Thus, given Vif's critical role in eliminating A3 function, it may be viewed as one of the most attractive pharmacologic targets for an anti-HIV drug, which would restore the activity of the intrinsic antiviral factor in the context of HIV infection. Here, we briefly review what is known about A3-Vif interactions and the subsequent ubiquitination, based on the available biological and structural information.

THE HUMAN A3 FAMILY OF CYTIDINE DEAMINASES

The seven members of the human A3 family have a defining feature: each protein has one or two conserved zinc (Z)-coordinating deaminase domains. Zinc coordination is mediated by a histidine and two cysteines, which form a catalytic center for a cytidine deaminase activity. Based on the phylogenetic analysis, the Z domains fall into three types: Z1 [A3A and the C-terminal half domains (CTD) of A3B and A3G], Z2 [A3C, both halves of A3DE and A3F, and the N-terminal domains (NTD) of A3B and A3G], and Z3 (A3H; LaRue et al., 2009; **Figure 1A**). Within the Z2 types, the domain can be further subdivided into three subgroups based on the identity of the amino acid sequence: (1) the A3F NTD; (2) the A3G NTD; (3) the A3F CTD (**Figure 1B**). Each subgroup has highly conserved amino acid sequences. For example, A3F CTD is 77 and 88% identical to A3C and A3DE CTD, respectively, whereas it is 42% identical to A3G NTD. As described in more detail below, only the Z3 type (A3H) and the Z2 type (more specifically, the A3G NTD and the A3F CTD subgroups) contain a critical interface for binding HIV-1 Vif (**Figure 1B**). It is thought that there is a common structural feature for the organization of cytidine deaminases: all Z domains are believed to have a conserved core structure composed of five β-strands (β1–β5) and six α-helices (α1–α6; **Figure 2A**). Although, to date, only the three-dimensional structure of the A3G CTD has been determined by NMR (Chen et al., 2008; Furukawa et al., 2009) or by X-ray crystallography

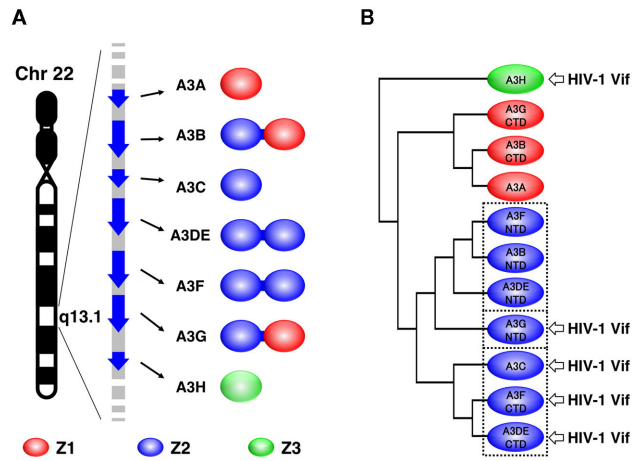

FIGURE 1 | Three types of Z domains in human A3 family. (A) Seven members of human A3 family, encoded by human chromosome 22, are illustrated. The protein products consist of one or two Z domains, each of which is phylogenetically grouped into three distinct types: Z1, Z2, and Z3. **(B)** Three subgroups of the Z2 domains are enclosed with dotted lines in the phylogenetic tree. The arrows point to the domains that are responsible for HIV-1 Vif interaction.

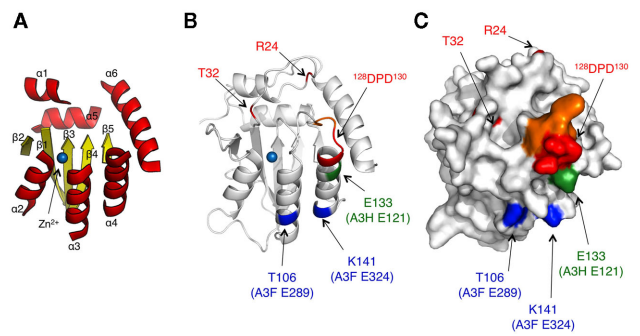

FIGURE 2 | Model structure of A3G NTD and location of responsible residues for Vif interaction. (A) Ribbon diagram of the A3 core structure for the model is depicted based on the crystal structure of the A3G CTD (PDB ID# 3IR2). The loop regions are removed. The α helices (α1–6) and β sheets (β1–5) are shown in red and yellow, respectively. **(B,C)** In the structure model, the amino acid determinants, T32, R24, and ^{128}DPD^{130}, for A3G are colored in red. The analogous residues T106 and K141 in A3F E289 and E324 (blue), and E133, corresponding to A3H E121 (green) are also shown. The critical residues, ^{125}YFW^{127}, for nucleic acid binding are colored in orange. **(C)** Predicted surface of the A3G NTD model is shown. All the critical residues are predicted to be surface exposed.

(Holden et al., 2008; Shandilya et al., 2010), no structure of the Z domain having an HIV-1 Vif interface has been solved yet.

THREE DISTINCT INTERFACES OF A3 Z DOMAINS INTERACT WITH HIV-1 VIF

The region in A3G responsible for binding to HIV-1 Vif was initially identified by comparative studies of the species specificity of A3G degradation by Vif. A single amino acid difference in hA3G, aspartic acid at position 128 (D128) versus lysine in the A3G of African green monkeys, determines species specificity by influencing Vif–A3G binding (Bogerd et al., 2004; Mangeat et al., 2004; Schrofelbauer et al., 2004; Xu et al., 2004). In addition, extensive site-direct mutagenesis revealed that the ^{128}DPD^{130} motif of A3G, located at the loop between β4 and α4 shown in red (**Figures 2B,C**), is crucial for direct binding to HIV-1 Vif (Huthoff and Malim, 2007). Furthermore, there is a report that residue T32, which may be potentially phosphorylated by protein kinase A, is also involved in the Vif–A3G interaction by collaborating with R24 (Shirakawa et al., 2008). All of these critical residues are mapped on the variable loop structure in proximity to the nucleic acid binding surface (**Figure 2B**).

In contrast, two independent studies have shown that two C-terminal A3F residues, E289 and E324, located in helices α3 and α4, respectively, are critical for the interaction with HIV-1 Vif (Albin et al., 2010; Smith and Pathak, 2010). Interestingly, in the structural model of the A3F CTD, these two residues are close to some negatively charged surface residues although the location of these residues is separate from ^{128}DPD^{130}. In accord with phylogenetic similarities, A3F E289 and E324 are highly conserved in hA3C (E106 and E141) and hA3DE CTD (E302 and E337). These findings suggest that structural features of the Vif-binding interfaces might be conserved among the A3F CTD, A3C, and A3DE CTD, but different from the A3G NTD. In the case of A3H, the interface for Vif is likely to have a surface area close to that of ^{128}DPD^{130} in the A3G NTD. The A3H gene is polymorphic, with four major haplotypes in humans. The four proteins have different levels of antiviral activity and sensitivity to HIV-1 Vif, in which haplotype II has the highest antiviral activity (Dang et al., 2008a; OhAinle et al., 2008; Harari et al., 2009; Tan et al., 2009; Li et al., 2010). By comparing the A3H variants, Zhen et al. (2010) identified a critical residue, E121, in A3H haplotype II for binding to HIV-1 (**Figures 2B,C**). Because the identity of amino acid sequences between Z2 and Z3 types, particularly the β4–α4 loop and the α4, is quite low, it is assumed that the putative Vif interface structure of A3H might be different from those of the A3G NTD or A3F CTD.

RESIDUES OF HIV-1 VIF THAT ARE CRITICAL FOR BINDING A3 PROTEINS

Extensive mutational analysis of HIV-1 Vif has led to the characterization of several distinct motifs in HIV-1 Vif that are required for formation of the Cul5-based E3 Ub ligase complex and recruitment of human A3 proteins (reviewed in Albin and Harris, 2010; **Figure 3**). The C-terminal half of Vif contains three conserved motifs: (1) the HCCH domain, which chelates zinc mediates the interaction with Cul5; (2) the SLQ motif, which binds elongin C (Elo C); and (3) the PPLP motif, which is important for Vif dimerization and recruitment of A3G, albeit by an unknown mechanism. Meanwhile, the N-terminal half of Vif is involved in the interaction with A3 proteins. **Figure 3** shows the compiled map of the critical residues that have been identified by several groups (Schrofelbauer et al., 2006; Tian et al., 2006; Russell and Pathak, 2007; He et al., 2008; Zhang et al., 2008; Chen et al., 2009; Pery et al., 2009; Zhen et al., 2010; Binka et al., 2011). Overall, it appears that the critical residues for binding to each Z domain type are discontinuous. This suggests that the interfaces in Vif might be determined by conformational constraints.

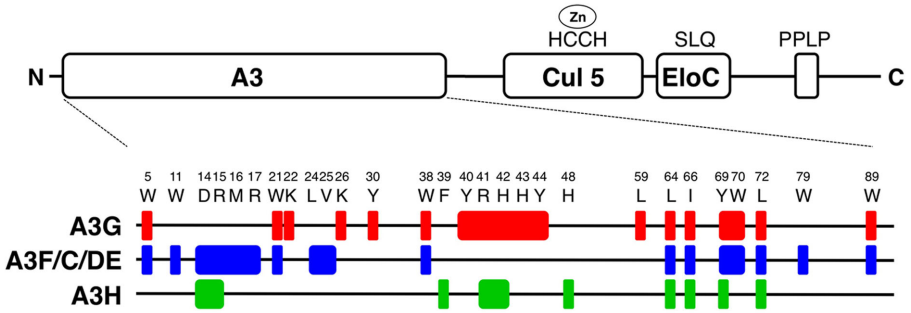

FIGURE 3 | Map of critical residues in HIV-1 Vif. Important domains in Vif (HIV-1 HXB2) are illustrated in the schematic diagram. The domains labeled "A3," "Cul5," and "Elo C" are responsible for Vif's functional interactions. The "A3" domain is responsible for binding to A3 family proteins. The amino acid sequence motifs, "HCCH," "SLQ," and "PPLP" are important for binding to Cul5, and Elo C, and Vif dimerization, respectively. The positions and the names of amino acid residues that were identified by several groups are shown. The residues that were identified as important for forming an interface with human A3 proteins are mapped in Vif, i.e., A3G (red), A3F, A3C, and A3DE (blue), and A3H (green).

Interestingly, some residues are unique among the three types of Z domains, suggesting that such residues might determine binding specificity. For example, K22, K26, Y30, Y40, H43, Y44, and L59 are important for interaction only with A3G, whereas the residues W11, M16, R17, L24, V25, and W79 are required for specific interactions with A3F. These residues tend to have two characteristics: they are positively charged or hydrophobic. Interestingly, the electrostatic charge of the Vif residues is mostly positive whereas the key residues that comprise the A3 interfaces are negatively charged. Thus, such electrostatic interactions might be one of the common features for binding between human A3 proteins and HIV-1 Vif. This could also determine the species-specific interactions between Vif and A3 proteins, as demonstrated in the case of Vif–A3G (Bogerd et al., 2004; Mangeat et al., 2004; Schrofelbauer et al., 2004; Xu et al., 2004). In contrast to the aforementioned regions, there are some aromatic or hydrophobic residues, W5, W21, W38, W70, and W89, which are commonly responsible for binding to two (the A3G NTD and the A3F CTD), or L64, I66, Y69, and L72 to all types of Z domains. These regions could play fundamental roles in maintaining the overall conformation of A3-binding interfaces or could form a partly shared structure of the interface for either two or all Z domains.

VIF-MEDIATED UBIQUITINATION/DEGRADATION

Information concerning the specific interaction between Vif and A3G in the E3 Ub ligase complex suggests that there may be a specific mechanism for Ub conjugation of the A3G protein. Previously, our studies using structure-guided mutagenesis demonstrated that four lysine residues (K297, 301, 303, and 334) near the C-terminal end of A3G are critical sites for HIV-1 Vif-mediated A3G ubiquitination and degradation (Iwatani et al., 2009). The data suggested that these sites, which are located on the opposite end of A3G relative to the Vif-binding interface, might be specifically dictated by the rigid structure of the Cul5-based scaffold. In addition, the study clearly demonstrated that the additional residues, particularly lysines near the C-terminal tag of A3G could be potential targets for Vif-induced ubiquitination. However, recently, Wang et al. (2011) showed that a detectable level of Vif-mediated ubiquitination occurs at the N-terminus in addition to certain lysine residues within 20 lysine residues of A3G. In contrast, another group could detect no N-terminal ubiquitination (Dang et al., 2008b). Although these apparent contradictions might be due to differences in the detection level of ubiquitination, it is important to consider the possibility that different tags attached at the C-terminal end of an A3G protein could create potential ubiquitination sites and/or mask the area where the four lysine residues are located (Iwatani et al., 2009). Moreover, while ubiquitination is associated primarily with the lysines in the CTD, the observation that there is also N-terminal ubiquitination could be of interest. The evidences of two distal ubiquitination sites in A3G may provide important structural insight, which implies two distinct types of structural configuration for Vif–A3G interaction. Further studies are needed to clarify Vif-mediated ubiquitination in the context of the E3 Ub ligase complex and to allow us to answer the following two questions: (1) How can we rationalize the relationship between the configuration of the N-terminal end and the proximal Vif-binding interface? (2) In particular, how can the Ub molecules be conjugated at the N-terminus, which is predicted to be a structurally flexible end?

CONCLUSION

Phylogenetic analyses and genetic studies of A3 and Vif have provided important evidence for three distinct types of interactions between human A3 and HIV-1 Vif proteins, which are determined by the characteristic Z domain types of A3G, A3F/C/DE, and A3H. Further understanding of Vif–A3 interactions could advance efforts to develop novel anti-HIV drugs, which would function as anti-Vif inhibitors. Although presenting a tremendous challenge, complementary studies focusing on the structure of the Vif-interactive A3 domain and Vif are also critical to accelerate future progress in this field.

ACKNOWLEDGMENTS

We thank Dr. Judith G. Levin (NIH, NICHD) for helpful discussions. This work was supported in part by a grant-in-aid for Scientific Research from the Ministry of Education, Culture, Sports, Science and Technology of Japan and by a grant for HIV/AIDS research from the Ministry of Health, Labor, and Welfare of Japan.

REFERENCES

Albin, J. S., and Harris, R. S. (2010). Interactions of host APOBEC3 restriction factors with HIV-1 in vivo: implications for therapeutics. *Expert Rev. Mol. Med.* 12, e4.

Albin, J. S., LaRue, R. S., Weaver, J. A., Brown, W. L., Shindo, K., Harjes, E., Matsuo, H., and Harris, R. S. (2010). A single amino acid in human APOBEC3F alters susceptibility to HIV-1 Vif. *J. Biol. Chem.* 285, 40785–40792.

Binka, M., Ooms, M., Steward, M., and Simon, V. (2011). The activity spectrum of Vif from multiple HIV-1 subtypes against APOBEC3G, APOBEC3F and APOBEC3H. *J. Virol.* (in press).

Bogerd, H. P., Doehle, B. P., Wiegand, H. L., and Cullen, B. R. (2004). A single amino acid difference in the host APOBEC3G protein controls the primate species specificity of HIV type 1 virion infectivity factor. *Proc. Natl. Acad. Sci. U.S.A.* 101, 3770–3774.

Chen, G., He, Z., Wang, T., Xu, R., and Yu, X. F. (2009). A patch of positively charged amino acids surrounding the human immunodeficiency virus type 1 Vif SLVx4Yx9Y motif influences its interaction with APOBEC3G. *J. Virol.* 83, 8674–8682.

Chen, K. M., Harjes, E., Gross, P. J., Fahmy, A., Lu, Y., Shindo, K., Harris, R. S., and Matsuo, H. (2008). Structure of the DNA deaminase domain of the HIV-1 restriction factor APOBEC3G. *Nature* 452, 116–119.

Dang, Y., Siew, L. M., Wang, X., Han, Y., Lampen, R., and Zheng, Y. H. (2008a). Human cytidine deaminase APOBEC3H restricts HIV-1 replication. *J. Biol. Chem.* 283, 11606–11614.

Dang, Y., Siew, L. M., and Zheng, Y. H. (2008b) APOBEC3G is degraded by the proteasomal pathway in a Vif-dependent manner without being polyubiquitylated. *J. Biol. Chem.* 283, 13124–13131.

Furukawa, A., Nagata, T., Matsugami, A., Habu, Y., Sugiyama, R., Hayashi, F., Kobayashi, N., Yokoyama, S., Takaku, H., and Katahira, M. (2009). Structure, interaction and real-time monitoring of the enzymatic reaction of wild-type APOBEC3G. *EMBO J.* 28, 440–451.

Goila-Gaur, R., and Strebel, K. (2008). HIV-1 Vif, APOBEC, and intrinsic immunity. *Retrovirology* 5, 51.

Harari, A., Ooms, M., Mulder, L. C., and Simon, V. (2009). Polymorphisms and splice variants influence the antiretroviral activity of human APOBEC3H. *J. Virol.* 83, 295–303.

He, Z., Zhang, W., Chen, G., Xu, R., and Yu, X. F. (2008). Characterization of conserved motifs in HIV-1 Vif required for APOBEC3G and APOBEC3F interaction. *J. Mol. Biol.* 381, 1000–1011.

Holden, L. G., Prochnow, C., Chang, Y. P., Bransteitter, R., Chelico, L., Sen, U., Stevens, R. C., Goodman, M. F., and Chen, X. S. (2008). Crystal structure of the anti-viral APOBEC3G catalytic domain and functional implications. *Nature* 456, 121–124.

Huthoff, H., and Malim, M. H. (2007). Identification of amino acid residues in APOBEC3G required for regulation by human immunodeficiency virus type 1 Vif and Virion encapsidation. *J. Virol.* 81, 3807–3815.

Iwatani, Y., Chan, D. S., Liu, L., Yoshii, H., Shibata, J., Yamamoto, N., Levin, J. G., Gronenborn, A. M., and Sugiura, W. (2009). HIV-1 Vif-mediated ubiquitination/degradation of APOBEC3G involves four critical lysine residues in its C-terminal domain. *Proc. Natl. Acad. Sci. U.S.A.* 106, 19539–19544.

Jarmuz, A., Chester, A., Bayliss, J., Gisbourne, J., Dunham, I., Scott, J., and Navaratnam, N. (2002). An anthropoid-specific locus of orphan C to U RNA-editing enzymes on chromosome 22. *Genomics* 79, 285–296.

LaRue, R. S., Andresdottir, V., Blanchard, Y., Conticello, S. G., Derse, D., Emerman, M., Greene, W. C., Jonsson, S. R., Landau, N. R., Lochelt, M., Malik, H. S., Malim, M. H., Munk, C., O'Brien, S. J., Pathak, V. K., Strebel, K., Wain-Hobson, S., Yu, X. F., Yuhki, N., and Harris, R. S. (2009). Guidelines for naming nonprimate APOBEC3 genes and proteins. *J. Virol.* 83, 494–497.

Li, M. M., Wu, L. I., and Emerman, M. (2010). The range of human APOBEC3H sensitivity to lentiviral Vif proteins. *J. Virol.* 84, 88–95.

Mangeat, B., Turelli, P., Liao, S., and Trono, D. (2004). A single amino acid determinant governs the species-specific sensitivity of APOBEC3G to Vif action. *J. Biol. Chem.* 279, 14481–14483.

Miyagi, E., Brown, C. R., Opi, S., Khan, M., Goila-Gaur, R., Kao, S., Walker, R. C. Jr., Hirsch, V., and Strebel, K. (2010). Stably expressed APOBEC3F has negligible antiviral activity. *J. Virol.* 84, 11067–11075.

OhAinle, M., Kerns, J. A., Li, M. M., Malik, H. S., and Emerman, M. (2008). Antiretroelement activity of APOBEC3H was lost twice in recent human evolution. *Cell Host Microbe* 4, 249–259.

Pery, E., Rajendran, K. S., Brazier, A. J., and Gabuzda, D. (2009). Regulation of APOBEC3 proteins by a novel YXXL motif in human immunodeficiency virus type 1 Vif and simian immunodeficiency virus SIVagm Vif. *J. Virol.* 83, 2374–2381.

Russell, R. A., and Pathak, V. K. (2007). Identification of two distinct human immunodeficiency virus type 1 Vif determinants critical for interactions with human APOBEC3G and APOBEC3F. *J. Virol.* 81, 8201–8210.

Schrofelbauer, B., Chen, D., and Landau, N. R. (2004). A single amino acid of APOBEC3G controls its species-specific interaction with virion infectivity factor (Vif). *Proc. Natl. Acad. Sci. U.S.A.* 101, 3927–3932.

Schrofelbauer, B., Senger, T., Manning, G., and Landau, N. R. (2006). Mutational alteration of human immunodeficiency virus type 1 Vif allows for functional interaction with nonhuman primate APOBEC3G. *J. Virol.* 80, 5984–5991.

Shandilya, S. M., Nalam, M. N., Nalivaika, E. A., Gross, P. J., Valesano, J. C., Shindo, K., Li, M., Munson, M., Royer, W. E., Harjes, E., Kono, T., Matsuo, H., Harris, R. S., Somasundaran, M., and Schiffer, C. A. (2010). Crystal structure of the APOBEC3G catalytic domain reveals potential oligomerization interfaces. *Structure* 18, 28–38.

Sheehy, A. M., Gaddis, N. C., Choi, J. D., and Malim, M. H. (2002). Isolation of a human gene that inhibits HIV-1 infection and is suppressed by the viral Vif protein. *Nature* 418, 646–650.

Shirakawa, K., Takaori-Kondo, A., Yokoyama, M., Izumi, T., Matsui, M., Io, K., Sato, T., Sato, H., and Uchiyama, T. (2008). Phosphorylation of APOBEC3G by protein kinase A regulates its interaction with HIV-1 Vif. *Nat. Struct. Mol. Biol.* 15, 1184–1191.

Simon, V., Zennou, V., Murray, D., Huang, Y., Ho, D. D., and Bieniasz, P. D. (2005). Natural variation in Vif: differential impact on APOBEC3G/3F and a potential role in HIV-1 diversification. *PLoS Pathog.* 1, e6. doi:10.1371/journal.ppat.0010006

Smith, J. L., and Pathak, V. K. (2010). Identification of specific determinants of human APOBEC3F, APOBEC3C, and APOBEC3DE and African green monkey APOBEC3F that interact with HIV-1 Vif. *J. Virol.* 84, 12599–12608.

Tan, L., Sarkis, P. T., Wang, T., Tian, C., and Yu, X. F. (2009). Sole copy of Z2-type human cytidine deaminase APOBEC3H has inhibitory activity against retrotransposons and HIV-1. *FASEB J.* 23, 279–287.

Tian, C., Yu, X., Zhang, W., Wang, T., Xu, R., and Yu, X. F. (2006). Differential requirement for conserved tryptophans in human immunodeficiency virus type 1 Vif for the selective suppression of APOBEC3G and APOBEC3F. *J. Virol.* 80, 3112–3115.

Wang, Y., Shao, Q., Yu, X., Kong, W., Hildreth, J. E., and Liu, B. (2011). N-terminal hemagglutinin tag renders lysine-deficient APOBEC3G resistant to HIV-1 Vif-induced degradation by reduced polyubiquitination. *J. Virol.* 85, 4510–4519.

Wedekind, J. E., Dance, G. S., Sowden, M. P., and Smith, H. C. (2003). Messenger RNA editing in mammals: new members of the APOBEC family seeking roles in the family business. *Trends Genet.* 19, 207–216.

Wiegand, H. L., Doehle, B. P., Bogerd, H. P., and Cullen, B. R. (2004). A second human antiretroviral factor, APOBEC3F, is suppressed by the HIV-1 and HIV-2 Vif proteins. *EMBO J.* 23, 2451–2458.

Xu, H., Svarovskaia, E. S., Barr, R., Zhang, Y., Khan, M. A., Strebel, K., and Pathak, V. K. (2004). A single amino acid substitution in human APOBEC3G antiretroviral enzyme confers resistance to HIV-1 virion infectivity factor-induced depletion. *Proc. Natl. Acad. Sci. U.S.A.* 101, 5652–5657.

Yu, X., Yu, Y., Liu, B., Luo, K., Kong, W., Mao, P., and Yu, X. F. (2003). Induction of APOBEC3G ubiquitination and degradation by an HIV-1 Vif-Cul5-SCF complex. *Science* 302, 1056–1060.

Yu, X. F. (2006). Innate cellular defenses of APOBEC3 cytidine deaminases and viral counter-defenses. *Curr. Opin. HIV AIDS* 1, 187–193.

Zhang, W., Chen, G., Niewiadomska, A. M., Xu, R., and Yu, X. F. (2008). Distinct determinants in HIV-1 Vif and human APOBEC3 proteins are required for the suppression of diverse host anti-viral proteins. *PLoS ONE* 3, e3963. doi:10.1371/journal.pone.0003963

Zhen, A., Wang, T., Zhao, K., Xiong, Y., and Yu, X. F. (2010). A single amino acid difference in human APOBEC3H variants determines HIV-1 Vif sensitivity. *J. Virol.* 84, 1902–1911.

Zheng, Y. H., Irwin, D., Kurosu, T., Tokunaga, K., Sata, T., and Peterlin, B. M. (2004). Human APOBEC3F is another host

factor that blocks human immunodeficiency virus type 1 replication. *J. Virol.* 78, 6073–6076.

Conflict of Interest Statement: The authors declare that the research was conducted in the absence of any commercial or financial relationships that could be construed as a potential conflict of interest.

Received: 14 November 2011; accepted: 02 December 2011; published online: 21 December 2011.
Citation: Kitamura S, Ode H and Iwatani Y (2011) Structural features of antiviral APOBEC3 proteins are linked to their functional activities. Front. Microbio. ***2****:258. doi: 10.3389/fmicb.2011.00258*
This article was submitted to Frontiers in Virology, a specialty of Frontiers in Microbiology.

frontiers in
MICROBIOLOGY

REVIEW ARTICLE
published: 12 December 2011
doi: 10.3389/fmicb.2011.00250

Structural basis for the antiviral activity of BST-2/tetherin and its viral antagonism

Juan F. Arias, Yukie Iwabu and Kenzo Tokunaga*

Department of Pathology, National Institute of Infectious Diseases, Tokyo, Japan

Edited by:
Akio Adachi, The University of Tokushima Graduate School, Japan

Reviewed by:
Masako Nomaguchi, The University of Tokushima Graduate School, Japan
Hirotaka Ode, National Hospital Organization Nagoya Medical Center, Japan

***Correspondence:**
Kenzo Tokunaga, Department of Pathology, National Institute of Infectious Diseases, Shinjuku-ku, Tokyo 162-8640, Japan.
e-mail: tokunaga@nih.go.jp

The interferon-inducible host restriction factor bone marrow stromal antigen 2 (BST-2/tetherin) blocks the release of HIV-1 and other enveloped viruses. In turn, these viruses have evolved specific antagonists to counteract this host antiviral molecule, such as the HIV-1 protein Vpu. BST-2 is a type II transmembrane protein with an unusual topology consisting of an N-terminal cytoplasmic tail (CT) followed by a single transmembrane (TM) domain, a coiled-coil extracellular (EC) domain, and a glycosylphosphatidylinositol (GPI) anchor at the C terminus. We and others showed that BST-2 restricts enveloped virus release by bridging the host and virion membranes with its two opposing membrane anchors and that deletion of either one completely abrogates antiviral activity. The EC domain also shows conserved structural properties that are required for antiviral function. It contains several destabilizing amino acids that confer the molecule with conformational flexibility to sustain the protein's function as a virion tether, and three conserved cysteine residues that mediate homodimerization of BST-2, as well as acting as a molecular ruler that separates the membrane anchors. Conversely, the efficient release of virions is promoted by the HIV-1 Vpu protein and other viral antagonists. Our group and others provided evidence from mutational analyses indicating that Vpu antagonism of BST-2-mediated viral restriction requires a highly specific interaction of their mutual TM domains. This interpretation is further supported and expanded by the findings of the latest structural modeling studies showing that critical amino acids in a conserved helical face of these TM domains are required for Vpu–BST-2 interaction and antagonism. In this review, we summarize the current advances in our understanding of the structural basis for BST-2 antiviral function as well as BST-2-specific viral antagonism.

Keywords: HIV-1, Vpu, BST-2, transmembrane, restriction factor, antagonist, interaction

INTRODUCTION

As a result of exposure to viral pathogens over millions of years, humans and other mammals evolved intrinsic immunity proteins that provide resistance to infection by directly interfering with different stages of the viral life cycle. These so-called host restriction factors are normally induced by interferon-α (IFN-α) during induction of the innate immune response by viral infection. A case in point is HIV-1, an extensively studied pathogen for which four major restriction factors have been identified: the apolipoprotein B mRNA-editing enzyme catalytic polypeptide-like 3 (APOBEC3) family of cytidine deaminases (Sheehy et al., 2002); the α-isoform of the tripartite motif-containing protein 5 (TRIM5α; Stremlau et al., 2004); the bone marrow stromal antigen 2 (Neil et al., 2008; Van Damme et al., 2008; BST-2, also known as tetherin or CD317, referred to hereafter as BST-2), which is the subject of this review article; and, more recently, SAMHD1 (Hrecka et al., 2011; Laguette et al., 2011). HIV-1, in turn, evolved countermeasures to overcome the antiviral activity of their host restriction factors, mainly by acquiring a series of *trans*-acting viral accessory proteins, including Vif and Vpu. Vif blocks the above-described APOBEC3 proteins that mediate extensive deamination of cytosines in single-stranded viral DNA, thus halting HIV replication. Vpu is another viral antagonist of the transmembrane BST-2 protein that blocks the release of enveloped viruses by physically binding the budding viral particles to the membrane of infected cells. Likewise, in HIV-2 and related simian immunodeficiency viruses, Vpx acts as an antagonist of SAMHD1 that blocks HIV-1 replication in dendritic and myeloid cells. It should be noted that HIV-1 is not susceptible to human TRIM5α antiviral action (Stremlau et al., 2004). In this review, we focus on current advances in structure-based analyses of BST-2 and viral antagonists.

BST-2: MOLECULAR CHARACTERISTICS

BST-2 is an interferon-induced type II membrane glycoprotein of unusual topology (Ishikawa et al., 1995; Kupzig et al., 2003), which efficiently blocks the release of diverse mammalian enveloped viruses by directly tethering viral particles to the membranes of infected cells. Viruses restricted by BST-2 are found among diverse families, including filoviruses, arenaviruses, paramyxoviruses (Jouvenet et al., 2009; Kaletsky et al., 2009; Sakuma et al., 2009a; Radoshitzky et al., 2010), gamma-herpesviruses (Mansouri et al., 2009; Pardieu et al., 2010), rhabdoviruses (Weidner et al., 2010), and a wide array of retroviruses from several mammal host species (Arnaud et al., 2010; Dietrich et al., 2011; Xu et al., 2011).

A recent study characterizing a feline BST-2 ortholog reported the protein's strong activity against FIV particle release *in vitro* (Dietrich et al., 2011). BST-2 comprises a short, 21-amino-acid cytoplasmic N-terminal tail (CT), followed by an α-helical transmembrane (TM) domain, an extracellular domain (EC) that is predominantly helical and contains an extended parallel coiled-coil, and a C-terminal glycosylphosphatidylinositol (GPI) component that acts as a second anchor linking the protein back to the cell membrane (Kupzig et al., 2003; **Figure 1A**). This double-anchor topology is extremely unusual and is only shared by an isoform of the prion protein (Moore et al., 1999).

Accumulating evidence supports the view that the structural features of BST-2 are key to its antiviral activity, as discussed in detail in the following sections. In agreement with a direct tethering mechanism, a requirement for both the TM and GPI anchors has been found for BST-2's antiviral activity (Neil et al., 2008; Iwabu et al., 2009; Perez-Caballero et al., 2009). Additionally, the EC of BST-2 contains a series of important residues that are conserved throughout the protein's mammalian orthologs, and these residues are essential to the inhibition of viral release (Van Damme et al., 2008; Andrew et al., 2009; Sakuma et al., 2009b). Whereas the stability of BST-2 is maintained by disulfide-links (Hinz et al., 2010; Schubert et al., 2010), the EC forms an extended coiled-coil domain that contains several conserved destabilizing amino acid residues, providing the conformational flexibility necessary for the molecule to sustain its role as a physical tether, as described later. Salient BST-2 structural motifs important for antiviral function are summarized in **Table 1**.

Based on the identification of these structural features critical for BST-2's antiviral activity, Perez-Caballero et al. (2009) through domain replacement experiments, were able to show that BST-2's configuration rather than its primary sequence is critical for antiviral activity. In an elegant demonstration, the authors generated a completely artificial BST-2-like protein made of structurally similar domains from three unrelated heterologous proteins (the TM from the transferrin receptor, the coiled-coil from dystrophia myotonica protein kinase, and the GPI anchor from the urokinase plasminogen activator receptor). Despite its lack of sequence homology with native BST-2, this artificial protein reproduced the latter's antiviral activity as it was able to inhibit the release of HIV-1 and Ebola virus-like-particles.

BOTH TM AND GPI ANCHOR ARE IMPORTANT FOR THE RESTRICTION OF VIRUS RELEASE

The TM (amino acid positions 22–43) of BST-2 is a short single-pass α-helix that anchors the molecule to the plasma membrane, while the GPI anchor is located at the C-terminal region of the protein (Kupzig et al., 2003). These two membrane anchors in part determine the antiviral function of BST-2. This unusual topology suggests a model that BST-2 directly tethers budding virions to the membrane of infected cells. Indeed, unequivocal support for this model has come from immunoelectron microscopy studies demonstrating that BST-2 is associated with virions and located between the viral and cell membranes as well as between tethered virions (Neil et al., 2008; Fitzpatrick et al., 2010; Hammonds et al., 2010).

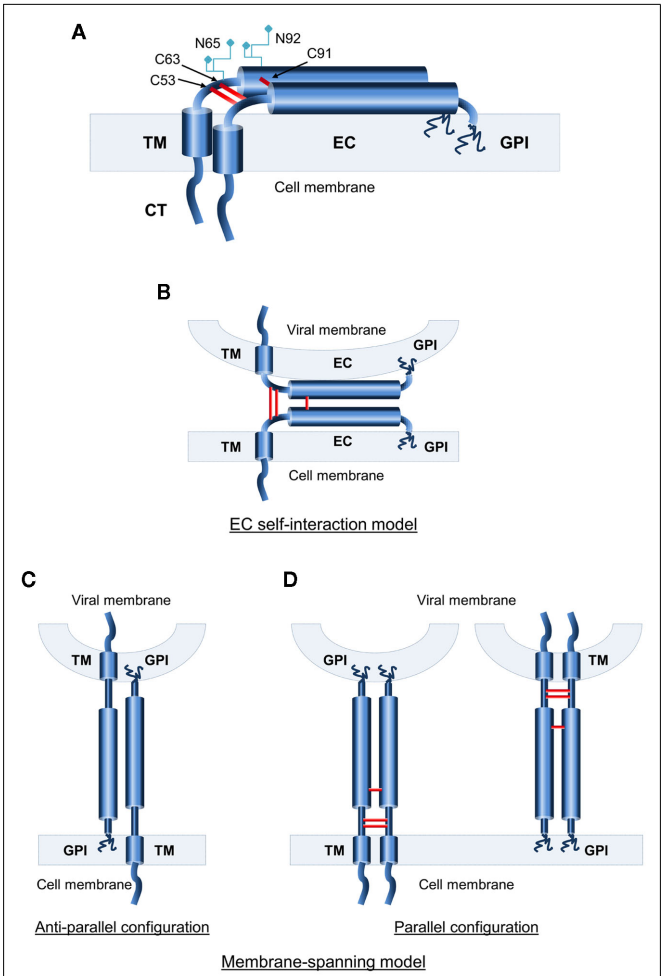

FIGURE 1 | Topological characteristics of human BST-2. (A) Schematic representation of the domain structure of BST-2, a type II transmembrane (TM) protein. BST-2 features a short cytoplasmic N-terminus followed by an α-helical single-pass TM domain and an extended coiled-coil extracellular domain that is linked back to the plasma membrane by a C-terminal GPI anchor. *N*-glycosylation sites and cysteine residues for disulfide-bond formation in the extracellular domain (EC) are noted. **(B–D)** Topological models of BST-2's functional state. **(B)** The EC self-interaction model, in which individual BST-2 monomers are anchored at both ends to the same membrane, with interaction between the ECs of cell-bound and virion-bound monomers. **(C)** Membrane-spanning anti-parallel model. Monomers are anchored in both membranes with opposing orientations. **(D)** Membrane-spanning parallel model. Monomers are anchored in both membranes with the same orientation.

As shown in **Table 1**, two structural elements are absolutely required for BST-2-mediated restriction of viral release; (1) the presence of both the TM and the GPI anchor (Neil et al., 2008; Van Damme et al., 2008; Iwabu et al., 2009; Perez-Caballero et al., 2009); and (2) homodimer formation through EC disulfide-bond interactions (Andrew et al., 2009; Perez-Caballero et al., 2009). The latter is discussed in greater detail in a later section of this review. These two elements form the basis of the two proposed topological models of BST-2. In the "EC self-interaction model (**Figure 1B**)," individual BST-2 monomers are anchored at

Table 1 | Salient structural features of human BST-2.

Domain	Structural motif	Function	Necessary for antiviral action?	Reference
CT (1–21)	$YxY_{6–8}$	Clathrin-dependent internalization	No	Masuyama et al. (2009), Rollason et al. (2007)
	$DDIWK_{14–18}$	Nef recognition sequence	No	Yang et al. (2010a), Sauter et al. (2009), Lim et al. (2010)
	K18	Putative ubiquitination site by K5	No	Mansouri et al. (2009), Pardieu et al. (2010)
TM (22–43)	Alpha-helix (22–43)	Membrane anchor	Yes	Neil et al. (2008), Perez-Caballero et al. (2009), Iwabu et al. (2009)
	I34, L37, L41	Vpu recognition face	No	Iwabu et al. (2009), Gupta et al. (2009a), Rong et al. (2009), McNatt et al. (2009), Kobayashi et al. (2011), Skasko et al. (2011b)
EC (44–160)	N65, N92	N-linked glycosylation	No	Sakuma et al. (2009a), Andrew et al. (2009), Ohtomo et al. (1999)
	C53, C63, C91	Putative disulfide-bond formation	Yes	Perez-Caballero et al. (2009), Andrew et al. (2009), Hinz et al. (2010)
	Coiled-coil (68–138)	Molecular ruler	Yes	Hinz et al. (2010), Yang et al. (2010a), Swiecki et al. (2011), Schubert et al. (2010)
	C91, V95, L98, L102, E105, V113, L116, I120, L123, L127, V134, L137	Destabilizing residues at core heptad positions	Yes	
GPI anchor	GPI signal peptide	Membrane anchor	Yes	Kupzig et al. (2003), Perez-Caballero et al. (2009), Iwabu et al. (2009)

both ends to the same membrane (cellular or viral), and interaction between the EC domains of cell-bound and virion-bound monomers is required for the restriction of virus release. The alternative is the "membrane-spanning model (**Figures 1C,D**)," in which both BST-2 end tails (TM and GPI anchor) are anchored in different membranes (i.e., cellular and viral). Theoretically, the BST-2 monomers in this model can be arranged in either an anti-parallel (**Figure 1C**) or parallel (**Figure 1D**) configuration.

The first approach to resolve the topology of BST-2 involves cleavage of the GPI anchor by treatment with the hydrolytic enzyme phosphatidyl inositol-specific phospholipase C (Pi–PLC). However, the enzymatic treatment does not effectively release restricted virions from the cell membrane (Fitzpatrick et al., 2010), supporting either a membrane-spanning anti-parallel configuration (**Figure 1C**) or the EC self-interaction model (**Figure 1B**), in which monomers would be able to remain attached to the respective membrane by the TM domain even after cleavage of the GPI anchor.

The second approach is to evaluate the gap between the cellular and viral membranes in electron microscopy studies. If the BST-2 monomers are positioned parallel to the cellular and viral membranes (EC self-interaction model; **Figure 1B**), virions would be tethered very close to the membrane, less than 3–5 nm, as described in (Hinz et al., 2010). However, imaging studies show larger distances between virions and cells (Neil et al., 2008; Perez-Caballero et al., 2009; Hammonds et al., 2010), thus supporting a membrane-spanning model (**Figures 1C,D**).

The third approach to this problem has been the systematic determination of BST-2 function in mutational analyses. We have previously shown that the anchoring of BST-2 through both its N-terminal and C-terminal regions is required for antiviral activity (Iwabu et al., 2009). Briefly, mutagenesis studies using GPI-anchor-deleted and CD4 signal peptide chimeric versions of BST-2, in which the protein is linked to the cell membrane only through one of its ends, showed that removal of either end abrogated the antiviral effect of BST-2 on virus production. Therefore, we concluded that membrane binding through both the TM and GPI anchor of BST-2 is critical for its antiviral activity, supporting the model of the membrane-spanning parallel configuration (**Figure 1D**). Further evidence for this parallel-dimer model comes from the analysis of residual BST-2 found in virions released through proteolytic treatment with subtilisin (Perez-Caballero et al., 2009).

Finally and more importantly, four different groups have combined high-resolution crystallography (1.6–2.8Å), and small-angle X-ray scattering-based modeling to determine the structures of the entire human and murine BST-2 EC, and have shown that BST-2 forms parallel coiled-coil arrangements (Hinz et al., 2010; Schubert et al., 2010; Yang et al., 2010a; Swiecki et al., 2011). Taken together, these observations suggest that the antiviral state of BST-2 present at the cell membrane corresponds to the membrane-spanning parallel configuration model as shown in **Figure 1D**.

THE EC MEDIATES HOMODIMERIZATION

The BST-2 EC (amino acid positions 44–160) is predominantly an α-helical coiled-coil structure that contains a series of residues highly conserved among mammalian orthologs: two asparagines that are N-linked glycosylation sites (N65, N92), and three cysteines (C53, C63, C91) responsible for intermolecular disulfide-bonds that result in homodimerization (**Figure 1A**; Ohtomo et al., 1999; Andrew et al., 2009). Disulfide linkage through these cysteine residues is critical for the restriction of HIV production

(**Table 1**). Mutational analyses demonstrate that partial disulfide-bond formation through at least one such cysteine residue is necessary for the retention of antiviral activity, whereas mutations at all three positions result in the total loss of antiviral function even though expression of the protein at the cell membrane remains unaltered (Andrew et al., 2009; Perez-Caballero et al., 2009; Hinz et al., 2010), although this is not the case for filovirus or arenavirus (Lassa virus) particles (Perez-Caballero et al., 2009; Sakuma et al., 2009a).

Several conserved amino acids within the EC domain, which are also thought to stabilize the dimers through weak coiled-coil domain interactions, include two interhelical salt bridges (E105–K106, and E133–R138) and one interhelical hydrogen bond (N141), and contribute to stabilize the EC domain interface (Hinz et al., 2010). Glycosylation of residues N65 and N92 was shown to contribute to anterograde transport and correct protein folding, but mutations in these positions had no effect on BST-2 antiviral activity (**Table 1**; Andrew et al., 2009; Sakuma et al., 2009a). In summary, all evidence thus far suggests that BST-2 EC contains a dimeric coiled-coil that is stabilized by C53–C53, C63–C63, and C91–C91 disulfide-bonds, with the conservation of at least one of these, along with weak interactions within the coiled-coil domain, and is required for dimer stability and the antiviral activity of BST-2.

THE BST-2 EC EXHIBITS CONFORMATIONAL FLEXIBILITY

The most recent structural studies provide valuable clues to the biological function of the EC while at the same time reconciling the topological models of BST-2 dimer configuration with available electron microscopy data, as outlined above. Resolution of the crystal structure of human BST-2 EC (Hinz et al., 2010; Schubert et al., 2010; Yang et al., 2010a) together with small-angle X-ray scattering data suggest an elongated extracellular domain forming a long rod-like structure and a greatly extended EC separating the two membrane anchors, acting as a molecular ruler with a predicted distance of 170Å (**Table 1**). This distance would correspond to the predicted separation between membrane-tethered virions and the plasma membrane of the host cells, or between tethered viral particles, and is in agreement with the separation determined in published electron micrographic studies. This finding seems to be consistent with the aforementioned membrane-spanning model (**Figure 1D**).

The authors of those studies also described the presence of irregularities in the 90-Å coiled-coil motif. The irregularities arise from the introduction of destabilizing residues (see **Table 1**) that are arranged regularly in core heptad positions, i.e., amino acid residues located at the center of the α–helix. The destabilizing residues loosen regular coiled-coil packing increasing the pitch and radius of the α-helix, accounting for the low stability of BST-2's coiled-coil under reducing conditions in vitro. These positions are conserved throughout all available BST-2 sequences, and their mutations result in loss of the antiviral function of BST-2 (Hinz et al., 2010). Yet, despite this intrinsic instability, the disulfide-bonds are still able to be formed, restabilizing the EC domains in a dimeric form. These findings suggest that conformational flexibility allows adaptation to the dynamic events of virion budding, while disulfide-bond-mediated dimerization prevents major separation of the coiled-coils. Together, these two properties result in a dynamic structure that permits dimer dissociation and restabilization during the process of virion trapping (Hinz et al., 2010; Swiecki et al., 2011). A high-resolution crystal structure of the full-length mouse BST-2 EC confirmed the presence of an elongated EC characteristically unstable due to the insertion of destabilizing residues (Swiecki et al., 2011). In that study, structural and biophysical analyses of murine and human BST-2 EC domains revealed that an unstable coiled-coil motif is evolutionarily conserved. This evidence provides further support for the aforementioned model of conformational flexibility.

THE GPI ANCHOR MEDIATES SURFACE LOCALIZATION AND THE CT IS CRITICAL FOR BST-2 TRAFFICKING

BST-2 localizes both to the plasma membrane and internal compartments, particularly the trans-Golgi network (TGN) and recycling endosomes (Kupzig et al., 2003; Rollason et al., 2007; Dube et al., 2009; Masuyama et al., 2009; Habermann et al., 2010). At the cell surface, BST-2 localizes into cholesterol-enriched lipid rafts, due to its GPI anchor. This localization is implicated in the promotion of clathrin-mediated endocytosis (Rollason et al., 2007; Masuyama et al., 2009) and, importantly, it allows BST-2 to directly interfere with the virion-release process, as lipid rafts are the preferential site of budding of several enveloped viruses (Aloia et al., 1993; Panchal et al., 2003; Waheed and Freed, 2009). This also positions BST-2 at the virological synapse (VS; Casartelli et al., 2010; Jolly et al., 2010; Pais-Correia et al., 2010), but its potential to restrict cell-to-cell viral spread remains controversial. With respect to internalization and cell trafficking, it was previously shown that rodent BST-2 is internalized from the cell surface in a clathrin-dependent manner (Rollason et al., 2007; Masuyama et al., 2009). Internalization requires a non-canonical dual tyrosine motif at amino acid positions 6 and 8 of the protein's CT ($YxY_{6–8}$; **Table 1**). This motif is highly conserved through all mammalian orthologs and sequentially participates in the interaction of BST-2 with the clathrin adaptors AP-2, which mediates internalization by endocytosis, and AP-1, which retrieves BST-2 to the TGN. The CT domain of BST-2 indirectly interacts with the underlying actin cytoskeleton through a series of adaptor proteins (RICH2, EBP50, ezrin), although additional studies are required to understand the implications of these interactions for BST-2 function (Rollason et al., 2009).

VIRAL ANTAGONISM OF BST-2

Since BST-2 targets the lipid bilayer of the host cell, viruses cannot evade it simply by escape mutations. Therefore, enveloped viruses had been obliged to evolve trans-acting countermeasures specifically to overcome BST-2 restriction. Among primate lentiviruses, three different viral gene products are known to antagonize BST-2. In most SIV strains, the viral Nef protein antagonizes primate BST-2, while in HIV-1 and HIV-2, the Vpu protein and the Env glycoprotein, respectively, antagonize human BST-2. Other BST-2 antagonists include the Kaposi's sarcoma-associated herpesvirus (KSHV) K5 protein and the Ebola virus glycoprotein (GP). With the exception of Ebola GP, all of these viral proteins downregulate BST-2 at the plasma membrane, thus effectively removing it from viral budding sites.

HIV-1 Vpu

Just as the study of HIV-1 Vif led to the discovery of APOBEC3 as a host restriction factor (Sheehy et al., 2002), BST-2 was identified by searching for the host restriction factor antagonized by the accessory viral protein Vpu. This 16-kDa type I transmembrane viral protein is a BST-2 antagonist and as such promotes the release of HIV-1 virions (Cohen et al., 1988; Strebel et al., 1988; Malim and Emerman, 2008). Importantly, Vpu can directly mediate the removal of BST-2 away from its site of action on the cell surface, although the mechanisms remain hotly debated (Van Damme et al., 2008; Iwabu et al., 2009, 2010; Ruiz et al., 2010; Lau et al., 2011). Thus far, it appears that Vpu recruits cellular proteins to remove BST-2 from the surface (**Figure 2A**). As we and others have shown, BST-2 downregulation by Vpu involves a beta-transducin repeat-containing protein (β-TrCP)-dependent mechanism (Douglas et al., 2009; Iwabu et al., 2009; Mangeat et al., 2009; Mitchell et al., 2009; Dubé et al., 2010; Tokarev et al., 2011); however, this only partially explains the underlying mechanism, since mutations in the β-TrCP-binding motif of Vpu do not entirely abrogate its antagonism of BST-2 (Schubert and Strebel, 1994; Van Damme et al., 2008; Iwabu et al., 2009).

Whereas several reports suggest that BST-2 downregulation in the presence of Vpu is accomplished at least in part through proteasomal degradation (Goffinet et al., 2009; Gupta et al., 2009a; Mangeat et al., 2009), evidence obtained by our group and others supports a model of BST-2 downregulation through lysosomal degradation (Douglas et al., 2009; Iwabu et al., 2009; Mitchell et al., 2009; Janvier et al., 2011). It is proposed that Vpu causes the retention of BST-2 within endosomes by blocking its recycling after endocytosis (Mitchell et al., 2009; Dubé et al., 2010; Lau et al., 2011). Alternatively, it is hypothesized that Vpu inhibits the membrane transport of BST-2 by causing its intracellular sequestration within the TGN (Dubé et al., 2010; Andrew et al., 2011; Lau et al., 2011). We and others suggested that Vpu directly internalizes BST-2 from the cell surface through TM interactions leading to lysosomes (Iwabu et al., 2009, 2010; Janvier et al., 2011; Skasko et al., 2011a). An additional level of complexity in the BST-2 downregulation mechanism stems from a report that in certain cell lines (CEMx174, H9), Vpu overexpression results in the enhancement of virion production, but without effectively reducing the surface levels of BST-2 (Miyagi et al., 2009). Thus, it is not yet clear how Vpu affects the internalization, recycling, or membrane transport, of BST-2.

Regardless of the mechanisms of Vpu-induced BST-2 downregulation, the ability of Vpu to bind to BST-2 is crucial for the antagonism of BST-2-mediated restriction (**Figure 2A**), as evidenced by data showing that the anti-BST-2 activity of Vpu is abrogated by mutations that disrupt TM-TM interaction. (Gupta et al., 2009a; Iwabu et al., 2009; McNatt et al., 2009; Rong et al., 2009; Skasko et al., 2011a). This interaction is highly specific since single point mutations in either BST-2 (I34, L37, L41; **Table 1**; Kobayashi et al., 2011) or Vpu (A14, A18, and W22; Vigan and Neil, 2010) render BST-2 resistant to Vpu antagonism. Their structural analyses showed that these residues form both hydrophobic faces of the helices, and therefore presumably contribute to their interacting surfaces. Recently, the aforementioned residues have been shown by NMR spectroscopy to interact directly in a membrane-embedded TM–TM interface (Skasko et al., 2011b).

Importantly, a high degree of species-specificity characterizes this interaction. Even though all primate BST-2 proteins are able to block HIV-1 virion-release, non-human BST-2 proteins are mostly insensitive to Vpu antagonism (Goffinet et al., 2009; Gupta et al., 2009a; Jia et al., 2009; Zhang et al., 2009). Analyses of codon-specific positive selection in the primate lineage showed that a mutation of residue T45 in human BST-2 is sufficient to reduce its sensitivity to Vpu (Gupta et al., 2009a). Likewise, the transfer of amino acid positions 30–45 of the human BST-2 TM domain into rhesus BST-2 was sufficient to render it Vpu-sensitive, while a single I48T mutation in rhesus BST-2 conferred partial Vpu sensitivity (Yoshida et al., 2011). These results suggest that this specificity of HIV-1 Vpu for BST-2 depends on conserved amino acids in the latter's TM domain (as described above) that are divergent between the human protein and its simian counterparts.

OTHER BST-2 ANTAGONISTS

Most of the primate lentiviruses that do not encode a Vpu protein instead use Nef to counteract BST-2's antiviral function (Jia et al., 2009; Sauter et al., 2009; Zhang et al., 2009). It should be noted that even though the primate ancestors of HIV-1, SIVcpz, and SIVgor from chimpanzees and gorillas encode Vpu, they also use Nef to antagonize BST-2 (Sauter et al., 2009; Yang et al., 2010b). Analogous to HIV-1 Vpu antagonism of human and chimpanzee, but not other primate BST-2 proteins (Goffinet et al., 2009; McNatt et al., 2009; Hauser et al., 2010), SIV Nef counteracts primate but not human BST-2 orthologs. This selectivity resides in the CT of non-human primate BST-2, which contains a discreet $DDIWK_{14–18}$ sequence (**Table 1**) that is required for the response to SIV Nef but is deleted in the protein's human counterparts (Sauter et al., 2009; Lim et al., 2010; Yang et al., 2010b). Furthermore, antagonism of non-human primate BST-2 is abrogated by mutations in the myristoylation site of SIV Nef (**Figure 2B**; Jia et al., 2009; Zhang et al., 2009). In addition, SIV Nef mutations that impair CD4 and CD28 downregulation also abrogate BST-2 antagonism, suggesting a similar mechanism of interaction (Zhang et al., 2009). By contrast, BST-2 antagonism by some strains of HIV-2 (as well as SIVtan from Tantalus monkeys) is mediated by the Env glycoprotein (**Figure 2C**; Bour and Strebel, 1996; Ritter et al., 1996; Abada et al., 2005; Gupta et al., 2009b). Although the exact determinants of interaction are not well understood, an endocytic motif (GYxxϕ) in the cytoplasmic region of gp41 (Boge et al., 1998) is known to be required to bind to AP-2, triggering BST-2 downregulation (Le Tortorec and Neil, 2009), while extracellular domains of HIV-2 Env apparently bind to the EC of BST-2. It was recently reported that an A100D point mutation of BST-2's EC abrogates the HIV-2 Env-mediated block of BST-2 restriction (Gupta et al., 2009b), supporting a model of interaction between HIV-2 Env and the EC of BST-2.

Other BST-2 antagonists include KSHV K5 protein, which ubiquitinates K18 residue in the CT domain of BST-2 (**Table 1**), leading to reduced surface and intracellular levels of BST-2, presumably through an endolysosomal process (**Figure 2D**; Mansouri et al., 2009; Pardieu et al., 2010). The Ebola virus GP2 appears to use a novel non-sequence-specific mechanism, overcoming

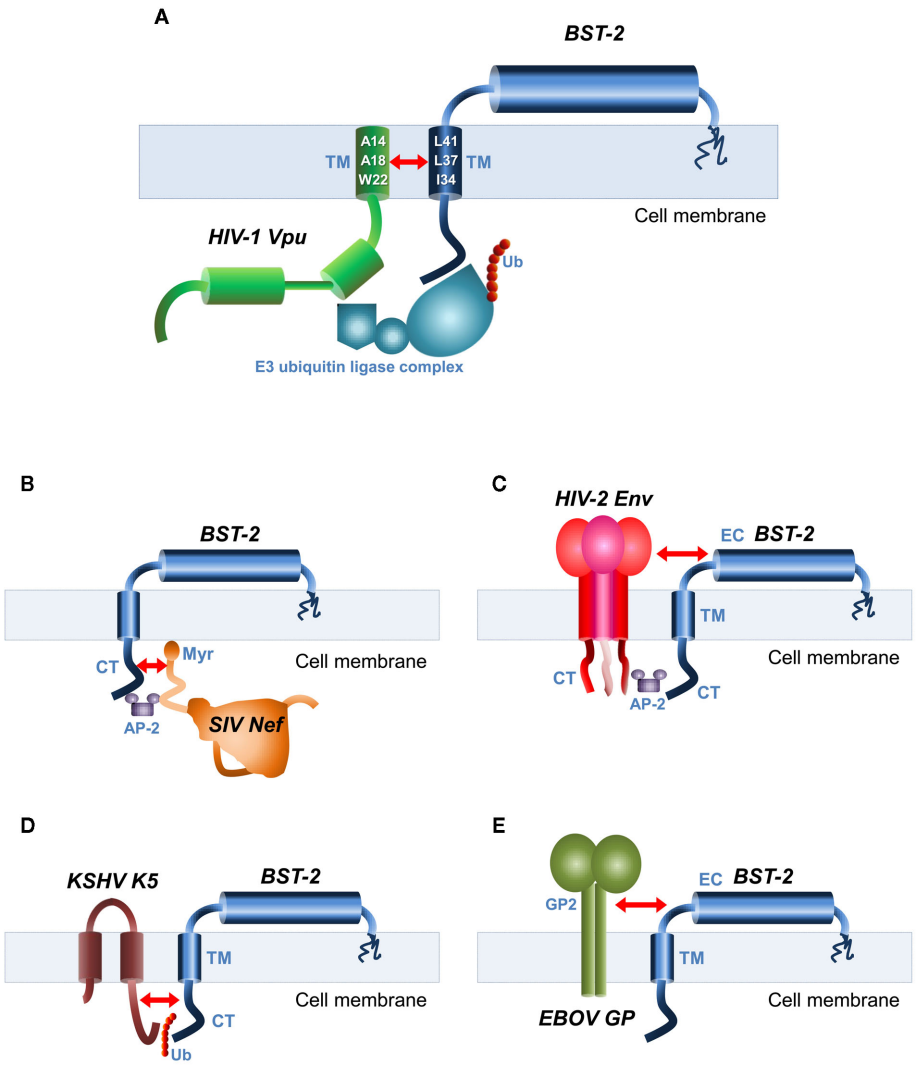

FIGURE 2 | Viral antagonists of BST-2 and their domains of interaction. Schematic representation of BST-2 and its known antagonists. The structural domains of interaction are indicated by red arrows. **(A)** HIV-1 Vpu and BST-2 interact through their mutual transmembrane (TM) domains. Key amino acid residues involved in the interaction are depicted in the TM helices. Also shown is the E3 ubiquitin (Ub) ligase complex required for BST-2 internalization. **(B)** SIV Nef recognizes the cytoplasmic (CT) domain of BST-2. The AP-2 clathrin adaptor recruited for BST-2 internalization is also shown. Myr, myristoylation site. **(C)** The envelope glycoprotein (Env) of HIV-2 and SIVtan binds to BST-2 through their mutual ectodomains (EC), and recruitment of AP-2 by the CT domain of Env required for internalization is also shown. **(D)** Kaposi's sarcoma-associated herpesvirus (KSHV) K5 protein that is an ubiquitin ligase ubiquitinates a target lysine motif in the CT domain of BST-2, resulting in its internalization. **(E)** The antagonistic mechanisms of the Ebola virus (EBOV) glycoprotein (GP) are unclear, but require interaction between GP2 subunit of EBOV–GP and BST-2 EC.

BST-2's restriction without significant removal of the protein from the cell surface (**Figure 2E**; Kaletsky et al., 2009; Lopez et al., 2010; Kühl et al., 2011). Influenza virus is suspected of harboring an unidentified viral antagonist against BST-2, since BST-2 expression was unable to block replication-competent influenza virus production but inhibited the release of influenza virus-like-particles (Watanabe et al., 2011).

CONCLUSION

Considerable progress was made recently in understanding the structure and function of BST-2, as well as the mechanisms by which viral antagonists counteract its activity. Through a combination of biological studies and structural analyses, the functional state of BST-2 is characterized as that of a parallel dimeric coiled-coil that, via its double-membrane anchors, physically binds budding virions to the infected cell. More importantly, current evidence shows that the unusual structural features of BST-2 determine its antiviral function independently of sequence homology. The EC has a prime role acting as a molecular ruler that separates the membrane anchors, in addition to allowing dimerization of BST-2 and providing conformational flexibility to sustain the protein's function as a viral particle tether. Likewise, loss of BST-2's double-membrane anchoring leads to the complete abrogation of the antiviral activity.

Although most of the evidence presented here was obtained from *in vitro* systems, a recent study using BST-2 knockout mice has shown that BST-2 inhibited the replication and release of a murine retrovirus *in vivo*, in a manner completely dependent on IFN-α production. Additionally, BST-2 restricted viral pathogenesis and delayed disease progression, suggesting that it has verifiable antiviral activity not only *in vitro* but also *in vivo*. (Liberatore and Bieniasz, 2011). Another study using rhesus macaques has confirmed the importance of the antagonism of BST-2 antiviral activity by Vpu *in vivo* (Shingai et al., 2011). Further investigation of the antiviral mechanisms exerted by host restriction factors, as well as the evolution of viral countermeasures, will not only advance our understanding of AIDS pathogenesis but also lead to the development of therapeutic alternatives.

ACKNOWLEDGMENTS

This work was supported by grants from the Ministry of Health, Labor and Welfare of Japan (Research on HIV/AIDS; H21–009), and from the Ministry of Education, Science, Technology, Sports and Culture of Japan.

REFERENCES

Abada, P., Noble, B., and Cannon, P. M. (2005). Functional domains within the human immunodeficiency virus type 2 envelope protein required to enhance virus production. *J. Virol.* 79, 3627–3638.

Aloia, R. C., Tian, H., and Jensen, F. C. (1993). Lipid composition and fluidity of the human immunodeficiency virus envelope and host cell plasma membranes. *Proc. Natl. Acad. Sci. U.S.A.* 90, 5181–5185.

Andrew, A. J., Miyagi, E., Kao, S., and Strebel, K. (2009). The formation of cysteine-linked dimers of BST-2/tetherin is important for inhibition of HIV-1 virus release but not for sensitivity to Vpu. *Retrovirology* 6, 80.

Andrew, A. J., Miyagi, E., and Strebel, K. (2011). Differential effects of human immunodeficiency virus type 1 Vpu on the stability of BST-2/tetherin. *J. Virol.* 85, 2611–2619.

Arnaud, F., Black, S. G., Murphy, L., Griffiths, D. J., Neil, S. J., Spencer, T. E., and Palmarini, M. (2010). Interplay between ovine bone marrow stromal cell antigen 2/tetherin and endogenous retroviruses. *J. Virol.* 84, 4415–4425.

Boge, M., Wyss, S., Bonifacino, J. S., and Thali, M. (1998). A membrane-proximal tyrosine-based signal mediates internalization of the HIV-1 envelope glycoprotein via interaction with the AP-2 clathrin adaptor. *J. Biol. Chem.* 273, 15773–15778.

Bour, S., and Strebel, K. (1996). The human immunodeficiency virus (HIV) type 2 envelope protein is a functional complement to HIV type 1 Vpu that enhances particle release of heterologous retroviruses. *J. Virol.* 70, 8285–8300.

Casartelli, N., Sourisseau, M., Feldmann, J., Guivel-Benhassine, F., Mallet, A., Marcelin, A.-G., Guatelli, J., and Schwartz, O. (2010). Tetherin restricts productive HIV-1 cell-to-cell transmission. *PLoS Pathog.* 6, e1000955. doi:10.1371/journal.ppat.1000955

Cohen, E. A., Terwilliger, E. F., Sodroski, J. G., and Haseltine, W. A. (1988). Identification of a protein encoded by the vpu gene of HIV-1. *Nature* 334, 532–534.

Dietrich, I., Hosie, M. J., and Willett, B. J. (2011). The role of BST2/tetherin in feline retrovirus infection. *Vet. Immunol. Immunopathol.* 143, 255–264.

Douglas, J. L., Viswanathan, K., Mccarroll, M. N., Gustin, J. K., Fruh, K., and Moses, A. V. (2009). Vpu Directs the degradation of the human immunodeficiency virus restriction factor BST-2/tetherin via a {beta}TrCP-dependent mechanism. *J. Virol.* 83, 7931–7947.

Dubé, M., Bhusan Roy, B., Guiot-Guillain, P., Binette, J., Mercier, J., Chiasson, A., and Cohen, É. A. (2010). Antagonism of tetherin restriction of HIV-1 release by Vpu involves binding and sequestration of the restriction factor in a perinuclear compartment. *PLoS Pathog.* 6, e1000856. doi:10.1371/journal.ppat.1000856

Dube, M., Roy, B. B., Guiot-Guillain, P., Mercier, J., Binette, J., Leung, G., and Cohen, E. A. (2009). Suppression of tetherin-restricting activity upon human immunodeficiency virus type 1 particle release correlates with localization of Vpu in the trans-Golgi network. *J. Virol.* 83, 4574–4590.

Fitzpatrick, K., Skasko, M., Deerinck, T. J., Crum, J., Ellisman, M. H., and Guatelli, J. (2010). Direct restriction of virus release and incorporation of the interferon-induced protein BST-2 into HIV-1 particles. *PLoS Pathog.* 6, e1000701. doi:10.1371/journal.ppat.1000701

Goffinet, C., Allespach, I., Homann, S., Tervo, H.-M., Habermann, A., Rupp, D., Oberbremer, L., Kern, C., Tibroni, N., Welsch, S., Krijnse-Locker, J., Banting, G., Kräusslich, H.-G., Fackler, O. T., and Keppler, O. T. (2009). HIV-1 Antagonism of CD317 is species specific and involves Vpu-mediated proteasomal degradation of the restriction factor. *Cell Host Microbe* 5, 285–297.

Gupta, R. K., Hué, S., Schaller, T., Verschoor, E., Pillay, D., and Towers, G. J. (2009a). Mutation of a single residue renders human tetherin resistant to HIV-1 Vpu-mediated depletion. *PLoS Pathog.* 5, e1000443. doi:10.1371/journal.ppat.1000443

Gupta, R. K., Mlcochova, P., Pelchen-Matthews, A., Petit, S. J., Mattiuzzo, G., Pillay, D., Takeuchi, Y., Marsh, M., and Towers, G. J. (2009b). Simian immunodeficiency virus envelope glycoprotein counteracts tetherin/BST-2/CD317 by intracellular sequestration. *Proc. Natl. Acad. Sci. U.S.A.* 106, 20889–20894.

Habermann, A., Krijnse-Locker, J., Oberwinkler, H., Eckhardt, M., Homann, S., Andrew, A., Strebel, K., and Krausslich, H.-G. (2010). CD317/tetherin is enriched in the HIV-1 envelope and downregulated from the plasma membrane upon virus infection. *J. Virol.* 84, 4646–4658.

Hammonds, J., Wang, J.-J., Yi, H., and Spearman, P. (2010). Immunoelectron microscopic evidence for tetherin/BST2 as the physical bridge between HIV-1 virions and the plasma membrane. *PLoS Pathog.* 6, e1000749. doi:10.1371/journal.ppat.1000749

Hauser, H., Lopez, L. A., Yang, S. J., Oldenburg, J. E., Exline, C. M., Guatelli, J. C., and Cannon, P. M. (2010). HIV-1 Vpu and HIV-2 Env counteract BST-2/tetherin by sequestration in a perinuclear compartment. *Retrovirology* 7, 51.

Hinz, A., Miguet, N., Natrajan, G., Usami, Y., Yamanaka, H., Renesto, P., Hartlieb, B., Mccarthy, A. A., Simorre, J.-P., Göttlinger, H., and Weissenhorn, W. (2010). Structural basis of HIV-1 tethering to membranes by the BST-2/tetherin ectodomain. *Cell Host Microbe* 7, 314–323.

Hrecka, K., Hao, C., Gierszewska, M., Swanson, S. K., Kesik-Brodacka, M., Srivastava, S., Florens, L., Washburn, M. P., and Skowronski, J. (2011). Vpx relieves inhibition of HIV-1 infection of macrophages mediated by the SAMHD1 protein. *Nature* 474, 658–661.

Ishikawa, J., Kaisho, T., Tomizawa, H., Lee, B. O., Kobune, Y., Inazawa, J., Oritani, K., Itoh, M., Ochi, T., Ishihara, K., and Hirano, T. (1995). Molecular cloning and chromosomal mapping of a bone marrow stromal cell surface gene, BST2, that may be involved in pre-B-cell growth. *Genomics* 26, 527–534.

Iwabu, Y., Fujita, H., Kinomoto, M., Kaneko, K., Ishizaka, Y., Tanaka, Y., Sata, T., and Tokunaga, K. (2009). HIV-1 accessory protein Vpu internalizes cell-surface BST-2/tetherin through transmembrane interactions leading to lysosomes. *J. Biol. Chem.* 284, 35060–35072.

Iwabu, Y., Fujita, H., Tanaka, Y., Sata, T., and Tokunaga, K. (2010). Direct internalization of cell-surface BST-2/tetherin by the HIV-1 accessory protein Vpu. *Commun. Integr. Biol.* 3, 366–369.

Janvier, K., Pelchen-Matthews, A., Renaud, J.-B., Caillet, M., Marsh, M., and Berlioz-Torrent, C. (2011). The ESCRT-0 component HRS is required for HIV-1 Vpu-mediated BST-2/tetherin down-regulation. *PLoS Pathog.* 7, e1001265. doi:10.1371/journal.ppat.1001265

Jia, B., Serra-Moreno, R., Neidermyer, W. Jr., Rahmberg, A., Mackey, J., Fofana, I. B., Johnson, W. E., Westmoreland, S., and Evans, D. T. (2009). Species-specific activity of SIV Nef and HIV-1 Vpu in overcoming restriction by tetherin/BST2. *PLoS Pathog.* 5, e1000429. doi:10.1371/journal.ppat.1000429

Jolly, C., Booth, N. J., and Neil, S. J. D. (2010). Cell-cell spread of human immunodeficiency virus type 1 overcomes tetherin/BST-2-mediated restriction in T cells. *J. Virol.* 84, 12185–12199.

Jouvenet, N., Neil, S. J., Zhadina, M., Zang, T., Kratovac, Z., Lee, Y., Mcnatt, M., Hatziioannou, T., and Bieniasz, P. D. (2009). Broad-spectrum inhibition of retroviral and filoviral particle release by tetherin. *J. Virol.* 83, 1837–1844.

Kaletsky, R. L., Francica, J. R., Agrawal-Gamse, C., and Bates, P. (2009). Tetherin-mediated restriction of filovirus budding is antagonized by the Ebola glycoprotein. *Proc. Natl. Acad. Sci. U.S.A.* 106, 2886–2891.

Kobayashi, T., Ode, H., Yoshida, T., Sato, K., Gee, P., Yamamoto, S. P., Ebina, H., Strebel, K., Sato, H., and Koyanagi, Y. (2011). Identification of amino acids in the human tetherin transmembrane domain responsible for HIV-1 Vpu interaction and susceptibility. *J. Virol.* 85, 932–945.

Kühl, A., Banning, C., Marzi, A., Votteler, J., Steffen, I., Bertram, S., Glowacka, I., Konrad, A., Stürzl, M., Guo, J.-T., Schubert, U., Feldmann, H., Behrens, G., Schindler, M., and Pöhlmann, S. (2011). The ebola virus glycoprotein and HIV-1 Vpu employ different strategies to counteract the antiviral factor tetherin. *J. Infect. Dis.* 204, S850–S860.

Kupzig, S., Korolchuk, V., Rollason, R., Sugden, A., Wilde, A., and Banting, G. (2003). Bst-2/HM1.24 is a raft-associated apical membrane protein with an unusual topology. *Traffic* 4, 694–709.

Laguette, N., Sobhian, B., Casartelli, N., Ringeard, M., Chable-Bessia, C., Segeral, E., Yatim, A., Emiliani, S., Schwartz, O., and Benkirane, M. (2011). SAMHD1 is the dendritic- and myeloid-cell-specific HIV-1 restriction factor counteracted by Vpx. *Nature* 474, 654–657.

Lau, D., Kwan, W., and Guatelli, J. (2011). Role of the endocytic pathway in the counteraction of BST-2 by human lentiviral pathogens. *J. Virol.* 85, 9834–9846.

Le Tortorec, A., and Neil, S. J. D. (2009). Antagonism to and intracellular sequestration of human tetherin by the human immunodeficiency virus type 2 envelope glycoprotein. *J. Virol.* 83, 11966–11978.

Liberatore, R. A., and Bieniasz, P. D. (2011). Tetherin is a key effector of the antiretroviral activity of type I interferon in vitro and in vivo. *Proc. Natl. Acad. Sci. U.S.A.* 108, 18097–18101.

Lim, E. S., Malik, H. S., and Emerman, M. (2010). Ancient adaptive evolution of tetherin shaped the functions of vpu and nef in human immunodeficiency virus and primate lentiviruses. *J. Virol.* 84, 7124–7134.

Lopez, L. A., Yang, S. J., Hauser, H., Exline, C. M., Haworth, K. G., Oldenburg, J., and Cannon, P. M. (2010). Ebola virus glycoprotein counteracts BST-2/tetherin restriction in a sequence-independent manner that does not require tetherin surface removal. *J. Virol.* 84, 7243–7255.

Malim, M. H., and Emerman, M. (2008). HIV-1 accessory proteins ensuring viral survival in a hostile environment. *Cell Host Microbe* 3, 388–398.

Mangeat, B., Gers-Huber, G., Lehmann, M., Zufferey, M., Luban, J., and Piguet, V. (2009). HIV-1 Vpu neutralizes the antiviral factor tetherin/BST-2 by binding it and directing its beta-TrCP2-dependent degradation. *PLoS Pathog.* 5, e1000574. doi:10.1371/journal.ppat.1000574

Mansouri, M., Viswanathan, K., Douglas, J. L., Hines, J., Gustin, J., Moses, A. V., and Fruh, K. (2009). Molecular mechanism of BST2/tetherin down-regulation by K5/MIR2 of Kaposi's sarcoma-associated herpesvirus. *J. Virol.* 83, 9672–9681.

Masuyama, N., Kuronita, T., Tanaka, R., Muto, T., Hirota, Y., Takigawa, A., Fujita, H., Aso, Y., Amano, J., and Tanaka, Y. (2009). HM1.24 is internalized from lipid rafts by clathrin-mediated endocytosis through interaction with α-adaptin. *J. Biol. Chem.* 284, 15927–15941.

McNatt, M. W., Zang, T., Hatziioannou, T., Bartlett, M., Fofana, I. B., Johnson, W. E., Neil, S. J. D., and Bieniasz, P. D. (2009). Species-specific activity of HIV-1 Vpu and positive selection of tetherin transmembrane domain variants. *PLoS Pathog.* 5, e1000300. doi:10.1371/journal.ppat.1000300

Mitchell, R. S., Katsura, C., Skasko, M. A., Fitzpatrick, K., Lau, D., Ruiz, A., Stephens, E. B., Margottin-Goguet, F., Benarous, R., and Guatelli, J. C. (2009). Vpu antagonizes BST-2–mediated restriction of HIV-1 release via β-TrCP and endo-lysosomal trafficking. *PLoS Pathog.* 5, e1000450. doi:10.1371/journal.ppat.1000450

Miyagi, E., Andrew, A. J., Kao, S., and Strebel, K. (2009). Vpu enhances HIV-1 virus release in the absence of Bst-2 cell surface down-modulation and intracellular depletion. *Proc. Natl. Acad. Sci. U.S.A.* 106, 2868–2873.

Moore, R. C., Lee, I. Y., Silverman, G. L., Harrison, P. M., Strome, R., Heinrich, C., Karunaratne, A., Pasternak, S. H., Chishti, M. A., Liang, Y., Mastrangelo, P., Wang, K., Smit, A. F. A., Katamine, S., Carlson, G. A., Cohen, F. E., Prusiner, S. B., Melton, D. W., Tremblay, P., Hood, L. E., and Westaway, D. (1999). Ataxia in prion protein (PrP)-deficient mice is associated with upregulation of the novel PrP-like protein doppel. *J. Mol. Biol.* 292, 797–817.

Neil, S. J., Zang, T., and Bieniasz, P. D. (2008). Tetherin inhibits retrovirus release and is antagonized by HIV-1 Vpu. *Nature* 451, 425–430.

Ohtomo, T., Sugamata, Y., Ozaki, Y., Ono, K., Yoshimura, Y., Kawai, S., Koishihara, Y., Ozaki, S., Kosaka, M., Hirano, T., and Tsuchiya, M. (1999). Molecular cloning and characterization of a surface antigen preferentially overexpressed on multiple myeloma cells. *Biochem. Biophys. Res. Commun.* 258, 583–591.

Pais-Correia, A.-M., Sachse, M., Guadagnini, S., Robbiati, V., Lasserre, R., Gessain, A., Gout, O., Alcover, A., and Thoulouze, M.-I. (2010). Biofilm-like extracellular viral assemblies mediate HTLV-1 cell-to-cell transmission at virological synapses. *Nat. Med.* 16, 83–89.

Panchal, R. G., Ruthel, G., Kenny, T. A., Kallstrom, G. H., Lane, D., Badie, S. S., Li, L., Bavari, S., and Aman, M. J. (2003). In vivo oligomerization and raft localization of Ebola virus protein VP40 during vesicular budding. *Proc. Natl. Acad. Sci. U.S.A.* 100, 15936–15941.

Pardieu, C., Vigan, R., Wilson, S. J., Calvi, A., Zang, T., Bieniasz, P., Kellam, P., Towers, G. J., and Neil, S. J. D. (2010). The RING-CH ligase K5 antagonizes restriction of KSHV and HIV-1 particle release by mediating ubiquitin-dependent endosomal degradation of tetherin. *PLoS Pathog.* 6, e1000843. doi:10.1371/journal.ppat.1000843

Perez-Caballero, D., Zang, T., Ebrahimi, A., Mcnatt, M. W., Gregory, D. A., Johnson, M. C., and Bieniasz, P. D. (2009). Tetherin inhibits HIV-1 release by directly tethering virions to cells. *Cell* 139, 499–511.

Radoshitzky, S. R., Dong, L., Chi, X., Clester, J. C., Retterer, C., Spurgers, K., Kuhn, J. H., Sandwick, S., Ruthel, G., Kota, K., Boltz, D., Warren, T., Kranzusch, P. J., Whelan, S. P., and Bavari, S. (2010). Infectious Lassa virus, but not filoviruses, is restricted by BST-2/tetherin. *J. Virol.* 84, 10569–10580.

Ritter, G. D. Jr., Yamshchikov, G., Cohen, S. J., and Mulligan, M. J. (1996). Human immunodeficiency virus type 2 glycoprotein enhancement of particle budding: role of the cytoplasmic domain. *J. Virol.* 70, 2669–2673.

Rollason, R., Korolchuk, V., Hamilton, C., Jepson, M., and Banting, G. (2009). A CD317/tetherin–RICH2 complex plays a critical role in the organization of the subapical actin cytoskeleton in polarized epithelial cells. *J. Cell Biol.* 184, 721–736.

Rollason, R., Korolchuk, V., Hamilton, C., Schu, P., and Banting, G. (2007). Clathrin-mediated endocytosis of a lipid-raft-associated protein is mediated through a dual tyrosine motif. *J. Cell. Sci.* 120, 3850–3858.

Rong, L., Zhang, J., Lu, J., Pan, Q., Lorgeoux, R.-P., Aloysius, C., Guo, F., Liu, S.-L., Wainberg, M. A., and Liang, C. (2009). The transmembrane domain of BST-2 determines its sensitivity to down-modulation by human immunodeficiency virus type 1 Vpu. *J. Virol.* 83, 7536–7546.

Ruiz, A., Hill, M. S., Schmitt, K., and Stephens, E. B. (2010). Membrane raft association of the Vpu protein of human immunodeficiency virus type 1 correlates with enhanced virus release. *Virology* 408, 89–102.

Sakuma, T., Noda, T., Urata, S., Kawaoka, Y., and Yasuda, J. (2009a). Inhibition of Lassa and Marburg virus production by tetherin. *J. Virol.* 83, 2382–2385.

Sakuma, T., Sakurai, A., and Yasuda, J. (2009b). Dimerization of tetherin is not essential for its antiviral activity against Lassa and Marburg viruses. *PLoS ONE* 4, e6934. doi:10.1371/journal.pone.0006934

Sauter, D., Schindler, M., Specht, A., Landford, W. N., Münch, J., Kim, K.-A., Votteler, J., Schubert, U., Bibollet-Ruche, F., Keele, B. F., Takehisa, J., Ogando, Y., Ochsenbauer, C., Kappes, J. C., Ayouba, A., Peeters, M., Learn, G. H., Shaw, G., Sharp, P. M., Bieniasz, P., Hahn, B. H., Hatziioannou, T., and Kirchhoff, F. (2009). Tetherin-driven adaptation of Vpu and Nef function and the evolution of pandemic and nonpandemic HIV-1 strains. *Cell Host Microbe* 6, 409–421.

Schubert, H. L., Zhai, Q., Sandrin, V., Eckert, D. M., Garcia-Maya, M., Saul, L., Sundquist, W. I., Steiner, R. A., and Hill, C. P. (2010). Structural and functional studies on the extracellular domain of BST2/tetherin in reduced and oxidized conformations. *Proc. Natl. Acad. Sci. U.S.A.* 107, 17951–17956.

Schubert, U., and Strebel, K. (1994). Differential activities of the human immunodeficiency virus type 1-encoded Vpu protein are regulated by phosphorylation and occur in different cellular compartments. *J. Virol.* 68, 2260–2271.

Sheehy, A. M., Gaddis, N. C., Choi, J. D., and Malim, M. H. (2002). Isolation of a human gene that inhibits HIV-1 infection and is suppressed by the viral Vif protein. *Nature* 418, 646–650.

Shingai, M., Yoshida, T., Martin, M. A., and Strebel, K. (2011). Some human immunodeficiency virus type 1 Vpu proteins are able to antagonize macaque BST-2 in vitro and in vivo: Vpu-negative simian-human immunodeficiency viruses are attenuated in vivo. *J. Virol.* 85, 9708–9715.

Skasko, M., Tokarev, A., Chen, C.-C., Fischer, W. B., Pillai, S. K., and Guatelli, J. (2011a). BST-2 is rapidly down-regulated from the cell surface by the HIV-1 protein Vpu: evidence for a post-ER mechanism of Vpu-action. *Virology* 411, 65–77.

Skasko, M., Wang, Y., Tian, Y., Tokarev, A., Munguia, J., Ruiz, A., Stephens, E. B., Opella, S. J., and Guatelli, J. (2011b). HIV-1 Vpu antagonizes the innate restriction factor BST-2 via lipid-embedded helix-helix interactions. *J. Biol. Chem.* doi: 10.1074/jbc.M111.296772. [Epub ahead of print].

Strebel, K., Klimkait, T., and Martin, M. A. (1988). A novel gene of HIV-1, vpu, and its 16-kilodalton product. *Science* 241, 1221–1223.

Stremlau, M., Owens, C. M., Perron, M. J., Kiessling, M., Autissier, P., and Sodroski, J. (2004). The cytoplasmic body component TRIM5alpha restricts HIV-1 infection in old world monkeys. *Nature* 427, 848–853.

Swiecki, M., Scheaffer, S. M., Allaire, M., Fremont, D. H., Colonna, M., and Brett, T. J. (2011). Structural and biophysical analysis of BST-2/tetherin ectodomains reveals an evolutionary conserved design to inhibit virus release. *J. Biol. Chem.* 286, 2987–2997.

Tokarev, A. A., Munguia, J., and Guatelli, J. C. (2011). Serine-threonine ubiquitination mediates downregulation of BST-2/tetherin and relief of restricted virion release by HIV-1 Vpu. *J. Virol.* 85, 51–63.

Van Damme, N., Goff, D., Katsura, C., Jorgenson, R. L., Mitchell, R., Johnson, M. C., Stephens, E. B., and Guatelli, J. (2008). The interferon-induced protein BST-2 restricts HIV-1 release and is downregulated from the cell surface by the viral Vpu protein. *Cell Host Microbe* 3, 245–252.

Vigan, R., and Neil, S. J. D. (2010). Determinants of tetherin antagonism in the transmembrane domain of the human immunodeficiency virus type 1 Vpu protein. *J. Virol.* 84, 12958–12970.

Waheed, A. A., and Freed, E. O. (2009). Lipids and membrane microdomains in HIV-1 replication. *Virus Res.* 143, 162–176.

Watanabe, R., Leser, G. P., and Lamb, R. A. (2011). Influenza virus is not restricted by tetherin whereas influenza VLP production is restricted by tetherin. *Virology* 417, 50–56.

Weidner, J. M., Jiang, D., Pan, X. B., Chang, J., Block, T. M., and Guo, J. T. (2010). Interferon-induced cell membrane proteins, IFITM3 and tetherin, inhibit vesicular stomatitis virus infection via distinct mechanisms. *J. Virol.* 84, 12646–12657.

Xu, F., Tan, J., Liu, R., Xu, D., Li, Y., Geng, Y., Liang, C., and Qiao, W. (2011). Tetherin inhibits prototypic foamy virus release. *Virol. J.* 8, 198.

Yang, H., Wang, J., Jia, X., Mcnatt, M. W., Zang, T., Pan, B., Meng, W., Wang, H.-W., Bieniasz, P. D., and Xiong, Y. (2010a). Structural insight into the mechanisms of enveloped virus tethering by tetherin. *Proc. Natl. Acad. Sci. U.S.A.* 107, 18428–18432.

Yang, S. J., Lopez, L. A., Hauser, H., Exline, C. M., Haworth, K. G., and Cannon, P. M. (2010b). Anti-tetherin activities in Vpu-expressing primate lentiviruses. *Retrovirology* 7, 13.

Yoshida, T., Kao, S., and Strebel, K. (2011). Identification of residues in the BST-2 TM domain important for antagonism by HIV-1 Vpu using a gain-of-function approach. *Front. Microbiol.* 2:35. doi:10.3389/fmicb.2011.00035

Zhang, F., Wilson, S. J., Landford, W. C., Virgen, B., Gregory, D., Johnson, M. C., Munch, J., Kirchhoff, F., Bieniasz, P. D., and Hatziioannou, T. (2009). Nef proteins from simian immunodeficiency viruses are tetherin antagonists. *Cell Host Microbe* 6, 54–67.

Conflict of Interest Statement: The authors declare that the research was conducted in the absence of any commercial or financial relationships that could be construed as a potential conflict of interest.

Received: 18 November 2011; accepted: 25 November 2011; published online: 12 December 2011.

Citation: Arias JF, Iwabu Y and Tokunaga K (2011) Structural basis for the antiviral activity of BST-2/tetherin and its viral antagonism. Front. Microbio. ***2****:250. doi: 10.3389/fmicb.2011.00250*

This article was submitted to Frontiers in Virology, a specialty of Frontiers in Microbiology.

frontiers in
MICROBIOLOGY

MINI REVIEW ARTICLE
published: 04 January 2012
doi: 10.3389/fmicb.2011.00267

CTL escape and viral fitness in HIV/SIV infection

Sayuri Seki [1,2] ***and Tetsuro Matano*** [1,2] ***

[1] *AIDS Research Center, National Institute of Infectious Diseases, Tokyo, Japan*
[2] *The Institute of Medical Science, The University of Tokyo, Tokyo, Japan*

Edited by:
Akio Adachi, The University of Tokushima Graduate School, Japan

Reviewed by:
Hirofumi Akari, Kyoto University, Japan
Yasuko Yokota, National Institute of Infectious Diseases, Japan

***Correspondence:**
Tetsuro Matano, AIDS Research Center, National Institute of Infectious Diseases, 1-23-1 Toyama, Shinjuku-ku, Tokyo 162-8640, Japan.
e-mail: tmatano@nih.go.jp

Cytotoxic T lymphocyte (CTL) responses exert a suppressive effect on HIV and simian immunodeficiency virus (SIV) replication. Under the CTL pressure, viral CTL escape mutations are frequently selected with viral fitness costs. Viruses with such CTL escape mutations often need additional viral genome mutations for recovery of viral fitness. Persistent HIV/SIV infection sometimes shows replacement of a CTL escape mutation with an alternative escape mutation toward higher viral fitness. Thus, multiple viral genome changes under CTL pressure are observed in the chronic phase of HIV/SIV infection. HIV/SIV transmission to HLA/MHC-mismatched hosts drives further viral genome changes including additional CTL escape mutations and reversions under different CTL pressure. Understanding of viral structure/function and host CTL responses would contribute to prediction of HIV evolution and control of HIV prevalence.

Keywords: HIV, SIV, MHC, cytotoxic T lymphocyte, escape mutation, viral fitness, capsid

INTRODUCTION

Virus-specific $CD8^+$ cytotoxic T lymphocyte (CTL) responses play a central role in the control of HIV and simian immunodeficiency virus (SIV) replication (Borrow et al., 1994; Koup et al., 1994; Matano et al., 1998; Jin et al., 1999; Schmitz et al., 1999; Goulder and Watkins, 2008). CTLs recognize viral antigen-derived peptides (epitopes) presented by major histocompatibility class I (MHC-I) molecules on the surface of viral-infected cells. Under the CTL pressure, viral mutations in and around epitope-coding regions which result in viral escape from CTL recognition are frequently selected with the cost of viral fitness (Phillips et al., 1991; Borrow et al., 1997; Goulder et al., 1997; Price et al., 1997). Thus, analysis of structural and functional constraints in viral proteins could facilitate determination of effective CTLs that can limit viral escape options, contributing to immunogen design in development of CTL-inducing AIDS vaccines.

We previously developed an AIDS vaccine using a Sendai virus vector expressing Gag (SeV-Gag), which induces Gag-specific CTL responses efficiently. Our analysis showed vaccine-based control of a SIVmac239 challenge in a group of Burmese rhesus macaques possessing the MHC-I haplotype *90-120-Ia* (Matano et al., 2004; Kawada et al., 2008). $Gag_{206–216}$ (IINEEAADWDL) epitope-specific CTL responses exert a suppressive effect on SIV replication and select for a CTL escape mutation, GagL216S, leading to a leucine (L)-to-serine (S) substitution at the 216th amino acid (aa) in Gag capsid (CA) with viral fitness costs (Kobayashi et al., 2005). Our studies starting with this finding revealed viral genome changes in persistent SIV infection, providing insights into HIV/SIV evolution.

LOSS OF VIRAL FITNESS BY ESCAPE MUTATIONS AND ITS RECOVERY BY COMPENSATORY MUTATIONS

In contrast to the SIVmac239 challenge experiment, *90-120-Ia*-positive vaccinees failed to control a challenge with another pathogenic SIV strain, SIVsmE543-3 (Hirsch et al., 1997), which has the same $Gag_{206–216}$ amino acid sequence with SIVmac239. SIVsmE543-3 has a different amino acid (glutamate [E]) from SIVmac239 (aspartate [D]) at Gag residue 205, and this GagD205E change resulted in escape from $Gag_{206–216}$-specific CTL recognition, leading to failure in control of SIVsmE543-3 replication in *90-120-Ia*-positive vaccinees (Moriya et al., 2008).

Theoretically, $Gag_{206–216}$-specific CTL responses can select for either GagD205E or GagL216S mutation. SIVmac239-infected *90-120-Ia*-positive macaques, however, select the latter GagL216S mutation but not GagD205E in a year postchallenge. This suggests a possibility that the GagD205E substitution in SIVmac239 results in larger reduction of viral fitness than GagL216S. Indeed, our analysis *in vitro* revealed much lower replicative ability of the virus with this GagD205E substitution, SIVmac239Gag205E, compared to the wild-type SIVmac239 (Inagaki et al., 2010). On LuSIV cells, which contain a luciferase indicator gene under the control of the SIVmac239 long terminal repeat, SIVmac239Gag205E infection showed significantly lower luciferase activity compared to wild-type SIVmac239, indicating suppression of the early phase of this mutant virus replication.

Further passage of SIVmac239Gag205E-infected culture supernatants *in vitro* found an additional mutation, GagV340M, resulting in a valine (V)-to-methionine (M) substitution at the 340th aa in Gag. Interestingly, SIVmac239 has V while SIVsmE543-3 has M at the Gag residue 340. SIVmac239Gag205E340M showed similar replication kinetics with wild-type SIVmac239, indicating compensation for loss of viral fitness in SIVmac239Gag205E by addition of the GagV340M substitution. Thus, CTL escape mutations resulting in loss of viral fitness could be selected with compensatory mutations. **Figure 1** is a schema indicating the interaction between escape and compensatory mutations.

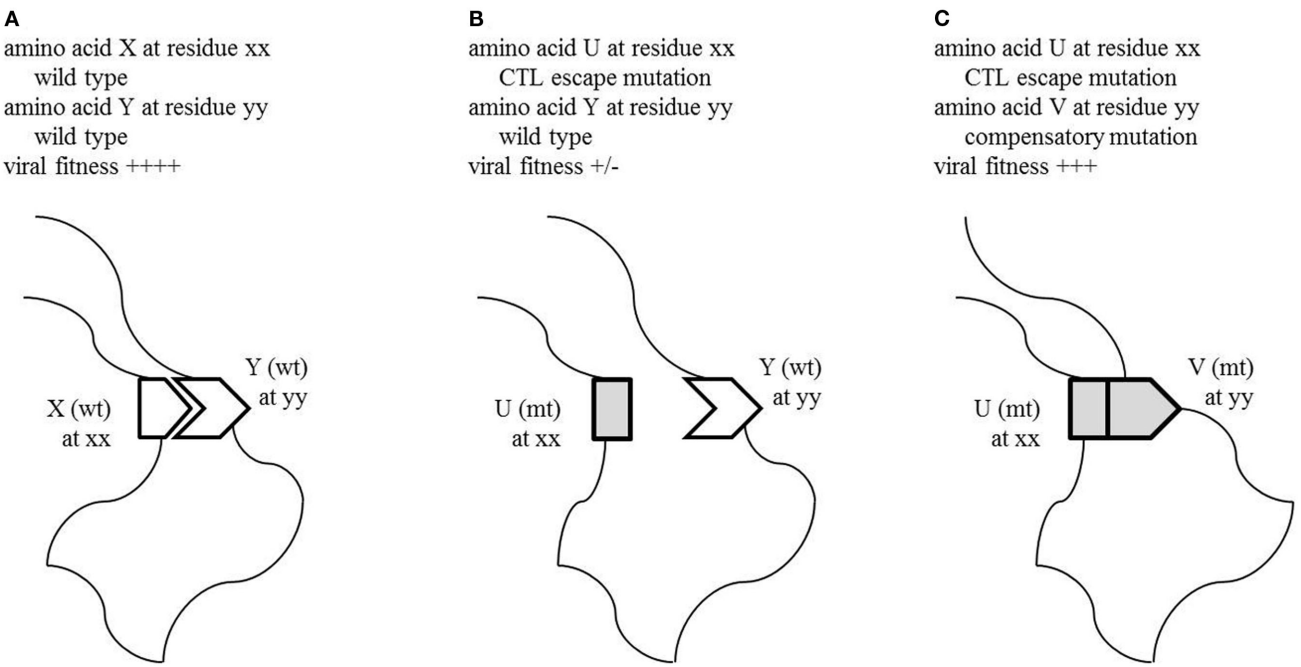

FIGURE 1 | Schema of recovery of viral fitness by a compensatory mutation. (A) Functional interaction between amino acid X at residue xx and Y at residue yy in wild-type viral protein is critical for viral replication. **(B)** A CTL escape mutation leading to an amino acid change from X to U at residue xx results in loss of viral fitness. **(C)** An additional compensatory mutation leading to an amino acid change from Y to V partially or fully restores viral function and replication.

GAG CA INTERMOLECULAR INTERACTION

The Gag CA is comprised of the N-terminal (NTD) and the C-terminal domains (CTD) (Momany et al., 1996; Gamble et al., 1997; Berthet-Colominas et al., 1999). Modeling of CA monomer structure showed that the Gag 205th residue is located in the helix 4 of CA NTD and the 340th is in the loop between helices 10 and 11 of CTD. A possibility of intramolecular contact between Gag residues 205 and 340 is not supported by this modeling. However, CA molecules are known to form hexamer lattice in mature virions (Ganser et al., 1999; Li et al., 2000; Ganser-Pornillos et al., 2007, 2008; Pornillos et al., 2009). Modeling of CA hexamer structure revealed that the Gag 205th residue is located in close proximity to the 340th of the adjacent CA molecule. The molecular model of CA hexamers incorporating the GagD205E substitution suggested shortening of the distance between Gag205 and Gag340 residues, which appeared compensated by GagV340M substitution. Thus, there may be intermolecular interaction between Gag residues 205 and 340 in CA hexamers. This is consistent with our results obtained by viral core stability assay. The core stability was reduced by the GagD205E substitution but recovered by the GagV340M substitution. Loss of viral fitness by GagD205E and its recovery by GagV340M implies a structural constraint for functional interaction between CA NTD and CTD involved in the formation of CA hexamers. In addition to previous reports on intramolecular compensation for loss of viral fitness by CTL escape mutations (Friedrich et al., 2004a; Crawford et al., 2007), our results present evidence indicating intermolecular compensation.

REPLACEMENT OF A CTL ESCAPE MUTATION WITH AN ALTERNATIVE ESCAPE MUTATION TOWARD HIGHER VIRAL FITNESS

As stated above, SIVmac239-infected *90-120-Ia*-positive macaques usually select the $Gag_{206–216}$-specific CTL escape mutation, GagL216S, but not GagD205E in a year postchallenge. After that, however, we found that the GagD205E mutation together with GagV340M became dominant instead of GagL216S in a *90-120-Ia*-positive macaque (Inagaki et al., 2010). In this macaque, neither GagD205E nor GagV340M was detected until week 123 after SIVmac239 challenge, but both became detectable at week 137 and were dominant at week 150. In contrast, the GagL216S mutation dominant until week 123 was undetectable at week 150. Thus, in this animal, SIVmac239Gag216S, whose replicative ability is lower than wild-type SIVmac239 but higher than SIVmac239Gag205E, became dominant under $Gag_{206–216}$-specific CTL pressure in the early phase, while in the later phase, this mutant virus was replaced with SIVmac239Gag205E340M, whose replicative ability is similar with the wild-type. This indicates replacement of a CTL escape mutation with an alternative escape mutation toward higher viral fitness in the chronic phase, implying persistent $Gag_{206–216}$-specific CTL pressure for more than 2 years after selection of the CTL escape mutation.

MULTIPLE VIRAL GENOME CHANGES UNDER CTL PRESSURE

In another study (Kawada et al., 2006), we observed accumulation of multiple CTL escape mutations in viral genomes in SIV-infected macaques. SeV-Gag-vaccinated animals possessing

MHC-I haplotype *90-120-Ia* elicited $Gag_{206–216}$-specific CTL responses and controlled viral replication with rapid selection of the GagL216S mutation after SIVmac239 challenge. Among these SIV controllers, two animals (V3 and V5) accumulated additional *gag* mutations and showed reappearance of plasma viremia around week 60 postchallenge. Both animals first selected a $Gag_{241–249}$ epitope-specific CTL escape mutation leading to a GagD244E (aspartic acid [D] to glutamic acid [E] at the 244th aa in Gag) substitution, and then, a $Gag_{373–380}$ epitope-specific CTL escape mutation leading to a GagA373T (alanine [A] to threonine [T] at the 373rd) or GagP376S (proline [P] to S at the 376th) substitution during the period of viral control. At the viremia reappearance, SIVmac239Gag216S244E247L312V373T with five *gag* mutations, L216S, D244E, I247L (isoleucine [I] to L at the 247th), A312V (A to V at the 312th), and A373T, became dominant in one of them (V5), and SIVmac239Gag145A216S244E376S with four *gag* mutations leading to V145A (V to A at the 145th), L216S, D244E, and P376S became dominant in the other (V3). These viruses with multiple *gag* mutations showed lower replicative ability *in vitro* than SIVmac239Gag216S carrying single GagL216S mutation. Indeed, SIVmac239Gag216S244E247L312V373T carrying five *gag* mutations had lower replicative ability *in vitro* compared to SIVmac239Gag216S244E373T carrying three *gag* mutations. These results suggest that selection of CTL escape mutations even with viral fitness costs could be advantageous for viral replication *in vivo* under CTL pressure.

SIV TRANSMISSION INTO MHC-MISMATCHED HOSTS DRIVES FURTHER VIRAL GENOME CHANGES

Previous studies (Friedrich et al., 2004b; Kobayashi et al., 2005; Loh et al., 2007) reported reversion of CTL escape mutations in the absence of CTL pressure by transmission of SIVs carrying single escape mutations between MHC-mismatched hosts. SIVs carrying CTL escape *gag* mutations selected in *90-120-Ia*-positive macaques showed lower replicative ability *in vitro*. We then examined *in vivo* replicative ability of those SIVs carrying CTL escape mutations in *90-120-Ia*-negative macaques (Seki et al., 2008). Coinoculation of macaques with SIVmac239GagL216S and SIVmac239Gag216S244E373T resulted in rapid selection of the former; i.e., D244E and A373T mutations were undetectable even in the acute phase, indicating lower replicative ability *in vivo* of the latter carrying three escape mutations than the former. Reversion of L216S was observed in a few months, confirming lower replicative ability *in vivo* of SIVmac239Gag216S than wild-type SIVmac239. Further competition indicated lower replicative ability *in vivo* of SIVmac239Gag216S244E247L312V373T carrying five *gag* mutations than SIVmac239Gag216S244E373T carrying three.

We next examined viral genome changes after challenge of *90-120-Ia*-negative macaques with SIVs carrying multiple CTL escape mutations selected in *90-120-Ia*-positive macaques. Challenge with SIVs carrying five *gag* mutations, L216S, D244E, I247L, A312V, and A373T, resulted in persistent viremia in all four *90-120-Ia*-negative macaques. Two animals exhibited higher viral

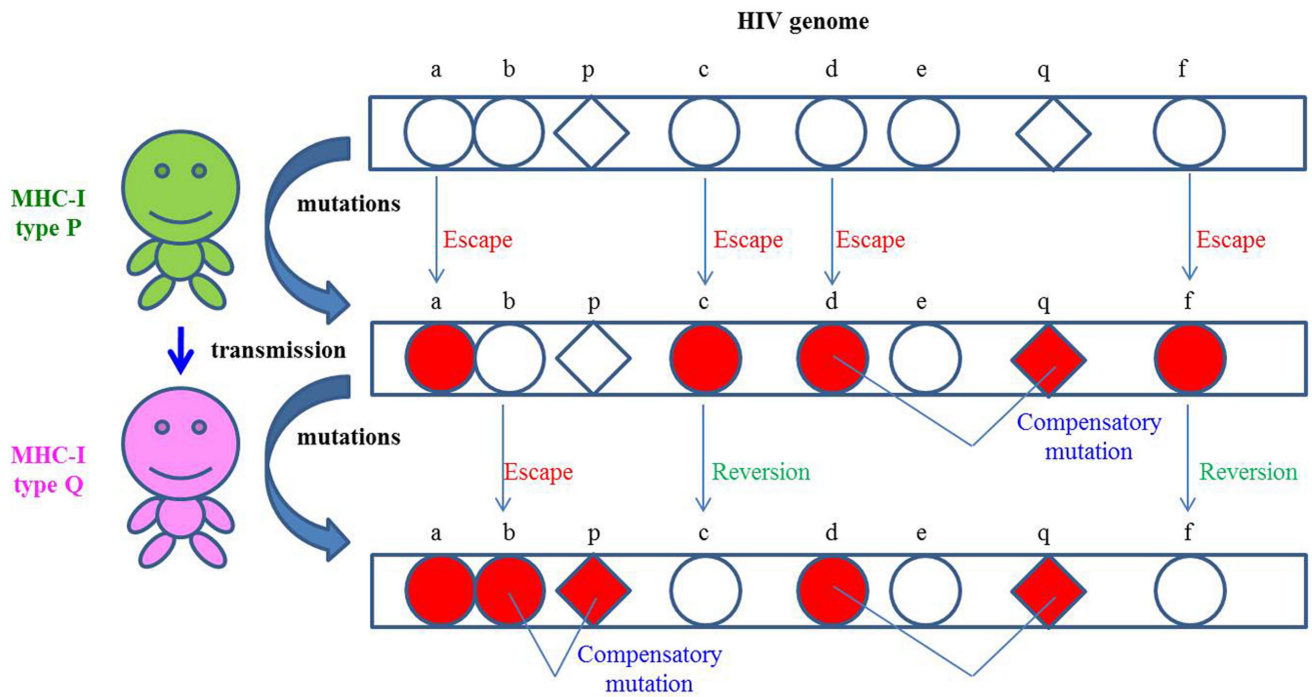

FIGURE 2 | Schema of HIV/SIV transmission resulting in accumulation of multiple viral mutations. Multiple CTL escape mutations resulting in viral fitness costs do not always revert rapidly even in the absence of CTL pressure after their transmission into HLA/MHC-mismatched hosts and such mutants can be transmitted further to other hosts. New escape mutations and compensatory mutations are also observed with transmissions. Thus, CTL affects HIV/SIV evolution in individuals with divergent HLA/MHC polymorphisms.

loads. One of them rapidly developed AIDS at week 18 while the other developed AIDS 2 years postchallenge. The former showed reversion of I247L and A312V but still had three CTL escape mutations, L216S, D244E, and A373T at AIDS onset. The latter showed reversion of four mutations in a year postchallenge, but the A373T mutation remained dominant without reversion until AIDS onset. In the remaining two animals that exhibited lower viral loads, multiple *gag* mutations including L216S and D244E were still dominant without reversion 1 year after challenge.

Thus, in the experiment of challenge with SIVs carrying multiple CTL escape mutations, the reversion of all the mutations was not required for AIDS onset, while transmission with SIVs carrying single CTL escape mutations showed their rapid reversion. This suggests that even HIVs accumulating multiple CTL escape mutations with viral fitness costs can induce persistent viral infection leading to AIDS progression after their transmission into HLA/MHC-mismatched individuals.

The reversion of the L216S mutation was delayed or not observed after challenge with SIVs carrying multiple *gag* mutations, whereas challenge with SIVmac239Gag216S resulted in its reversion in a few months. This may be due to the predominant selection of the reversion of other mutations, compensatory mutations, or to lower viral replication efficiency in the former case. Our results suggest that CTL escape mutations resulting in viral fitness costs may not always revert rapidly after their transmission into MHC-mismatched hosts and can be transmitted further to other hosts, driving further viral genome changes with accumulation of mutations (**Figure 2**). These results provide an important insight into HIV evolution in human individuals with divergent HLA/MHC polymorphisms.

CONCLUDING REMARKS

Cytotoxic T lymphocyte responses exert strong selective pressure on HIV and play a central role in viral evolution (Kaslow et al., 1996; Brander and Walker, 2003; Kiepiela et al., 2004; O'Connor et al., 2004). Correlation of frequencies of viral epitope variants with prevalence of restricting HLA alleles has been shown, indicating HIV adaptation to HLA polymorphisms at a population level (Kawashima et al., 2009). Loss of viral fitness by CTL escape mutations may contribute to HIV control (Martinez-Picado et al., 2006; Schneidewind et al., 2007), but our results indicate the potential of even such HIVs with lower viral fitness to induce AIDS progression. Elucidation of structural constraints of viral antigens for viral function would lead to determination of conserved, escape-resistant epitopes whose mutations largely diminish viral replicative ability (Dahirel et al., 2011), contributing to immunogen design in development of CTL-inducing AIDS vaccines.

REFERENCES

Berthet-Colominas, C., Monaco, S., Novelli, A., Sibai, G., Mallet, F., and Cusack, S. (1999). Head-to-tail dimers and interdomain flexibility revealed by the crystal structure of HIV-1 capsid protein (p24) complexed with a monoclonal antibody Fab. *EMBO J.* 18, 1124–1136.

Borrow, P., Lewicki, H., Hahn, B. H., Shaw, G. M., and Oldstone, M. B. (1994). Virus-specific CD8+ cytotoxic T-lymphocyte activity associated with control of viremia in primary human immunodeficiency virus type 1 infection. *J. Virol.* 68, 6103–6110.

Borrow, P., Lewicki, H., Wei, X., Horwitz, M. S., Peffer, N., Meyers, H., Nelson, J. A., Gairin, J. E., Hahn, B. H., Oldstone, M. B., and Shaw, G. M. (1997). Antiviral pressure exerted by HIV-1-specific cytotoxic T lymphocytes (CTL) during primary infection demonstrated by rapid selection of CTL escape virus. *Nat. Med.* 3, 205–211.

Brander, C., and Walker, B. D. (2003). Gradual adaptation of HIV to human host populations: good or bad news? *Nat. Med.* 9, 1359–1362.

Crawford, H., Prado, J. G., Leslie, A., Hué, S., Honeyborne, I., Reddy, S., van der Stok, M., Mncube, Z., Brander, C., Rousseau, C., Mullins, J. I., Kaslow, R., Goepfert, P., Allen, S., Hunter, E., Mulenga, J., Kiepiela, P., Walker, B. D., and Goulder, P. J. R. (2007). Compensatory mutation partially restores fitness and delays reversion of escape mutation within the immunodominant HLA-B*5703-restricted Gag epitope in chronic human immunodeficiency virus type 1 infection. *J. Virol.* 81, 8346–8351.

Dahirel, V., Shekhar, K., Pereyra, F., Miura, T., Artyomov, M., Talsania, S., Allen, T. M., Altfeld, M., Carrington, M., Irvine, D. J., Walker, B. D., and Chakraborty, A. K. (2011). Coordinate linkage of HIV evolution reveals regions of immunological vulnerability. *Proc. Natl. Acad. Sci. U.S.A.* 108, 11530–11535.

Friedrich, T. C., Frye, C. A., Yant, L. J., O'Connor, D. H., Kriewaldt, N. A., Benson, M., Vojnov, L., Dodds, E. J., Cullen, C., Rudersdorf, R., Hughes, A. L., Wilson, N., and Watkins, D. I. (2004a). Extra-epitopic compensatory substitutions partially restore fitness to simian immunodeficiency virus variants that escape from an immunodominant cytotoxic T-lymphocyte response. *J. Virol.* 78, 2581–2585.

Friedrich, T. C., Dodds, E. J., Yant, L. J., Vojnov, L., Rudersdorf, R., Cullen, C., Evans, D. T., Desrosiers, R. C., Mothé, B. R., Sidney, J., Sette, A., Kunstman, K., Wolinsky, S., Piatak, M., Lifson, J., Hughes, A. L., Wilson, N., O'Connor, D. H., and Watkins, D. I. (2004b). Reversion of CTL escape-variant immunodeficiency viruses in vivo. *Nat. Med.* 10, 275–281.

Gamble, T. R., Yoo, S., Vajdos, F. F., von Schwedler, U. K., Worthylake, D. K., Wang, H., McCutcheon, J. P., Sundquist, W. I., and Hill, C. P. (1997). Structure of the carboxyl-terminal dimerization domain of the HIV-1 capsid protein. *Science* 278, 849–853.

Ganser, B. K., Li, S., Klishko, V. Y., Finch, J. T., and Sundquist, W. I. (1999). Assembly and analysis of conical models for the HIV-1 core. *Science* 283, 80–83.

Ganser-Pornillos, B. K., Cheng, A., and Yeager, M. (2007). Structure of full-length HIV-1 CA: a model for the mature capsid lattice. *Cell* 131, 70–79.

Ganser-Pornillos, B. K., Yeager, M., and Sundquist, W. I. (2008). The structural biology of HIV assembly. *Curr. Opin. Struct. Biol.* 18, 203–217.

Goulder, P. J., Phillips, R. E., Colbert, R. A., McAdam, S., Ogg, G., Nowak, M. A., Giangrande, P., Luzzi, G., Morgana, B., Edwards, A., McMichael, A. J., and Rowland-Jones, S. (1997). Late escape from an immunodominant cytotoxic T-lymphocyte response associated with progression to AIDS. *Nat. Med.* 3, 212–217.

Goulder, P. J. R., and Watkins, D. I. (2008). Impact of MHC class I diversity on immune control of immunodeficiency virus replication. *Nat. Rev. Immunol.* 8, 619–630.

Hirsch, V., Adger-Johnson, D., Campbell, B., Goldstein, S., Brown, C., Elkins, W., and Montefiori, D. (1997). A molecularly cloned, pathogenic, neutralization-resistant simian immunodeficiency virus, SIVsmE543-3. *J. Virol.* 71, 1608–1620.

Inagaki, N., Takeuchi, H., Yokoyama, M., Sato, H., Ryo, A., Yamamoto, H., Kawada, M., and Matano, T. (2010). A structural constraint for functional interaction between N-terminal and C-terminal domains in simian immunodeficiency virus capsid proteins. *Retrovirology* 7, 90.

Jin, X., Bauer, D. E., Tuttleton, S. E., Lewin, S., Gettie, A., Blanchard, J., Irwin, C. E., Safrit, J. T., Mittler, J., Weinberger, L., Kostrikis, L. G., Zhang, L., Perelson, A. S., and Ho, D. D. (1999). Dramatic rise in plasma viremia after CD8+ T cell depletion in simian immunodeficiency virus-infected macaques. *J. Exp. Med.* 189, 991–998.

Kaslow, R. A., Carrington, M., Apple, R., Park, L., Muñoz, A., Saah, A. J., Goedert, J. J., Winkler, C., O'Brien, S. J., Rinaldo, C., Detels, R., Blattner, W., Phair, J., Erlich, H., and Mann, D. L. (1996). Influence of combinations of human major histocompatibility complex genes on the course of HIV-1 infection. *Nat. Med.* 2, 405–411.

Kawada, M., Igarashi, H., Takeda, A., Tsukamoto, T., Yamamoto, H., Dohki, S., Takiguchi, M., and Matano, T. (2006). Involvement of multiple epitope-specific cytotoxic T lymphocyte responses in vaccine-based control of simian immunodeficiency virus replication in rhesus macaques. *J. Virol.* 80, 1949–1958.

Kawada, M., Tsukamoto, T., Yamamoto, H., Iwamoto, N., Kurihara, K., Takeda, A., Moriya, C., Takeuchi, H., Akari, H., and Matano, T. (2008). Gag-specific cytotoxic T lymphocyte-based control of primary simian immunodeficiency virus replication in a vaccine trial. *J. Virol.* 82, 10199–10206.

Kawashima, Y., Pfafferott, K., Frater, J., Matthews, P., Payne, R., Addo, M., Gatanaga, H., Fujiwara, M., Hachiya, A., Koizumi, H., Kuse, N., Oka, S., Duda, A., Prendergast, A., Crawford, H., Leslie, A., Brumme, Z., Brumme, C., Allen, T., Brander, C., Kaslow, R., Tang, J., Hunter, E., Allen, S., Mulenga, J., Branch, S., Roach, T., John, M., Mallal, S., Ogwu, A., Shapiro, R., Prado, J. G., Fidler, S., Weber, J., Pybus, O. G., Klenerman, P., Ndung'u, T., Phillips, R., Heckerman, D., Harrigan, P. R., Walker, B. D., Takiguchi, M., and Goulder, P. (2009). Adaptation of HIV-1 to human leukocyte antigen class I. *Nature* 458, 641–645.

Kiepiela, P., Leslie, A. J., Honeyborne, I., Ramduth, D., Thobakgale, C., Chetty, S., Rathnavalu, P., Moore, C., Pfafferott, K. J., Hilton, L., Zimbwa, P., Moore, S., Allen, T., Brander, C., Addo, M. M., Altfeld, M., James, I., Mallal, S., Bunce, M., Barber, L. D., Szinger, J., Day, C., Klenerman, P., Mullins, J., Korber, B., Coovadia, H. M., Walker, B. D., and Goulder, P. J. (2004). Dominant influence of HLA-B in mediating the potential co-evolution of HIV and HLA. *Nature* 432, 769–775.

Kobayashi, M., Igarashi, H., Takeda, A., Kato, M., and Matano, T. (2005). Reversion in vivo after inoculation of a molecular proviral DNA clone of simian immunodeficiency virus with a cytotoxic-T-lymphocyte escape mutation. *J. Virol.* 79, 11529–11532.

Koup, R. A., Safrit, J. T., Cao, Y., Andrews, C. A., McLeod, G., Borkowsky, W., Farthing, C., and Ho, D. D. (1994). Temporal association of cellular immune responses with the initial control of viremia in primary human immunodeficiency virus type 1 syndrome. *J. Virol.* 68, 4650–4655.

Li, S., Hill, C. P., Sundquist, W. I., and Finch, J. T. (2000). Image reconstructions of helical assemblies of the HIV-1 CA protein. *Nature* 407, 409–413.

Loh, L., Batten, C. J., Petravic, J., Davenport, M. P., and Kent, S. J. (2007). In vivo fitness costs of different Gag CD8 T-cell escape mutant simian-human immunodeficiency viruses for macaques. *J. Virol.* 81, 5418–5422.

Martinez-Picado, J., Prado, J. G., Fry, E. E., Pfafferott, K., Leslie, A., Chetty, S., Thobakgale, C., Honeyborne, I., Crawford, H., Matthews, P., Pillay, T., Rousseau, C., Mullins, J. I., Brander, C., Walker, B. D., Stuart, D. I., Kiepiela, P., and Goulder, P. (2006). Fitness cost of escape mutations in p24 Gag in association with control of human immunodeficiency virus type 1. *J. Virol.* 80, 3617–3623.

Matano, T., Kobayashi, M., Igarashi, H., Takeda, A., Nakamura, H., Kano, M., Sugimoto, C., Mori, K., Iida, A., Hirata, T., Hasegawa, M., Yuasa, T., Miyazawa, M., Takahashi, Y., Yasunami, M., Kimura, A., O'Connor, D. H., Watkins, D. I., and Nagai, Y. (2004). Cytotoxic T lymphocyte-based control of simian immunodeficiency virus replication in a preclinical AIDS vaccine trial. *J. Exp. Med.* 199, 1709–1718.

Matano, T., Shibata, R., Siemon, C., Connors, M., Lane, H. C., and Martin, M. A. (1998). Administration of an anti-CD8 monoclonal antibody interferes with the clearance of chimeric simian/human immunodeficiency virus during primary infections of rhesus macaques. *J. Virol.* 72, 164–169.

Momany, C., Kovari, L. C., Prongay, A. J., Keller, W., Gitti, R. K., Lee, B. M., Gorbalenya, A. E., Tong, L., McClure, J., Ehrlich, L. S., Summers, M. F., Carter, C., and Rossmann, M. G. (1996). Crystal structure of dimeric HIV-1 capsid protein. *Nat. Struct. Mol. Biol.* 3, 763–770.

Moriya, C., Igarashi, H., Takeda, A., Tsukamoto, T., Kawada, M., Yamamoto, H., Inoue, M., Iida, A., Shu, T., Hasegawa, M., Nagai, Y., and Matano, T. (2008). Abrogation of AIDS vaccine-induced cytotoxic T lymphocyte efficacy in vivo due to a change in viral epitope flanking sequences. *Microbes Infect.* 10, 285–292.

O'Connor, D. H., McDermott, A. B., Krebs, K. C., Dodds, E. J., Miller, J. E., Gonzalez, E. J., Jacoby, T. J., Yant, L., Piontkivska, H., Pantophlet, R., Burton, D. R., Rehrauer, W. M., Wilson, N., Hughes, A. L., and Watkins, D. I. (2004). A dominant role for CD8-T-lymphocyte selection in simian immunodeficiency virus sequence variation. *J. Virol.* 78, 14012–14022.

Phillips, R. E., Rowland-Jones, S., Nixon, D. F., Gotch, F. M., Edwards, J. P., Ogunlesi, A. O., Elvin, J. G., Rothbard, J. A., Bangham, C. R., Rizza, C. R., and McMichael, A. J. (1991). Human immunodeficiency virus genetic variation that can escape cytotoxic T cell recognition. *Nature* 354, 453–459.

Pornillos, O., Ganser-Pornillos, B. K., Kelly, B. N., Hua, Y., Whitby, F. G., Stout, C. D., Sundquist, W. I., Hill, C. P., and Yeager, M. (2009). X-Ray Structures of the hexameric building block of the HIV capsid. *Cell* 137, 1282–1292.

Price, D. A., Goulder, P. J., Klenerman, P., Sewell, A. K., Easterbrook, P. J., Troop, M., Bangham, C. R., and Phillips, R. E. (1997). Positive selection of HIV-1 cytotoxic T lymphocyte escape variants during primary infection. *Proc. Natl. Acad. Sci. U.S.A.* 94, 1890–1895.

Schmitz, J. E., Kuroda, M. J., Santra, S., Sasseville, V. G., Simon, M. A., Lifton, M. A., Racz, P., Tenner-Racz, K., Dalesandro, M., Scallon, B. J., Ghrayeb, J., Forman, M. A., Montefiori, D. C., Rieber, E. P., Letvin, N. L., and Reimann, K. A. (1999). Control of viremia in simian immunodeficiency virus infection by CD8+ lymphocytes. *Science* 283, 857–860.

Schneidewind, A., Brockman, M. A., Yang, R., Adam, R. I., Li, B., Le Gall, S., Rinaldo, C. R., Craggs, S. L., Allgaier, R. L., Power, K. A., Kuntzen, T., Tung, C. S., LaBute, M. X., Mueller, S. M., Harrer, T., McMichael, A. J., Goulder, P. J., Aiken, C., Brander, C., Kelleher, A. D., and Allen, T. M. (2007). Escape from the dominant HLA-B27-restricted cytotoxic T-lymphocyte response in Gag is associated with a dramatic reduction in human immunodeficiency virus type 1 replication. *J. Virol.* 81, 12382–12393.

Seki, S., Kawada, M., Takeda, A., Igarashi, H., Sata, T., and Matano, T. (2008). Transmission of simian immunodeficiency virus carrying multiple cytotoxic T-lymphocyte escape mutations with diminished replicative ability can result in AIDS progression in rhesus macaques. *J. Virol.* 82, 5093–5098.

Conflict of Interest Statement: The authors declare that the research was conducted in the absence of any commercial or financial relationships that could be construed as a potential conflict of interest.

Received: 15 November 2011; accepted: 16 December 2011; published online: 04 January 2012.

Citation: Seki S and Matano T (2012) CTL escape and viral fitness in HIV/SIV infection. Front. Microbio. ***2****:267. doi: 10.3389/fmicb.2011.00267*

This article was submitted to Frontiers in Virology, a specialty of Frontiers in Microbiology.

frontiers in
MICROBIOLOGY

REVIEW ARTICLE
published: 29 December 2011
doi: 10.3389/fmicb.2011.00264

Structural dynamics of retroviral genome and the packaging

Yasuyuki Miyazaki*, Ariko Miyake, Masako Nomaguchi and Akio Adachi

Department of Microbiology, Institute of Health Biosciences, The University of Tokushima Graduate School, Tokushima, Japan

Edited by:
Mikako Fujita, Kumamoto University, Japan

Reviewed by:
Mikako Fujita, Kumamoto University, Japan
Jun-ichi Sakuragi, Osaka University, Japan

****Correspondence:***
Yasuyuki Miyazaki, Department of Microbiology, Institute of Health Biosciences, The University of Tokushima Graduate School, 3-18-15 Kuramoto, Tokushima 770-8503, Japan.
e-mail: ymiyazaki@basic.med.tokushima-u.ac.jp

Retroviruses can cause diseases such as AIDS, leukemia, and tumors, but are also used as vectors for human gene therapy. All retroviruses, except foamy viruses, package two copies of unspliced genomic RNA into their progeny viruses. Understanding the molecular mechanisms of retroviral genome packaging will aid the design of new anti-retroviral drugs targeting the packaging process and improve the efficacy of retroviral vectors. Retroviral genomes have to be specifically recognized by the cognate nucleocapsid domain of the Gag polyprotein from among an excess of cellular and spliced viral mRNA. Extensive virological and structural studies have revealed how retroviral genomic RNA is selectively packaged into the viral particles. The genomic area responsible for the packaging is generally located in the 5′ untranslated region (5′ UTR), and contains dimerization site(s). Recent studies have shown that retroviral genome packaging is modulated by structural changes of RNA at the 5′ UTR accompanied by the dimerization. In this review, we focus on three representative retroviruses, Moloney murine leukemia virus, human immunodeficiency virus type 1 and 2, and describe the molecular mechanism of retroviral genome packaging.

Keywords: retrovirus, genome, RNA, NC, structure, dimerization, packaging

INTRODUCTION

Retroviruses belong to a diverse family of RNA viruses causing various diseases, such as leukemia, tumors, demyelinization disease, and AIDS. One unique feature of retroviruses is their integration of reverse transcribed genome into the host chromosome as a provirus. Some retroviruses have been engineered to function as vectors for the delivery of corrective human genes, and vectors derived from the Moloney murine leukemia virus (MoMLV) have been used for the treatment of severe combined immunodeficiency (Nelson et al., 2003). An understanding of the molecular mechanism of retroviral replication is needed for the development of anti-retroviral therapies as well as retroviral vectors.

All retroviruses, except foamy viruses, package two copies of full-length genomic RNA into progeny viruses, the genomic RNA having to be specifically selected from among a large amount of spliced viral and cellular RNA (**Figure 1**; Berkowitz et al., 1996). Virological and genetic studies have shown that the specific packaging of retroviral genomic RNA is mediated via interaction with the nucleocapsid (NC) domain of the Gag polyprotein (Rein, 1994; Berkowitz et al., 1996; Jewell and Mansky, 2000; Greatorex, 2004; Paillart et al., 2004b; Russell et al., 2004). Retroviral NC domains are generally highly basic and contain one or two zinc knuckle motifs composed of C–C–H–C arrays (Henderson et al., 1981; Summers et al., 1990; Kodera et al., 1998; D'Souza and Summers, 2004; Matsui et al., 2007). The zinc knuckles form a metal-coordinating "reverse turn" stabilized by NH–S hydrogen bonds. Most retroviral zinc knuckles contain a hydrophobic cleft on the surface of the mini globular domain, recognizing specific structures of RNA or DNA. The basic N- and C-terminal tails of NC domains are conformationally labile (Summers et al., 1992).

Retroviral genomes are known to be non-covalently dimerized in progeny virions (Rizvi and Panganiban, 1993). The region responsible for retroviral genome packaging is generally located between the splice donor (SD) site and the *gag* start codon in the 5′ leader region (Watanabe and Temin, 1982; Mann and Baltimore, 1985; Lever et al., 1989; Mansky et al., 1995; Kaye and Lever, 1999; Browning et al., 2003; Mustafa et al., 2004). Interestingly, the packaging signal generally overlaps with the site of dimerization (Paillart et al., 1996, 2004a; Greatorex, 2004; Hibbert et al., 2004), implying that the packaging event is coupled with genome dimerization (Russell et al., 2004). Inhibition of genome dimerization by deletion or insertion mutations at dimer initiation sites (DIS) causes a drastic reduction in genome packaging (Berkhout, 1996; Paillart et al., 1996; Laughrea et al., 1997; McBride and Panganiban, 1997). Moreover, studies with mutant viruses containing two 5′ untranslated region (UTR) packaged monomeric genome, indicate that genome packaging is achieved by the interaction of two 5′ UTRs (Sakuragi et al., 2001, 2002). Experiments with MoMLV have indicated that the conformational change induced by genome dimerization causes the exposure of NC-binding sites (D'Souza and Summers, 2004). A recent study also indicated that human immunodeficiency virus type 1 (HIV-1) employs a similar strategy for genome packaging (Lu et al., 2011a). In addition, several structures have been determined among complexes of NC and RNA fragments functioning in genome packaging, which provide the molecular mechanism for retroviral genome recognition of NC at the atomic level. In this review, we describe the molecular mechanisms of retroviral genome packaging.

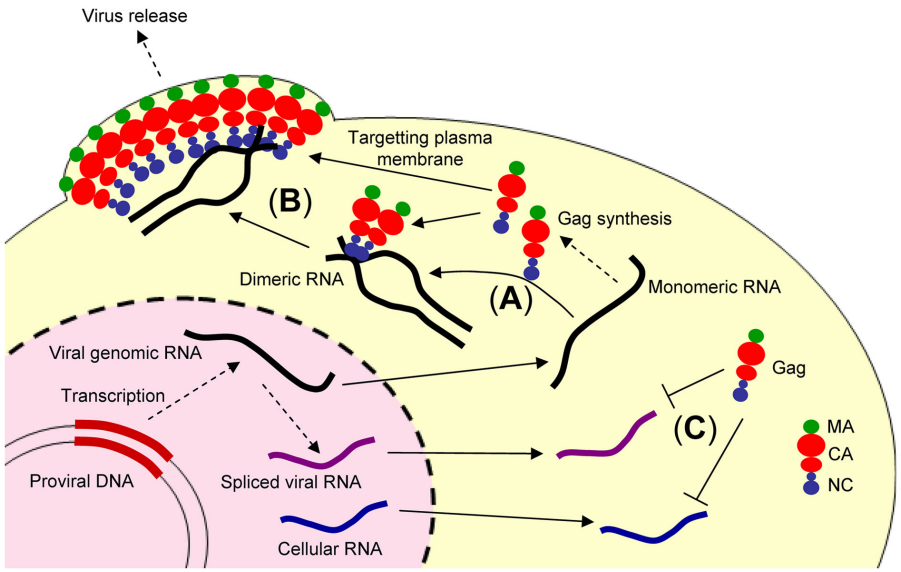

FIGURE 1 | Illustration showing retroviral genome packaging events. The retroviral genomic RNA is exported from the nucleus to cytoplasm and used as the mRNA for ribosomal synthesis of the Gag and Gag–Pol polyproteins. **(A)** The retroviral genomic RNA promotes conversion of the dimeric form of genomic RNA via the NC domain of Gag. **(B)** The Gag and retroviral genomic RNA complex is transported to the plasma membrane, where further assembly and budding occur, mediated by the myristoylated MA domain of Gag. **(C)** In contrast, spliced viral RNA or cellular RNA is not bound to the NC domain of Gag or may be bound to a small number of Gag polyproteins insufficient for trafficking to the plasma membrane.

MOLONEY MURINE LEUKEMIA VIRUS

Moloney murine leukemia virus is a simple prototypical retrovirus, with a single splicing event producing a spliced RNA for synthesizing Env during its life cycle. MoMLV is one of the most extensively studied retroviruses. Nucleotides 215–565 of the 5′ UTR have been identified as a responsible site for genome packaging (Ψ-site; Mann et al., 1983). The secondary structure of the 5′ UTR was determined by RNase protection assays using cross-linking reagents combined with computational analyses such as phylogenetic and free-energy calculations (Tounekti et al., 1992; Mougel et al., 1993). The monomeric Ψ-site is composed of a series of RNA stem-loops. Differences in RNase protection patterns were observed for the dimeric Ψ-site (Tounekti et al., 1992; Mougel et al., 1993; D'Souza and Summers, 2005). It was reported that a dimerized RNA fragment containing the entire Ψ-site was bound to a significant number of NCs (Miyazaki et al., 2010a). Meanwhile, a mutant RNA fragment that inhibited dimerization was bound to a few NCs. Thus, dimerization-dependent genome packaging is strongly indicated in MoMLV.

The minimum region sufficient for genome packaging is referred to as the core encapsidation signal (Ψ^{CES}), though a virus containing only Ψ^{CES} exhibits less efficient packaging than a virus containing the entire Ψ-site (Bender et al., 1987; Adam and Miller, 1988; Murphy and Goff, 1989; Mougel and Barklis, 1997; Yu et al., 2000). Ψ^{CES} consists of three RNA stem-loops (DIS-2, SL-C, and SL-D, see **Figures 2A,B**). DIS-2 harbors a palindromic sequence and is able to convert heterologous extended dimers. The structure of NC in a complex with a mutant RNA of Ψ^{CES} mimicking the dimer-like conformation was determined by nuclear magnetic resonance (NMR) spectroscopy (**Figures 2C,D**; D'Souza and Summers, 2004). UAUCUG residues sequestered by base-pairing in the monomeric conformation are exposed as a linker by dimerization. NC recognizes the UCUG sequence. NC is a highly basic protein, consisting of a zinc knuckle motif and labile tails in both the N- and C-terminus. Biophysical study indicated that NC specifically recognizes RNA fragments including a Py (C or U) – Py-Py-G sequence (Dey et al., 2005). The interface of NC–UCUG is complementary in both shape and charge (D'Souza and Summers, 2004; Dey et al., 2005). The guanosine base attaches to the deep hydrophobic pocket of the zinc knuckle via hydrophobic and hydrogen bonds. The three upstream nucleotides make contact with hydrophobic residues on the surface of the zinc knuckle.

SL-C and SL-D, which are part of Ψ^{CES}, promote genome packaging (Mougel et al., 1996; Mougel and Barklis, 1997; Fisher and Goff, 1998). Both are highly conserved among gammaretroviruses and contain GACG loops (Konings et al., 1992; Kim and Tinoco, 2000; D'Souza et al., 2001). A stem loop RNA fragment containing the GACG tetra-loop has a unique property (Kim and Tinoco, 2000). The C and G (3′) residues of the loop undergo intermolecular base-pairing (kissing interactions). This property of the stem loop containing GACG has led to speculation that SL-C and SL-D function in genome dimerization (Kim and Tinoco, 2000; D'Souza et al., 2001; Hibbert et al., 2004). Interestingly, the RNA fragment of SL-C forms two alternative conformations (one containing the GACG tetra-loop and the other, a CGAGU loop; Miyazaki et al., 2010b). NMR data showed that SL–CD was in a state of equilibrium between kissing and non-kissing interactions even at a high sample concentration and physiological ion-strength. The two alternative conformations of SL-C may regulate genome dimerization though the biological meaning of this is not yet clear.

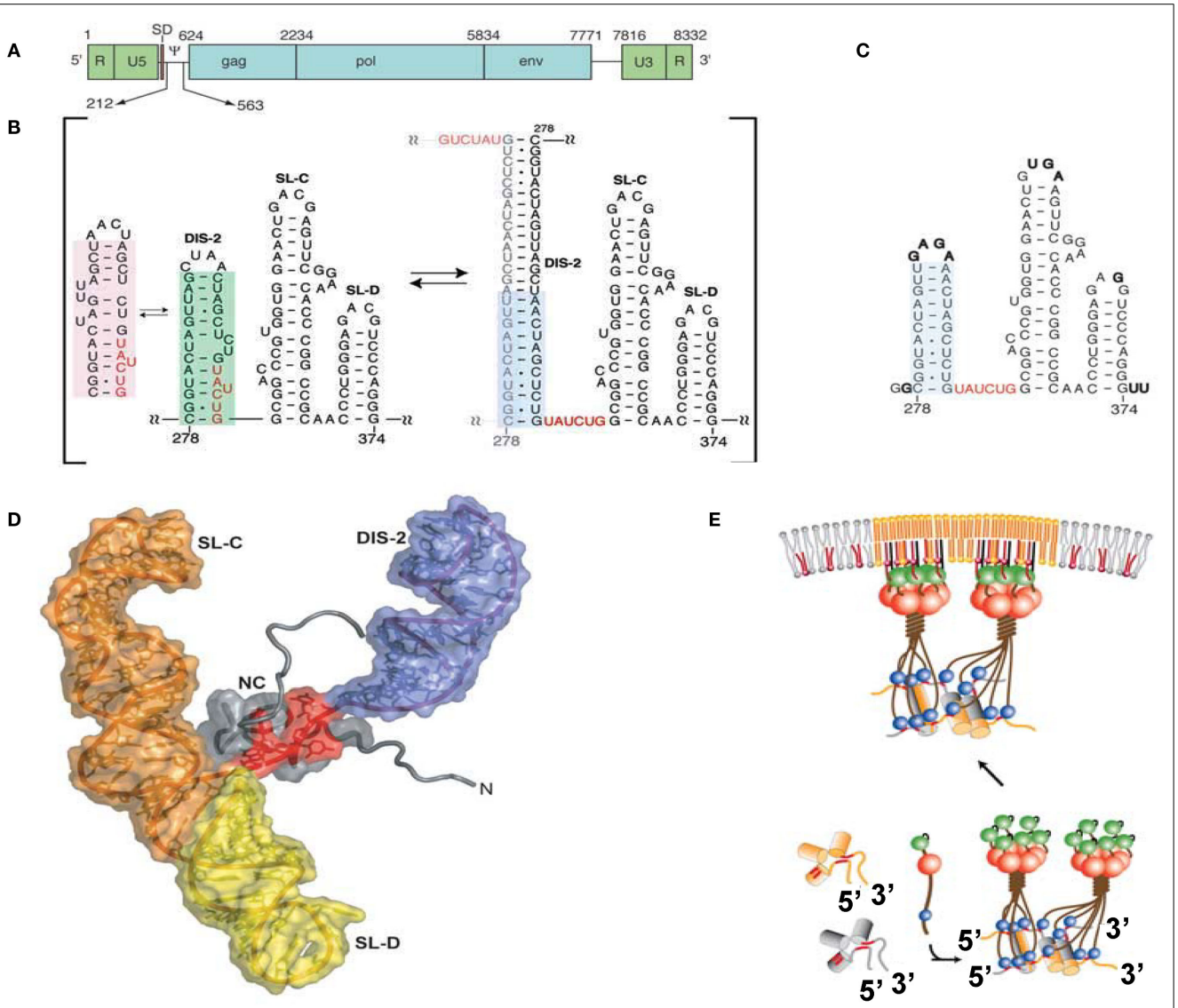

FIGURE 2 | (A) Genomic organization of MoMLV. **(B)** Secondary structure of the core encapsidation signal (Ψ^{CES}). Dimerization of DIS-2 induces a frame shift, exposing a UCUG element as a linker. **(C)** Secondary structure of mutant Ψ^{CES} that mimics the dimer-like conformation. **(D)** The complex of NC and mutant Ψ^{CES}. **(E)** Hypothetical mechanism for the genome packaging of MoMuLV. Upon dimerization, SL-CD exhibits a cross-kissing interaction, promoting the proximity of NC-binding sites. The SL–CD dimer functions as a scaffold that facilitates the Gag–Gag interaction. The ribonucleoprotein complex is transported to the plasma membrane. Reprinted with permission from [**(A–D)**: D'Souza and Summers, 2004; **(E)**: Miyazaki et al., 2010b].

The tertiary structure of a RNA fragment of a SL–CD mutant locking to form a single conformation containing the GACG terra-loop was determined by NMR spectroscopy and confirmed by Cryo-electron tomography (Miyazaki et al., 2010b). The structure revealed that SL–CD is dimerized by intermolecular cross-kissing (SL-C to SL-D′ and SL-D to SL-C′). These intermolecular cross-kissing interactions were also proposed based on selective 2′-Hydroxyl acylation analyzed by primer extension (SHAPE; Gherghe and Weeks, 2006; Gherghe et al., 2010). In addition, SL-C and SL-D stack end to end. Consequently, the two residues at the 5′-end of the SL–CD dimer are separated by ∼20 Å. There are two UCUG sequences just upstream of SL-C. The intermolecular kissing interactions of SL-C and SL-D induce the proximity of four of the NC-binding sites. The genomic RNA has been suggested to promote the retroviral Gag/Gag interaction (Dawson and Yu, 1998; Burniston et al., 1999; Campbell and Rein, 1999; Cimarelli et al., 2000; Sandefur et al., 2000; Khorchid et al., 2002; Huseby et al., 2005). Both the DIS DIS-1 and DIS-2 are followed by two UCUG elements. The abundance and proximity of exposed UCUG and related elements within the dimeric 5′ UTR may facilitate Gag–Gag interactions (**Figure 2E**).

Of note, a totally different monomeric structure for a portion of the Ψ-site (nucleotides 205–374) was proposed based on SHAPE (Gherghe and Weeks, 2006), where the RNA region spanning nucleotides 231–315 forms a large stem-loop structure, which contains residues corresponding to DIS-2. SL-C also differed from

the structure previously reported, where the bottom of the stem is unstructured. It is suggested that the intermolecular kissing interactions of SL-C and SL-D induce the conformational change of SL-C and promote the dimerization of DIS-2. The difference in RNA structures may be due to the difference of RNA fragments used in those studies.

HUMAN IMMUNODEFICIENCY VIRUS TYPE 1

Virological studies have indicated the HIV-1 5′ leader region including the entire 5′ UTR and a portion of the *gag* coding region to be involved in genome packaging (Lever et al., 1989; Aldovini and Young, 1990; Clavel and Orenstein, 1990; Poznansky et al., 1991; Buchschacher and Panganiban, 1992; Kim et al., 1994; Luban and Goff, 1994; Parolin et al., 1994; Berkowitz et al., 1995; McBride and Panganiban, 1996, 1997; McBride et al., 1997; Harrison et al., 1998; Helga-Maria et al., 1999; Clever et al., 2002; Russell et al., 2002; Sakuragi et al., 2003, 2007). The 5′ leader RNA consists of a series of RNA stem-loops referred to as the transacting responsive element (TAR), primer-binding site (PBS), polyadenylation signal [poly(A)], DIS, SD, and residues spanning the *gag* start codon (AUG; **Figure 3**; Hayashi et al., 1992, 1993; Baudin et al., 1993; Skripkin et al., 1994; Clever et al., 1995; McBride and Panganiban, 1996, 1997; Clever and Parslow, 1997; Harrison et al., 1998; Damgaard et al., 2004; Wilkinson et al., 2008; Watts et al., 2009). It has been suggested that an RNA fragment of the 5′ leader RNA has two alternative conformations, whose secondary structure has been determined by chemical probing assays (Berkhout and van Wamel, 2000). One conformation is referred to as the long distance interaction (LDI) structure, in which the residues of DIS are base-paired with those of poly(A) and SD. The other conformation is referred to as the branched multiple hairpin structure (BMH), in which the residues of DIS, SD, and Ψ form a stem-loop structure as indicated before (Huthoff and Berkhout, 2001). In addition, the residues of AUG form base-pairs with the residues of the unique 5′ region (U5). Of note, it has been proposed a lot of secondary structural models for the 5′ leader (Lu et al., 2011b). NC catalyzes LDI to BMH. DIS is exposed as a stem-loop in BMH, which promotes the kissing dimer conformation and following the genome packaging event. However, the BMH structure is mostly observed in HIV-1-infected cells, but the LDI structure fails to be detected (Paillart et al., 2004a). Thus, the biological significance of the BMH/LDI riboswitch model remains to be elucidated.

RNA fragments of DIS, SD, Ψ, and AUG have been studied extensively since the region from DIS to AUG was initially identified as a Ψ-site (Lever et al., 1989; Aldovini and Young, 1990; Clavel and Orenstein, 1990; Poznansky et al., 1991; Harrison and Lever, 1992; Kim et al., 1994; McBride and Panganiban, 1996, 1997; Harrison et al., 1998). The RNA fragments of SD and Ψ are bound to NC with high affinity (Clever et al., 1995; Amarasinghe et al., 2000a,b), whereas the RNA fragments of DIS and AUG are bound to NC with relatively low affinity (Darlix et al., 1990; Amarasinghe et al., 2001; Lawrence et al., 2003). The RNA fragment of Ψ is bound to NC with the highest affinity ($K_d = 100$ nM) among these four RNA fragments (Amarasinghe et al., 2000b). Deletion or destabilization of the stem of Ψ results in a significant reduction in genome packaging efficiency (Clever and Parslow, 1997; McBride and Panganiban, 1997). This indicates that the stem-loop

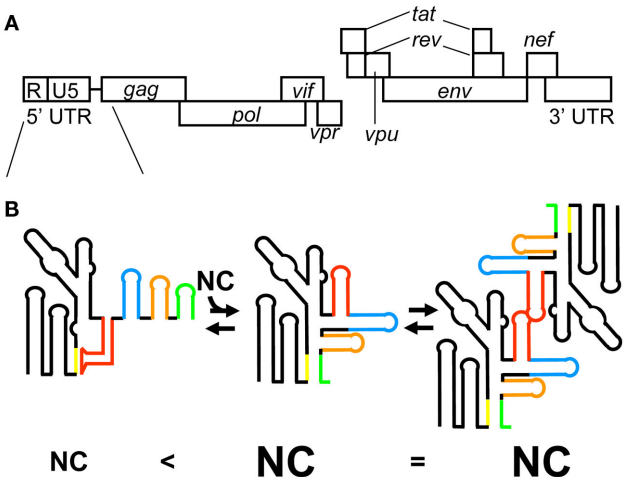

FIGURE 3 | (A) Genomic organization of HIV-1. **(B)** The latest model for HIV-1 genome packaging. Conformational change of RNA in the 5′ leader region regulates genome dimerization and genome packaging. The stem-loop structure of AUG causes sequestering of DIS via long range interaction with the residues of U5, resulting in the inhibition of HIV-1 genome dimerization (left). In this conformation of the 5′ leader RNA, a small number of NCs are capable of binding the 5′ leader RNA. In contrast, the interaction of AUG with U5 residues promotes genome dimerization via exposure of DIS (center). In this conformation of the 5′ leader RNA, a greater number of NCs are capable of binding the 5′ leader RNA. The different RNA elements in the 5′ leader region are color coded: DIS (red), SD (blue), Ψ (orange), and AUG (green).

structure of Ψ is important for genome packaging. Ψ consists of a GGAG tetra-loop and a stem. The structure of the ribonucleoprotein complex NC–Ψ has been determined by NMR spectroscopy. Guanosine residues of the GGAG tetra-loop are inserted into the hydrophobic clefts of both the N- and C-terminal zinc knuckles (De Guzman et al., 1998). The adenosine residue of the loop packs against the N-terminal zinc knuckle and an N-terminal alpha-helix domain binds to the major groove of the RNA stem. Thus, overall, NC residues are involved in binding with Ψ RNA, by which the tight binding of NC–Ψ is achieved. In addition, the intramolecular interaction of two zinc knuckles may help to stabilize the complex of NC and Ψ RNA.

The RNA fragment of SD is also bound to NC with high affinity though the binding is slightly weaker than that of Ψ (Amarasinghe et al., 2000a). SD RNA contains a GGUG tetra-loop and a stem containing a characteristic AUA triple base-pairing structure. All guanosine residues of the loop inserted into the hydrophobic clefts of zinc knuckles as observed in the complex of NC and Ψ RNA. A major structural difference between the NC and SD RNA complex and the NC and Ψ RNA complex is the orientation of the N-terminal alpha-helix domain of NC. The domain does not stick into SD RNA and is exposed outside of SD RNA. The N-terminal zinc knuckle interacts with an AUA triple base-pairing motif in the minor groove of the SD RNA stem. A mutant virus with a disrupted lower stem structure of SD exhibited a 20% reduction in genome packaging compared with the wild-type virus, despite the robust binding of Ψ RNA and NC (McBride and Panganiban,

1997). Further study will be needed to clarify the link between the tight binding of SD RNA with NC and its biological relevance.

Dimer initiation site contains a GC-rich palindromic sequence and an inner bulge (G-AGG) in the middle of the stem. This inner bulge is recognized by NC. As described above, guanosine residues not in base-pairs possibly play an important role in the binding to NC (Mihailescu and Marino, 2004). However, the binding affinity of NC–DIS is relatively weak (approximately five times weaker than that of NC–SD/ Ψ; Lawrence et al., 2003). NC catalyzes the conversion of DIS from a kissing dimer to a more stable extended duplex conformation (Darlix et al., 1990; Feng et al., 1996). Virological studies have suggested that interaction between the two 5′ UTR is required for genome packaging (Sakuragi et al., 2001, 2002). A very recent study indicated that genome dimerization is controlled by a unique strategy (**Figure 3B**). RNA containing the entire 5′ UTR and the first 21 residues of the *gag* coding region forms two alternative conformations (Lu et al., 2011a). In one conformation, DIS is sequestered via a long range interaction with U5, which inhibits genome dimerization. In the other conformation, DIS is exposed by release from the interaction with U5, which promotes genome dimerization.

AUG was believed to form a stem-loop structure, consisting of a GAGA tetra-loop and an unstable short stem containing two wobble G–U base-pairs (Amarasinghe et al., 2001). The GAGA tetra-loop is a type of GNRA (N is A, C, G, or U; R is A or G) tetra-loop, which is frequently observed in ribosomal RNA. GNRA tetra-loop helps fold stem-loops, and one Watson–Crick base-pair is enough to close off the RNA fragment. However, it has been suggested that AUG does not form a stem-loop structure and a portion of the residues of AUG may have a long range interaction with the residues of U5 as indicated in the BMH structure (Abbink and Berkhout, 2003; Damgaard et al., 2004; Spriggs et al., 2008; Wilkinson et al., 2008; Watts et al., 2009). Studies using deletion mutants indicate that the entire 5′ UTR and *gag* coding regions are important for genome packaging (Buchschacher and Panganiban, 1992; Luban and Goff, 1994; Parolin et al., 1994; Clever et al., 2002; Russell et al., 2002). Evidence of the importance of long range interactions for genome packaging was reported recently (**Figure 3B**; Lu et al., 2011a). It shows that AUG regulates genome dimerization. AUG forms two alternative conformations. One is a stem-loop conformation as initially suggested. The other is a complex with the residues of U5. The interaction of AUG with U5 leads to the exposure of DIS, promoting genome dimerization. Of note, when the residues of AUG form a stem-loop structure, in which the dimerization of the 5′ leader RNA is inhibited, a small number of NCs can bind the 5′ leader RNA (**Figure 3B**). On the other hand, when the residues of AUG interact with the residues of U5, a greater number of NCs can bind the 5′ leader RNA. Thus, AUG has a critical role in genome dimerization and genome packaging. In addition, it is suggested that the residues ranging from the end of Ψ to the start of AUG form base-pairing with the residues of the 3′ terminus of PBS. That is also proposed by earlier work Lu et al. (2011b). In fact, Sakuragi et al. (2003, 2007) indicate these residues are indispensable both for genome dimerization and genome packaging *in vivo*.

It is suggested that the HIV-1 genome's dimerization and packaging are controlled by dynamic changes of the 5′ leader's conformation as indicated in MoMLV (D'Souza and Summers, 2004; Miyazaki et al., 2010a; Lu et al., 2011a). Ψ is indicated to be important for genome packaging, however, it is not clear how Ψ works in the model suggested by Lu et al. (2011a). This will be the next question to answer for a better understanding of the molecular mechanism of HIV-1 genome packaging.

HUMAN IMMUNODEFICIENCY VIRUS TYPE 2

Human immunodeficiency virus type 2 (HIV-2) is one of two human lentiviruses that can cause AIDS. HIV-1 and HIV-2 exhibit approximately 55% nucleotide sequence identity. However, they differ significantly in their 5′ UTR. For example, the 5′ UTR of HIV-2 (HIV-2_{ROD}) consists of 535 nucleotides, whereas that of HIV-1 (HIV-1_{NL432}) consists of 335 nucleotides. The 5′ leader RNA of HIV-2 contains three unique RNA elements referred to as Ψ-1, Ψ-2, and Ψ-3 in addition to a series of RNA stem-loops, TAR, poly(A), PBS, DIS, SD, and AUG, those are commonly observed in the 5′ leader of HIV-1 (**Figure 4**; Berkhout, 1996). The structure of HIV-2 NC also exhibits some different features. A major difference in NC between HIV-2 and HIV-1 is the structure of the N-terminal flanking domain (Berkhout, 1996; Jewell and Mansky, 2000; Matsui et al., 2009). The N-terminal domain of HIV-1 NC forms an alpha-helix, whereas that of HIV-2 NC is too short to do so. Another difference is the intra-molecular interaction of two zinc knuckles of HIV-2 NC, by which HIV-2 NC forms a more globular structure than HIV-1 NC. These structural differences of NCs between HIV-1 and HIV-2 may affect RNA recognition.

It has been suggested that Ψ-3 can be bound to NC (Tsukahara et al., 1996; Damgaard et al., 1998). A study using RNase protection assays suggested that the NC–Ψ-3 ribonucleoprotein exhibited strong protection at the loop of Ψ-3. This was supported by NMR experiments. The guanosine residue of the UUAGAC loop is inserted into the hydrophobic cleft of the C-terminal zinc knuckle (Matsui et al., 2009). The N-terminal zinc knuckle does not bind the RNA fragment of Ψ-3. However, virological study has suggested that Ψ-3 is not essential for either genome dimerization or genome packaging (McCann and Lever, 1997). In agreement with that, a recent study showed that NC binds the RNA fragment of Ψ-3 with 100 times lower affinity than HIV-1 NC binds the RNA fragment of HIV-1 Ψ (Purzycka et al., 2011).

The RNA fragment of DIS is bound to NC with high affinity ($K_d = 100$ nM), equivalent to the affinity of HIV-1 Ψ RNA and the cognate NC (Purzycka et al., 2011). HIV-2 NC recognizes the inner bulge of DIS, and does not bind to the loop. HIV-1 DIS is weakly bound to the cognate NC (Lawrence et al., 2003; Andersen et al., 2004). Interestingly, HIV-2 TAR and poly(A) is bound to the NCs with relatively high affinity (TAR–NC Kd = 450 nM, poly(A) – NC Kd = 550 nM). All the tight NC-binding sites [DIS, TAR, and poly(A)] are located upstream of SD. The regions responsible for the genome packaging of retroviruses are generally located downstream of SD, by which the genomic RNA is selectively packaged from an excess amount of spliced viral RNA. It is suggested that HIV-2 genome packaging is primarily mediated by *cis* packaging mechanism (Kaye and Lever, 1999; Griffin et al., 2001; L'Hernault et al., 2007). The Gag packages genomic RNA from which it is translated. Therefore, the HIV-2 Gag is not required to distinguish the genomic RNA from viral spliced RNAs. Recent

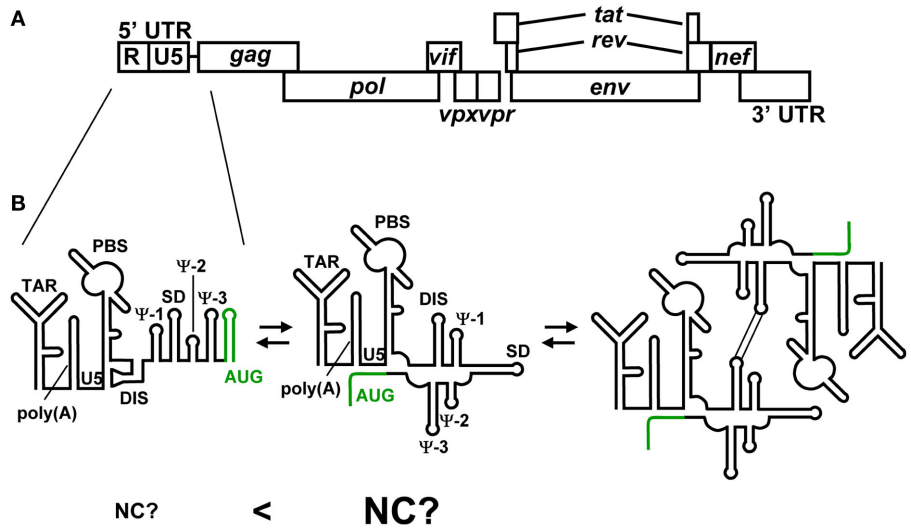

FIGURE 4 | (A) Genomic organization of HIV-2. **(B)** Representative secondary structures predicted for the 5′ UTR of HIV-2. Variations among recent predictions for AUG (green) are shown. The residues of AUG have been suggested to form a stem-loop structure and show long range interaction with the residues of U5. It has been suggested that HIV-2 genome's dimerization is employed the same mechanism as HIV-1. However, it remains to be clear whether NC preferentially binds the 5′ leader RNA containing the U5–AUG interaction.

studies, however, indicated that HIV-2 genome packaging is primarily mediated by *trans* packaging mechanism (Ni et al., 2011). TAR contains a palindromic sequence and has been suggested to form a dimer (Berkhout et al., 1993; Andersen et al., 2004). The dimerization of TAR may also function for efficient genome packaging. Further study will be needed to determine how the RNA elements located upstream of SD are involved in genome packaging.

Despite significant differences in the recognition of NC by the 5′ leader RNA, HIV-1, and HIV-2 may employ similar mechanisms for genome packaging. Dirac et al. (2002) observed that the RNA fragment of the 5′ leader region forms two alternative conformations as observed for the HIV-1 RNA fragments of the 5′ leader region. The long range interaction of U5–AUG is observed for the BMH conformation though it is not clear whether the LDI/BMH riboswitch mechanism is utilized for genome packaging *in vivo*. Recent study also indicated the U5–AUG interaction by SHAPE analysis (Purzycka et al., 2011). Of note, it is suggested that the U5–AUG interaction regulates the HIV-2 genome dimerization as indicated in HIV-1 (Baig et al., 2008). Lu et al. (2011a) suggest that the 5′ leader RNA containing the U5–AUG interaction of HIV-1 is preferentially bound to the cognate NC. A major question is whether the U5–AUG interaction of HIV-2 also promotes the NC-binding to the 5′ leader RNA (**Figure 4B**). Phylogenetic and computational analyses suggested that the U5–AUG long range interaction is widely conserved among retroviruses (Damgaard et al., 2004). The long range interaction of U5–AUG may be important for retroviral genome dimerization and genome packaging.

PERSPECTIVES

It has been indicated that the MoMLV NC domain of Gag binds predominantly to dimeric genomes (D'Souza and Summers, 2004; Miyazaki et al., 2010a). HIV-1 was indicated to have a similar system (Lu et al., 2011a). MoMLV showed proximal NC-binding motifs in Ψ^{CES}, implying that Gag–Gag multimerization is initiated by genomic RNA (Miyazaki et al., 2010b). A major question is whether the proximity of NC-binding motifs is observed for other retroviruses such as HIV-1 and HIV-2. In addition, is the proximity of NC-binding motifs essential for retroviral genome packaging? Further study for these questions will lead to a better understanding for the molecular mechanism underlying retroviral genome packaging.

ACKNOWLEDGMENTS

This work was supported in part by a Grant-in-Aid for Scientific Research (B) from the Japan Society for the Promotion of Science (ID no. 21390141).

REFERENCES

Abbink, T. E. M., and Berkhout, B. (2003). A novel long distance base-pairing interaction in human immunodeficiency virus type 1 RNA occludes the Gag start codon. *J. Biol. Chem.* 278, 11601–11611.

Adam, M. A., and Miller, A. D. (1988). Identification of a signal in a murine retrovirus that is sufficient for packaging of nonretroviral RNA into virions. *J. Virol.* 62, 3802–3806.

Aldovini, A., and Young, R. A. (1990). Mutations of RNA and protein sequences involved in human immunodeficiency virus type 1 packaging result in production of noninfectious virus. *J. Virol.* 64, 1920–1926.

Amarasinghe, G. K., De Guzman, R. N., Turner, R. B., Chancellor, K. J., Wu, Z. R., and Summers, M. F. (2000a). NMR structure of the HIV-1 nucleocapsid protein bound to stem-loop SL2 of the psi-RNA packaging signal. Implications for genome recognition. *J. Mol. Biol.* 301, 491–511.

Amarasinghe, G. K., De Guzman, R. N., Turner, R. B., and Summers, M. F. (2000b). NMR structure of stem-loop SL2 of the HIV-1 psi RNA packaging signal reveals a novel A-U-A base-triple platform. *J. Mol. Biol.* 299, 145–156.

Amarasinghe, G. K., Zhou, J., Miskimon, M., Chancellor, K. J., McDonald, J. A., Matthews, A. G., Miller, R. R., Rouse, M. D., and Summers, M. F. (2001). Stem-loop SL4 of the HIV-1 psi RNA packaging signal exhibits weak affinity for the nucleocapsid protein. Structural studies and implications for genome recognition. *J. Mol. Biol.* 314, 961–970.

Andersen, E. S., Contera, S. A., Knudsen, B., Damgaard, C. K., Besenbacher, F., and Kjems, J. (2004). Role of the trans-activation response element in dimerization of HIV-1 RNA. *J. Biol. Chem.* 279, 22243–22249.

Baig, T. T., Strong, C. L., Lodmell, J. S., and Lanchy, J. M. (2008). Regulation of primate lentiviral RNA dimerization by structural entrapment. *Retrovirology* 5, 65.

Baudin, F., Marquet, R., Isel, C., Darlix, J. L., Ehresmann, B., and Ehresmann, C. (1993). Functional sites in the 5′ region of human immunodeficiency virus type 1 RNA form defined structural domains. *J. Mol. Biol.* 229, 382–397.

Bender, M. A., Palmer, T. D., Gelinas, R. E., and Miller, A. D. (1987). Evidence that the packaging signal of Moloney murine leukemia virus extends into the gag region. *J. Virol.* 61, 1639–1646.

Berkhout, B. (1996). Structure and function of the human immunodeficiency virus leader RNA. *Prog. Nucleic Acid Res. Mol. Biol.* 54, 1–34.

Berkhout, B., Essink, B. B., and Schoneveld, I. (1993). In vitro dimerization of HIV-2 leader RNA in the absence of PuGGAPuA motifs. *FASEB J.* 7, 181–187.

Berkhout, B., and van Wamel, J. L. (2000). The leader of the HIV-1 RNA genome forms a compactly folded tertiary structure. *RNA* 6, 282–295.

Berkowitz, R., Fisher, J., and Goff, S. P. (1996). RNA packaging. *Curr. Top. Microbiol. Immunol.* 214, 177–218.

Berkowitz, R. D., Hammarskjöld, M. L., Helga-Maria, C., Rekosh, D., and Goff, S. P. (1995). 5′ Regions of HIV-1 RNAs are not sufficient for encapsidation: implications for the HIV-1 packaging signal. *Virology* 212, 718–723.

Browning, M. T., Mustafa, F., Schmidt, R. D., Lew, K. A., and Rizvi, T. A. (2003). Delineation of sequences important for efficient packaging of feline immunodeficiency virus RNA. *J. Gen. Virol.* 84, 621–627.

Buchschacher, G. L., and Panganiban, A. T. (1992). Human immunodeficiency virus vectors for inducible expression of foreign genes. *J. Virol.* 66, 2731–2739.

Burniston, M. T., Cimarelli, A., Colgan, J., Curtis, S. P., and Luban, J. (1999). Human immunodeficiency virus type 1 Gag polyprotein multimerization requires the nucleocapsid domain and RNA and is promoted by the capsid-dimer interface and the basic region of matrix protein. *J. Virol.* 73, 8527–8540.

Campbell, S., and Rein, A. (1999). In vitro assembly properties of human immunodeficiency virus type 1 Gag protein lacking the p6 domain. *J. Virol.* 73, 2270–2279.

Cimarelli, A., Sandin, S., Höglund, S., and Luban, J. (2000). Basic residues in human immunodeficiency virus type 1 nucleocapsid promote virion assembly via interaction with RNA. *J. Virol.* 74, 3046–3057.

Clavel, F., and Orenstein, J. M. (1990). A mutant of human immunodeficiency virus with reduced RNA packaging and abnormal particle morphology. *J. Virol.* 64, 5230–5234.

Clever, J., Sassetti, C., and Parslow, T. G. (1995). RNA secondary structure and binding sites for gag gene products in the 5′ packaging signal of human immunodeficiency virus type 1. *J. Virol.* 69, 2101–2109.

Clever, J. L., Miranda, D., and Parslow, T. G. (2002). RNA structure and packaging signals in the 5′ leader region of the human immunodeficiency virus type 1 genome. *J. Virol.* 76, 12381–12387.

Clever, J. L., and Parslow, T. G. (1997). Mutant human immunodeficiency virus type 1 genomes with defects in RNA dimerization or encapsidation. *J. Virol.* 71, 3407–3414.

Damgaard, C. K., Andersen, E. S., Knudsen, B., Gorodkin, J., and Kjems, J. (2004). RNA interactions in the 5′ region of the HIV-1 genome. *J. Mol. Biol.* 336, 369–379.

Damgaard, C. K., Dyhr-Mikkelsen, H., and Kjems, J. (1998). Mapping the RNA binding sites for human immunodeficiency virus type-1 gag and NC proteins within the complete HIV-1 and -2 untranslated leader regions. *Nucleic Acids Res.* 26, 3667–3676.

Darlix, J. L., Gabus, C., Nugeyre, M. T., Clavel, F., and Barré-Sinoussi, F. (1990). *Cis* elements and trans-acting factors involved in the RNA dimerization of the human immunodeficiency virus HIV-1. *J. Mol. Biol.* 216, 689–699.

Dawson, L., and Yu, X. F. (1998). The role of nucleocapsid of HIV-1 in virus assembly. *Virology* 251, 141–157.

De Guzman, R. N., Wu, Z. R., Stalling, C. C., Pappalardo, L., Borer, P. N., and Summers, M. F. (1998). Structure of the HIV-1 nucleocapsid protein bound to the SL3 psi-RNA recognition element. *Science* 279, 384–388.

Dey, A., York, D., Smalls-Mantey, A., and Summers, M. F. (2005). Composition and sequence-dependent binding of RNA to the nucleocapsid protein of Moloney murine leukemia virus. *Biochemistry* 44, 3735–3744.

Dirac, A. M. G., Huthoff, H., Kjems, J., and Berkhout, B. (2002). Regulated HIV-2 RNA dimerization by means of alternative RNA conformations. *Nucleic Acids Res.* 30, 2647–2655.

D'Souza, V., Melamed, J., Habib, D., Pullen, K., Wallace, K., and Summers, M. F. (2001). Identification of a high affinity nucleocapsid protein binding element within the Moloney murine leukemia virus Psi-RNA packaging signal: implications for genome recognition. *J. Mol. Biol.* 314, 217–232.

D'Souza, V., and Summers, M. F. (2004). Structural basis for packaging the dimeric genome of Moloney murine leukaemia virus. *Nature* 431, 586–590.

D'Souza, V., and Summers, M. F. (2005). How retroviruses select their genomes. *Nat. Rev. Microbiol.* 3, 643–655.

Feng, Y. X., Copeland, T. D., Henderson, L. E., Gorelick, R. J., Bosche, W. J., Levin, J. G., and Rein, A. (1996). HIV-1 nucleocapsid protein induces "maturation" of dimeric retroviral RNA in vitro. *Proc. Natl. Acad. Sci. U.S.A.* 93, 7577–7581.

Fisher, J., and Goff, S. P. (1998). Mutational analysis of stem-loops in the RNA packaging signal of the Moloney murine leukemia virus. *Virology* 244, 133–145.

Gherghe, C., Leonard, C. W., Gorelick, R. J., and Weeks, K. M. (2010). Secondary structure of the mature ex virio Moloney murine leukemia virus genomic RNA dimerization domain. *J. Virol.* 84, 898–906.

Gherghe, C., and Weeks, K. M. (2006). The SL1-SL2 (stem-loop) domain is the primary determinant for stability of the gamma retroviral genomic RNA dimer. *J. Biol. Chem.* 281, 37952–37961.

Greatorex, J. (2004). The retroviral RNA dimer linkage: different structures may reflect different roles. *Retrovirology* 1, 22.

Griffin, S. D., Allen, J. F., and Lever, A. M. (2001). The major human immunodeficiency virus type 2 (HIV-2) packaging signal is present on all HIV-2 RNA species: cotranslational RNA encapsidation and limitation of Gag protein confer specificity. *J. Virol.* 75, 12058–12069.

Harrison, G. P., and Lever, A. M. (1992). The human immunodeficiency virus type 1 packaging signal and major splice donor region have a conserved stable secondary structure. *J. Virol.* 66, 4144–4153.

Harrison, G. P., Miele, G., Hunter, E., and Lever, A. M. (1998). Functional analysis of the core human immunodeficiency virus type 1 packaging signal in a permissive cell line. *J. Virol.* 72, 5886–5896.

Hayashi, T., Shioda, T., Iwakura, Y., and Shibuta, H. (1992). RNA packaging signal of human immunodeficiency virus type 1. *Virology* 188, 590–599.

Hayashi, T., Ueno, Y., and Okamoto, T. (1993). Elucidation of a conserved RNA stem-loop structure in the packaging signal of human immunodeficiency virus type 1. *FEBS Lett.* 327, 213–218.

Helga-Maria, C., Hammarskjöld, M. L., and Rekosh, D. (1999). An intact TAR element and cytoplasmic localization are necessary for efficient packaging of human immunodeficiency virus type 1 genomic RNA. *J. Virol.* 73, 4127–4135.

Henderson, L. E., Copeland, T. D., Sowder, R. C., Smythers, G. W., and Oroszlan, S. (1981). Primary structure of the low molecular weight nucleic acid-binding proteins of murine leukemia viruses. *J. Biol. Chem.* 256, 8400–8406.

Hibbert, C. S., Mirro, J., and Rein, A. (2004). mRNA molecules containing murine leukemia virus packaging signals are encapsidated as dimers. *J. Virol.* 78, 10927–10938.

Huseby, D., Barklis, R. L., Alfadhli, A., and Barklis, E. (2005). Assembly of human immunodeficiency virus precursor gag proteins. *J. Biol. Chem.* 280, 17664–17670.

Huthoff, H., and Berkhout, B. (2001). Two alternating structures of the HIV-1 leader RNA. *RNA* 7, 143–157.

Jewell, N. A., and Mansky, L. M. (2000). In the beginning: genome recognition, RNA encapsidation and the initiation of complex retrovirus assembly. *J. Gen. Virol.* 81, 1889–1899.

Kaye, J. F., and Lever, A. M. (1999). Human immunodeficiency virus types 1 and 2 differ in the predominant mechanism used for selection of genomic RNA for encapsidation. *J. Virol.* 73, 3023–3031.

Khorchid, A., Halwani, R., Wainberg, M. A., and Kleiman, L. (2002). Role of RNA in facilitating Gag/Gag-Pol interaction. *J. Virol.* 76, 4131–4137.

Kim, C. H., and Tinoco, I. (2000). A retroviral RNA kissing complex containing only two GC base pairs. *Proc. Natl. Acad. Sci. U.S.A.* 97, 9396–9401.

Kim, H. J., Lee, K., and O'Rear, J. J. (1994). A short sequence upstream of the 5′ major splice site is important for encapsidation of HIV-1 genomic RNA. *Virology* 198, 336–340.

Kodera, Y., Sato, K., Tsukahara, T., Komatsu, H., Maeda, T., and Kohno, T. (1998). High-resolution solution NMR structure of the minimal active domain of the human immunodeficiency virus type-2 nucleocapsid protein. *Biochemistry* 37, 17704–17713.

Konings, D. A., Nash, M. A., Maizel, J. V., and Arlinghaus, R. B. (1992). Novel GACG-hairpin pair motif in the 5′ untranslated region of type C retroviruses related to murine leukemia virus. *J. Virol.* 66, 632–640.

Laughrea, M., Jetté, L., Mak, J., Kleiman, L., Liang, C., and Wainberg, M. A. (1997). Mutations in the kissing-loop hairpin of human immunodeficiency virus type 1 reduce viral infectivity as well as genomic RNA packaging and dimerization. *J. Virol.* 71, 3397–3406.

Lawrence, D. C., Stover, C. C., Noznitsky, J., Wu, Z., and Summers, M. F. (2003). Structure of the intact stem and bulge of HIV-1 Psi-RNA stem-loop SL1. *J. Mol. Biol.* 326, 529–542.

Lever, A., Gottlinger, H., Haseltine, W., and Sodroski, J. (1989). Identification of a sequence required for efficient packaging of human immunodeficiency virus type 1 RNA into virions. *J. Virol.* 63, 4085–4087.

L'Hernault, A., Greatorex, J. S., Crowther, R. A., and Lever, A. M. L. (2007). Dimerisation of HIV-2 genomic RNA is linked to efficient RNA packaging, normal particle maturation and viral infectivity. *Retrovirology* 4, 90.

Lu, K., Heng, X., Garyu, L., Monti, S., Garcia, E. L., Kharytonchyk, S., Dorjsuren, B., Kulandaivel, G., Jones, S., Hiremath, A., Divakaruni, S. S., LaCotti, C., Barton, S., Tummillo, D., Hosic, A., Edme, K., Albrecht, S., Telesnitsky, A., and Summers, M. F. (2011a). NMR detection of structures in the HIV-1 5 ′-leader RNA that regulate genome packaging. *Science* 334, 242–245.

Lu, K., Heng, X., and Summers, M. F. (2011b). Structural determinants and mechanism of HIV-1 genome packaging. *J. Mol. Biol.* 410, 609–633.

Luban, J., and Goff, S. P. (1994). Mutational analysis of *cis*-acting packaging signals in human immunodeficiency virus type 1 RNA. *J. Virol.* 68, 3784–3793.

Mann, R., and Baltimore, D. (1985). Varying the position of a retrovirus packaging sequence results in the encapsidation of both unspliced and spliced RNAs. *J. Virol.* 54, 401–407.

Mann, R., Mulligan, R. C., and Baltimore, D. (1983). Construction of a retrovirus packaging mutant and its use to produce helper-free defective retrovirus. *Cell* 33, 153–159.

Mansky, L. M., Krueger, A. E., and Temin, H. M. (1995). The bovine leukemia virus encapsidation signal is discontinuous and extends into the 5′ end of the gag gene. *J. Virol.* 69, 3282–3289.

Matsui, T., Kodera, Y., Miyauchi, E., Tanaka, H., Endoh, H., Komatsu, H., Tanaka, T., Kohno, T., and Maeda, T. (2007). Structural role of the secondary active domain of HIV-2 NCp8 in multi-functionality. *Biochem. Biophys. Res. Commun.* 358, 673–678.

Matsui, T., Tanaka, T., Endoh, H., Sato, K., Tanaka, H., Miyauchi, E., Kawashima, Y., Nagai-Makabe, M., Komatsu, H., Kohno, T., Maeda, T., and Kodera, Y. (2009). The RNA recognition mechanism of human immunodeficiency virus (HIV) type 2 NCp8 is different from that of HIV-1 NCp7. *Biochemistry* 48, 4314–4323.

McBride, M. S., and Panganiban, A. T. (1996). The human immunodeficiency virus type 1 encapsidation site is a multipartite RNA element composed of functional hairpin structures. *J. Virol.* 70, 2963–2973.

McBride, M. S., and Panganiban, A. T. (1997). Position dependence of functional hairpins important for human immunodeficiency virus type 1 RNA encapsidation in vivo. *J. Virol.* 71, 2050–2058.

McBride, M. S., Schwartz, M. D., and Panganiban, A. T. (1997). Efficient encapsidation of human immunodeficiency virus type 1 vectors and further characterization of *cis* elements required for encapsidation. *J. Virol.* 71, 4544–5454.

McCann, E. M., and Lever, A. M. (1997). Location of *cis*-acting signals important for RNA encapsidation in the leader sequence of human immunodeficiency virus type 2. *J. Virol.* 71, 4133–41337.

Mihailescu, M. -R., and Marino, J. P. (2004). A proton-coupled dynamic conformational switch in the HIV-1 dimerization initiation site kissing complex. *Proc. Natl. Acad. Sci. U.S.A.* 101, 1189–1194.

Miyazaki, Y., Garcia, E. L., King, S. R., Iyalla, K., Loeliger, K., Starck, P., Syed, S., Telesnitsky, A., and Summers, M. F. (2010a). An RNA structural switch regulates diploid genome packaging by Moloney murine leukemia virus. *J. Mol. Biol.* 396, 141–152.

Miyazaki, Y., Irobalieva, R. N., Tolbert, B. S., Smalls-Mantey, A., Iyalla, K., Loeliger, K., D'Souza, V., Khant, H., Schmid, M. F., Garcia, E. L., Telesnitsky, A., Chiu, W., and Summers, M. F. (2010b). Structure of a conserved retroviral RNA packaging element by NMR spectroscopy and cryo-electron tomography. *J. Mol. Biol.* 404, 751–772.

Mougel, M., and Barklis, E. (1997). A role for two hairpin structures as a core RNA encapsidation signal in murine leukemia virus virions. *J. Virol.* 71, 8061–8065.

Mougel, M., Tounekti, N., Darlix, J. L., Paoletti, J., Ehresmann, B., and Ehresmann, C. (1993). Conformational analysis of the 5′ leader and the gag initiation site of Mo-MuLV RNA and allosteric transitions induced by dimerization. *Nucleic Acids Res.* 21, 4677–4684.

Mougel, M., Zhang, Y., and Barklis, E. (1996). *cis*-active structural motifs involved in specific encapsidation of Moloney murine leukemia virus RNA. *J. Virol.* 70, 5043–5050.

Murphy, J. E., and Goff, S. P. (1989). Construction and analysis of deletion mutations in the U5 region of Moloney murine leukemia virus: effects on RNA packaging and reverse transcription. *J. Virol.* 63, 319–327.

Mustafa, F., Lew, K. A., Schmidt, R. D., Browning, M. T., and Rizvi, T. A. (2004). Mutational analysis of the predicted secondary RNA structure of the Mason-Pfizer monkey virus packaging signal. *Virus Res.* 99, 35–46.

Nelson, P. N., Carnegie, P. R., Martin, J., Davari Ejtehadi, H., Hooley, P., Roden, D., Rowland-Jones, S., Warren, P., Astley, J., and Murray, P. G. (2003). Demystified. Human endogenous retroviruses. *Mol. Pathol.* 56, 11–18.

Ni, N., Nikolaitchik, O. A., Dilley, K. A., Chen, J., Galli, A., Fu, W., Prasad, V. V. S. P., Ptak, R. G., Pathak, V. K., and Hu, W. S. (2011). Mechanisms of human immunodeficiency virus type 2 RNA packaging: efficient *trans* packaging and selection of RNA copackaging partners. *J. Virol.* 85, 7603–7612.

Paillart, J. C., Dettenhofer, M., Yu, X. -F., Ehresmann, C., Ehresmann, B., and Marquet, R. (2004a). First snapshots of the HIV-1 RNA structure in infected cells and in virions. *J. Biol. Chem.* 279, 48397–48403.

Paillart, J. C., Shehu-Xhilaga, M., Marquet, R., and Mak, J. (2004b). Dimerization of retroviral RNA genomes: an inseparable pair. *Nat. Rev. Microbiol.* 2, 461–472.

Paillart, J. C., Marquet, R., Skripkin, E., Ehresmann, C., and Ehresmann, B. (1996). Dimerization of retroviral genomic RNAs: structural and functional implications. *Biochimie* 78, 639–653.

Parolin, C., Dorfman, T., Palú, G., Göttlinger, H., and Sodroski, J. (1994). Analysis in human immunodeficiency virus type 1 vectors of *cis*-acting sequences that affect gene transfer into human lymphocytes. *J. Virol.* 68, 3888–3895.

Poznansky, M., Lever, A., Bergeron, L., Haseltine, W., and Sodroski, J. (1991). Gene transfer into human lymphocytes by a defective human immunodeficiency virus type 1 vector. *J. Virol.* 65, 532–536.

Purzycka, K. J., Pachulska-Wieczorek, K., and Adamiak, R. W. (2011). The in vitro loose dimer structure and rearrangements of the HIV-2 leader RNA. *Nucleic Acids Res.* 39, 7234–7248.

Rein, A. (1994). Retroviral RNA packaging: a review. *Arch. Virol.* 9, 513–522.

Rizvi, T. A., and Panganiban, A. T. (1993). Simian immunodeficiency virus RNA is efficiently encapsidated by human immunodeficiency virus type 1 particles. *J. Virol.* 67, 2681–2688.

Russell, R. S., Hu, J., Laughrea, M., Wainberg, M. A., and Liang, C. (2002). Deficient dimerization of human immunodeficiency virus type 1 RNA caused by mutations of the u5 RNA sequences. *Virology* 303, 152–163.

Russell, R. S., Liang, C., and Wainberg, M. A. (2004). Is HIV-1 RNA dimerization a prerequisite for packaging? Yes, no, probably? *Retrovirology* 1, 23.

Sakuragi, J., Iwamoto, A., and Shioda, T. (2002). Dissociation of genome dimerization from packaging functions and virion maturation of human immunodeficiency virus type 1. *J. Virol.* 76, 959–967.

Sakuragi, J., Sakuragi, S., and Shioda, T. (2007). Minimal region sufficient for genome dimerization in the human immunodeficiency virus type 1 virion and its potential roles in the early stages of viral replication. *J. Virol.* 81, 7985–7992.

Sakuragi, J., Shioda, T., and Panganiban, A. T. (2001). Duplication of the primary encapsidation and dimer linkage region of human immunodeficiency virus type 1 RNA results in the appearance of monomeric RNA in virions. *J. Virol.* 75, 2557–2565.

Sakuragi, J., Ueda, S., Iwamoto, A., and Shioda, T. (2003). Possible role of dimerization in human immunodeficiency virus type 1 genome RNA packaging. *J. Virol.* 77, 4060–4069.

Sandefur, S., Smith, R. M., Varthakavi, V., and Spearman, P. (2000). Mapping and characterization of the N-terminal I domain of human immunodeficiency virus type 1 Pr55(Gag). *J. Virol.* 74, 7238–7249.

Skripkin, E., Paillart, J. C., Marquet, R., Ehresmann, B., and Ehresmann, C. (1994). Identification of the primary site of the human immunodeficiency virus type 1 RNA dimerization in vitro. *Proc. Natl. Acad. Sci. U.S.A.* 91, 4945–4949.

Spriggs, S., Garyu, L., Connor, R., and Summers, M. F. (2008). Potential intra- and intermolecular interactions involving the unique-5′ region of the HIV-1 5′-UTR. *Biochemistry* 47, 13064–13073.

Summers, M. F., Henderson, L. E., Chance, M. R., Bess, J. W., South, T. L., Blake, P. R., Sagi, I., Perez-Alvarado, G., Sowder, R. C., and Hare, D. R. (1992). Nucleocapsid zinc fingers detected in retroviruses: EXAFS studies of intact viruses and the solution-state structure of the nucleocapsid protein from HIV-1. *Protein Sci.* 1, 563–574.

Summers, M. F., South, T. L., Kim, B., and Hare, D. R. (1990). High-resolution structure of an HIV zinc fingerlike domain via a new NMR-based distance geometry approach. *Biochemistry* 29, 329–340.

Tounekti, N., Mougel, M., Roy, C., Marquet, R., Darlix, J. L., Paoletti, J., Ehresmann, B., and Ehresmann, C. (1992). Effect of dimerization on the conformation of the encapsidation Psi domain of Moloney murine leukemia virus RNA. *J. Mol. Biol.* 223, 205–220.

Tsukahara, T., Komatsu, H., Kubo, M., Obata, F., and Tozawa, H. (1996). Binding properties of human immunodeficiency virus type-2 (HIV-2) RNA corresponding to the packaging signal to its nucleocapsid protein. *Biochem. Mol. Biol. Int.* 40, 33–42.

Watanabe, S., and Temin, H. M. (1982). Encapsidation sequences for spleen necrosis virus, an avian retrovirus, are between the 5′ long terminal repeat and the start of the gag gene. *Proc. Natl. Acad. Sci. U.S.A.* 79, 5986–5990.

Watts, J. M., Dang, K. K., Gorelick, R. J., Leonard, C. W., Bess, J. W., Swanstrom, R., Burch, C. L., and Weeks, K. M. (2009). Architecture and secondary structure of an entire HIV-1 RNA genome. *Nature* 460, 711–716.

Wilkinson, K. A., Gorelick, R. J., Vasa, S. M., Guex, N., Rein, A., Mathews, D. H., Giddings, M. C., and Weeks, K. M. (2008). High-throughput SHAPE analysis reveals structures in HIV-1 genomic RNA strongly conserved across distinct biological states. *PLoS Biol.* 6, e96. doi:10.1371/journal.pbio.0060096

Yu, S. S., Kim, J. M., and Kim, S. (2000). The 17 nucleotides downstream from the env gene stop codon are important for murine leukemia virus packaging. *J. Virol.* 74, 8775–8780.

Conflict of Interest Statement: The authors declare that the research was conducted in the absence of any commercial or financial relationships that could be construed as a potential conflict of interest.

Received: 28 November 2011; paper pending published: 08 December 2011; accepted: 11 December 2011; published online: 29 December 2011.

*Citation: Miyazaki Y, Miyake A, Nomaguchi M and Adachi A (2011) Structural dynamics of retroviral genome and the packaging. Front. Microbio. **2**:264. doi: 10.3389/fmicb.2011.00264*

This article was submitted to Frontiers in Virology, a specialty of Frontiers in Microbiology.

frontiers in
MICROBIOLOGY

MINI REVIEW ARTICLE
published: 08 February 2012
doi: 10.3389/fmicb.2012.00029

Aptamers in virology: recent advances and challenges

Jennifer M. Binning[1,2], Daisy W. Leung[1] and Gaya K. Amarasinghe[1]*

[1] *Department of Pathology and Immunology, Washington University School of Medicine, St. Louis, MO, USA*
[2] *Biochemistry Graduate Program, Department of Biochemistry, Biophysics and Molecular Biology, Iowa State University, Ames, IA, USA*

Edited by:
Akio Adachi, University of Tokushima Graduate School, Japan

Reviewed by:
Mikako Fujita, Kumamoto University, Japan
Yasuyuki Miyazaki, University of Tokushima Graduate School, Japan

***Correspondence:**
Gaya K. Amarasinghe, Department of Pathology and Immunology, Washington University School of Medicine, Campus Box 8118, 660 South Euclid Avenue, St. Louis, MO 63110, USA.
e-mail: gamarasinghe@path.wustl.edu

Aptamers generated from randomized libraries of nucleic acids have found utility in a wide variety of fields and in the clinic. Aptamers can be used to target both intracellular and extracellular components, including small molecules, proteins, cells, and viruses. With recent technological developments in stringent selection and rapid isolation strategies, it is likely that aptamers will continue to make an impact as useful tools and reagents. Although many recently developed aptamers are intended for use as therapeutic and diagnostic agents, use of aptamers for basic research, including target validation, remains an active area with high potential to impact our understanding of molecular mechanisms and for drug discovery. In this brief review, we will discuss recent aptamer discoveries, their potential role in structural virology, as well as challenges and future prospects.

Keywords: aptamer, therapeutic and diagnostic agents, structural virology, research tools

INTRODUCTION

Aptamers are *in vitro* selected nucleic acid molecules that bind to a broad range of targets with high affinity and specificity. The basic isolation process, termed "systematic evolution of ligands by exponential enrichment" or SELEX (Ellington and Szostak, 1990; Robertson and Joyce, 1990; Tuerk and Gold, 1990), utilizes a large initial pool of randomized nucleic acids from which high affinity binders are isolated and enriched through subsequent rounds of selection (**Figure 1**). Different *in vitro* isolation strategies can be used to generate aptamers against many diverse targets under different selection and counter selection conditions, leading to facile identification of aptamers that bind targets ranging from a few atoms (small molecules) to many atoms (macromolecules) to intact cells and viruses. Most aptamers characterized to date are single stranded DNA or RNA molecules ranging from 20 to 90 bases, although longer aptamers have been generated. These single stranded polynucleotide sequences can fold into a variety of secondary structural elements, including double stranded RNA (dsRNA) or dsDNA, stem loops, pseudoknots, kinks, and bulges, providing multiple recognition surfaces for target binding.

Aptamers are often compared to antibodies, due to the high specificity for their targets generated through stringent *in vitro* selection. However, aptamers have notable advantages over antibodies, including low immunogenicity and the potential for chemical derivatization to enhance *in vivo* stability and bioavailability (Jellinek et al., 1995; Chelliserrykattil and Ellington, 2004; Kato et al., 2005). The aptamer selection process can be carried out in as little as 2–4 weeks, which is significantly shorter compared to antibody development (months). Since the initial description of the SELEX process over two decades ago, general principles guiding the selection process have remained largely unaltered. However, modifications to the original process now allow for highly efficient and extremely stringent selection strategies to be employed against a diverse array of targets. Identified aptamers can be further optimized using biased libraries that result in aptamer subpopulations with higher specificity and/or affinity and other desirable characteristics, such as membrane permeability. Coupling SELEX methods with other techniques, such as capillary electrophoresis and surface plasmon resonance (SPR), can reduce the number of selection rounds and shorten the period for aptamer discovery against a given target. In addition, facile generation of modified aptamers allows for coupling of diagnostic tags, which can extend the use of aptamers through prolonged lifetimes in serum. Given the traditional comparisons with antibodies, the utility of aptamers in the clinic is taking longer than anticipated from the outset of discovery. Nonetheless, with the 2004 FDA approval of pegaptanib, an aptamer-based drug used to treat wet age-related muscular degeneration, and others in the pipeline, it is clear that aptamers will continue to contribute to our understanding of normal and aberrant cellular processes as well as disease treatment. Recent comprehensive reviews highlight advances in basic research (James, 2001, 2007; Syed and Pervaiz, 2010; Sun et al., 2011) and clinical settings (Bunka and Stockley, 2006; Gopinath, 2007, 2008; Meyer et al., 2011). These developments have positioned aptamers to make a significant impact in many areas.

APTAMERS AND VIRUSES

The host–viral interface has become an increasingly popular target for aptamers because interactions between nucleic acids and proteins are critical to viral replication (**Figure 2**). Although not a prerequisite, targeting nucleic acid binding proteins by aptamers has a high probability of success due to the presence of basic surface charges on most nucleic acid binding proteins. Below we summarize select studies in order to highlight the use of aptamers against viral components and discuss challenges and future prospects of the field.

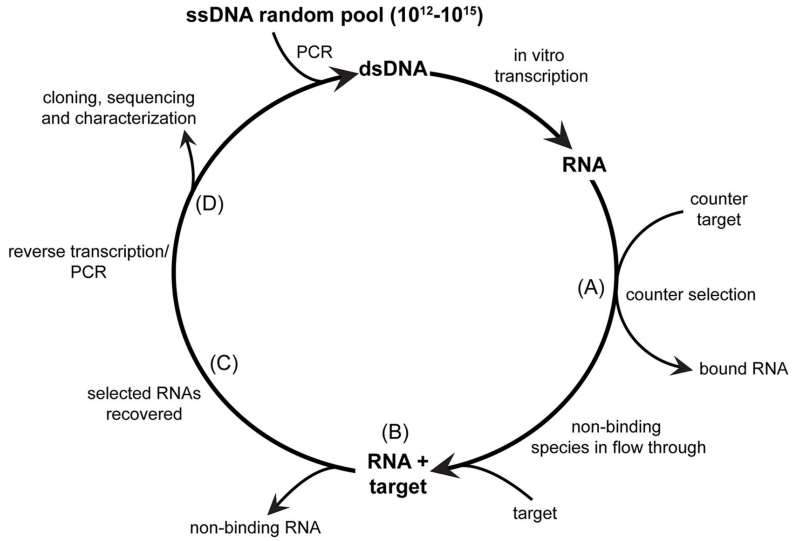

FIGURE 1 | The SELEX process. An initial pool of dsDNA is *in vitro* transcribed. The resulting pool of RNA is subjected to (A) counter selection and/or (B) selection by filter binding. (C) Selected RNA is recovered, reverse transcribed, and amplified by PCR. (D) The resulting RNA pool is subjected to another round of SELEX for enrichment or cloned and sequenced.

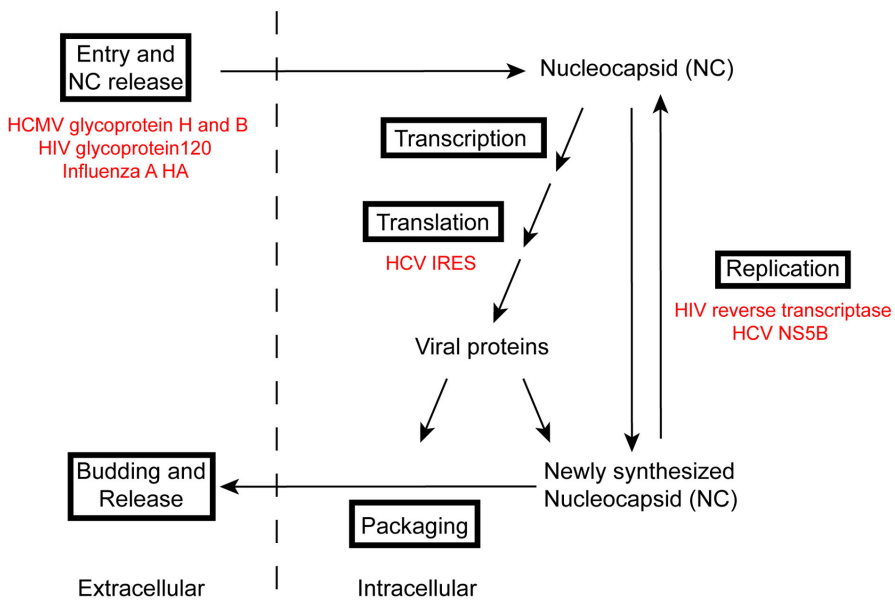

FIGURE 2 | Key steps in the viral replication cycle are targets for aptamer development. Examples of viral proteins targeted by aptamers are identified in red.

APTAMERS IN THERAPEUTICS

Aptamers provide an alternative method for the development of therapeutic agents to counter viral infections. Aptamers can be used to inhibit viral infectivity at any stage in the viral replication cycle, including viral entry, which has the potential to prevent initial infection. The development of aptamers against the human immunodeficiency virus HIV-1 has been of interest for drug discovery. In order to target HIV entry into helper T-cells, aptamers generated against HIV glycoprotein 120 (gp120) competes with the HIV co-receptor, CCR5. The aptamer binding site is located in a highly conserved region of gp120, allowing neutralization of a broad range of HIV isolates by disrupting the gp120–CCR5 interaction (Dey et al., 2005a,b). Binding to a conserved region of gp120 is critical due to the propensity of HIV to undergo mutagenesis that results in drug-resistance. The anti-gp120 aptamer has not been approved for clinical trials, but has

been used as a basis for developing chimeric aptamers (Neff et al., 2011; Wheeler et al., 2011; Zhou et al., 2011). Coupling of siRNA and the anti-gp120 aptamer through phi29 packaging RNA combines two functions (Zhou et al., 2011). The anti-gp120 aptamer has an inhibitory effect, while siRNA downregulates the expression of its target.

Aptamer generation against human cytomegalovirus (HCMV) particles was carried out without prior information on specific targets (Wang et al., 2000). Two aptamers, L13 and L19, were isolated that inhibit HCMV plaque formation and growth. The antiviral activity of L13 and L19 aptamers identified HCMV glycoproteins B and H as targets, respectively, by binding to the glycoproteins and blocking viral entry.

Viral RNA-dependent RNA polymerases have been a common target because viral polymerases use RNA as the template during genome replication. For example, the hepatitis C virus (HCV) polymerase non-structural protein 5B (NS5B), is required for transcribing the HCV genome and has been used to generate both anti-NS5B RNA and DNA aptamers (Biroccio et al., 2002; Bellecave et al., 2003, 2008). Both sets of aptamers have been shown to bind to NS5B with high affinity and inhibit polymerase activity. The mechanism of inhibition of the anti-NS5B RNA aptamer is non-competitive with regards to the template RNA, and mutagenesis studies revealed that a basic patch within the thumb domain of NS5B is the aptamer binding site (Biroccio et al., 2002). Only one anti-NS5B DNA aptamer inhibits replication by competing with the RNA template; the other inhibits through a non-competitive mechanism in which initiation and post initiation events are disrupted. RNA aptamers capable of inhibiting NS5B polymerase activity were further optimized through the use of deletion clones and point mutagenesis, which identified a GC-rich motif and a stem-loop with a bulge as important features for aptamer binding to NS5B (Kanamori et al., 2009).

In the context of HIV pathogenesis, viral reverse transcriptase (RT) converts the single stranded RNA (ssRNA) viral genome into dsDNA. RNA aptamers that target HIV-RT effectively inhibit the synthesis of cDNA (Tuerk et al., 1992). The ligand 1.1 aptamer targeting HIV-RT is postulated to reduce adverse side effects, a main concern with current HIV-RT drugs, such as 3′-azido-3′-deoxythymidine (AZT) and dideoxyinosine. Moreover, by targeting an enzyme early in the HIV-1 replication cycle, the likelihood that mutations will arise resulting in drug-resistance should diminish. These factors make aptamers generated against HIV-RT promising candidates for drug development.

Inhibition of protein translation is a key host defense mechanism against viral infections since viruses are completely dependent on the host machinery for protein synthesis. However, viruses have developed various means to evade host defenses and hijack the host translational machinery. For example, the HCV mRNA has an internal ribosome entry site (IRES), a structured region within the mRNA that binds the ribosome and initiates cap-independent translation, allowing HCV to circumvent the requirement for host initiation and elongation factors. Aptamers targeting the HCV IRES inhibit IRES-dependent translation of HCV proteins (Aldaz-Carroll et al., 2002; Kikuchi et al., 2003, 2005; Da Rocha Gomes et al., 2004). Furthermore, many of these HCV IRES aptamers inhibit translation both *in vitro* and *in vivo*, highlighting the potential therapeutic value of these aptamers since they target RNA secondary structure that is characteristic of select viral mRNAs but not host mRNA. Therefore, such selection may result in a reduction of negative side effects. The viral inhibitory properties of HCV anti-IRES aptamers can be enhanced through conjugation to other aptamers, which target different binding sites within the HCV IRES. This results in a conjugated anti-IRES aptamer that binds the HCV IRES with a higher affinity and is functionally more effective than the unconjugated aptamers (Kikuchi et al., 2009). Alternatively, HCV anti-IRES aptamers can be coupled to the hammerhead ribozyme to prevent translation. The chimeric RNA molecule, HH363-50, inhibits IRES-dependent translation *in vitro* likely through disruption of 80S complex formation with no effect on IRES-independent translation. HH363-50 also reduced the level of HCV RNA due to the ribozyme activity of the molecule (Romero-Lopez et al., 2009).

APTAMERS IN VIRAL DIAGNOSTICS

Early and reliable detection of pathogens is a critical step in the successful treatment of infection. Due to many potential advantages aptamers provide, aptamers are also ideal tools for diagnostics. Many examples of aptamers as a detection tool have been described. These studies include simple modifications to the enzyme linked immunosorbent assay (ELISA) as well as more complex diagnostic systems, such as those that use inhibitory aptamers to suppress multi turnover enzymes (Zhou et al., 2010).

The Influenza A virus hemagglutinin (HA) and neuraminidase (NA) antigens are glycoproteins found on the surface of the viral particle, and serve important roles in host membrane fusion. A number of aptamers have been isolated against Influenza A HA that inhibit viral infectivity (Jeon et al., 2004; Misono and Kumar, 2005; Gopinath et al., 2006; Dhar and Datta, 2009; Park et al., 2011). In addition to disrupting viral HA-mediated membrane fusion, the P30-10-16 aptamer can distinguish between closely related Influenza A strains. This aptamer property is novel, considering that most monoclonal antibodies against HA have been unsuccessful at differentiating among influenza subtypes. Although initial studies were carried out by SPR-based detection, coupling of these aptamers to fluorophores or other signaling molecules could provide facile detection of virus subtypes. Development of these aptamers for viral subtype diagnostics will provide a significant advancement in our ability to differentiate highly pathogenic influenza strains from those that are less virulent and will likely yield important insights into its mechanism of action.

The Hepatitis B virus (HBV) surface antigen (HBsAg) is found on the membrane of HBV-infected hepatocytes. A fluorescently labeled aptamer targeting HBsAg, HBs-A22, was used to isolate cells expressing HBsAg. Use of fluorescence microscopy showed that that anti-HBsAg aptamer bound to the HBsAg-positive cell line (HepG2.2.15) but not to the HBsAg-negative cell line (HepG2). These results establish the use of aptamers for imaging, but also provide the first HBV specific antigen aptamer that could be used for early detection and treatment of HBV-infected cells (Liu et al., 2010).

Aptamers can also function as diagnostic tools when coupled to existing biosensors (Davis et al., 1998; Jhaveri et al., 2000;

Fang et al., 2001; O'Sullivan, 2002). Biosensors utilize a biological recognition element, such as aptamers, and a transducer for easier detection and quantification. An aptamer-based biosensor, or aptasensor, was isolated against the trans-activator of transcription (Tat) of HIV-1, which is important for regulating the early phases of HIV-1 infection (Chang et al., 1997; Mucha et al., 2002). The Tat aptasensor was generated by immobilizing the aptamer on a piezoelectric quartz-crystal, the transduction component of the aptasensor. Comparison of the Tat aptasensor to a corresponding immunosensor that uses an anti-Tat monoclonal antibody showed that the two biosensors are similar in terms of sensitivity and reproducibility (Minunni et al., 2004).

A multicomponent reporter system consisting of an inhibitory aptamer bound to a restriction endonuclease and a target complement/trigger system was successful in differentiating Dengue virus serotypes (Fletcher et al., 2010). One of the key advantages of this method is that the same aptamer/enzyme complex can be used since only the nucleic acid complement/trigger needs modification to detect new targets. Such a system can be more sensitive due to the multi-turnover nature of the endonuclease. Further development of these aptasensors and incorporating more stable chemical derivatives will likely overcome some of the limitations of current aptasensors.

APTAMERS IN BASIC RESEARCH

In addition to diagnostic and therapeutic applications, aptamers can be used as laboratory reagents in a number of biochemical and cell-based assays, similar to antibodies. Aptamers have key advantages over antibodies in that they often have higher affinity and specificity for their targets with some binding constants (K_D) < 1 nM, which results in an enhanced signal-to-noise ratio. Additionally, aptamers can be generated against almost any target ranging from small organic molecules to proteins to whole cells (Jayasena, 1999), and they are often times smaller than antibodies (7–30 kDa for aptamers vs. ∼150 kDa for antibodies) allowing them to bind regions inaccessible to antibodies.

By utilizing aptamers that disrupt protein–protein interactions, one can begin to dissect and characterize cellular pathways. The human T-cell leukemia virus type 1 Tax protein is a trans-activator that regulates the expression of various viral and cellular genes. Tax cannot directly bind DNA in the absence of certain host transcription factors, suggesting that protein–protein interactions are essential for Tax function. The YT1 aptamer disrupts Tax interactions with the cyclic AMP-response element binding protein (CREB) and NF-κB, but not serum response factor (SRF), all of which are known to interact with Tax proteins (Tian et al., 1995). These results suggest that the CREB and NF-κB binding interfaces on Tax may potentially overlap or are in close proximity, whereas the SRF binding site occupies a different surface on Tax. Therefore, aptamers provide a potential tool to map interaction surfaces between binding partners.

Assembly of the viral nucleocapsid (NC) requires multiple protein–protein and protein–nucleic acid interactions. The HIV NC is a highly conserved protein that plays a key role in RNA encapsidation and viral replication, and specifically binds viral genomic RNA through the psi sequence. An aptamer generated against NC competes with the psi sequence and prevents proper encapsidation of the viral genome, which likely inhibits proper packaging of the genomic RNA (Kim et al., 2002). Other HIV-1 NC aptamers against the HIV-1 Gag protein bind the matrix and the NC domains of Gag and reduced HIV replication in cultured cells. The inhibitory effect of these aptamers was not due to a defect in virion release but the downregulation of intracellular Gag protein and mRNA. A subset of aptamers which specifically bound NC competes with the psi packing signal of HIV-1, and disrupts interactions between Gag and viral RNA (Ramalingam et al., 2011). Unlike other aptamers that inhibit early stages in viral infection, the NC aptamer targets events that occur after viral entry, and therefore, allows one to study the intracellular effects of viral infection.

Using aptamers to specifically target and modulate functions of proteins within cellular pathways or the viral replication cycle can provide invaluable information about these respective systems. Nonetheless, an additional advantage of using aptamers to investigate cellular signaling is the ability to selectively turn the aptamers "on" and "off" with effectors. Further advances in the spatial and temporal regulation of aptamers will be important for enhancing our understanding of viral/host interactions. The potential regulation of aptamers with effector molecules is highlighted by Vuyisich and Beal (2002) in the regulation of formamidopyrimidine glycosylase (Fpg), a bacterial enzyme involved in DNA repair. A modified SELEX protocol was used where RNA-bound Fpg was treated with neomycin in order to elute the bound RNA. The Fpg aptamer inhibited Fpg activity, but the functionality was restored in the presence of neomycin. Rusconi et al. (2002) utilized antisense RNA in order to regulate the function of an aptamer targeted against the blood coagulation factor IXa. The anti-sense RNA base pairs to complementary regions within the aptamer and disrupts aptamer function. The factor IXa aptamer and anti-sense RNA antidote pair was an effective, reversible anticoagulant and shows potential for clinical application.

FUTURE PROSPECTS

Many viral proteins bind nucleic acids, although not a required characteristic, makes viruses good targets for aptamer development. As outlined above, aptamers have been used in a variety of studies to characterize and counter host–viral interactions, including targeting individual viral components or whole cells. A significant advantage of the aptamer technology lies in its ability to identify aptamers against a given target without *a priori* knowledge of the exact site or target. With limited information on the binding site, aptamers can be generated toward a given target and subsequently tested for regulatory activity either *in vitro* or *in vivo*. Similarly, aptamers can be used in target validation, where judicious use of aptamers can provide distinct advantages. Aptamers can also be used to dissect protein–protein interfaces and to validate traditional targets for small molecules, such as enzyme active sites. Current selection of small molecules toward known targets often depend on a variety of factors, including the availability of validating functional assays, structural and biochemical data, prior to initiating drug discovery efforts, which consume large amounts of time and resources. In contrast, one can develop aptamers with a fraction of the cost and time in a laboratory setting.

It is interesting to note that most aptamers form unusual and dynamic conformations that can potentially allow aptamers to target protein–protein, protein–nucleic acid, and small molecule interactions. However, in many of the examples reviewed, there is limited knowledge on the structural and biochemical aspects of these aptamer/target interactions, and available data are primarily restricted to secondary structure predictions or mapping. The addition of structural and biochemical studies of aptamer/target pairs can enhance the utility of these aptamers by providing new information on the aptamer/target interfaces and by providing information for structure-based optimization of aptamers. Continual development and optimization of multifunctional, chimeric aptamers, and aptamer libraries for strain specific viral identification will lead to more broadly applicable therapeutic and diagnostic applications in the future.

ACKNOWLEDGMENTS

Work in our laboratory is supported by NIH grants [AI089547 to Gaya K. Amarasinghe (CF Basler-PI) and AI059536]. We thank P. Ramanan for critical reading of the manuscript.

REFERENCES

Aldaz-Carroll, L., Tallet, B., Dausse, E., Yurchenko, L., and Toulme, J. J. (2002). Apical loop-internal loop interactions: a new RNA-RNA recognition motif identified through in vitro selection against RNA hairpins of the hepatitis C virus mRNA. *Biochemistry* 41, 5883–5893.

Bellecave, P., Andreola, M. L., Ventura, M., Tarrago-Litvak, L., Litvak, S., and Astier-Gin, T. (2003). Selection of DNA aptamers that bind the RNA-dependent RNA polymerase of hepatitis C virus and inhibit viral RNA synthesis in vitro. *Oligonucleotides* 13, 455–463.

Bellecave, P., Cazenave, C., Rumi, J., Staedel, C., Cosnefroy, O., Andreola, M. L., Ventura, M., Tarrago-Litvak, L., and Astier-Gin, T. (2008). Inhibition of hepatitis C virus (HCV) RNA polymerase by DNA aptamers: mechanism of inhibition of in vitro RNA synthesis and effect on HCV-infected cells. *Antimicrob. Agents Chemother.* 52, 2097–2110.

Biroccio, A., Hamm, J., Incitti, I., De Francesco, R., and Tomei, L. (2002). Selection of RNA aptamers that are specific and high-affinity ligands of the hepatitis C virus RNA-dependent RNA polymerase. *J. Virol.* 76, 3688–3696.

Bunka, D. H., and Stockley, P. G. (2006). Aptamers come of age – at last. *Nat. Rev. Microbiol.* 4, 588–596.

Chang, H. C., Samaniego, F., Nair, B. C., Buonaguro, L., and Ensoli, B. (1997). HIV-1 Tat protein exits from cells via a leaderless secretory pathway and binds to extracellular matrix-associated heparan sulfate proteoglycans through its basic region. *AIDS* 11, 1421–1431.

Chelliserrykattil, J., and Ellington, A. D. (2004). Evolution of a T7 RNA polymerase variant that transcribes 2′-*O*-methyl RNA. *Nat. Biotechnol.* 22, 1155–1160.

Da Rocha Gomes, S., Dausse, E., and Toulme, J. J. (2004). Determinants of apical loop-internal loop RNA-RNA interactions involving the HCV IRES. *Biochem. Biophys. Res. Commun.* 322, 820–826.

Davis, K. A., Lin, Y., Abrams, B., and Jayasena, S. D. (1998). Staining of cell surface human CD4 with 2′-*F*-pyrimidine-containing RNA aptamers for flow cytometry. *Nucleic Acids Res.* 26, 3915–3924.

Dey, A. K., Griffiths, C., Lea, S. M., and James, W. (2005a). Structural characterization of an anti-gp120 RNA aptamer that neutralizes R5 strains of HIV-1. *RNA* 11, 873–884.

Dey, A. K., Khati, M., Tang, M., Wyatt, R., Lea, S. M., and James, W. (2005b). An aptamer that neutralizes R5 strains of human immunodeficiency virus type 1 blocks gp120-CCR5 interaction. *J. Virol.* 79, 13806–13810.

Dhar, G. S., and Datta, A. (2009). Targeting pseudoknots in H5N1 hemagglutinin using designed aptamers. *Bioinformation* 4, 193–196.

Ellington, A. D., and Szostak, J. W. (1990). In vitro selection of RNA molecules that bind specific ligands. *Nature* 346, 818–822.

Fang, X., Cao, Z., Beck, T., and Tan, W. (2001). Molecular aptamer for real-time oncoprotein platelet-derived growth factor monitoring by fluorescence anisotropy. *Anal. Chem.* 73, 5752–5757.

Fletcher, S. J., Phillips, L. W., Milligan, A. S., and Rodda, S. J. (2010). Toward specific detection of Dengue virus serotypes using a novel modular biosensor. *Biosens. Bioelectron.* 26, 1696–1700.

Gopinath, S. C. (2007). Antiviral aptamers. *Arch. Virol.* 152, 2137–2157.

Gopinath, S. C. (2008). Anti-coagulant aptamers. *Thromb. Res.* 122, 838–847.

Gopinath, S. C., Misono, T. S., Kawasaki, K., Mizuno, T., Imai, M., Odagiri, T., and Kumar, P. K. (2006). An RNA aptamer that distinguishes between closely related human influenza viruses and inhibits haemagglutinin-mediated membrane fusion. *J. Gen. Virol.* 87, 479–487.

James, W. (2001). Nucleic acid and polypeptide aptamers: a powerful approach to ligand discovery. *Curr. Opin. Pharmacol.* 1, 540–546.

James, W. (2007). Aptamers in the virologists' toolkit. *J. Gen. Virol.* 88, 351–364.

Jayasena, S. D. (1999). Aptamers: an emerging class of molecules that rival antibodies in diagnostics. *Clin. Chem.* 45, 1628–1650.

Jellinek, D., Green, L. S., Bell, C., Lynott, C. K., Gill, N., Vargeese, C., Kirschenheuter, G., Mcgee, D. P., Abesinghe, P., Pieken, W. A., Shapiro, R., Rifkin, D. B., Moscatelli, D., and Janjic, N. (1995). Potent 2′-amino-2′-deoxypyrimidine RNA inhibitors of basic fibroblast growth factor. *Biochemistry* 34, 11363–11372.

Jeon, S. H., Kayhan, B., Ben-Yedidia, T., and Arnon, R. (2004). A DNA aptamer prevents influenza infection by blocking the receptor binding region of the viral hemagglutinin. *J. Biol. Chem.* 279, 48410–48419.

Jhaveri, S., Rajendran, M., and Ellington, A. D. (2000). In vitro selection of signaling aptamers. *Nat. Biotechnol.* 18, 1293–1297.

Kanamori, H., Yuhashi, K., Uchiyama, Y., Kodama, T., and Ohnishi, S. (2009). In vitro selection of RNA aptamers that bind the RNA-dependent RNA polymerase of hepatitis C virus: a possible role of GC-rich RNA motifs in NS5B binding. *Virology* 388, 91–102.

Kato, Y., Minakawa, N., Komatsu, Y., Kamiya, H., Ogawa, N., Harashima, H., and Matsuda, A. (2005). New NTP analogs: the synthesis of 4′-thioUTP and 4′-thioCTP and their utility for SELEX. *Nucleic Acids Res.* 33, 2942–2951.

Kikuchi, K., Umehara, T., Fukuda, K., Hwang, J., Kuno, A., Hasegawa, T., and Nishikawa, S. (2003). RNA aptamers targeted to domain II of hepatitis C virus IRES that bind to its apical loop region. *J. Biochem.* 133, 263–270.

Kikuchi, K., Umehara, T., Fukuda, K., Kuno, A., Hasegawa, T., and Nishikawa, S. (2005). A hepatitis C virus (HCV) internal ribosome entry site (IRES) domain III-IV-targeted aptamer inhibits translation by binding to an apical loop of domain IIId. *Nucleic Acids Res.* 33, 683–692.

Kikuchi, K., Umehara, T., Nishikawa, F., Fukuda, K., Hasegawa, T., and Nishikawa, S. (2009). Increased inhibitory ability of conjugated RNA aptamers against the HCV IRES. *Biochem. Biophys. Res. Commun.* 386, 118–123.

Kim, S. J., Kim, M. Y., Lee, J. H., You, J. C., and Jeong, S. (2002). Selection and stabilization of the RNA aptamers against the human immunodeficiency virus type-1 nucleocapsid protein. *Biochem. Biophys. Res. Commun.* 291, 925–931.

Liu, J., Yang, Y., Hu, B., Ma, Z. Y., Huang, H. P., Yu, Y., Liu, S. P., Lu, M. J., and Yang, D. L. (2010). Development of HBsAg-binding aptamers that bind HepG2.2.15 cells via HBV surface antigen. *Virol. Sin.* 25, 27–35.

Meyer, C., Hahn, U., and Rentmeister, A. (2011). Cell-specific aptamers as emerging therapeutics. *J. Nucleic Acids* 2011, 904750.

Minunni, M., Tombelli, S., Gullotto, A., Luzi, E., and Mascini, M. (2004). Development of biosensors with aptamers as bio-recognition element: the case of HIV-1 Tat protein. *Biosens. Bioelectron.* 15, 1149–1156.

Misono, T. S., and Kumar, P. K. (2005). Selection of RNA aptamers against human influenza virus hemagglutinin using surface plasmon resonance. *Anal. Biochem.* 342, 312–317.

Mucha, P., Szyk, A., Rekowski, P., and Barciszewski, J. (2002). Structural requirements for conserved Arg52 residue for interaction of the human immunodeficiency virus type 1 trans-activation responsive element with trans-activator of transcription protein (49-57). Capillary electrophoresis mobility shift assay. *J. Chromatogr. A* 968, 211–220.

Neff, C. P., Zhou, J., Remling, L., Kuruvilla, J., Zhang, J., Li, H., Smith, D. D., Swiderski, P., Rossi, J. J., and Akkina, R. (2011). An aptamer-siRNA chimera suppresses HIV-1 viral loads and protects from helper CD4(+) T cell decline in humanized mice. *Sci. Transl. Med.* 3, 66ra66.

O'Sullivan, C. K. (2002). Aptasensors – the future of biosensing? *Anal. Bioanal. Chem.* 372, 44–48.

Park, S. Y., Kim, S., Yoon, H., Kim, K. B., Kalme, S. S., Oh, S., Song, C. S., and Kim, D. E. (2011). Selection of an antiviral RNA aptamer against hemagglutinin of the subtype H5 avian influenza virus. *Nucleic Acid Ther.* 21, 395–402.

Ramalingam, D., Duclair, S., Datta, S. A., Ellington, A., Rein, A., and Prasad, V. R. (2011). RNA aptamers directed to human immunodeficiency virus type 1 Gag polyprotein bind to the matrix and nucleocapsid domains and inhibit virus production. *J. Virol.* 85, 305–314.

Robertson, D. L., and Joyce, G. F. (1990). Selection in vitro of an RNA enzyme that specifically cleaves single-stranded DNA. *Nature* 344, 467–468.

Romero-Lopez, C., Diaz-Gonzalez, R., Barroso-Deljesus, A., and Berzal-Herranz, A. (2009). Inhibition of hepatitis C virus replication and internal ribosome entry site-dependent translation by an RNA molecule. *J. Gen. Virol.* 90, 1659–1669.

Rusconi, C. P., Scardino, E., Layzer, J., Pitoc, G. A., Ortel, T. L., Monroe, D., and Sullenger, B. A. (2002). RNA aptamers as reversible antagonists of coagulation factor IXa. *Nature* 419, 90–94.

Sun, W., Du, L., and Li, M. (2011). Advances and perspectives in cell-specific aptamers. *Curr. Pharm. Des.* 17, 80–91.

Syed, M. A., and Pervaiz, S. (2010). Advances in aptamers. *Oligonucleotides* 20, 215–224.

Tian, Y., Adya, N., Wagner, S., Giam, C. Z., Green, M. R., and Ellington, A. D. (1995). Dissecting protein:protein interactions between transcription factors with an RNA aptamer. *RNA* 1, 317–326.

Tuerk, C., and Gold, L. (1990). Systematic evolution of ligands by exponential enrichment: RNA ligands to bacteriophage T4 DNA polymerase. *Science* 249, 505–510.

Tuerk, C., Macdougal, S., and Gold, L. (1992). RNA pseudoknots that inhibit human immunodeficiency virus type 1 reverse transcriptase. *Proc. Natl. Acad. Sci. U.S.A.* 89, 6988–6992.

Vuyisich, M., and Beal, P. A. (2002). Controlling protein activity with ligand-regulated RNA aptamers. *Chem. Biol.* 9, 907–913.

Wang, J., Jiang, H., and Liu, F. (2000). In vitro selection of novel RNA ligands that bind human cytomegalovirus and block viral infection. *RNA* 6, 571–583.

Wheeler, L. A., Trifonova, R., Vrbanac, V., Basar, E., Mckernan, S., Xu, Z., Seung, E., Deruaz, M., Dudek, T., Einarsson, J. I., Yang, L., Allen, T. M., Luster, A. D., Tager, A. M., Dykxhoorn, D. M., and Lieberman, J. (2011). Inhibition of HIV transmission in human cervicovaginal explants and humanized mice using CD4 aptamer-siRNA chimeras. *J. Clin. Invest.* 121, 2401–2412.

Zhou, J., Battig, M. R., and Wang, Y. (2010). Aptamer-based molecular recognition for biosensor development. *Anal. Bioanal. Chem.* 398, 2471–2480.

Zhou, J., Shu, Y., Guo, P., Smith, D. D., and Rossi, J. J. (2011). Dual functional RNA nanoparticles containing phi29 motor pRNA and anti-gp120 aptamer for cell-type specific delivery and HIV-1 inhibition. *Methods* 54, 284–294.

Conflict of Interest Statement: The authors declare that the research was conducted in the absence of any commercial or financial relationships that could be construed as a potential conflict of interest.

Received: 05 January 2012; accepted: 17 January 2012; published online: 08 February 2012.

Citation: Binning JM, Leung DW and Amarasinghe GK (2012) Aptamers in virology: recent advances and challenges. Front. Microbio. ***3****:29. doi: 10.3389/fmicb.2012.00029*

This article was submitted to Frontiers in Virology, a specialty of Frontiers in Microbiology.

frontiers in
MICROBIOLOGY

GENERAL COMMENTARY
published: 14 February 2012
doi: 10.3389/fmicb.2012.00052

Commentary on aptamers for virus research

Yasuyuki Miyazaki[1]* and Mikako Fujita[2]

[1] *Department of Microbiology, Institute of Health Biosciences, The University of Tokushima Graduate School, Tokushima, Japan*
[2] *Research Institute for Drug Discovery, School of Pharmacy, Kumamoto University, Kumamoto, Japan*
**Correspondence: ymiyazaki@basic.med.tokushima-u.ac.jp*

A commentary on

Aptamers in virology: recent advances and challenges
by Binning, J. M., Leung, D. W., and Amarasinghe, G. K. (2012). Front. Microbiol. 3:29. doi: 10.3389/fmicb.2012.00029

Aptamers are oligonucleotide ligands that form unique secondary and tertiary structures, such as stem loops, kinks, bulges, and pseudoknots. Each aptamer exhibits a unique interface, through its structure, that specifically recognizes the target molecule. In fact, the target recognition of aptamers is highly specific, and it has been reported that an aptamer is able to discriminate between closely related isoforms or different conformational states of the same molecule (Conrad and Ellington, 1996; Proske et al., 2002).

Aptamers are often compared with antibodies due to their high specificity and affinity to the targets; however, they have some advantages over antibodies. For instance, antibodies require animals to be generated. Aptamers are generated by *in vitro* chemical synthesis, which enables chemical modification to control their stability or to add fluorescent dye on demand. Moreover, antibodies basically function in extracellular regions, whereas aptamers are easily introduced into the intra-cellular compartment by transfection. Loss-of-function technologies such as gene knockout, antisense oligonucleotide, and RNA interference (RNAi) are actively utilized for gene targeting. These aim to address the function of a target product through gene inactivation at the genomic or transcriptional level. Proteins often have multiple functions and work as part of multiprotein complex. It is often difficult to validate the functional relevance of the proteins by deletion at the genomic or transcriptional level. Aptamers are applicable to these proteins since aptamers can directly bind target proteins. As protein-based target validation reagents other than antibodies, peptides derived from phage display libraries are available. These peptides, however, require *in vivo* production, and in part, exhibit poor specificity to the target molecules, which remains to be overcome for general application. Thus, aptamers have some advantages over other technologies currently used, and have potential for a broad range of application, such as diagnostic, therapeutic, and basic research (**Figure 1**).

Binning et al. (2012) summarized the recent developments and future prospects of aptamers in the virus research field. Early and reliable detection of pathogens is important for the successful treatment and prevention of virus epidemics. As a diagnostic tool, aptamers have ideal properties, such as (1) highly specific and tight affinity to target molecule, (2) facilitation of modification, and (3) stability. Due to these advantages, aptamers are being actively investigated as a diagnostic tool. In addition, aptamers can be coupled to existing biosensors, achieving very high sensitivity (Zhou et al., 2010). Aptamers can also be exploited as therapeutic reagents. As mentioned above, aptamers can be located in both extra- and intra-cellular regions, where they are capable of targeting any viral components. In fact, aptamers have been reported to work in various viral replication steps, such as entry, transcription, translation, and genome packaging (Binning et al., 2012). Furthermore, aptamers exhibit little or no immunogenicity and toxicity. Since oligonucleotides, especially RNAs, are readily broken down by nucleases in organisms, aptamers have to evade from attack of nucleases for therapeutic use. 2′-Fluoropyrimidine modification, 2′-*O*-methyl nucleotides, or 3′ end cap modification has been developed to achieve resistance to nucleases (Keefe and Cload, 2008). Thus, aptamers are potent therapeutic reagents. In addition, aptamers can be an excellent tool for drug discovery, and a competitive screening method has been developed (Green et al., 2001). A large pool of chemical compounds is screened against an aptamer/target complex. Only a chemical compound capable of binding the target molecule with equivalent or higher affinity than the aptamer/target can displace the aptamer from the target molecule. This aptamer approach enables high-throughput screening of potent drug candidates. Of note, the aptamer approach is applicable even if the natural ligand/substrate is unknown. Aptamers can also be a useful tool for basic research by specifically targeting and disrupting the functions of viral or host protein involved in viral replications. For example, Binning et al. (2012) described an aptamer targeting Tax of human T-cell leukemia virus and those targeting NC of human immunodeficiency virus. Thus, aptamers can provide invaluable insight into viral replication.

Over two decades have passed since the initial description of a screening method of aptamers, so called systematic evolution of ligands by exponential enrichment (SELEX; Ellington and Szostak, 1990; Tuerk and Gold, 1990) and applications using aptamers have become more sophisticated and are increasing. Now is a good time for all researchers in the virus research field to consider the use of aptamers.

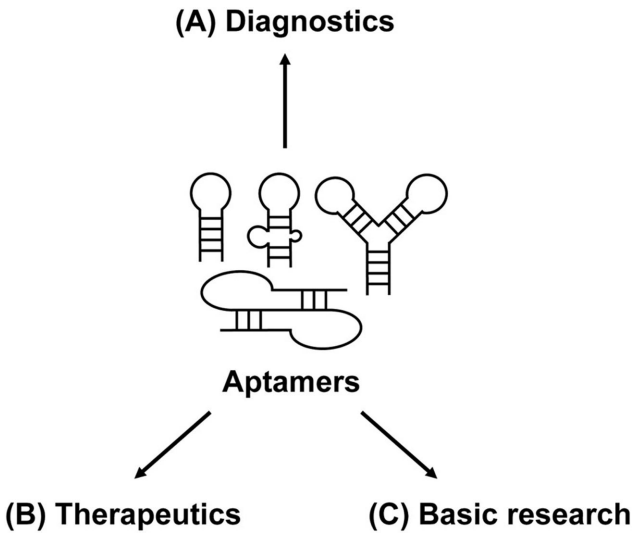

FIGURE 1 | Possible applications of aptamers in virus research. (A) Aptamers as diagnostic tools. Aptamers exhibit highly specific recognition with very tight affinity (K_d < 1 nM) to the target molecules. Aptamer-based detection assays are expected to reach lower detection limits than conventional antibody-based detection assays such as ELISA. **(B)** Aptamers as therapeutics. Due to specific and tight affinity to the target molecules, and low or no immunogenicity and toxicity, aptamers are expected to be effective therapeutic reagents. Moreover, aptamers are capable of existing in extra- and intra-cellular regions, indicating that any viral components can be targeted by aptamers. **(C)** Aptamers as a basic research tool. Antibodies or peptides derived from phage display libraries are generally used for protein-based target validation. Aptamers have some advantages over these methods because of their short development time, *in vitro* synthesis, and high specificity.

REFERENCES

Binning, J. K., Leung, D. W., and Amarasinghe, G. K. (2012). Aptamers in virology: recent advances and challenges. *Front. Microbiol.* 3:29. doi: 10.3389/fmicb.2012.00029

Conrad, R., and Ellington, A. D. (1996). Detecting immobilized protein kinase C isozymes with RNA aptamers. *Anal. Biochem.* 242, 261–265.

Ellington, A. D., and Szostak, J. W. (1990). In vitro selection of RNA molecules that bind specific ligands. *Nature* 346, 818–822.

Green, L. S., Bell, C., and Janjic, N. (2001). Aptamers as reagents for high-throughput screening. *BioTechniques* 30, 1094–1100.

Keefe, A. D., and Cload, S. T. (2008). SELEX with modified nucleotides. *Curr. Opin. Chem. Biol.* 12, 448–456.

Proske, D., Höfliger, M., Söll, R. M., Beck-Sickinger, A. G., and Famulok, M. (2002). A Y2 receptor mimetic aptamer directed against neuropeptide Y. *J. Biol. Chem.* 277, 11416–11422.

Tuerk, C., and Gold, L. (1990). Systematic evolution of ligands by exponential enrichment: RNA ligands to bacteriophage T4 DNA polymerase. *Science* 249, 505–510.

Zhou, J., Battig, M. R., and Wang, Y. (2010). Aptamer-based molecular recognition for biosensor development. *Anal. Bioanal. Chem.* 398, 2471–2480.

Received: 26 January 2012; accepted: 31 January 2012; published online: 14 February 2012.

*Citation: Miyazaki Y and Fujita M (2012) Commentary on aptamers for virus research. Front. Microbio. **3**:52. doi: 10.3389/fmicb.2012.00052*

This article was submitted to Frontiers in Virology, a specialty of Frontiers in Microbiology.

frontiers in
MICROBIOLOGY

GENERAL COMMENTARY
published: 08 September 2011
doi: 10.3389/fmicb.2011.00186

Commentary on a new era of investigating 3D structure-based human–virus protein network dynamics

***Shun Adachi*[1], *Akio Adachi*[2] *and Masako Nomaguchi*[2]*

[1] *Multicellular Society Laboratory, Center for Frontier Research, National Institute of Genetics, Mishima, Japan*
[2] *Department of Microbiology, Institute of Health Biosciences, The University of Tokushima Graduate School, Tokushima, Japan*
**Correspondence: nomaguchi@basic.med.tokushima-u.ac.jp*

A commentary on

Structural principles within the human–virus protein-protein interaction network *by Franzosa, E. A., and Xia, Y. (2011). Proc. Natl. Acad. Sci. U.S.A. 108, 10538–10543.*

Virology is a fundamental research field for viruses that encompasses studies on minimum replication units, rapid evolution, and clinical applications. Similar to the other biological systems, structural study of viral system is based on three distinct phases of understanding: (I) modeling of steady-state network; (II) involvement of spatial confinements to the model; (III) involvement of timing asymmetry to the model. Most molecular biological understandings are limited to phase (I), rendering later phases to be investigated by future systems biology.

Even in phase (I), complexities of protein–protein network system make the researchers puzzled over examining actual underlying principles in the observed data sets. One type of solution for such an abstraction of the principles is to model a protein–protein interaction network based on graph theory; a theory of pair-wise relations between objects of a certain collection. Graph is constituted of nodes (for protein of interests in this case) and edges (for a certain protein–protein interaction), sometimes accompanied by different evaluation weights for an expected dynamics. Scale-free network, in which a small number of nodes act as hubs and the other nodes possess extremely small numbers of links, is supposed to be a characteristic of actual protein–protein interaction network in biological system. This type of network is prominent when the network encounters adding-on system for growth and selection bias for linking nodes act as hubs. However, it is not clear whether an input and output of such an abstracted system represents actual dynamics of original biological system, and what biological significances of parameters characterizing the networks are, i.e., density, transitivity, reciprocity, centrality etc. Progressing of the type of study requires further information to analyze the network elegantly.

In the article that deals with underlying principles of human–virus protein interaction network (*Proc. Natl. Acad. Sci. U.S.A.* 108, 10538–10543), Drs Franzosa and Xia have reported the results from 3D surface structure-based protein interaction network system. Based on 3039 endogenous interactions among 2435 human proteins as well as 53 exogenous interactions among 50 viral proteins from 36 viral species and their 50 human target proteins, they developed combined method of BLAST homology evaluation algorithm and MSMS program based on solvent-accessible surface area (SASA). The unique properties of this model case study are (i) detection of convergent evolution (mimicking evolution of viral protein surfaces to non-homological host human protein surfaces, in contrast to host gene duplication resulted in overlapping protein surface interactions) and evolutionary "arms race" (fast evolving trait of exogenous interactions due to cutting-off and catching-up interactions between human target proteins and viral proteins) due to rapid evolution and highly antagonistic manner of viral proteins and their target proteins, in contrast to cooperative interaction of endogenous human protein interactions; (ii) higher resolution of data based on more information from 3D surface structure interface. The original idea of using 3D surface information to network analysis is from the yeast study by Kim et al. (2006). In contrast to Kim's work, the patterns of evolution became much clearer based on fast evolving antagonistic viral proteins of absolutely different origins from host human. Compared to endogenous interactions, exogenous interactions exhibit transient structure, increase in number of interacting proteins, higher tendency of regulatory function, and faster evolution. Addition of BLAST information elucidates co-evolutionary information such as convergent evolution and evolutionary arms race.

Although the researchers are still struggling in phase (I), the application of 3D structural information to a graph of protein–protein network is very useful for investigating the evolutionary dynamics of the network of interests applying huge sum of mechanical interactive information to a simple graph of the interaction network. Additional investigation by commonly used BLAST algorithm will be useful expecting clinical application of drug design to highly conserved protein–protein interaction, instead of fast evolving highly adaptive region for target viruses.

REFERENCE

Kim, P. M., Lu, L. J., Xia, Y., and Gerstein, M. B. (2006). Relating three-dimensional structures to protein networks provides evolutionary insights. *Science* 314, 1938–1941.

Received: 22 August 2011; accepted: 22 August 2011; published online: 08 September 2011.
Citation: Adachi S, Adachi A and Nomaguchi M (2011) Commentary on a new era of investigating 3D structure-based human-virus protein network dynamics. Front. Microbio. 2:186. doi: 10.3389/fmicb.2011.00186
This article was submitted to Frontiers in Virology, a specialty of Frontiers in Microbiology.